

The cover art depicts a vast, desolate landscape of Europa, characterized by rugged, snow-covered mountains and a flat, icy plain. In the upper right corner, the massive, swirling clouds of Jupiter are visible against the dark, star-filled sky of space.

# **EUROPA STUDY 2012 REPORT**

## **EUROPA ORBITER MISSION**

**Europa Study Team, 1 May 2012, JPL D-71990**  
Task Order NMO711062 Outer Planets Flagship Mission

**Cover art Michael Carroll**



# Europa Study Final Report—Orbiter

## Contents

B.	Orbiter Mission.....	B-2
B.1	Science of the Orbiter Mission .....	B-6
B.1.1	Orbiter Science .....	B-6
B.1.2	Orbiter Traceability Matrix.....	B-13
B.1.3	Science Instrument Complement.....	B-22
B.2	Orbiter Mission Concept.....	B-24
B.2.1	Orbiter Study Scope and Driving Requirements .....	B-24
B.2.2	Orbiter Mission Concept Overview .....	B-25
B.2.3	Orbiter Mission Elements.....	B-26
B.2.4	Orbiter Mission Architecture Overview.....	B-26
B.2.5	Science Instrumentation .....	B-26
B.2.6	Mission Design .....	B-41
B.2.7	Flight System Design and Development.....	B-48
B.2.8	Mission Operations .....	B-96
B.2.9	Systems Engineering.....	B-100
B.3	Programmatics.....	B-113
B.3.1	Management Approach .....	B-113
B.3.2	WBS .....	B-114
B.3.3	Schedule.....	B-114
B.3.4	Risk and Mitigation Plan .....	B-118
B.3.5	Cost .....	B-120
B.4	Appendices .....	B-127
B.4.1	References .....	B-127
B.4.2	Acronyms and Abbreviations .....	B-133
B.4.3	Master Equipment List.....	B-138
B.4.4	Europa Orbiter Mission Senior Review Board Report.....	B-139
B.4.5	Aerospace Independent Orbiter Concept CATE: Cost and Technical Evaluation.....	B-143

*This research was carried out at the Jet Propulsion Laboratory, California Institute of Technology, under a contract with the National Aeronautics and Space Administration, with contributions from the Applied Physics Laboratory, Johns Hopkins University.*

*The cost information contained in this document is of budgetary and planning nature and is intended for informational purposes only. It does not constitute a commitment on the part of JPL and/or Caltech.*



## B. ORBITER MISSION

*The Europa Orbiter Mission would explore Europa to investigate its habitability, delivering cost-effective, low-risk science.*

### *Executive Summary*

#### *Background*

The 2011 Planetary Science Decadal Survey recommended an immediate effort to find major cost reductions for the Jupiter Europa Orbiter (JEO) concept. To that end, NASA Headquarters appointed a Science Definition Team (SDT) and directed the Europa Study Team, guided by the SDT, to redefine a set of minimal science missions to Europa. The cost target was \$2.25B (\$FY15, excluding launch vehicle) and additional guidelines were levied, as described in §A. Independent cost and technical review was to be performed on all study results. These studies, independent reviews, and all deliverables were delivered to NASA Headquarters on May 1, 2012.

One of these mission concepts, a Europa Orbiter Mission, is well suited to addressing the

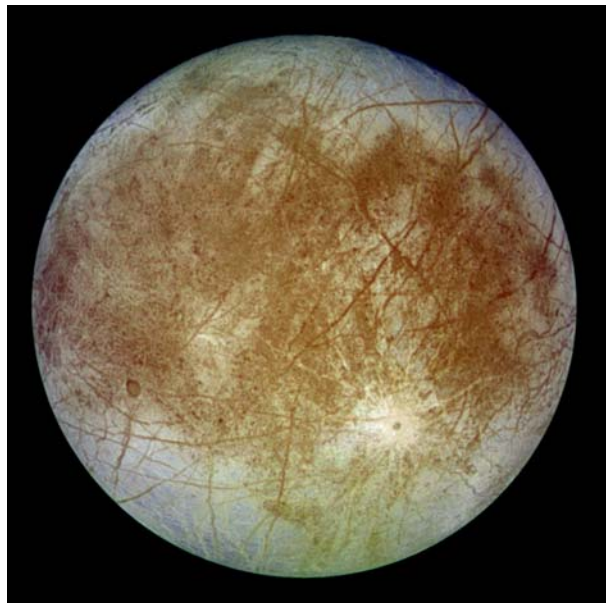


**Figure B-1.** Europa: a world of rock, ice, and water the size of the Earth's moon. The 2011 Planetary Decadal Survey identifies exploration of Europa as “the first step in understanding the potential of the outer solar system as an abode for life” (Space Studies Board 2011, p. 1).

ocean and geology themes of Europa exploration. It would involve a spacecraft low circular polar orbit around Europa, uniformly covering the entire moon to form global imagery, gravity and magnetometry data sets allowing investigation of the interior ocean, ice shell and surface geology. This concept, as detailed below, represents the combined effort since April 2011 of the SDT and a technical team from the Jet Propulsion Laboratory (JPL) and Johns Hopkins University's Applied Physics Laboratory (APL).

#### *Rationale for Orbiter Science*

The 2003 Planetary Decadal Survey, “New Horizons in the Solar System,” and 2011 Planetary Decadal Survey, “Vision and Voyages” (Space Studies Board 2003, 2011), both emphasize the importance of Europa exploration. The 2011 Decadal Survey discusses the likelihood of contemporary habitats with the necessary conditions for life, stressing the inherent motivation for “a Europa mission with the goal of confirming the presence of an interior ocean, characterizing the satellite's ice shell, and understanding its geological history” (Space Studies Board 2011, pp. 1–2).

Understanding the global-scale structure of Europa, with emphasis on the ocean, along with the distribution of landforms is key to evaluating the habitability of this moon. Within this goal, the Orbiter Mission objectives—(1) to characterize the extent of the ocean and its relation to the deeper interior and (2) to understand the formation of surface features, including sites of recent or current activity, and characterize high-science-interest localities—require global data sets obtained under relatively uniform conditions. As such, these data sets are best suited to collection from a platform that is in orbit around Europa. Within this report, the science to be achieved is discussed, the data types that are needed, and the means by which they can be acquired. The Europa Orbiter Mission would be directly responsive to the Deca-

dal Survey’s recommendations for Europa science.

#### *Science Objectives*

Understanding planetary processes and habitability is a key driver for Europa exploration. Thus, the goal adopted for the Europa Study is to “Explore Europa to investigate its habitability.” The phrase “investigate its habitability” recognizes the significance of Europa’s astrobiological potential. “Habitability” includes characterizing any water within and beneath Europa’s ice shell, investigating the chemistry of the surface and ocean, and evaluating geological processes that might permit Europa’s ocean to possess the chemical energy necessary for life (Figure B-2). Understanding Europa’s habitability is intimately tied to understanding the three “ingredients” for life: water, chemistry, and energy. The Europa Orbiter Mission objectives are categorized in priority order as exploration of Europa’s ocean and exploration of Europa’s geology to understand their contributions to the ingredients for life.

The complete traceability from top level mission goal and objectives to example measurements and the model instruments that could accomplish them is compiled and contained in this report. The example measurements and the notional instruments are provided as a proof of concept to demonstrate the types of measurements that could address the investigations, objectives, and goals. These are not meant to be exclusive of other measurements and instruments that might be able to address

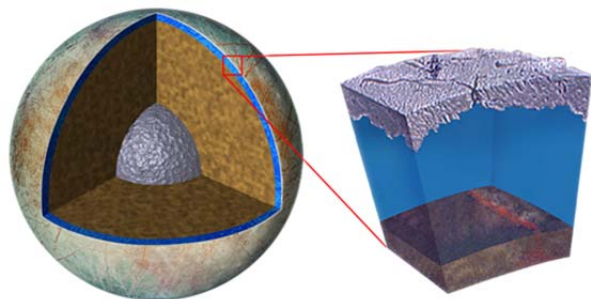


**Figure B-2.** Diagram of Europa’s subsurface ocean: our Solar System’s best chance for extant life beyond Earth?

the investigations and objectives in other ways. The model planning payload selected for the Europa Orbiter Mission consists of a notional set of remote-sensing instruments (Laser Altimeter [LA] and Mapping Camera [MC]), in situ instruments (Magnetometer [MAG] and Langmuir Probe [LP]), and a telecommunications system that provides Doppler and range data for accurate orbit reconstruction in support of geophysical objectives. NASA will ultimately select the payload through a formal Announcement of Opportunity (AO) process.

A traceability matrix (Foldout B-1 [FO B-1]), with its overarching goal to “Explore Europa to investigate its habitability,” provides specific objectives (in priority order), along with specific investigations (in priority order), and example measurements (in priority order) for each investigation. Each objective and its investigations are described in this report, along with the corresponding example measurements that could address them.

#### *Architecture Implementation*

Careful analysis and detailed understanding of the science objectives and traceability matrix led the team to determine that an orbiter mission architecture is the optimal approach to satisfying the science objectives in the most cost-effective, lowest-risk manner. This approach allows the acquisition of a uniform, well controlled data set, while exposing the flight hardware to a lower radiation dose compared to JEO.

The mission concept has been designed to provide global coverage of the European surface by means of a circular polar orbit. This orbit, in association with an instrument scan platform, allows mapping coverage across all latitudes at uniform lighting conditions with concurrent acquisition of magnetometry and gravity science measurements. Science measurement requirements are fully met with the current mission design with several areas of further refinement available to improve overall

mission robustness. The Europa Orbiter Mission instruments are light, require only a modest amount of power and produce a data at a modest and manageable rate. These characteristics are ideal for deployment into Europa orbit where insertion mass, power requirements and data return constraints dominate. Additionally, science operations are very repetitive, which leads to low-cost operations. The instrument interface and accommodations allow for delivery late in system-level integration and test, providing program flexibility.

The flight system (Figure B-3) uses a modular architecture, which greatly facilitates the implementation, assembly, and testing of the system. The 3-axis-stabilized spacecraft would utilize four Advanced Stirling Radioisotope Generators (ASRGs) for power. A innovative propulsion system accommodation, along with a Juno-style electronics vault and a nested shielding strategy, would provide significant protection from the radiation environment, allowing the use of existing parts qualified for Earth geosynchronous or medium earth orbit applications. Europa planetary protection requirements would be met through system-level dry-heat microbial reduction in a thermal-vacuum chamber at the launch site. Technical margins for the mission design are extremely robust, with 43% mass margin, 39% power margin during science operations, and 71% downlink margin.

*Schedule and Cost*

A top-level development schedule is shown in

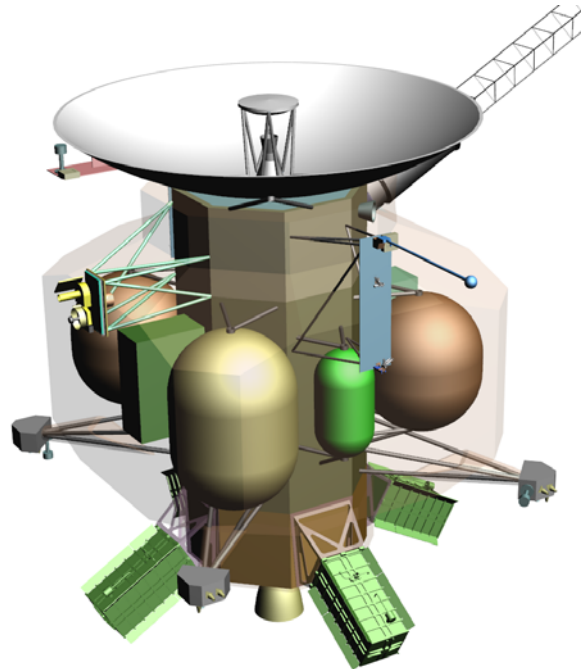


**Figure B-3.** The Europa Orbiter Mission flight system provides a robust platform to collect and transmit science data.

Figure B-4. The phase durations are conservative and draw on experience from previous outer planets missions. This schedule would enable front-loading of requirements development, significant time for instrument development to understand the actual design implications for radiation and planetary protection, and a flatter than typical mission funding profile, all consistent with newly drafted NASA NPR 7120.5E requirements.

The Orbiter Mission study used a model based costing methodology deriving driving flight

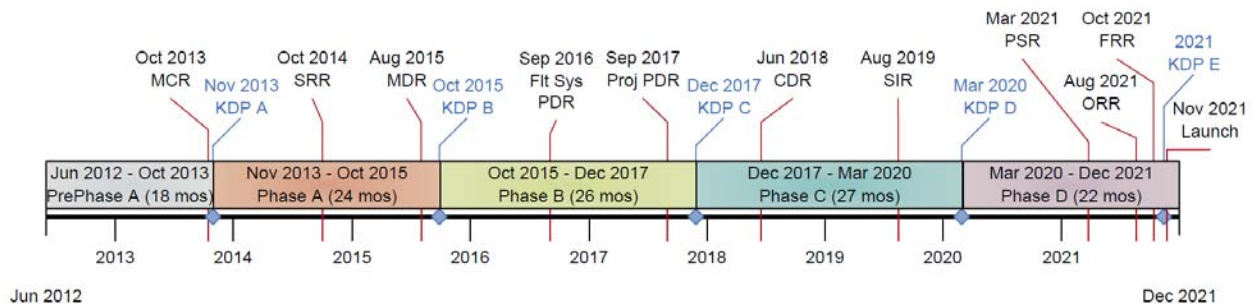


**Figure B-4.** Top-level development schedule with conservative durations provides appropriate time to address radiation and planetary protection challenges.

system costs from two cost models (PRICE-H, SEER) and payload costs from the NASA Instrument Cost Model (NICM). Experience based percentage wrap factors were then applied to derive supporting Work Breakdown Structure (WBS) elements. JPL Team X estimates were obtained as internally independent validation of the estimated cost and the Aerospace Corporation was retained to perform an external independent CATE cost estimate. The mission Phase A–E lifecycle cost is estimated to be \$1.7B (FY15\$, w/o Launch Vehicle), 70th-percentile confidence. The Aerospace Corporation performed an independent cost analysis and found \$1.8B (FY15\$, w/o Launch Vehicle).

#### *Summary*

The challenge from NASA and the Decadal Survey has been met with the Europa Orbiter Mission concept. The Europa Orbiter Mission is in compliance with NASA Headquarters direction and guidelines. It has been descoped relative to JEO, yet still retains exceptional science merit. The mission design is conservative with large margins, and meets the NASA cost target \$2.25B (FY15\$, w/o Launch Vehicle). The Europa Orbiter Mission was presented to the Outer Planets Assessment Group (OPAG) in October 2011, to extremely positive community feedback. An independent technical review of the Europa Orbiter Mission concept was conducted, chaired by Scott Hubbard. The key findings were:

- The overall approach to modularity and radiation shielding was universally lauded as a creative approach to reducing technical risk and cost;
- No engineering “showstoppers” were identified;
- The Orbiter concept satisfied the “existence proof” test as a mission that met Europa science requirements, could be conducted within the cost constraints provided and has substantial margins;

- Two technical risks were identified: ASRG and radiation mitigation for instrument detectors.

The review board’s report is included in Appendix B.4.4.

#### *NASA Headquarters Guidelines*

Key guidelines from NASA Headquarters included the following:

- **Science Objectives:** The primary science objective of the mission concept is Europa. The science content of the Europa Jupiter System Mission (EJSM) JEO concept presented to the Decadal Survey is expected to be descoped. The mission concepts are expected to represent the minimum science missions that are at or very near the acceptable science “floor” below which the mission concept is not worth pursuing at the cost estimate.
- **International Contributions:** The study shall limit international contributions to no more than half of the payload.
- **Launch Vehicle:** The study shall limit its launch vehicle options to those expected to be available and approved for nuclear payloads by 2020. The study shall delineate the launch vehicle cost, but these costs are not to be included in the cost target.
- **Power System:** The study shall limit the power systems under consideration to solar arrays, ASRGs, batteries, or any combination thereof. The number of ASRG units available is not specified, but should be minimized. The study should assume an ASRG cost of \$50M/unit.
- **Science Definition Team:** The study shall utilize a small, well-focused SDT to provide guidance on the scientific objectives, measurements, and priorities for the mission concept. The SDT shall be composed of US scientists only and shall be kept to a reasonable

size. A European Space Agency (ESA) observer might be attending some meetings, but is not expected to contribute.

- Presentations of the mission to the science community, including but not limited to OPAG and other advisory groups as requested by HQ.

## B.1 Science of the Orbiter Mission

### B.1.1 Orbiter Science

Europa is a potentially habitable world that is likely active today. As outlined in this section, there are many well-defined and focused science questions to be addressed by exploring Europa. Both the 2003 Planetary Decadal Survey, *New Horizons in the Solar System*, and the 2011 Planetary Decadal Survey, *Vision and Voyages*, emphasize the importance of Europa exploration (Space Studies Board 2003, 2011). Both Decadal Surveys discuss Europa's relevance to understanding issues of habitability in the solar system, stressing this as the inherent motivation for Europa exploration.

*“The first step in understanding the potential of the outer solar system as an abode for life is a Europa mission with the goal of confirming the presence of an interior ocean, characterizing the satellite's ice shell, and understanding its geological history” (Space Studies Board 2011).*

Understanding Europa's habitability is intimately tied to understanding the three “ingredients” for life: water, chemistry, and energy (see §A). A spacecraft in orbit around Europa is an excellent platform to understand the global-scale structure of Europa, with emphasis on the ocean, the distribution of landforms, and evaluation of the link between the interior and the surface. To fulfill these types of investigations, a focus on geophysical and geologic measurements is required, necessitating global data sets obtained under relatively uniform conditions. These data are best suited to be collected from orbit around Europa. In this

section, we discuss the science background of an orbiter mission that concentrates on geophysical measurements to address Europa's habitability.

#### B.1.1.1 Ocean

As it orbits Jupiter, Europa is continually flexed, tugged, and deformed by the gravity of this gas giant. Consequently, the satellite's response of bending, breaking, flowing, heating, and churning enable the characteristics of its ocean and ice to be observed and inferred. Europa also experiences the varying magnetic field of Jupiter, which generates induction currents in the satellite's interior and reveals the conductivity structure through its response. These external influences, in addition to Europa's internal thermal and chemical properties, create the possibility that Europa's interior is volcanically active. Geophysics both dictates and elucidates the characteristics of Europa's ocean, as well as its ice shell and deeper interior.

The surface of Europa suggests recently active processes operating in the ice shell. Jupiter raises gravitational tides on Europa, which 1) contribute to thermal energy in the ice shell and rocky interior (Ojakangas and Stevenson 1989, Sotin et al. 2009), 2) produce near-surface stresses responsible for some surface features (Greeley et al. 2004), and 3) might drive currents in the ocean. Although relatively little is known about the internal structure, most models include an outer ice shell underlain by liquid water, a silicate mantle, and iron-rich core (Anderson et al. 1998, Schubert et al. 2009). Possible means to constrain these models include measurements of the gravitational and magnetic fields, topographic shape, and rotational state of Europa, each of which includes steady-state and time-dependent components. Additionally, the surface heat flux and local thermal anomalies might yield constraints on the satellite's internal heat production and activity. Taken together, results from measuring a range of geophysical parameters would be fundamental to characterizing

the ocean and the overlying ice shell and would provide constraints on deep interior structure and processes.

#### B.1.1.1.1 Gravity

Observations of the gravitational field of a planetary body provide information about the interior mass distribution. For a spherically symmetric body, all points on the surface would have the same gravitational acceleration; in those regions with more than average mass, however, gravity would be greater. Lateral variations in gravitational field strength, therefore, indicate lateral variations in internal density structure.

Within Europa, principal sources of static gravity anomalies could be those due to 1) ice shell thickness variations, 2) topography on the ocean floor, or 3) internal density variations within the silicate mantle. If the ice shell is isostatically compensated, it would only yield very small anomalies. Gravity anomalies that are not spatially coherent with ice surface topography are presumed to arise from greater depths. Radio Doppler tracking over repeat orbits at 100- km altitude could resolve seamount ridges or other topographic features hundreds of kilometers wide on the ocean floor; note, however, that unique determination of the nature of these features would require additional knowledge acquired via other geophysical measurements (e.g., high-order induced magnetic field measurements).

One of the most diagnostic gravitational features is the amplitude and phase of the time-dependent signal due to tidal deformation (Moore and Schubert 2000). The forcing from Jupiter's gravitational field is well known, and Europa's tidal response would be much larger if a fluid layer decouples the ice from the interior, permitting the unambiguous detection of an ocean and characterization of the ocean and the bulk properties of the overlying ice shell. With an ocean that decouples the surface ice from the rocky interior, the amplitude of the semi-diurnal tide on Europa is roughly 30 m,

which is in clear contrast to the  $\sim 1$  m tide in the absence of an ocean (Moore and Schubert 2000). Because the distance to Jupiter is 430 times the mean radius of Europa, only the lowest degree tides are expected to be detectable. Figure B.1.1-1 illustrates the degree-two tidal potential variations on Europa during a single orbital cycle. The tidal amplitude is directly proportional to this potential.

#### B.1.1.1.2 Topography

Characterizing Europa's topography is important for several reasons. At long wavelengths (hemispheric-scale), topography is mainly a response to tides and possibly shell-thickness variations driven by tidal heating

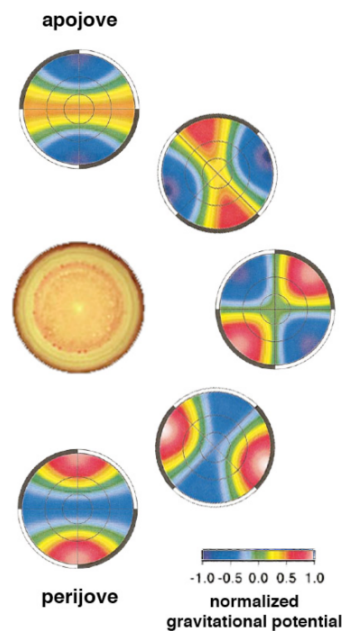


**Figure B.1.1-1.** Europa experiences a time-varying gravitational potential field as it moves in its eccentric orbit about Jupiter (eccentricity = 0.0094), with a 3.551-day (1 eurosol) period. Europa's tidal amplitude varies proportionally to the gravitational potential, so the satellite flexes measurably as it orbits. This adaptation of a figure from Moore and Schubert (2000), looks down on the north pole of Jupiter as Europa orbits counterclockwise with its prime meridian pointed approximately toward Jupiter. Measuring the varying gravity field and tidal amplitude simultaneously allows the interior rigidity structure of the satellite to be derived, revealing the properties of its ocean and ice shell.

(Ojakangas and Stevenson 1989, Nimmo and Manga 2009) and is, thus, diagnostic of internal tidal processes. At intermediate wavelengths (hundreds of kilometers), the topographic amplitudes and correlation with gravity are diagnostic of the density and thickness of the ice shell. The view of Mars provided by the MOLA laser altimeter (Zuber et al. 1992) revolutionized geophysical study of that body; if similar measurements were achieved, then the same advancement of our understanding of Europa would be expected. The limited topographic information currently available shows Europa to be very smooth on a global scale, but topographically diverse on regional to local scales (Schenk 2009). At the shortest wavelengths (kilometer-scale), small geologic features would tend to have topographic signatures diagnostic of formational processes.

#### *B.1.1.1.3 Rotation*

Tidal dissipation within Europa probably drives its rotation into equilibrium, with implications for both the direction and rate of rotation. The mean rotation period should almost exactly match the mean orbital period, so that the sub-Jupiter point would librate in longitude, with an amplitude equal to twice the orbital eccentricity. If the body behaves rigidly, the amplitude of this forced libration is expected to be ~100 m (Comstock and Bills 2003); however, if the ice shell is mechanically decoupled from the silicate interior, the libration could be three times larger. Similar forced librations in latitude are due to the finite obliquity and are diagnostic of internal structure in the same way. The rate of rotation would also change in response to tidal modulation of the shape of the body and corresponding changes in the moments of inertia (Yoder et al. 1981).

The spin pole is expected to occupy a Cassini state (Peale 1976), similar to that of Earth's Moon. The gravitational torque exerted by Jupiter on Europa would cause Europa's spin pole to precess about the orbit pole, while the

orbit pole in turn precesses about Jupiter's spin pole, with all three axes remaining coplanar. The obliquity required for Europa to achieve this state is ~0.1 degree, but depends upon the moments of inertia and is, thus, diagnostic of internal density structure (Bills 2005, Bills et al. 2009).

Obtaining a wide variety of different geophysical observations, all relevant to the internal structure of Europa, reduces the ambiguity inherent in interpretations of measurements.

#### *B.1.1.1.4 Magnetic Field*

Magnetic fields interact with conducting matter at length scales ranging from atomic to galactic. Magnetic fields are produced when currents flow in response to electric potential differences between interacting conducting fluids or solids. Many planets generate their own stable internal magnetic fields in convecting cores or inner shells through dynamos powered by internal heat or gravitational settling of the interior. Europa, however, does not generate its own magnetic field, suggesting that its core has either frozen or is still fluid but not convecting.

Europa is known to respond to the rotating magnetic field of Jupiter through electromagnetic induction (Khurana et al. 1998, 2009). In this process, eddy currents are generated on the surface of a conductor to shield its interior from changing external electric and magnetic fields. The eddy currents generate their own magnetic field—called the induction field—external to the conductor. This secondary field is readily measured by a magnetometer located outside the conductor.

The induction technique exploits the fact that the primary alternating magnetic field at Europa is provided by Jupiter, because its rotation and magnetic dipole axes are not aligned. It is now widely believed that the induction signal seen in Galileo magnetometer data (Khurana et al. 1998) arises within a subsurface ocean in Europa. The measured signal was shown to remain in phase with the primary field of Jovi-

an origin (Kivelson et al. 2000), thus unambiguously proving that the perturbation signal is a response to Jupiter's field.

Although clearly indicative of a European ocean, modeling of the measured induction signal suffers from non-uniqueness in the derived parameters because of the limited data. From a short series of measurements, such as those obtained by the Galileo spacecraft, the induction field components cannot be separated uniquely, forcing assumptions that the inducing signal is composed of a single frequency corresponding to the synodic rotation period of Jupiter. Unfortunately, single frequency data cannot be inverted to determine independently both the ocean thickness and the conductivity. Nevertheless, the single frequency analysis of Zimmer et al. (2000) reveals that the ocean must have a conductivity of at least 0.06 S/m. Work by Schilling et al. (2004) suggests the ratio of induction field to primary field is 0.97, from which Hand and Chyba (2007) infer that the ice shell is <15 km thick and the ocean water conductivity >6 S/m (see also Hand et al. 2009).

The large uncertainty in the conductivity estimates of the ocean water results from the poor signal-to-noise (S/N) ratio of the induction signature obtainable from relatively short segments of Galileo flyby data. Observations from a Europa orbiter could improve the S/N ratio of the induction field by several orders of magnitude.

To determine the ocean thickness and conductivity, magnetic sounding of the ocean at multiple frequencies is required. The depth to which an electromagnetic wave penetrates is inversely proportional to the square root of its frequency. Thus, longer period waves sound deeper and could provide information on the ocean's thickness, the mantle, and the metallic core. Electromagnetic sounding at multiple frequencies is routinely used to study Earth's mantle and core from surface magnetic data (Dyal and Parkin 1973, Parkinson 1983). Recently, Tyler et al. (2003) and Constable and

Constable (2004) demonstrated that data from orbit could be used for electromagnetic induction sounding at multiple frequencies. In the case of Europa, the two dominant frequencies are those of Jupiter's synodic rotation period (~11 hr) and Europa's orbital period (~85 hr). Observing the induction response at these two frequencies would likely allow determination of both the ocean thickness and the conductivity.

Some remaining key questions to be addressed regarding Europa's ocean, bulk ice shell properties, and deeper interior include:

- Does Europa undoubtedly have a subsurface ocean?
- What are the salinity and thickness of Europa's ocean?
- What is the internal structure of Europa's outermost H<sub>2</sub>O-rich layers?
- Does Europa have a non-zero obliquity and, if so, what controls it?
- Does Europa possess an Io-like mantle?
- Does Europa exhibit kilometer-scale variations in ice shell thickness across the globe?

#### B.1.1.2 Geology

By understanding Europa's varied and complex geology, the moon's past and present processes are deciphered, along with implications for habitability. An understanding of Europa's geology provides clues about geological processes on other icy satellites with similar surface features, such as Miranda, Triton, and Enceladus.

The relative youth of Europa's surface is inherently linked to the ocean and the effects of gravitational tides, which trigger processes that include cracking of the ice shell, resurfacing, and possibly release of materials from the interior. Clues to these and other processes are provided by spectacular surface features, such as linear fractures and ridges, chaotic terrain, and impact craters.

### B.1.1.2.1 Linear Features

Europa's unusual surface is dominated by tectonic features in the form of linear ridges, bands, and fractures (Figure B.1.1-2). The class of linear features includes simple troughs and scarps (e.g., Figure B.1.1-2g), double ridges separated by a trough, and intertwining ridge-complexes. Whether these represent different processes or stages of the same process is unknown. Ridges are the most common feature type on Europa and appear to have formed throughout the satellite's visible history (Figures B.1.1-2j and l). These ridges range

from 0.1 to > 500 km long, are as wide as 2 km, and could be several hundred meters high. Cycloidal ridges are similar to double ridges, but form chains of linked arcs.

Most models of linear feature formation involve fracturing in response to processes within the ice shell (Greeley et al. 2004, Kattenhorn and Hurford 2009, Prockter and Patterson 2009). Some models suggest that liquid oceanic material or warm mobile subsurface ice squeezes through fractures to form the ridge; other models suggest that ridges form by fric-

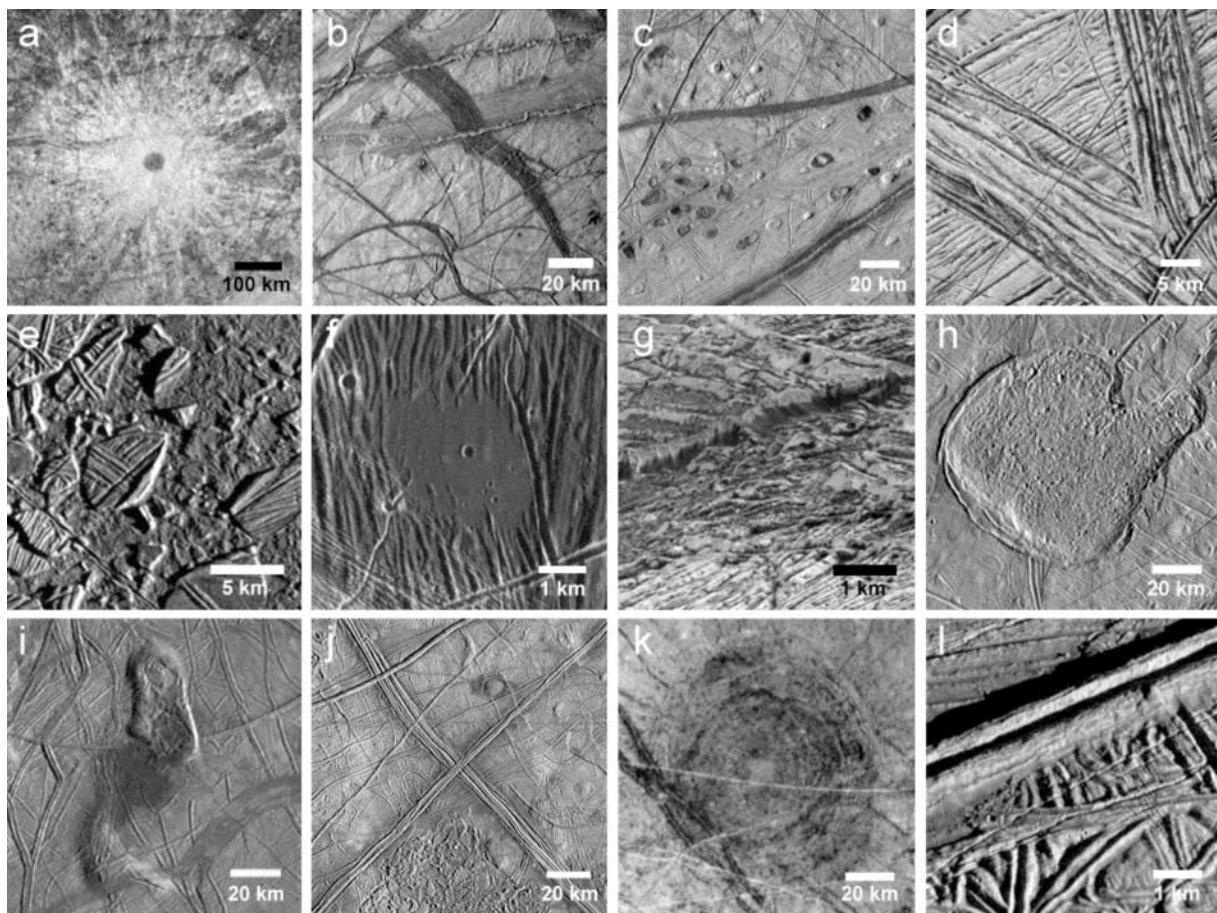


**Figure B.1.1-2.** Europa is a cryological wonderland, with a wide variety of surface features. Many appear to be unique to this icy moon. While much was learned from Galileo, it is still not understood how many of these features form or their implications for Europa's evolution. Shown here are: (a) the impact crater Pwyll, the youngest large crater on Europa; (b) pull-apart bands; (c) lenticulae; (d) pull-apart band at high resolution; (e) Conamara Chaos; (f) dark plains material in a topographic low, (g) a very-high resolution image of a cliff, showing evidence of mass wasting; (h) Murias Chaos, a cryovolcanic feature that has appears to have flowed a short distance across the surface; (i) the Castalia Macula region, wherein the northernmost dome contains chaos and is ~900 m high; (j) a regional view of two very large ridge complexes in the Conamara region; (k) a Tyre impact feature, showing multiple rings; and (l) one of Europa's ubiquitous ridges, at high resolution.

tional heating and, possibly, melting along the fracture shear zone. Thus, ridges might represent regions of material exchange between the surface, ice shell, and ocean, plausibly providing a means for surface oxidants to enter the ocean. Some features, such as cycloidal ridges, appear to initiate as a direct result of Europa's tidal cycle (Hoppa et al. 1999).

Bands reflect fracturing and lithospheric separation, much like sea-floor spreading on Earth; most bands display bilateral symmetry (e.g., Sullivan et al. 1998) (Figures B.1.1-2b and d). Their surfaces vary from relatively smooth to heavily fractured. The youngest bands tend to be dark, while older bands are bright, suggesting that they brighten with time. Geometric reconstruction of bands suggests that a spreading model is appropriate, indicating extension in these areas and possible contact with the ocean (Tufts et al. 2000, Prockter et al. 2002).

The accommodation of extensional features remains a significant outstanding question regarding Europa's geology. A small number of contractional folds were found on the surface (Prockter and Pappalardo 2000), and some sites of apparent convergence within bands have been suggested (Sarid et al. 2002); these features are, however, insufficient to accommodate the extension documented across Europa's surface. Although some models suggest that ridges and local folds could reflect such contraction, the current lack of global images, topographic information, and knowledge of subsurface structure precludes testing these ideas.

Fractures are narrow (from hundreds of meters to the ~10-m limit of image resolution) and some exceed 1000 km in length. Some fractures cut across nearly all surface features, indicating that the ice shell is subject to deformation on the most recent time-scales. The youngest ridges and fractures could be active today in response to tidal flexing. Young ridges might be places where there has been material exchange between the ocean and the

surface and would be prime targets as potential habitable niches.

#### B.1.1.2.2 Chaotic Terrain

Europa's surface has been disrupted to form regions of chaotic terrain, as subcircular features termed lenticulae, and irregular-shaped, generally larger chaos zones (Collins and Nimmo 2009). Lenticulae include pits, spots of dark material, and domes where the surface is upwarped and commonly broken (Figures B.1.1-2c and f). Pappalardo et al. (1998, 1999) argued that these features are typically ~10 km across and were possibly formed by upwelling of compositionally or thermally buoyant ice diapirs through the ice shell. In such a case, their size distribution would imply the thickness of the ice shell to be at least 10–20 km at the time of formation.

An alternative model suggests that there is no dominant size distribution and that lenticulae are small members of chaos (Greenberg et al. 1999), formed through either direct material exchange (through melting) or indirect exchange (through convection) between the ocean and surface (e.g., Carr et al. 1998). Thus, global mapping of the size distribution of these features could address their origin.

Chaos is generally characterized by fractured plates of ice that have been shifted into new positions within a background matrix (Figure B.1.1-2e). Much like a jigsaw puzzle, many plates could be fit back together, and some ice blocks appear to have disaggregated and “foundered” into the surrounding finer-textured matrix. Some chaos areas stand higher than the surrounding terrain (Figures B.1.1-2h and i). Models of chaos formation suggest whole or partial melting of the ice shell, perhaps enhanced by local pockets of brine (Head and Pappalardo 1999). Chaos and lenticulae commonly have associated dark, reddish zones thought to be material derived from the subsurface, possibly from the ocean. However, these and related models are poorly constrained because the total energy

partitioning within Europa is not known, nor are details of the composition of non-ice components. Subsurface sounding, surface imaging, and topographic mapping (e.g., Schenk and Pappalardo 2004) are required to understand the formation of chaotic terrain and its implications for habitability.

#### *B.1.1.2.3 Impact Features*

Only 24 impact craters with diameters of  $\geq 10$  km have been identified on Europa (Schenk et al. 2004), reflecting the youth of the surface. This is remarkable in comparison to Earth's Moon, which is only slightly larger but far more heavily cratered. The youngest European crater is thought to be the 24-km-diameter Pwyll, (Figure B.1.1-2a), which still retains its bright rays and likely formed less than 5 Myr ago (Zahnle et al. 1998, Bierhaus et al. 2009). Complete global imaging would provide a full crater inventory, allowing a more comprehensive determination of the age of Europa's surface and helping to identify the very youngest areas.

Crater morphology and topography provide insight into ice layer thickness at the time of the impact. Morphologies vary from bowl-shaped depressions with crisp rims, to shallow depressions with smaller depth-to-diameter ratios. Craters of up to 25–30 km in diameter have morphologies consistent with formation in a warm but solid ice shell, while the two largest impacts, Tyre (Figure B.1.1-2k) and Callanish, might have punched through brittle ice approximately 20 km thick into a liquid zone (Moore et al. 2001, Schenk et al. 2004, Schenk and Turtle 2009).

#### *B.1.1.2.4 Geological History*

Determining the geological histories of planetary surfaces requires identifying and mapping surface units and structures and placing them into a time-sequence.

In the absence of absolute ages derived from isotopic measurements of rocks, planetary surface ages are commonly assessed from

impact crater distributions, with more heavily cratered regions reflecting greater ages. The paucity of impact craters on Europa limits this technique. Thus, superposition (i.e., younger materials burying older materials) and cross-cutting relations are used to assess sequences of formation (Figueredo and Greeley 2004, Doggett et al. 2009). Unfortunately, only 10% of Europa has been imaged at a sufficient resolution to understand temporal relationships among surface features; for most of Europa, imaging data is both incomplete and disconnected from region to region, making the global surface history difficult to decipher.

Where images of sufficient resolution (better than 200 m/pixel) exist, it appears that the style of deformation evolved through time from ridge and band formation to chaotic terrain (Greeley et al. 2004), although there are areas of the surface where this sequence is less certain (e.g., Riley et al. 2000). The mechanism for the change in geological style is uncertain, but a plausible mechanism for the change is one in which Europa's ocean is slowly cooling and freezing out as the ice above it is thickening. Once the ice shell reaches a critical thickness, solid-state convection may be initiated, allowing diapiric material to be convected toward the surface. A thickening ice shell could be related to a waning intensity of geological activity.

Given the relative youth of Europa's surface, such a fundamental change in style might seem unlikely over the last ~1% of the satellite's history, and its activity over the rest of its ~4.5 billion year existence could only be speculated. Four possible scenarios have been proposed (see Figure B.1.1-3):

- (a) Europa resurfaces itself in a steady-state and relatively constant, but patchy style.
- (b) Europa is at a unique time in its history, having undergone a recent major resurfacing event.
- (c) Global resurfacing is episodic or sporadic.

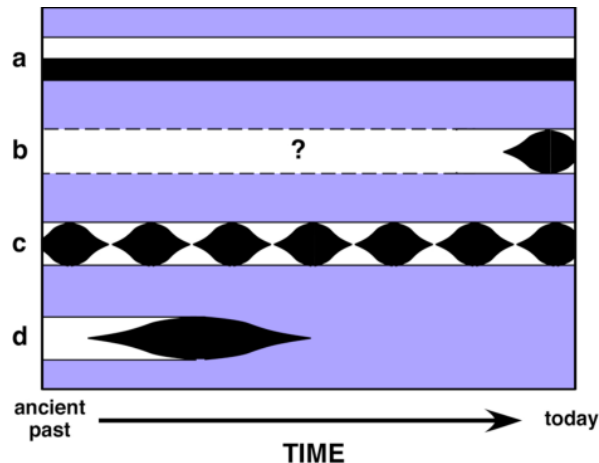


**Figure B.1.1-3.** Possible evolutionary scenarios for Europa's surface: (a) steady-state, relatively constant resurfacing; (b) the satellite is at a unique time in history, with a recent major resurfacing event; (c) global resurfacing is episodic or sporadic; and (d) the surface is older than cratering models suggest. After Pappalardo et al. (1999).

(d) Europa's surface is actually much older than current cratering models suggest (Zahnle et al. 2003).

From the standpoint of the dynamical evolution of the Galilean satellite system, there is good reason to believe that Europa's surface evolution could be cyclical. If so, Europa could experience cyclical variations in its orbital characteristics and tidal heating on time scales of perhaps 100 million years (Hussman and Spohn 2004).

Global imaging, coupled with topography, would enable these evolutionary models to be tested. Europa's surface features generally brighten and become less red through time, so albedo and color could serve as a proxy for age (Geissler et al. 1998, Moore et al. 2009). Quantitative topographic data (Schenk and Pappalardo 2004) could provide information on the origin of geologic features and might show trends with age. Profiles across ridges, bands, and various chaotic terrains would aid in constraining their modes of origin. Moreover, flexural signatures are expected to be indicative of local elastic lithosphere thickness at the time of their formation and might provide evidence of

topographic relaxation (e.g., Nimmo et al. 2003, Billings and Kattenhorn 2005).

Some remaining outstanding questions related to Europa's geology include:

- Do Europa's ridges, bands, chaos, and/or multi-ringed structures require the presence of near-surface liquid water to form?
- Where are Europa's youngest regions?

### B.1.2 Orbiter Traceability Matrix

As outlined in Section B.1.1, multiple well-defined and focused science questions can be addressed by exploring Europa to understand the potential for life in the outer solar system. Interrelated physical processes and habitability are key drivers for Europa exploration. Thus, the goal adopted for the Europa orbiter mission concept is:

*Explore Europa to investigate its habitability.*

This goal implies understanding processes, origin, and evolution. These include testing the numerous scientific questions described above. "Investigate its habitability" recognizes the significance of Europa's astrobiological potential. "Habitability" includes confirming the existence and determining the characteristics of water below Europa's icy surface, investigating the evolution of the surface and ocean, and evaluating the processes that have affected Europa through time. A Europa orbiter supplies critical information for investigating the extent of Europa's ocean and the cycling of energy from its interior to its surface.

The Europa orbiter mission objectives flow from the key science issues outlined above. These objectives represent a key subset of Europa science best accomplished by a Europa orbiter mission. These objectives are categorized in priority order as:

- O. Europa's Ocean: Characterize the extent of the ocean and its relation to the deeper interior.
- G. Europa's Geology: Understand the formation of surface features, including

sites of recent or current activity to understand regional and global evolution

The traceability matrix, compiled in Foldout B-1, maps the orbiter objectives (in priority order) to specific investigations (in priority order within each objective) to address the overarching mission goal. The specific measurements for each investigation are also listed in priority order. The orbiter objectives and investigations are discussed in detail in Sections B.1.2.1 and B.1.2.2.

#### B.1.2.1 Europa's Ocean

Galileo observations—in particular, the magnetometer data—provide evidence that the presence of a sub-surface ocean is very likely. Given the critical importance of such an ocean to Europa's astrobiological potential, it is important to first confirm its existence.

In the likely instance that an ocean exists, several geophysical measurements would place constraints on its depth, extent, and physical state (e.g., salinity). Several of these techniques would also help to characterize the deeper interior structure of Europa (the mantle and core). Doing so is important because of the coupling that takes place between the near-surface and deeper layers: for instance, an Io-like mantle implies a vigorously convecting ocean and a relatively thin ice shell. The investigations and corresponding measurement techniques are as follows.

##### *B.1.2.1.1 Investigation O.1: Determine the amplitude and phase of the gravitational tides.*

Perhaps the most direct way of confirming the presence of an ocean is to measure the time-variable gravity and topography due to the tides raised by Jupiter. In the absence of an ocean, Europa's ice shell would be coupled directly to the rocky core, and the time-dependent tidal surface displacement would be a few meters (Moore and Schubert 2000). If, on the other hand, Europa has a liquid water ocean beneath a relatively thin ice shell, the displacement amplitude would be 30 m over one orbit (Fig-

ure B.1.2-1). The surface displacement would also cause a measurable periodic gravity signal. Thus, measurement of the tidally driven time-variable topography or gravity (described by the Love numbers  $h_2$  and  $k_2$ , respectively) would provide a simple and definitive test of the existence of a sub-ice ocean.

The Love number  $k_2$  is estimated from the time-variable gravitational field of Europa. Simulations show that measurements of the Doppler shift of the spacecraft radio signal could be used to estimate  $k_2$ , the mantle and ice shell libration amplitudes and phase lag angle, and the static gravitational field parameters, which are estimated along with the spacecraft trajectory information (Wu et al. 2001). Simulations adding altimetry measurements show that the tidal Love number  $h_2$  could also be estimated (Wahr et al. 2006).

Observations from many orbits are required to estimate the body gravity field, including the tidal response, because the spacecraft orbit has to be determined at the same time. Orbit determination is improved by crossover analysis using altimetry measurements. If the spacecraft measures different distances to the same spot on the surface during different orbits, then (neglecting tides) the change must be due to the changing spacecraft altitude. In this manner, the spacecraft position could be accurately determined as at Mars (Neumann et al. 2001). This approach could also take into account the fact that the surface undergoes periodic displacements, due to tides and librations.

In addition to testing the ocean hypothesis,  $h_2$  and  $k_2$  could be used to investigate the ice shell thickness. Figure B.1.2-1 shows how these quantities vary with ice shell thickness and rigidity. Based on simulations of plausible internal structures, measurement uncertainties of  $\pm 0.0005$  for  $k_2$  and  $\pm 0.01$  for  $h_2$  would permit the actual  $k_2$  and  $h_2$  of Europa to be inferred with sufficient accuracy such that the combination places bounds on the depth of the ocean and the thickness of the ice shell (Wu et al. 2001, Wahr et al. 2006).

Goal	Objective	Investigation	Measurement	Model Instrument	Mission Constraints/Requirements	Water	Chemistry	Energy
Explore Europa to investigate its habitability	O. Ocean	O.1 Determine the amplitude and phase of gravitational tides.	O.1a Measure degree two-time dependent gravity field, to recover $k_2$ amplitude at Europa's orbital frequency to 0.003 absolute accuracy, and the phase to 1 degree.	Radio Subsystem (RS)	(1) Low altitude (100 km; < 200 km should be sufficient), circular, near-polar (within 5° to 10° of the pole) orbit, for at least 30 days (baseline), 18 days (floor); (2) Range-rate measurements with an accuracy better than 0.1 mm/s at 60 sec integration time to determine spacecraft orbit to better than 1-meter (rms) in radial direction over several tidal cycles; (3) Several "unperturbed" days for the data arcs (preferably at least one rotation of Europa) for gravity. Limit spacecraft momentum dumping or thrusting to an interval of 3 to 4 days, if possible.	✓		
			O.1b Determine topographic differences from globally distributed repeat measurements to recover spacecraft altitude at crossover points to 1-meter vertical accuracy.	Laser Altimeter (LA)	(1) Low altitude (100 km; < 200 km should be sufficient), circular, near polar (within 5° to 10° of the pole) orbit, for at least 30 days (baseline and floor); (2) Near continuous global ranging to the surface with 10-cm accuracy (baseline); floor of 20-cm accuracy; (3) Range-rate measurements with accuracy better than 0.1 mm/s at 60-sec integration time.	✓		
			O.1c Determine the orbital position of Europa's center of mass, relative to Jupiter, during the lifetime of the mission to better than 10 meters.	Radio Subsystem (RS)	(1) Low altitude (100 km; < 200 km should be sufficient), circular, near-polar (within 5° to 10° of the pole) orbit, for at least 30 days (baseline), 18 days (floor); (2) Range-rate measurements with an accuracy better than 0.1 mm/s at 60 sec integration time to determine spacecraft orbit to better than 1-meter (rms) in radial direction throughout the lifetime of the orbiter; (3) Limit spacecraft momentum dumping or thrusting to 3 to 4 days, if possible.	✓		
		O.2 Determine Europa's magnetic induction response.	O.2a Measure three-axis magnetic field components at 8 vectors/s, and a sensitivity of 0.1 nT, near-continuously to determine the induction response at multiple frequencies (orbital as well as Jupiter rotation time scales) to an accuracy of 0.1 nT.	Magnetometer (MAG)	(1) Low altitude (100 km; < 200 km should be sufficient), circular, near-polar (within 5° to 10° of the pole) orbit, for at least 30 days (baseline), 18 days (floor).	✓	✓	
			O.2b Characterize the local plasma density, temperature and flow to constrain (in conjunction with modeling) the contribution from currents not related to the surface and ocean.	Langmuir Probe (LP)	(1) Low altitude (100 km; < 200 km should be sufficient), circular, near-polar (within 5° to 10° of the pole) orbit, for at least 30 days; (2) Operation in "sweep" mode to measure ion currents; (3) 4π coverage (multiple probes with differential measurements); (4) Cover approximately 12 hours of local time (Europa local time) by spanning noon to dusk (or dawn) on the dayside hemisphere, which would also capture midnight to dawn (or dusk) on the nightside hemisphere.	✓		
			O.2c Determine electric field vectors (near DC to 3 MHz), and measure electron and ion density, as well as electron temperature, for local conductivity and electrical currents determination	Langmuir Probe (LP)	(1) Low altitude (100 km; < 200 km should be sufficient), circular, near-polar (within 5° to 10° of the pole) orbit, for at least 30 days; (2) Operation in "sweep" mode to measure ion currents; (3) 4π coverage (multiple probes with differential measurements); (4) Cover approximately 12 hours of local time (Europa local time) by spanning noon to dusk (or dawn) on the dayside hemisphere, which would also capture midnight to dawn (or dusk) on the nightside hemisphere.	✓		
		O.3 Determine the amplitude and phase of topographic tides.	O.3a Determine topographic differences from globally distributed repeat measurements at varying orbital phases, with better than or equal to 1-meter vertical accuracy, to recover $h_2$ to 0.01 (at the orbital frequency).	Laser Altimeter (LA)	(1) Low altitude (100 km; < 200 km should be sufficient), circular, near polar (within 5° to 10° of the pole) orbit, for at least 30 days (baseline and floor); (2) Near continuous global ranging to the surface with 10-cm accuracy (baseline); floor of 20-cm accuracy; (3) Range-rate measurements with accuracy better than 0.1 mm/s at 60-sec integration time.	✓		
			O.3b Measure spacecraft velocity to constrain the position of the spacecraft to better than 1 meter (rms).	Radio Subsystem (RS)	(1) Low altitude (100 km; < 200 km should be sufficient), circular, near-polar (within 5° to 10° of the pole) orbit, for at least 30 days (baseline), 18 days (floor); (2) Range-rate measurements with an accuracy better than 0.1 mm/s at 60 sec integration time to determine spacecraft orbit to better than 1-meter (rms) in radial direction throughout the lifetime of the orbiter; (3) Limit spacecraft momentum dumping or thrusting to 3 to 4 days, if possible.	✓		

Floor  
 Baseline only

**Water:** Water in its liquid form as pertaining to habitability as an oxidizer and medium for the transport of chemical constituents.

**Energy:** Energy that supports and fosters a means for potential metabolism to be established and sustained.

**Chemistry:** The constituents that foster and sustain the processes and environment for metabolic activity.

		Objective	Investigation	Measurement	Model Instrument	Mission Constraints/Requirements	Water	Chemistry	Energy
Explore Europa to investigate its habitability	O. Ocean	Characterize the extent of the ocean and its relation to the deeper interior	O.4 Determine Europa's rotation state.	O.4a Determine the mean spin pole direction (obliquity) to better than or equal to 10 meters, through development of an altimetry corrected geodetic control network from imaging at better than or equal to 100-m/pixel.	Laser Altimeter (LA), Mapping Camera (MC)	(1) Low altitude (100 km; < 200 km should be sufficient), circular, near polar (within 5° to 10° of the pole) orbit, for at least 30 days (baseline and floor); (2) Near continuous global ranging to the surface with 10-cm accuracy (baseline); floor of 20-cm accuracy; (3) Range-rate measurements with an accuracy better than 0.1 mm/s at 60 sec integration time; (4) Near-uniform lighting conditions preferred. To the extent possible, imaging should be at solar incidence angles greater than 45°. Ideally the incidence angle would be 70°; (5) Baseline: ≥80% global mapping at better or equal 100 m/pixel; Floor: ≥80% global mapping at better or equal 200 m/pixel.	✓		
				O.4b Determine the forced nutation and the amplitude of the forced libration of the spin pole at the orbital period to better than or equal to 1 meter, through development of a geodetic control network to better than or equal to 10-meter spatial scale at multiple tidal phases.	Laser Altimeter (LA)	(1) Low altitude (100 km; < 200 km should be sufficient), circular, near polar (within 5° to 10° of the pole) orbit, for at least 30 days (baseline and floor); (2) Near continuous global ranging to the surface with 10-cm accuracy (baseline); floor of 20-cm accuracy; (3) Range-rate measurements with accuracy better than 0.1 mm/s at 60-sec integration time.	✓		
			O.5 Investigate the deeper interior.	O.5a Resolve the static gravity field to degree and order 20 (floor); 30 (baseline) or better.	Radio Subsystem (RS)	(1) Low altitude (100 km; < 200 km should be sufficient), circular, near-polar (within 5° to 10° of the pole) orbit, for at least 30 days (baseline), 18 days (floor); (2) Range-rate measurements with an accuracy better than 0.1 mm/s at 60 sec integration time to determine spacecraft orbit to better than 1-meter (rms) in radial direction; (3) Several "unperturbed" days for the data arcs (preferably at least one rotation of Europa) for gravity. Limit spacecraft momentum dumping or thrusting to an interval of 3 to 4 days, if possible.	✓		
				O.5b Make topographic measurements to resolve coherence with gravity to degree 20 (floor); 30 (baseline) or better, with better than or equal to 1-meter vertical accuracy.	Laser Altimeter (LA)	(1) Low altitude (100 km; < 200 km should be sufficient), circular, near polar (within 5° to 10° of the pole) orbit, for at least 30 days (baseline and floor); (2) Near continuous global ranging to the surface with 10-cm accuracy (baseline); floor of 20-cm accuracy; (3) Range-rate measurements with accuracy better than 0.1 mm/s at 60-sec integration time.	✓		
				O.5c Characterize the local plasma density, temperature and flow to constrain (in conjunction with modeling) the contribution from currents not related to the surface and ocean.	Langmuir Probe (LP)	(1) Low altitude (100 km; < 200 km should be sufficient), circular, near-polar (within 5° to 10° of the pole) orbit, for at least 30 days; (2) Operation in "sweep" mode to measure ion currents; (3) 4π coverage (multiple probes with differential measurements); (4) Cover approximately 12 hours of local time (Europa local time) by spanning noon to dusk (or dawn) on the dayside hemisphere, which would also capture midnight to dawn (or dusk) on the nightside hemisphere.	✓		✓
				O.5d Measure three-axis magnetic field components at 8 vectors/s with a sensitivity of 0.1 nT.	Magnetometer (MAG)	(1) Low altitude (100 km; < 200 km should be sufficient), circular, near polar (within 5° to 10° of the pole) orbit, for at least 30 days (baseline and floor).	✓	✓	✓
	G. Geology	Understand the formation of surface features, including sites of recent or current activity to understand regional and global evolution	G1. Determine the distribution, formation, and three-dimensional characteristics of magmatic, tectonic, and impact landforms.	G.1a Constrain regional and global stratigraphic relationships by determining surface morphological characteristics at ~100-m/pixel scale.	Mapping Camera (MC)	(1) Near-uniform lighting conditions preferred. To the extent possible, imaging should be at solar incidence angles greater than 45°. Ideally the incidence angle would be 70°; (2) Baseline: ≥80% global mapping at better or equal 100 m/pixel; Floor: ≥80% global mapping at better than or equal to 200 m/pixel.	✓		✓
				G.1b Determine topography at better than or equal to 300-m/pixel horizontal footprint resolution (elevation posting from 100-m/pixel image data) and better than or equal to 30-meter vertical resolution (presumably through stereo imaging coverage), over as much of the surface as feasible.	Mapping Camera (MC), Laser Altimeter (LA)	(1) Stereo imaging: either have sufficient along-track or cross track FOV so that adjacent tracts cover at least half of each other for stereo, or else image the surface twice, the second time off nadir; (2) Laser altimetry is preferably simultaneous with imaging; (3) Baseline: ≥80% global mapping at better or equal 100 m/pixel; Floor: ≥80% global mapping at better or equal 200 m/pixel.	✓		✓

Floor  
 Baseline only

**Water:** Water in its liquid form as pertaining to habitability as an oxidizer and medium for the transport of chemical constituents.  
**Energy:** Energy that supports and fosters a means for potential metabolism to be established and sustained.  
**Chemistry:** The constituents that foster and sustain the processes and environment for metabolic activity.

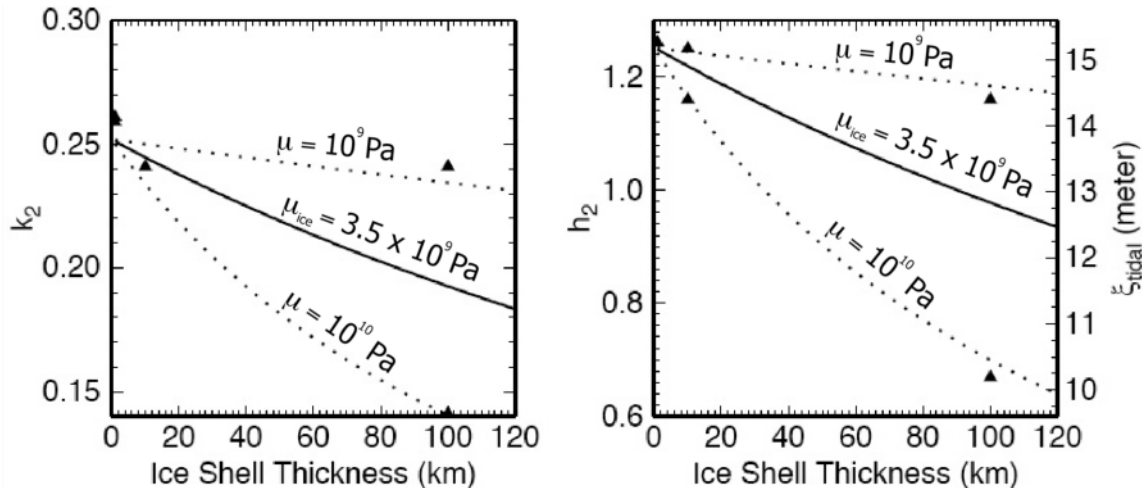


**Figure B.1.2-1.** Sensitivity of Love numbers  $k_2$  (left) and  $h_2$  (right) to ice shell thickness and rigidity, with the assumption of a subsurface ocean. For the same curves that depict  $h_2$ , the right-hand axis shows the amplitude  $\zeta_{\text{tidal}}$  (which is half of the total measurable tide) as a function of ice shell thickness. For a relatively thin ice shell above an ocean, the tidal amplitude is  $\zeta_{\text{tidal}} \sim 15$  m (total measurable tide  $\sim 30$  m), while in the absence of an ocean  $\zeta_{\text{tidal}} \sim 1$  m (Moore and Schubert 2000). Solid curves show the  $h_2$  and corresponding  $\zeta_{\text{tidal}}$  for an ice shell rigidity of  $\mu_{\text{ice}} = 3.5 \times 10^9$  Pa, while the dotted lines bound a plausible range for ice rigidity. A rocky core is assumed, with a radius 1449 km and rigidity  $\mu_{\text{rock}} = 10^{11}$  Pa, and the assumed ice + ocean thickness = 120 km. Triangles show the reported values from Moore and Schubert (2000), which did not include a core. Figure courtesy Amy Barr.

#### B.1.2.1.1.1 Measurement Techniques—Radio Subsystem and Laser Altimetry

To detect the radio Doppler shift caused by the spacecraft motion in the line-of-sight to Earth, two frequency bands have been considered. X-band (near 8 GHz) would be used for spacecraft commanding and Ka-band (near 32 GHz) would be used for transmission of spacecraft data to Earth. With the X-band uplink, Doppler measurement accuracy is limited by fluctuations in the solar plasma. An accuracy of 0.1 mm/s for 60 s integration times is typical, but varies as a function of solar elongation.

Doppler-only simulations (Wu et al. 2001) show that the Love number  $k_2$  could be determined with an accuracy of approximately 0.0005, or 0.25%, using either X/X or X/Ka Doppler tracking over 15 days when fit simultaneously with the Europa gravity field, librations, and spacecraft trajectory. In the same estimation the radial position of the spacecraft could be determined to an accuracy of 2 m, close to the desired orbit reconstruction accu-

racy, but about 10 times worse than currently being achieved with Mars orbiting spacecraft using much longer data arcs (Konopliv et al. 2006). The expected accuracy in determining  $k_2$  is easily sufficient to distinguish between an ocean-bearing and ocean-free Europa.

Range-rate measurements would also permit precise determination of the position of Europa's center of mass relative to Jupiter during the lifetime of the mission. This is necessary for determining the spacecraft orbit to better than 1-meter (rms) throughout the orbiter lifetime.

The Love number  $h_2$  is derived by measuring the time-variable topography of Europa; specifically, by measuring topography at cross-over points. This measurement can be readily achieved with a laser altimeter (Figure B.1.2-2); in fact, the technique has been demonstrated for the Earth (Luthcke et al. 2002 2005) and Mars (Rowlands et al. 1999, Neumann et al. 2001). After  $\sim 30$  days in orbit about Europa, the sub-spacecraft track would form a reasonably dense grid ( $\sim 25$ -km spacing

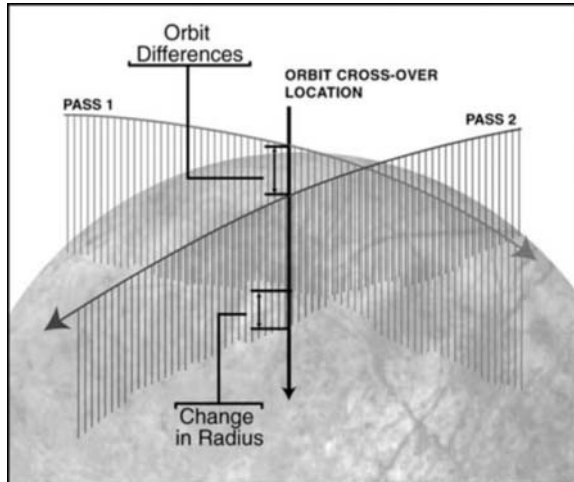


**Figure B.1.2-2.** Illustration of the cross-over technique. The actual change in the radius of Europa due to tidal and librational motions is determined by measuring altitude from the spacecraft to the surface and by accounting for the distance of the spacecraft from the center of mass by means of Doppler tracking (Wahr et al. 2006).

at the equator), comprised of a number  $N$  of ( $\sim 340$ ) great circle segments over the surface of Europa in 30 days. Each of the  $N$  arcs intersects each of the remaining  $N-1$  arcs at two roughly antipodal locations; at these cross-over locations, the static components of gravity and topography should agree. As illustrated in Figure B.1.2-2, differences in the measured values at cross-over points are equal to the sum of actual change in radius caused by tides and libration, combined with the difference in orbital altitude, along with any errors in range to the center of the body or orbital position. The errors are dominated by long wavelength effects and could be represented by 4 sine and cosine terms in each orbital component (radial, along track, and cross track). The tidal effects in gravity and topography have known spatial and temporal patterns and could each be represented globally by two parameters: an amplitude and a phase. The librations are effectively periodic rigid rotations with specified axes and periods and, again, an amplitude and a phase parameter.

#### B.1.2.1.2 Investigation O.2: Determine Europa's magnetic induction response.

The strongest current evidence for Europa's ocean is the induction signature apparently generated by Jupiter's time-dependent magnetic field interacting with a shallow conductive layer, presumably a salty ocean. However, because the Galileo spacecraft was effectively measuring the induction response at a single frequency during its flybys, only the product of the layer thickness and conductivity could be established. By contrast, an orbiter could determine both thickness and conductivity by measuring the induction response at multiple frequencies.

Europa is immersed in various low-frequency waves that could be used for magnetic sounding, some of which arise from Io's torus at the outer edge of Europa's orbit. Waves of different frequencies penetrate to different depths within the satellite and exhibit different induction responses. Dominant frequencies occur at the synodic rotation period of Jupiter (period  $\sim 11$  hr) and the orbital period of Europa (period = 3.55 days = 85.2 hr). Over a broad range of parameter space, the induction curves at two frequencies intersect (Khurana et al. 2002). In this range, the ocean thickness and conductivity (which constrains the salinity) could be determined uniquely. In order to sound the ocean at these two frequencies, continuous data are required from low altitude over times of at least one month.

##### B.1.2.1.2.1 Measurement Technique—Magnetometry & Plasma Measurements (Langmuir Probe)

Magnetometry requires near-continuous observations from Europa orbit for at least 8–10 eurosols (i.e., at least one month). A high cadence of 8 vectors/s is required to remove the effects of moon-plasma interactions from the data, and knowledge of spacecraft orientation is required to  $0.1^\circ$ . In addition, measurements of the electron and ion density, electron temperature, and electrical currents (Langmuir

Probe) generated in Europa's vicinity are necessary to facilitate removing their contributions from the measured magnetic field.

**B.1.2.1.3** *Investigation O.3: Determine the amplitude and phase of topographic tides.*

The time-dependent tidal deformation of Europa's surface, characterized by the Love number  $h_2$ , provides a strong test for the existence of an ocean. It could also be used in conjunction with the  $k_2$  Love number to constrain the ice shell thickness.

**B.1.2.1.3.1** *Measurement Technique—Laser Altimetry and Radio Subsystem*

The method to achieve the desired measurements is through quantifying topographic differences at the same surface point while Europa is located at different positions in its orbit. The details of how this can be accomplished are described in section B.1.2.1.1.2.

**B.1.2.1.4** *Investigation O.4: Determine Europa's rotation state.*

Europa's rotation pole position and its librations in both longitude and latitude would be determined as part of the orbit determination and crossover analysis necessary to determine  $h_2$  and  $k_2$  (Sections B.1.2.1.1). These quantities all depend on Europa's internal structure; thus, they provide additional, largely independent, constraints on the presence or absence of an ocean and the polar moment of inertia B. This latter quantity contains information about the distribution of mass within the satellite.

Librations in longitude and latitude are driven by the non-zero eccentricity and obliquity of the satellite, respectively. The amplitude of forced librations in longitude gives the combination  $(B-A)/C$  for the principal moments of inertia  $A < B < C$ , as has been done for Earth's Moon (Newhall and Williams 1997). The quantity  $(B-A)$  depends on the degree-two static gravity coefficients, which would be determined to high accuracy, and, thus, the polar moment of inertia C could be determined. If the ice shell is decoupled from the

interior by an ocean, the libration amplitude would be a factor of three larger than for a solid Europa (Comstock and Bills 2003). Similar constraints would be provided by determination of the latitudinal libration amplitude.

If there is an ocean, there might be two librational signals: one from the ice shell and another from the deeper interior. The shell's signal would be revealed in both gravity and topography data, whereas the deeper signal would appear only in the gravity.

Europa's obliquity—the angular separation between its spin and orbit poles—provides another constraint on its polar moment of inertia B. If its spin state is tidally damped, the obliquity is expected to be  $\sim 0.1^\circ$  (Bills 2005), with the exact amplitude depending on C (Ward 1975, Bills and Nimmo 2008).

**B.1.2.1.4.1** *Measurement Technique—Laser Altimetry and Mapping Camera*

The dynamical rotational state (spin rate and orientation, libration amplitudes) of Europa would be determined using Doppler tracking data and a laser altimetry crossover technique supplemented by a geodetic control network derived from imaging data at better than 100 m/pixel. Initially assuming both steady rotation and zero obliquity, the cross-over analysis described above (Section 1.2.1.1.2) would be used to adjust the spacecraft orbit estimate and to determine the dynamical rotation as well as the tidal flexing of Europa.

**B.1.2.1.5** *Investigation O.5: Investigate the deeper interior.*

Whether Europa's silicate interior is Io-like and dissipative or cold and inactive has important consequences for the likely thickness of the shell and for silicate-ocean interchange. Clues to the nature of the deeper interior could be obtained from gravity, topographic, and magnetic observations.

Static gravity observations, made using the same techniques as outlined above, could be used to investigate the topography at the silicate-ocean interface. Figure B.1.2-3 illustrates

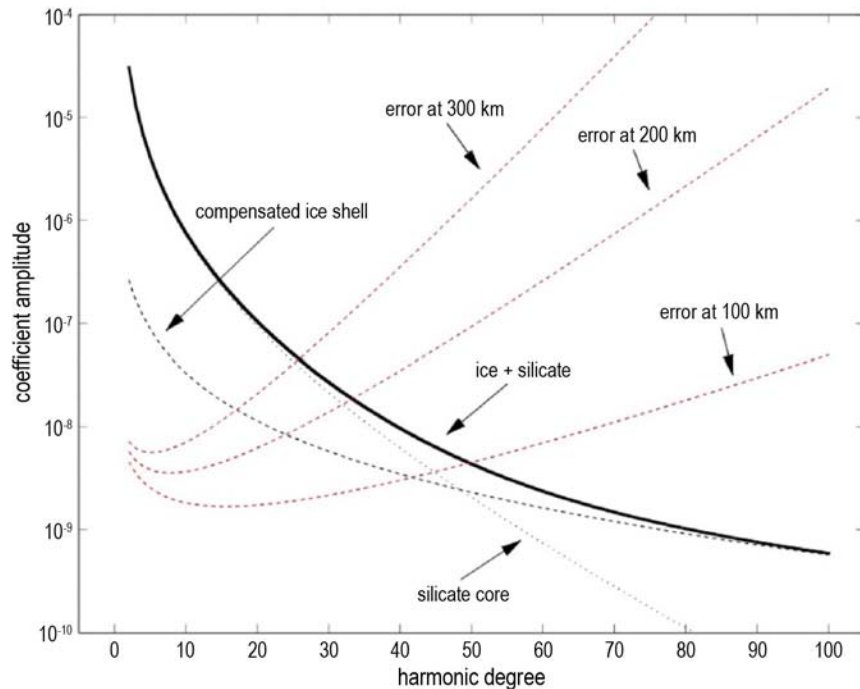


**Figure B.1.2-3.** Models of Europa's gravity spectrum, assuming an ice shell 10-km thick with isostatically compensated topography above an ocean and a silicate interior with a mean surface 100 km below the ice surface. The variance spectra of the ice topography and silicate gravity are assumed similar to those seen on terrestrial planets (Bills and Lemoine 1995). The signal has contributions from the silicate mantle and ice shell. The error spectra represent 30 days at fixed altitude and reflect variations in sensitivity with altitude. The error spectra at different orbital altitudes do not have the same shape because the longer wavelength anomalies are attenuated less at higher altitudes. During a few days at these altitudes, the improvement is linear with time; for longer times, repeat sampling leads to improvement proportional to square root of time.

the estimated gravitational spectrum for Europa, with separate contributions from an ice shell and a silicate interior, along with simulated error spectra for 30 days of tracking at each of three representative orbital altitudes (see Wu et al. 2001). To be conservative, only the X-band error estimate has been used. The recovered gravity errors are smaller at lower altitudes because the spacecraft is closer to the anomalies and, thus, experiences larger perturbations.

At long wavelengths, the gravity signal is dominated by the silicates. Because the water-silicate density contrast likely greatly exceeds density variations within the mantle, long-wavelength gravity anomalies would

provide evidence for seafloor topography and might point to the existence of seamounts or volcanic rises. Such long-wavelength gravity anomalies might also result in potentially measurable surface topographic variations (as with the sea surface on Earth).

At shorter wavelengths, the signal is dominated by shallower ice-shell contributions and the topography and gravity should be spatially coherent (Luttrell and Sandwell 2006). Isostatically supported topography in the ice shell produces a gravity anomaly that is larger for thicker shells. If the wavelength at which the transition from silicate-dominated to ice-dominated signals could be determined, this would provide a constraint on the thickness of the ice shell (assuming isostatic com-

pensation). Such a transition is potentially detectable at a 100-km orbit altitude.

#### B.1.2.1.5.1 *Measurement Technique—Radio Subsystem, Laser Altimetry, Magnetometry & Plasma Measurements (Langmuir Probe)*

Time-dependent gravity and static topography measurements might also provide constraints on Europa's deep interior: for instance, a fluid-like Love number ( $k_2 \sim 2.5$ ) would imply a low-rigidity mantle and core, as well as a subsurface ocean.

Magnetometer measurements of very low-frequency magnetic variations (periods of several weeks) would shed light on the magnetic properties of the deep interior, including

**Table B.1.2-1.** Hypothesis Tests to Address Selected Key Questions Regarding Europa's Ocean and Interior.

Example Hypothesis Questions	Example Hypothesis Tests
Does Europa undoubtedly have a subsurface ocean?	Measure the gravity field at Europa over the diurnal cycle.
What are the salinity and thickness of Europa's ocean?	Determine the magnetic induction signal over multiple frequencies to derive ocean salinity and thickness.
What is the internal structure of Europa's outermost H <sub>2</sub> O-rich layers?	Use measurements of the time-variable topography to derive the Love number $h_2$ , to relate the ice shell and ocean layer thicknesses.
Does Europa have a non-zero obliquity and, if so, what controls it?	Use gravitational and topographic measurements of the tides to infer obliquity, which, in turn, constrains moments of inertia, especially in combination with libration amplitude(s).
Does Europa possess an Io-like mantle?	Magnetic and/or gravitational inferences of the ice shell thickness constrain how much heat the silicate interior is producing; magnetometer inferences of ocean salinity constrain the rate of chemical exchange between silicates and water and the conductivity structure of the deep interior; time-variable gravity place bounds on the rigidity of the silicate interior.
Does Europa exhibit kilometer-scale variations in ice shell thickness across the globe?	Measure high degree and order gravity field and topography to determine coherence

the core. For instance, a partially molten, Io-like mantle is expected to have a higher conductivity than a cold, inactive interior. Such measurements need to be taken over a period of several months. Simultaneous plasma measurements are necessary to remove the effects of moon-plasma interactions from the data.

The key outstanding questions relating to Europa's ocean could be linked to and addressed by the investigations described above, as summarized in Table B.1.2-1.

### B.1.2.2 Europa's Geology

Europa's landforms are enigmatic; there exist a wide variety of hypotheses for explaining the formation of these landforms. The search for geologic activity is significant for understanding Europa's potential for habitability, especially with respect to the question of how material is transported between the surface and the subsurface, including the ocean.

#### B.1.2.2.1 *Investigation G.1: Determine the distribution, formation, and three-dimensional characteristics of magmatic, tectonic, and impact landforms.*

Geologically active sites are the most promising for astrobiology. Europa's continuous tidal activity leads to predictions that some landforms might be actively forming today and are

the most likely locations for near-surface liquid (see Section B.1.2.1). The most promising regions for current activity are 1) regions of chaos wherein thermally or compositionally buoyant diapirs rise to the surface or 2) cracks that have recently formed in response to tidal stresses. Low-albedo smooth-plains material associated with some chaotic terrains might be subsurface material (such as brines) that have been emplaced onto the surface (Collins and Nimmo 2009, Schmidt et al. 2011); these locations might therefore, represent sites of high scientific interest. Recently or currently active regions are expected to best illustrate the processes involved in the formation of some surface structures, showing pristine morphologies and distinct geologic relationships, and, perhaps, exhibiting associated plume activity such as that seen on Enceladus.

Determining the relative ages of Europa's surface features allows the evolution of the surface to be unraveled. Indication of relative age comes from the stratigraphy, derived from cross-cutting and embayment relationships, and the relative density of small primary impact craters. These relationships enable a time history to be assembled within regions that can be extrapolated globally across Europa. Without a global map, the relative ages of different regions cannot be determined because they cannot be linked; this is the current problem in

understanding Europa’s stratigraphy based on Galileo imaging.

**B.1.2.2.1.1 Measurement Technique—  
Mapping Camera**

Of first-order importance is characterization of surface features—their distribution, morphologies, and topography—at regional scales to understand the processes by which they formed. Galileo images demonstrate that regional-scale data (~100 m/pixel), is excellent for a geologic study of Europa; however, less than 10% of the surface was imaged at better than 250 m/pixel (Figure B.1.2-4). Near-global coverage (>80% of the surface) at 100 m/pixel would ensure characterization of landforms across the satellite.

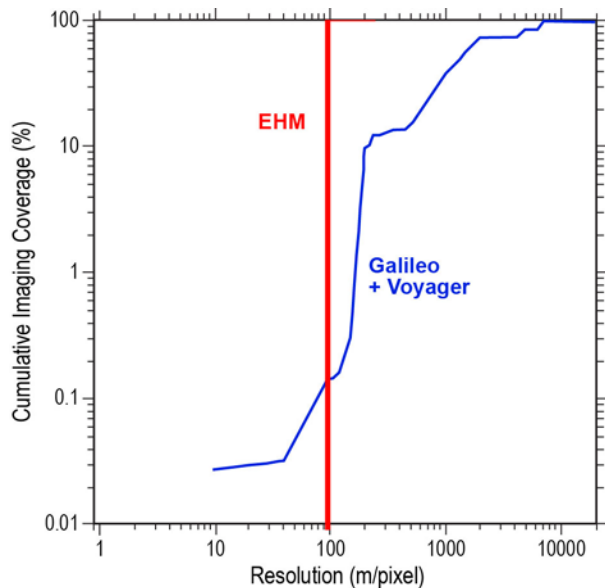


**Figure B.1.2-4.** Cumulative imaging coverage of Europa’s surface as a function of imaging resolution, illustrating the improvement of planned EHM imaging coverage relative to that from Voyager and Galileo combined.

Topographic mapping through stereo images (and correlated with laser altimetry data) at a regional scale can permit construction of digital elevation models with vertical resolution of ~30 m and horizontal resolution of 300 m, which would greatly aid morphologic characterization and geological interpretation. Stereo imaging could be achieved through horizontal overlap of adjacent Mapping Camera image tracks, resulting in approximately 30-m vertical-height accuracy with 100 m/pixel wide-angle camera images.

The key outstanding questions relating to Europa geology can be addressed by the Objective G investigations described above are summarized in Table B.1.2-2.

**B.1.3 Science Instrument Complement**

**B.1.3.1 Mission Goal Relation to Core Measurements and Instrumentation**

The overarching goal of an orbiter mission is to determine the habitability of Europa. As such, the recommended scientific measurements and scientific payload follow objectives (§B.1.1) of examining the presence of liquid water (the occurrence and extent of a subsurface ocean) and the regional and global geologic history (stratigraphic history, geologic processes, and exchange of material between the subsurface ocean and the surface). In this way, the payload links tightly with the three science themes that relate to Water, Chemistry, and Energy. In particular to Europa, the presence of a subsurface ocean, the overall structure and thickness of the ice shell and the exchange of material between the subsurface (ice shell and ocean) and the surface layer over time, followed by the physical evolution of the surface, leads to a complex story of Europa

**Table B.1.2-2.** Hypothesis Tests to Address Selected Key Questions Regarding Europa’s Geology.

Example Hypothesis Questions		Example Hypothesis Tests
G.1	Do Europa’s ridges, bands, chaos, and multi-ringed structures require the presence of near-surface liquid water to form?	Imaging to determine the style of surface deformation and the links to interior structure and water.
G.1	Where are the youngest regions on Europa and how old are they?	Stereo imaging to determine detailed stratigraphic relations on a global scale.

habitability. Unraveling this story requires an integrated package of instruments that work ideally and effectively in coordination. An orbiter mission offers unique abilities to observe the surface and unambiguously address the goal of understanding Europa's habitability.

The recommended science measurements and payload utilize the strengths of each archetypal instrument and technique to address key questions:

- What is the depth and salinity of the ocean, ice shell thickness and structure, and pathways by which ocean water may exchange with the surface?
- What are the geological signatures of surface-ocean exchange of materials and the surface history observed at scales of hundreds of meters?

#### B.1.3.2 Integration of Instrument Categories

Coordination and integration of observations and measurements acquired by different instruments is central to determining Europa's habitability. Spatially or temporally coordinated observations greatly enhance the scientific value of the mission. For example, obtaining clear insight into the internal structure of Europa requires various types of measurements working in concert. Probing the interior of Europa requires knowledge of the subsurface distribution of mass as manifested in variations of the gravity field. Combining this with time-dependent assessment of topographic due to tides and estimates of ocean salinity as derived from induced magnetization, a full picture of the ocean and ice shell is achieved. With this view in hand, global imaging provides a means to decipher the surface signature of interac-

tions between the icy crust and the watery interior. In this way the suite of instruments integrates to address the broader questions of habitability in a way that cannot be accomplished by each instrument alone.

#### B.1.3.3 Instrument Payload

The choice of instruments for the scientific payload is driven by the need for specific types of measurements that trace from the overarching goal of Europa's habitability, as detailed in the Europa orbiter traceability matrix (Fold-out B-1). These measurements focus on the geophysical characteristics of Europa's ocean and overlying ice shell along with the global-scale structure and stratigraphic history of exchange between the subsurface ocean and the observed surface. These fundamental measurements drive the recommendation of model instruments. These include active (such as topographic ranging) along with passive measurements (such as context imaging, magnetometry and gravity science). The notional payload (Table B.1.3-1) defined by the Science Definition Team (SDT) is the minimum required to achieve the required science objectives. Thus, it represents both the baseline and floor set of instruments. It was the SDT's judgment that more tolerable descopes would reflect a reduction in capability rather than the elimination of a specific instrument.

These model instruments work in concert to fully realize the value of data collected. For example, The Radio Subsystem (RS) would be used for gravity tracking of the spacecraft to determine gravity tides and the static field to probe the deep interior. Simultaneously, over a period of at least 5 Eurosols (18 days), the Laser Altimeter (LA) would determine surface

**Table B.1.3-1.** Scientific instruments of the model payload.

Model Instrument	Key Science Investigations and Measurements
Radio Subsystem (RS)	Gravitational tides and static gravity field to determine interior mass distribution to and characterize an interior ocean.
Laser Altimeter (LA)	Time-dependent topography as a function of Europa's position in its tidal cycle.
Magnetometer (MAG)	Magnetic measurements to derive ocean thickness and bulk salinity.
Langmuir Probe (LP)	Plasma correction for magnetic measurements
Mapping Camera (MC)	Formational mechanisms of surface features on regional to global scales

**Table B.1.3-2.** Potential enhanced instruments, not included in baseline model payload.

Model Instrument	Key Science Investigations and Measurements
Ion and Neutral Mass Spectrometer (INMS)	Atmospheric composition and chemistry through mass spectrometry.

elevations which, at crossover points, would be used to derive amplitude variations as a function of tidal cycle and the response to the ocean. Just as important as the LA and RS measurement, the Magnetometer (MAG) and Langmuir Probe (LP) would measure the time-variable induced magnetic field and plasma environment respectively so as to constrain the ocean salinity and hence the ice and water layer thicknesses. As the spacecraft makes successive orbits of Europa, the Mapping Camera (MC) would build up a global visual picture of Europa. Combining the image data with LA measurements, a three-dimensional view of geologic features, their stratigraphic relations and association with the deeper crustal processes can be achieved. The geophysical investigations achievable from an orbiter would fundamentally advance the state of knowledge and understanding of the habitability of Europa.

#### B.1.3.4 Europa Composition science from an Orbiter Mission

One additional instrument was considered by the SDT as potentially attractive to enhance the scientific return of a Europa Orbiter Mission by addressing composition science (Table B.1.3-2). However, this was not included in the baseline model payload because the Flyby Mission would be the more appropriate platform for the associated measurements. If an Orbiter Mission were chosen for Europa, then consideration of this valuable instrument might be made in considering the optimal payload for an Orbiter mission, to address a portion of the composition science.

The science of the Europa Flyby Mission (§C) includes investigation of the composition and chemistry of the surface and atmosphere. The potential inclusion of an Ion and Neutral Mass Spectrometer (INMS) on an Orbiter mission

would allow the first *in situ* assessment of the chemistry of material derived from the surface. Taken in concert with the ocean focused Orbiter measurements, inclusion of an INMS would provide insight into processes of interaction between the ocean, ice shell, and surface.

The sections that follow will provide details of the mission implementation approach and discuss the specific characteristic of each instrument.

## B.2 Orbiter Mission Concept

### B.2.1 Orbiter Study Scope and Driving Requirements

The purpose of the 2011 Europa Orbiter Mission study was to determine the existence of a feasible, cost effective, scientifically compelling mission concept. In order to be determined feasible, the mission had to have the following qualities:

- Accommodate the measurements and model payload elements delineated in the Science Traceability Matrix.
- Launch in the 2018-2024 timeframe w/ annual backup opportunities
- Use existing Atlas V 551 launch vehicle or smaller
- Utilize ASRGs. No limit on number, but strong desire to minimize <sup>238</sup>Pu usage
- Mission duration < 10 years, launch to EOM
- Use existing aerospace radiation hardened parts rated at 300 krad or less
- Optimize design for cost; looking for minimal cost while achieving baseline science
- Maintain robust technical margins to support cost commitment

The study team's strategy in investigating this concept was to develop a well-defined, well-documented architecture description early in the mission life cycle. From that architecture space, more compact design solutions were favored to reduce shielding and overall system mass. Hardware procurement, implementation, and integration were simplified by using a modular design. Mission operation costs were reduced by increasing system robustness and fault tolerance to allow for extended periods of minimally monitored operations during the long interplanetary cruise. Radiation dose at the part level was reduced to currently existing aerospace part tolerances. Specifically, the part total dose was reduced to levels demonstrated by geosynchronous and medium earth orbit satellites components.

Together, it was felt that each of these strategies contributes to an overall reduction in mission cost while maintaining a compelling, high reliability mission.

### **B.2.2 Orbiter Mission Concept Overview**

The orbiter mission concept centers on deploying a highly capable, radiation tolerant spacecraft into orbit around the Jovian moon Europa to collect a global data set mapping the moon's surface morphology, measuring its tidal cycle through gravity fluctuations, and measuring its ocean induction signature through investigation of Europa's interaction with the Jovian magnetosphere. These measurements are performed from a 100 km, 2-4pm local solar time near-polar orbit over the course of a 30-day science mission.

A representative Orbiter mission would launch from Cape Canaveral Air Force Station in November 2021 and spend 6.5 years travelling in solar orbit to Jupiter. During this time, the mission would perform gravity assist flybys of first Venus then two flybys of Earth before swinging out to Jupiter. All terrestrial body flybys would have altitudes greater than 500 km.

Jupiter orbit insertion occurs in April 2028 when the vehicle performs a nearly 2-hour main engine burn to impart a 900 m/s velocity change on the spacecraft. This maneuver places the spacecraft in an initial 200 day Jovian orbit. An additional burn at apoJove raises the periJove altitude and reduces the orbital period. The spacecraft then performs fifteen gravity assist flybys of Ganymede and Callisto over the course of eighteen months to reduce orbital energy and align the trajectory with Europa.

A 600 m/s Europa Orbit Insertion (EOI) burn places the spacecraft directly into a 100 km circular near-polar orbit. After a short check-out period, science observations begin. The spacecraft is oriented to point the high gain antenna (HGA) at Earth continuously during this time. A scan platform allows nadir pointing of the mapping camera and laser altimeter while maintaining HGA on earth-point. During the sunlit side of each orbit, the high resolution mapping camera collects 94 km wide swaths of imagery below the orbiter while the laser altimeter collects vertical topography data at 26 measurements per second throughout the orbit. Simultaneously, the magnetometer monitors changes in the local magnetic field as the spacecraft orbits Europa and Europa orbits Jupiter. Finally, maintaining continuous HGA-to-Earth pointing allows high precision radio science measurements of changes in Europa's gravitational field, a measurement expected to give significant insight into Europa's tidal amplitude and cycle.

The science measurement campaign would last a minimum of 30 days forming a statistically significant magnetic and gravitation data set for model correlation and allowing for at least eight opportunities to map any given location on Europa's surface. Extended mission objectives are possible and could be executed until critical spacecraft functionality is lost due to exposure to the intense radiation environment surrounding Europa. The spacecraft would be decommissioned by either commanding active

deorbit to the surface or by passive orbital decay due to third body gravitational perturbations.

### **B.2.3 Orbiter Mission Elements**

The Orbiter mission would be composed of a flight system and a ground system. The ground system is responsible for planning, testing, transmitting and monitoring all command sequences executed by the flight system, monitoring the flight system's health, and planning and executing any anomaly recovery activities required to maintain system health and mission robustness.

The flight system is a modularly designed spacecraft composed of three main modules: Avionics, Propulsion, and Power Source.

The Avionics Module hosts the bulk of the flight system's powered elements including the computers, power conditioning and distribution electronics, radios, and mass memory. These units are housed in a vault structure that provides significant radiation shielding. The upper section of the Avionics Module is called the Upper Equipment Section and hosts the batteries, reaction wheels, and star trackers, as well as the payload elements.

The Propulsion Module supports the fuel, oxidizer, and pressurant tanks, as well as the pressurant control assembly and the propellant isolation assembly. Four thruster clusters supported by tripod booms at the base of the Propulsion Module each contain four 1-lb reaction control system thrusters and one 20-lb thrust vector control thruster. The main engine would be mounted to a baseplate suspended from the bottom of the Propulsion Module main structure.

The Power Source Module would be composed of a ring and four vibration isolation systems each supporting an Advanced Stirling Radioisotope Generator (ASRG). The control boxes for the ASRGs would be mounted directly to the Power Source Module's main ring structure.

### **B.2.4 Orbiter Mission Architecture Overview**

Architecturally, the flight system's modular design offers several advantages and efficiencies. First, the Avionics Module is designed to place radiation sensitive components in a central vault structure. Centralization of sensitive components provides significant self-shielding benefits from passive spacecraft components that are then enhanced by the vault structure. Late in the integration flow, the Avionics Module is stacked onto the Propulsion Module. This configuration places the avionics vault structure in the core of the spacecraft; surrounded on all sides by the Propulsion Module's structure and propellant tanks. During the majority of the mission, these tanks would contain a significant amount of propellant. This configuration allows propellant to act as additional radiation shielding. In this way, dedicated, single purpose radiation shielding mass is minimized while still providing an internal vault radiation environment comparable to the doses received by geosynchronous satellites after a 20-year mission.

Additionally, the central vault avionics configuration allows waste heat from the avionics to be applied directly to keeping the propellant warm eliminating the need for dedicating significant electrical power to propellant tank heaters. There is sufficient heat emitted by the avionics to keep the propellant above 15 deg C for the life of the mission.

Finally, the modular design allows for a flexible procurement, integration, and testing strategy where each module is assembled and tested separately with schedule margin. Delays or problems on one module do not perturb the testing schedules of the other modules.

### **B.2.5 Science Instrumentation**

*A viable science instrument planning payload will provide the required science measurements, can be accommodated on the spacecraft, and can be implemented to operate successfully in the mission environment using only current technology.*

### B.2.5.1 Planning Payload

The Europa Orbiter planning payload, while notional, is used to quantify engineering aspects of the mission and spacecraft design and to define the operational scenarios required to obtain data necessary to meet the science objectives. For the purposes of this study, instruments were defined to demonstrate a viable approach to 1) meeting the measurement objectives, 2) performing in the radiation environment, and 3) meeting the planetary protection requirements. Therefore, instrument descriptions are provided here to show proof of concept. Heritage or similarities discussed refer to instrument techniques and basic design approaches. Physical and electrical modifications of previous heritage designs will be required for all instruments to function within the context of the mission requirements. These modifications are all judged feasible with current technology, and reasonable resource allocations are included in the mass and cost estimates. Instrument performance estimates assume only currently available detector technology. Development costs have been included in the cost estimates, but their projected performance improvements have not been assumed in these performance calculations. Alternative instrument concepts and tech-

niques that meet the mission objectives might be selected via NASA's AO process. Such options can be accommodated in the present concept. The instrument capabilities presented here are not meant to prejudge AO solicitation outcome.

The model planning payload selected for the Europa Orbiter study consists of a notional set of remote sensing instruments, *in situ* instruments, and a telecommunications system that provides Doppler and range data for accurate orbit reconstruction in support of geophysical objectives. Instrument representatives on the SDT (or identified by SDT members) were utilized extensively to understand the requirements for each instrument. Table B.2.5-1 presents the estimated resource requirements for each instrument and for the total planning payload.

Table B.2.5-2 summarizes the instruments and their capabilities. A more detailed mass estimate for each instrument is included in the Master Equipment List (MEL, Section B.4.3) as input for the NASA Instrument Cost Model (NICM).

#### B.2.5.1.1 Payload Accommodation

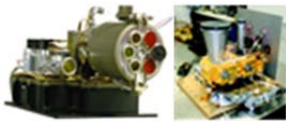
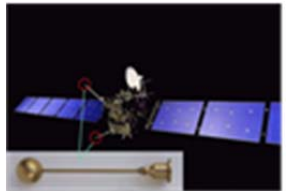
All remote-sensing instruments in the planning payload require view in the nadir direction

**Table B.2.5-1.** Europa Orbiter planning payload resource requirements and accommodations are met by the Europa Orbiter spacecraft.

Instrument	Mass		Total Mass (kg)	Operating Power (W)	Instantaneous Telemetry		Science Electronics		Pointing
	Un-shielded Mass (kg)	Shielding Mass (kg)			Telemetry Bandwidth (kbps)	Telemetry Interface	Chassis Board Ct.	Field of View	
Laser Altimeter (LA)	5.5	4.7	10.2	15	2	SpaceWire	2	0.029° dia. spot	Nadir
Mapping Camera (MC)	2.5	1.5	4.0	6	126	SpaceWire	1	50° × 0.049°	Nadir
Magnetometer (MAG)	3.3	0.0	3.3	4	4	SpaceWire	1	N/A	
Langmuir Probe (LP)	2.7	0.0	2.7	2.3	2	SpaceWire	2	Omni Electrons: 4π	
<b>Total All Instruments</b>	<b>14.0</b>	<b>6.2</b>	<b>20.2</b>	<b>27.3</b>			<b>6</b>		

Note: Resource requirements for the transponder used for radio science are carried as part of the spacecraft telecommunications system (see Section B.2.7.6.1).

**Table B.2.5-2.** Capable science instruments draw on previous flight designs.

Instrument	Characteristics	Similar Instruments	
Laser Altimeter	<b>Time-of-Flight Laser Rangefinder</b> Transmitter: 1.064 $\mu\text{m}$ laser Detector: Avalanche Photodiode Resolution: better than 1 m vertical Spatial: 50-m laser spot size, 26-Hz pulse rate	NEAR NLR MESSENGER MLA LRO LOLA	
Mapping Camera	<b>Pushbroom Imager</b> with fixed color filters and along-track stereo channel Detector: CMOS or CCD line arrays (5) Detector size: 1024 pixels wide Color bands: 560, 760, 950 nm Spatial resolution: 85 m from 100-km orbit FOV: 50° cross track; IFOV: 0.85 mrad	MRO MARCI Nozomi MIC MPL/MSL/MARDI MESSENGER MDIS New Horizons MVIC	
Magnetometer	<b>Dual 3-axis Fluxgate Magnetometer</b> Boom: 10 m Sensor location: 5 m and 10 m from S/C Dynamic range: 3000 nT Sensitivity: 0.1 nT Sampling resolution: 0.01 nT Maximum sampling rate: 32 Hz	MESSENGER MAG Galileo MAG	
Langmuir Probe	<b>Dual Langmuir Probe</b> Local plasma density, temperature, and flow Electric field vectors (near-DC to 3 MHz) Electron temperature Coverage: 4 $\pi$ steradian Booms: 1-m oriented 180° apart; at least one sensor always free of S/C wake	Rosetta LAP Cassini RPWS	

when in orbit around Europa, as shown in Figure B.2.5-1. Because the Orbiter spacecraft has adopted a fixed high-gain antenna (HGA) and the gravity science requires nearly continuous Doppler tracking with the HGA pointed to Earth, the remote sensing instruments are mounted on a two-axis gimballed platform to permit continuous nadir viewing and cross-track orientation of the camera field of view (FOV). The LP requires a wide, unimpeded FOV and is located to minimize obstructions to that field of view. Instrument mounting and accommodation requirements are summarized in Table B.2.5-2.

The Europa Orbiter Mission design calls for a near-circular, high-inclination orbit around Europa with local time such that the HGA end of the spacecraft is pointed close to the Sun while keeping the gimballed platform side oriented toward Europa. This geometry provides favorable viewing direction for thermal

radiators to dark space. The science payload is expected to contain instruments with detectors requiring cooling to as low as 170 K for proper operation while dissipating around 300 mW of heat. Cooling to this level can be accomplished via a passive radiator, mounted so that its view is directed away from the Sun and Europa at all times. Jupiter will move across the radiator FOV every 3.5 days, subtending a small portion of the radiator FOV but presenting only a minor transient perturbation to instrument thermal system performance.

The remote sensing instruments will require spacecraft pointing control to better than or equal to 2°, stability to 5 mrad/s, and reconstruction to 0.9 mrad. Pointing requirements are driven by the MC; however, these pointing requirements are less demanding than the HGA pointing requirements. To achieve the Europa geophysical science objectives connected with characterizing the topographic

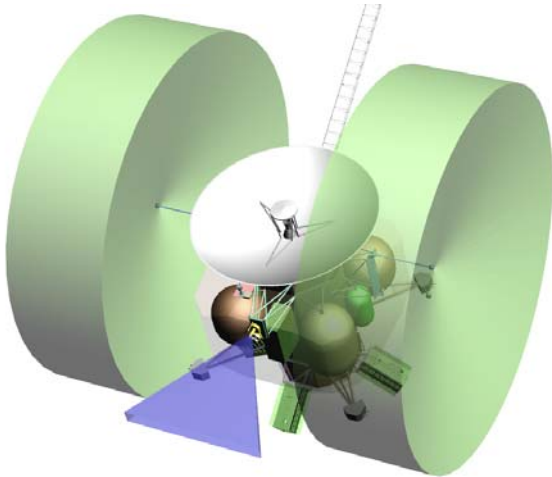


**Figure B.2.5-1.** The spacecraft configuration provides clear instrument FOVs.

tides, the Europa Orbiter orbit must be reconstructed to an accuracy of 1 m in the radial direction. To achieve this level of accuracy, Doppler radio tracking must be performed for several orbits (5–10 orbits), unperturbed by thruster firings.

The payload data rate is sufficiently low that an onboard science data storage volume of only about 2 Gb is needed to cover for the loss of a single DSN station pass. This volume is readily available on current generations of the RAD750 computer card without requiring an additional solid-state recorder. The notional planning payload block diagram (Figure B.2.5-2) assumes a data system architecture with SpaceWire interfaces baselined for all instruments.

The project will support the instrument AO process by providing NASA HQ with a Proposal Information Package (PIP) and any other advice as requested. To ensure compatibility between the selected instruments and the Orbiter flight system, the PIP is expected to specify a common instrument interface, provide an approved parts list, offer housing of instrument electronics in a centralized radiation-shielded vault, and require compatibility with Dry Heat Microbial Reduction (DHMR).

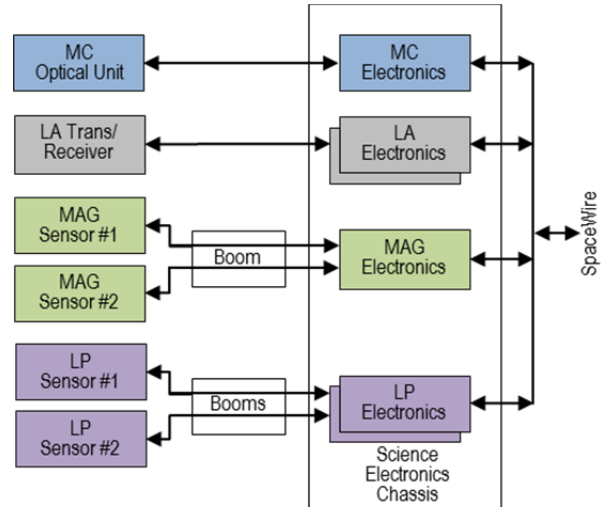


**Figure B.2.5-2.** Instrument electronics are colocated for efficient radiation shielding.

The instrument electronics are currently baselined to be accommodated with each instrument, shielded separately. However, the spacecraft concept accommodates an additional science chassis that can house all of the payload electronics, as well as perform some of the data reduction for IPR. This approach results in a conservative mass estimate, adding further margin in radiation shielding. Further trades need to be conducted on the benefits of a separate science chassis and its functionality. Since the presented model payload is notional, the payload trade will have to be re-evaluated once the flight instruments are selected.

#### B.2.5.1.2 Radiation and Planetary Protection

The severe radiation environment at Europa presents significant challenges for the science instruments, as does the need to meet the planetary protection requirements outlined in Section B.2.9.2. These challenges have been addressed by a notional payload architecture that efficiently implements radiation shielding and the use of radiation-hardened parts throughout the payload. A thorough study of both the radiation effects and the impact of planetary protection protocols on detectors was conducted for the 2008 JEO study by a Detector Working Group (DWG). The DWG developed a methodology for determining the required radiation

shielding for successful instrument operation in the severe transient radiation environment at Europa, assessed degradation of detectors due to total dose and displacement damage effects, and assessed the compatibility of candidate detectors with the planetary protection protocols. The DWG determined that there were no major issues associated with the types of detectors included in this planning payload.

#### *Payload Architecture*

The mission radiation design point is 1.56 Mrad behind 100 mils of aluminum shielding (Si) without a design margin, as shown in Section B.2.9.1. Note that energetic particle fluxes are high at Europa; therefore, sensors and supporting electronics require significant shielding. The most mass-efficient approach to providing radiation shielding is to centrally locate as much of the instrument electronics as possible, minimizing the electronics that must be co-located with the sensor portion of the instrument. The planning payload design presented here assumes instrument partitioning in this manner, as shown in Figure B.2.5-1, and includes a science electronics chassis implemented using the industry standard 6U Compact PCI form-factor. Space for six electronics boards is baselined, with radiation shielding sufficient to allow the use of components hardened to 300 krad without additional spot shielding. Internal partitioning of the science electronics is baselined to provide electrical isolation between instruments and to mitigate electromagnetic interference (EMI).

#### *Detector Radiation Noise Methodology*

The impact of radiation-induced transient noise on detectors was analyzed by estimating the number of high-energy electrons and protons penetrating the radiation shield and assessing their effect on the detector material. The flux of incident electrons reaching the detector for different radiation shielding thicknesses  $T$  can be estimated by applying the cutoff energy  $E$  determined from

$$E(\text{MeV}) = [T(\text{gm/cm}^2) + 0.106]/0.53$$

(Zombeck 1982) to the external integral electron flux. For 1 cm of Ta shielding, an estimated  $4.3 \times 10^5$  electrons/cm<sup>2</sup>·s and 50 protons/cm<sup>2</sup>·s would reach the detector while in orbit at Europa. The predominance of electrons in the Jovian environment is the determining factor for the detector radiation shielding analysis presented in subsequent sections.

#### *Detector Working Group*

The DWG concluded that the radiation and planetary protection challenges facing the planning payload are well understood. The question of detector survivability and science data quality is not considered to be a significant risk provided appropriate shielding is allocated to reduce cumulative TID, DDD, and instantaneous electron and proton flux at the detector. The full DWG assessment report can be found under separate cover (Boldt et al. 2008). Specific activities to support early education of potential instrument providers regarding the complexity of meeting radiation and planetary protection requirements were identified, and a series of instrument workshops was completed as part of the JEO study effort.

#### *Planetary Protection Protocols*

The approach to planetary protection compliance for the Europa Orbiter Mission is presented in full in Section B.2.9.2 and can be summarized as follows:

- Prelaunch sterilization to control the bioburden for areas not sterilized in flight
- In-flight sterilization via radiation prior to Europa Orbit Insertion (EOI)

The preferred method of sterilization is DHMR. Our plan is to sterilize the entire spacecraft upon completion of the flight assembly. Current planetary protection protocols include a time vs. temperature profile ranging from 125°C for 5 hours to 110°C for 50 hours.

Early in the instrument selection process, the project will generate and disseminate planetary protection guidelines to potential instrument providers, thereby allowing these providers to adequately address planetary protection issues. A mid-Phase B Payload Planetary Protection Review is baselined so that issues and mitigation strategies can be identified and addressed. Instrument-specific planetary protection concerns will be addressed in subsequent sections.

### B.2.5.2 Instrument Descriptions

#### B.2.5.2.1 Laser Altimeter

The notional Laser Altimeter (LA) is a diode-pumped Cr:Nd:YAG Q-switched laser transmitting at 1.064  $\mu\text{m}$  with an optical receiver and time-of-flight (TOF) sensing electronics. The notional design employs elements of the Lunar Orbiter Laser Altimeter (LOLA), the Mercury Laser Altimeter (MLA), and the NEAR Laser Rangefinder (NLR). The LA baselined for the Europa Orbiter is tailored to satisfy the following science requirements, as identified in Section B.1:

- Topographic differences to 1-m vertical accuracy at globally distributed crossover points at varying Europa orbital phases.
- Better than or equal to 10-cm ranging accuracy (to allow for  $\sim$ 1-m spacecraft orbit determination accuracy).

Simultaneous ranging with stereo imagery is desired.

#### Instrument Description

The notional LA includes a 0.5-mrad beam expander to produce a single 50-m laser spot from the 100-km orbit. A pulse rate of 26 Hz provides contiguous spots and 50-m along-track resolution, assuming a 1300-m/s ground track rate from the 100-km orbit. With each orbit crossing every previous orbit twice, in the course of 30 days more than 500,000 points are available for crossover analysis.

The notional laser transmitter is based upon the “Heritage Laser” developed by the multi-

year NASA Laser Risk Reduction Program (LRRP) (Seas et al. 2007) and shown in Figure B.2.5-3. The Heritage Laser design incorporates elements of the MLA and LOLA instruments and lessons learned from the LRRP effort itself. The baseline characteristics of the passively Q-switched, diode-pumped Cr:Nd:YAG laser allow up to 30-mJ, 6-ns pulses at rates of up to 150 Hz. For the Europa Orbiter, a nominal output of 2.7 mJ at 26 Hz is baselined, maintaining similarity to the LOLA laser transmitter. The Cr:Nd:YAG slab is assumed to be side pumped with a gallium arsenide (GaAs) diode array at 809 nm, similar to that used by NLR.

The notional optical receiver is based on a scaled version of the lightweight reflective telescope used by NLR and shown in Table B.2.5-2. The output of the telescope is passed through a spectral filter and presented to an avalanche photodiode (APD) operating in linear mode with gain of  $\sim$ 100 (per NLR) to minimize radiation effects.

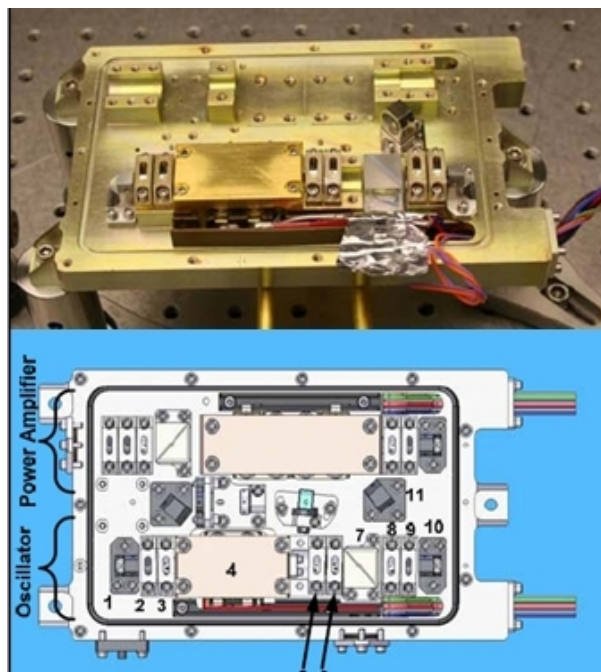


**Figure B.2.5-3.** The heritage laser developed by the NASA Laser Risk-Reduction Program is baselined for the notional Europa Orbiter Laser Altimeter.

Telescope sizing is obtained by comparison to the NLR link analysis, which assumes a 15-mJ transmitter, 8.9-cm-diameter receiver telescope with  $\sim 50\text{-cm}^2$  unobscured collecting area, and 15% surface albedo. While initially designed for a 50-km range, NLR achieved a 95% probability of detection for a single shot at 160-km range using 15 mJ of transmit power (vs. the initially specified 5 mJ) (Cole et al. 1997). Scaling for lower transmit power (2.7 mJ is assumed per the LOLA transmitter), a range of 200 km, and a surface albedo of 67% at Europa, an unobscured collecting area of  $\sim 100\text{ cm}^2$  is required for the notional LA. Assuming the same obscuration ratio as the NLR telescope, a 12.5-cm-diameter receiver telescope is baselined for Europa Orbiter. Comparisons to MLA and LOLA link analysis provided similar results.

The notional TOF system is a low-power design based on the range measurement system used by MLA, which employs a coarse counter (5 MHz) and precision timing offset measurements made using multiple radiation hardened TOF ASICs to achieve timing resolution equivalent to a 2-GHz counter (Cavanaugh et al. 2007). A commandable range gate masks system noise during laser firings and masks transient background radiation noise in the APD detector. The MLA range-measurement scheme can acquire and downlink multiple returns per shot, and this system can be

adapted to directly measure return pulse dilation to correct for topographically induced range-walk. The MLA range error budget (Cavanaugh et al. 2007) totals 1 m rms, with errors dominated by spacecraft orbit knowledge errors (0.75 m) and spacecraft pointing angle uncertainty (0.13 mrad). The expected performance of the Europa Orbiter spacecraft ( $\leq 1\text{-m}$  radial orbit knowledge with Ka-band and 0.25 mrad pointing uncertainty) allows the notional LA to meet the 1-m rms vertical-accuracy requirement.

A conceptual physical diagram of LA is shown in Figure B.2.5-4. The laser transmitter and optical receiver are located on the nadir-facing gimbaled platform of the spacecraft. The laser transmitter power supply, TOF system, system controller, and spacecraft interface electronics are packaged as two 6U cPCI boards and located in the science electronics chassis, which provides radiation shielding sufficient for components tolerant of 300 krad.

#### *Radiation Effects and Shielding*

The LA laser transmitter contains four main components requiring radiation shielding: GaAs laser diodes, a Cr:Nd:YAG laser slab, a LiNbO<sub>3</sub> Q-switch, and the fiber optic pickoff that provides the start pulse to the TOF system. The significant radiation issue for GaAs laser diodes is proton displacement damage. Testing with 5.5-MeV protons to a level of  $6 \times 10^9$  MeV/g, beyond the expected Europa

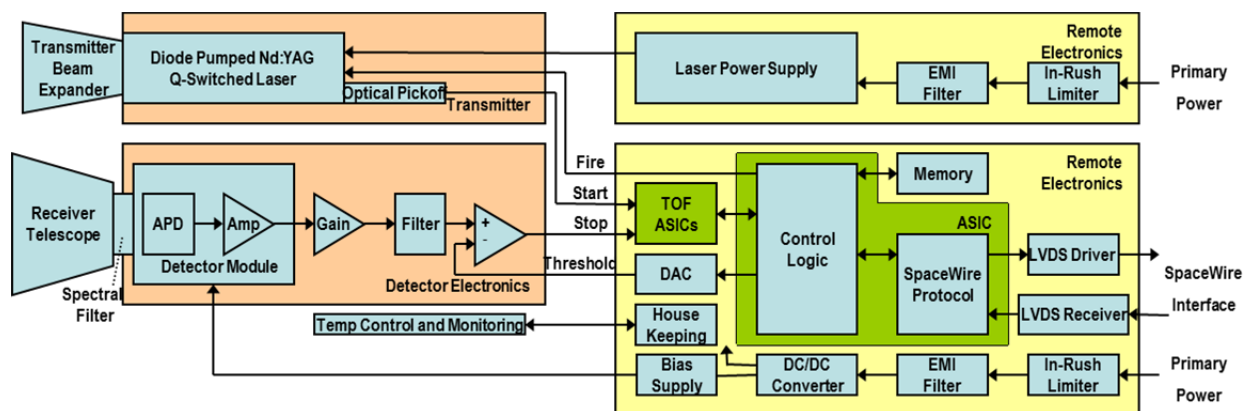


**Figure B.2.5-4.** The notional Laser Altimeter block diagram shows the remote electronics in a radiation-shielded enclosure.

Orbiter end-of-mission dose, showed only a minor shift in threshold current and no change in quantum efficiency (Johnston 2001). The significant radiation issue for Cr:Nd:YAG is total dose. Testing to 500 krad showed a negligible change in output power, with the level of Cr<sub>3</sub><sup>+</sup> doping a determining factor (Rose et al. 1995). Significant radiation issues for LiNbO<sub>3</sub> are total dose and displacement damage. Gamma irradiation of LiNbO<sub>3</sub> to levels far beyond that expected by Europa Orbiter showed a minimal change of insertion loss (Tsang and Radeka 1995). No corresponding data on displacement damage were reviewed for this study. The significant radiation issue for fiber optics is total dose. Testing observed only a 0.5 dB/m transmission loss in single-mode Ge-doped fiber optics after irradiation with 1×10<sup>6</sup> gray (Gy) (Henschel et al. 1995). While an exhaustive survey of radiation test results for the materials required for the LA laser transmitter is beyond the scope of this study, sufficient information has been reviewed and summarized in Boldt et al. (2008) to indicate the feasibility of operating a laser transmitter for the duration of the Europa Orbiter Mission. Based on this information, shielding of the LA laser transmitter to a level allowing use of materials tolerant of 400 krad is assumed.

The LA optical receiver uses an APD operating in linear mode to detect the return signal from the laser transmitter. Both silicon and germanium devices experience dark current increases due to total dose and proton damage and are susceptible to transient background radiation, which can create a signal larger than that produced by the optical return. The large detector area, typically 0.5 mm<sup>2</sup>, results in a high probability of a transient radiation event during the period of the range gate, assumed to be 67 μs for this analysis, and corresponding to an altitude range of 10 km. With 1 cm of Ta shielding, an estimated 4.3×10<sup>5</sup> electrons/cm<sup>2</sup>·s and 50 protons/cm<sup>2</sup>·s reach the APD through the shield while in orbit at Europa.

With the notional detector area and range gate, an estimated 14% of laser firings will be corrupted by background radiation. Increasing the shielding to 3 cm of Ta reduces the estimate to ~1.5% of laser firings. This level of shielding reduces the total dose seen by the detector to 10 krad and requires a detector tolerant of 20 krad, assuming 2× design margin. At this level of dose, dark current increases are modest (Becker et al. 2003) and can be accommodated by electronic adjustments and detector cooling.

#### *Resource Estimates*

The mass estimate for the LA is based on NLR (5 kg), adjusted for receiver telescope size, the mass of LRRP Heritage Laser, and radiation shielding of the laser transmitter, APD detector and detector electronics. The LRRP Heritage Laser, implemented with an aluminum chassis, is ~1.1 kg, with ~300-mil chassis walls (equivalent to 0.125 cm Ta) and interior dimensions of ~13×9×2 cm. To allow components tolerant to 300 krad, 0.3 cm of Ta shielding is required. The additional 0.175 cm of Ta shielding for the LA laser transmitter is estimated at 0.94 kg. Shielding of the APD (a small device) with 3 cm of Ta is estimated at 2.96 kg. Shielding of the detector electronics (assumed to require an 8×8×2 cm interior volume) with 0.2 cm Ta (1-Mrad components) is estimated at 0.6 kg. Shielding of the fiber optic is allocated 0.2 kg, resulting in an overall mass estimate for the notional LA of 10.2 kg.

The power estimate for the LA is 15 W based on NLR and assumptions for simplification of LOLA from a five-spot, five-receiver system to a single-spot, single-receiver system. The telemetry rate is estimated at 2 kbps, which allows output of ~75 bits per shot. A 100% duty cycle is assumed in Europa orbit.

#### *Planetary Protection*

Planetary protection concerns can be met for the LA through dry heat microbial reduction. Temperature effects on the nonimaging reflective optics are not considered to be an issue.

Temperature effects on the laser transmitter materials themselves are not likely to be problematic, although maintaining alignment of the transmitter components over a wide temperature range will require careful design and a thorough test program.

#### B.2.5.2.2 Radio Science

The Europa Orbiter spacecraft telecommunications system includes redundant small deep-space transponders (SDSTs) that receive commands from Earth tracking stations at X-band and transmit data to Earth at Ka-band, a configuration used on the Deep Space 1 and Kepler projects. The SDST also supports X/Ka Doppler range and delta-differential one-way range ( $\Delta$ DOR) for orbit determination. The SDST-based Doppler measurement accuracy is better than 0.1 mm/s for a 60-s integration time. Downlink tracking arcs free of spacecraft perturbations are required over several orbits, and range-rate measurements spanning several Europa tidal cycles are required. As discussed in Section B.1, simulations (Wu et al. 2001) show that these measurements can determine the radial component of the orbit about Europa to 1-m accuracy as well as allow determination of gravity and tidal parameters to useful accuracies. The approach to accommodation and radiation protection for the telecomm subsystem elements are addressed in Section B.2.7.6.1.

#### B.2.5.2.3 Mapping Camera

The MC consists of a wide-angle camera with basic functionality similar to that of the MRO Mars Color Imager (MARCI), the Nozomi Mars Imaging Camera (MIC), and MPL/MSL Mars Descent Imager (MARDI) instrument shown on Table B.2.5-2. The MC imager will be used in Europa orbit to provide global stereo landform mapping and to enable a search for evidence of surface/subsurface material exchange. The MC baselined for Europa Orbiter is tailored to satisfy the following science measurement requirements identified in Section B.1:

- Global stereo mapping:
  - Better than 100-m/pixel spatial resolution from a 100-km orbit.
  - 30-m vertical resolution at  $\leq 300$  m/pixel spatial scale.
  - Greater than 80% surface coverage.
- Color imaging:
  - Better than 100-m/pixel spatial resolution from a 100-km orbit.
  - Panchromatic plus three color bands.

#### Instrument Description

Collection of a global map with 100-m spatial resolution within 3 Eurosols ( $\sim 35\%$  of the nominal mission at Europa) requires an image swath width  $> 80$  km. This swath width results in a requirement for  $> 800$  pixels cross-track; a 1024-pixel-wide line array image sensor operating in pushbroom mode is baselined to allow for ample cross-track swath overlap for robust inter-swath tiepointing. The 1024-pixel-wide image sensor results in an instrument FOV of  $\sim 50^\circ$  full angle. A compact wide-angle refractive telescope similar to that of the MARDI instrument and a detector configuration similar to that of the New Horizons Multispectral Visible Imaging Camera (MVIC) are baselined. The notional MC has a 0.85-mrad IFOV to produce an 85-m pixel footprint at nadir and 120-m cross-track pixel footprint at the edge of the swath from the 100-km orbit. The radiation-shielded focal plane, similar to that of the New Horizons MVIC shown in Figure B.2.5-5, is envisioned to include 5 separate line arrays: four nadir viewing (one panchromatic and 3 color bands) plus one offset to view  $\sim 40^\circ$  forward or aft of nadir to enable near-simultaneous in-track stereo coverage. Vertical resolution provided by stereo imaging from the 100-km orbit is shown in Figure B.2.5-6. A digital elevation model (DEM) vertical resolution of 30-m is achieved at a stereo convergence angle of  $40^\circ$ . Fixed-color filters superimposed directly on the color line arrays satisfy the color imaging requirement with a minimum of complexity. The color and

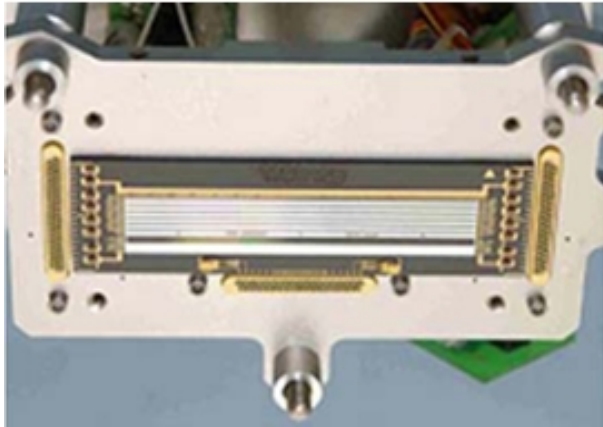


**Figure B.2.5-5.** The New Horizons MVIC detector, which contains multiple line arrays on a single substrate, is indicative of the notional MC detector.

stereo bands can be operated or not, as selected by ground command.

Preliminary MC performance analysis has been completed using the pixel characteristics (quantum efficiency, 13- $\mu\text{m}$  pixel size, 100-Ke<sup>-</sup> well depth) of the e2v CCD47-20BT image sensor used by the New Horizons Long-Range Reconnaissance Imager (LORRI) instrument as *an example* of the performance expected from the MC image sensor. The measured LORRI system readout noise of 20 electrons was assumed, although the LORRI pixel readout rate is considerably higher than that required for the MC (1.2 MHz vs. 13.3 kHz). Nominal selections for the color filters are

- Band #1: 540-580 nm.
- Band #2: 730-790 nm.
- Band #3: 900-1000 nm.

The wavelength-dependent quantum efficiency of the CCD47-20BT (*example only*) indicates that the line arrays for Band #1 and Band #2 will receive  $\sim 1/10$  of the illumination of the panchromatic channel, while the line array for Band #3 will receive  $\sim 1/20$  of the illumination. To balance the exposure times between the panchromatic and color channels, a neutral density filter, nominally ND-1, can be assumed in lieu of independent exposure control for each line array element.

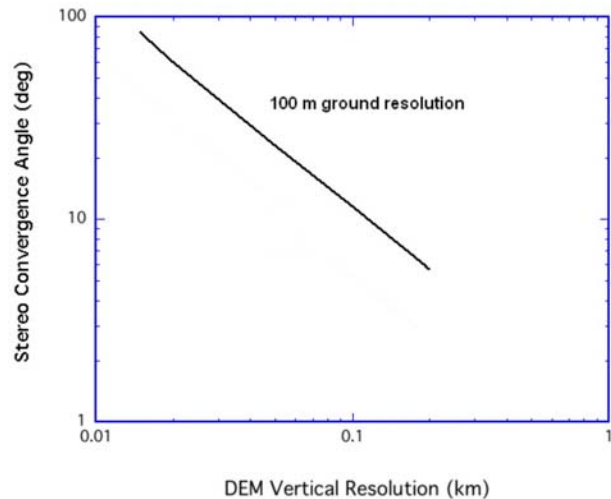


**Figure B.2.5-6.** The predicted MC vertical resolution obtained by stereo imagery based on parallax computations and use of modern auto-correlators will meet the science measurement requirements for surface topographic mapping.

Assuming a 15-mm focal length telescope with 3-mm aperture ( $f/5$ ), an ND-1 filter on the panchromatic channel, an optical efficiency of 75%, and a surface reflectance of 30%, a 50-Ke<sup>-</sup> signal level is reached in  $\sim 25$  ms, or  $\sim 40\%$  of the 63-ms integration time available while moving one pixel along track. Barring radiation-induced transient noise, this exposure results in a very high SNR ( $>200$ ) driven by photon noise rather than system noise and allows for longer exposure times over low-contrast surfaces. The performance of Band #1 and Band #2 will be similar to that of the panchromatic band with an ND-1 filter applied. The SNR of Band #3, which receives about half the light of the other bands, is  $\sim 160$ .

A conceptual physical block diagram of the MC is given in Figure B.2.5-7.

Consistent with the instrument architecture described in Section B.1.3.3, minimal electronics are packaged at the focal plane with the detector. The signal chain shown in the focal plane electronics contains elements required for a charge-coupled device (CCD) image sensor (clock drivers, correlated double sampler, A/D conversion) that either are unnecessary or are typically implemented within a

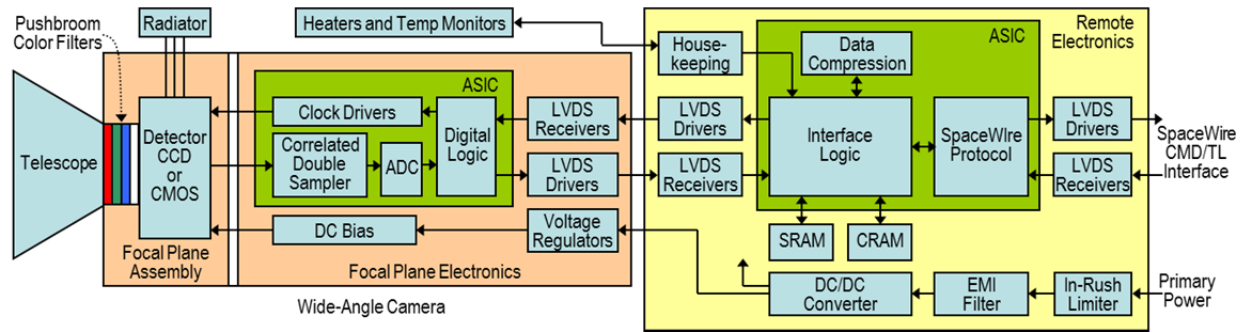


**Figure B.2.5-7.** Block diagram of the notional MC locates remote electronics in a radiation-shielded enclosure.

complementary metal-oxide semiconductor (CMOS) active pixel sensor (APS) device. A highly integrated CMOS APS device is an ideal solution, as it minimizes components at the focal plane that require radiation shielding. A passive thermal design is baselined for the MC with an cold space facing radiator used for detector cooling.

The MC is baselined with one electronics board (6U cPCI format) housed remotely in the science electronics chassis. The board provides DC/DC power conversion for both the camera and the electronics board itself. Data compression is assumed to be wavelet based, with commandable degrees of compression. Radiation-hardened static RAM (currently available as 16-Mb devices) is included for buffering incoming imager data, data compression intermediate products, and incoming and outgoing SpaceWire command and telemetry data.

#### *Radiation Effects and Shielding*

To protect the MC image sensor from total dose, displacement damage, and transient radiation noise, radiation shielding with 1 cm of Ta, comparable to that used by the Galileo Solid-State Imager (SSI), is baselined. Radiation dose analysis indicates a  $\sim 35$  krad total dose behind 1 cm of Ta shielding, which, assuming a required design margin of 2, allows use of detectors tolerant of 70 krad. While a CMOS APS device is favored for the notional Europa Orbiter MC due to its potential for high radiation tolerance, this dose level allows a choice of silicon device technologies, includ-

ing CMOS APS, P-channel CCD, and (arguably) N-channel CCD. Shielding mass of 1.5 kg is allocated for a 1-cm Ta,  $5 \times 3 \times 4$  cm enclosure similar to that shown in Figure B.2.5-8, which is designed to house a STAR1000-based CMOS APS and its interface electronics.

The impact of radiation background noise on the MC has been analyzed by estimating the number of high-energy electrons and protons penetrating the 1-cm Ta shield and assessing their effect on the silicon detector. An estimated  $4.3 \times 10^5$  electrons/cm<sup>2</sup>·s would reach the detector through 1 cm of Ta shielding. For a typical silicon image sensor, each incident electron can be expected to generate an average of 2000 signal electrons in the detector (per Boldt et al. 2008). Assuming 13- $\mu$ m pixels and a maximum exposure time of 63 ms for the notional MC, a “hit rate” of 4.6% of pixels per integration time is expected in orbit at



**Figure B.2.5-8.** Ample radiation shielding encloses a miniature focal plane assembly for a STAR1000 CMOS APS.

Europa. With the assumption that the signal-electrons generated by the incident particles are concentrated on a single pixel, the method of calculating the SNR adopted for the Galileo SSI camera can be employed (Klaassen et al. 1984). Based on empirical data, the radiation-induced noise is approximated as  $35 \times \text{SQRT}$  (mean radiation signal per pixel). For a 4.6% hit rate and 2000 electrons per hit, the radiation-induced noise would contribute 340 electrons to the MC SNR calculation if the radiation noise were uniformly distributed across the array. This would reduce the average MC SNR to  $\sim 120$  ( $\sim 70$  for the 950-nm band). However, since  $>90\%$  of the pixels would be unaffected by radiation-induced signal, they would retain their normal SNR value, while a small minority of pixels would have severely reduced SNR ( $\sim 25$ ), most of which can be repaired during ground processing. The number of incident protons reaching the detector through the 1 cm Ta shield can be estimated using the external integral 100-MeV flux level at Europa. The expected  $50 \text{ protons/cm}^2 \cdot \text{s}$ , when combined with  $13\text{-}\mu\text{m}$  pixels and a maximum 63-ms exposure time, result in a hit rate of 0.0053% of pixels per integration time in orbit at Europa. While the proton is expected to cause a strong signal ( $\sim 10,000$  signal-electrons) in a pixel or pixel group at the impact site, the low number of occurrences,  $\sim 5$  per 1-Mpixel image, and the strong signal are expected to have no significant impact on Europa science after ground-based post-processing to remove artifacts.

The MC electronics present no significant radiation concerns beyond those particular to the detector, and use of parts tolerant to 300 krad is assumed. Total dose and displacement damage effects on optical materials can be mitigated through use of a combination of fused silica and radiation-hardened glasses. In a system with a refractive telescope, the telescope itself acts as a “forward shield” for the image sensor, with the remainder of the image sensor surrounded by radiation shielding mate-

rial. In a system with a reflective telescope, a folded off-axis design can act as a “baffle” for radiation shielding of the detector, enabling shielding of the image sensor from all radiation input angles.

#### *Resource Estimates*

Mass estimates for the MC (4 kg including 1.5 kg of radiation shielding) are derived from similarity to the camera subassemblies of the Mercury Dual Imaging System (MDIS) on the Mercury Surface, Space Environment, Geochemistry, and Ranging (MESSENGER) mission and from estimated values for the harness mass and the 6U cPCI electronics boards. Power estimates for WAC (6 W) are based on measured values of the MESSENGER MDIS camera subassemblies and New Horizons LORRI electronics.

For an orbital ground track speed of 1300 m/s in the 100-km orbit, the MC line period is 63 ms. Assuming 12 bits/pixel from each of the line arrays, the MC uncompressed data rate is 189 kbps per channel, and the compressed data rate (with compression factor of 3 assumed) is 63 kbps/channel or 126 kbps for simultaneous stereo.

#### *Planetary Protection*

Planetary protection concerns for the MC will be met through dry heat microbial reduction. Temperature effects on optical materials, optical mounts and the image sensor will be a key aspect of the component and material selection process.

#### *B.2.5.2.4 Magnetometer*

The notional Magnetometer (MAG) measures the magnetic field at Europa with sufficient sensitivity to resolve the induction signal generated in Europa’s ocean as a response to Jupiter’s magnetic field. Operation in Europa orbit for an extended period allows sounding at multiple frequencies to determine ocean thickness and conductivity. Performing a role similar to that of the Galileo MAG, the notional MAG is adapted from more recent designs,

such as the MESSENGER MAG, and from ongoing developments in ASIC design for highly integrated MAG electronics. The MAG baselined for Europa Orbiter is tailored to satisfy the following science requirements identified in Section B.1:

- Characterize the magnetic environment at Europa to determine the induction response from the ocean:
  - Measurement rate: 8 vectors/s.
  - Measurement sensitivity: better than 0.1 nT.

#### *Instrument Description*

The notional MAG contains two sensors located on a 10-m boom: one at the tip and the other at the halfway point. The dual-MAG configuration can quantify and separate the spacecraft field from the background field, thereby improving the overall sensitivity of the system. The dual sensors also provide a level of redundancy once inflight calibrations are performed to assess the spacecraft-generated magnetic field. The expected magnetic field range over the full Europa Orbiter Mission is 0–500 nT. To achieve the required sensitivity, a magnetic cleanliness program is required to limit the magnetic field of the spacecraft at the 10-m point of the boom to <0.25 nT, with variation of <0.05 nT. An analysis of the effect of using ASRGs as the spacecraft power source confirmed that this level of cleanliness could be achieved with a 10-m boom.

The notional MAG sensors use three orthogonally mounted ring-core fluxgate sensors and are based on the MESSENGER MAG sensor assembly shown in Figure B.2.5-1. The sensors are excited by an AC signal that is also used to synchronously detect the signals from the fluxgate sensors. In an analog fluxgate MAG, the output from each synchronous detector is applied to an integrator, which supplies the feedback current used to null the field seen by the sensor. The output of the integrator is directly proportional to the component of the magnetic field along each orthogonal axis

and is sampled by a high-bit-count A/D converter. In a digital fluxgate MAG, the output from each synchronous detector is applied to an integrator whose output is digitized by an A/D converter. All subsequent filtering is done in the digital domain, and feedback to null the field seen by the sensor is generated by a D/A converter.

Digital fluxgate MAGs capable of meeting the Europa Orbiter science requirements have been demonstrated (O'Brien et al. 2007), and substantial progress has been made in developing a MAG front-end ASIC (MFA) that incorporates a complete MAG signal chain, including synchronous detection, high-bit-count  $\Sigma\Delta$  A/D converters, digital filtering,  $\Sigma\Delta$  D/A converters for sensor feedback, and basic output data formatting into a single device (Valavanoglou et al. 2007). Although current versions of MFA do not meet all of the Europa Orbiter radiation requirements, with further development this technology is likely to be available for Europa Orbiter; consequently, this approach is baselined for the notional MAG instrument.

A conceptual physical block diagram of the notional MAG is shown in Figure B.2.5-9. A single 6U cPCI electronics board located in the science electronics chassis contains ASICs for MAG signal processing, spacecraft interface electronics, and a low-voltage power supply.

Fluxgate sensors suffer from small drifts in their zero levels that require periodic calibration. During the Cruise Phase, calibrations can be achieved using the rotational nature of the interplanetary magnetic field. Once inside Jupiter's magnetosphere, slow spacecraft spins around two orthogonal axes will be required every 2 to 4 weeks.

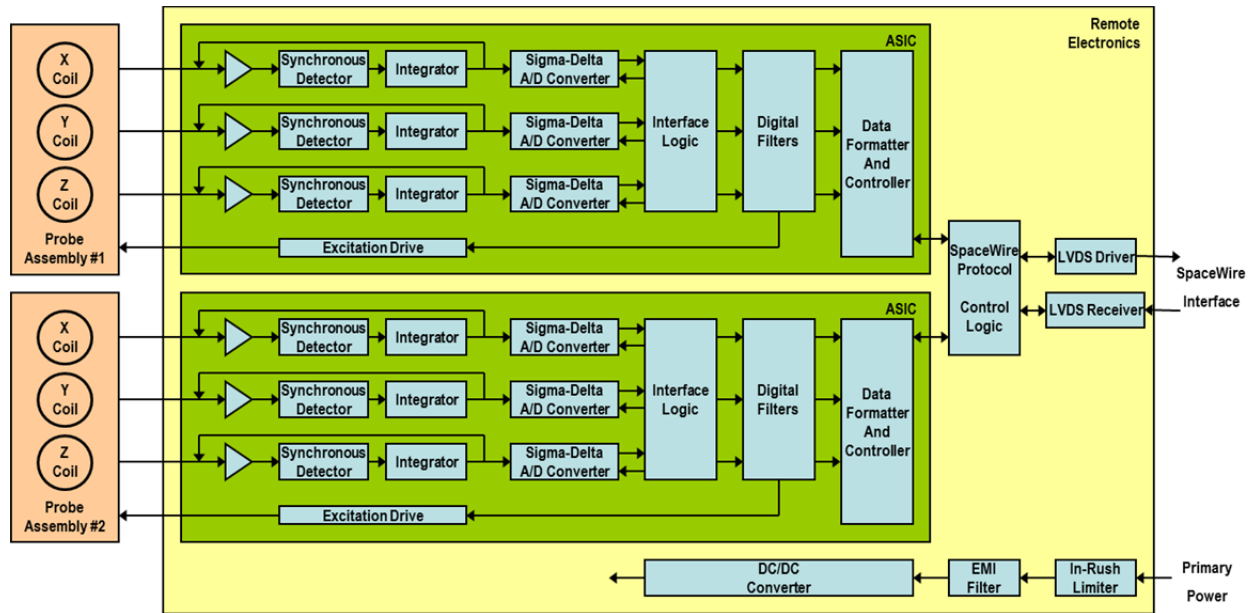


**Figure B.2.5-9.** Block diagram of the notional MAG locates remote electronics in a radiation-shielded enclosure.

#### *Radiation Effects and Shielding*

Fluxgate MAG sensors contain no active electrical parts and, with proper selection of materials, present no issues in meeting the Europa Orbiter radiation requirements. The notional MAG electronics are located in the science electronics chassis, which provides radiation shielding sufficient for components hardened to 300 krad. A fully radiation-hardened MAG signal-chain ASIC similar to the current MFA is assumed for the notional Europa Orbiter MAG.

#### *Resource Estimates*

The mass estimate for the notional MAG is based on the as-built mass of the MESSENGER MAG sensor (250 g), the as-built mass per unit length of the MESSENGER MAG harness (113 g/m), and the estimated mass of a 6U cPCI board. The total mass estimate for MAG is 3.3 kg, slightly more than half of which is required by harnessing. The estimated 19.2 kg mass of the supporting boom and deployment structure is not included in this instrument mass estimate, but rather included in the engineering structures mass rollup. See section B.4.3 for the Master Equipment List.

MAG power dissipation is estimated at 4 W based on scaling measured performance of the MESSENGER MAG for two probes. The MAG telemetry rate is estimated at 4 kbps based on scaling of the MESSENGER MAG telemetry rate for a higher sampling rate (32 Hz max) and two sensors.

#### *Planetary Protection*

Planetary protection concerns for MAG will be met through dry heat microbial reduction. With proper selection of materials for the MAG sensor, no issues are expected.

#### *B.2.5.2.5 Langmuir Probe*

The notional dual Langmuir probe (LP) instrument will characterize the local plasma and electric field in order to support the MAG determination of Europa's magnetic induction response. The LP will satisfy the following science measurement requirements identified in Section B.1:

- Electron number density ( $N_e$ ) up to  $10^6 \text{ cm}^{-3}$ , sampled at frequencies from 0 (dc) to 20 kHz.
- Ion density up to  $10^6 \text{ cm}^{-3}$  for sampling frequencies up to 1 Hz.

- Electron temperatures ( $T_e$ ) in the range of 0.01 to a few eV for sampling frequencies up to 1 Hz.
- Ion drift speed ( $v_{di}$ ) in the range 1-200 km/s, depending on density, for sampling frequencies up to 1 Hz.
- Electric field component (1 Hz to 3 MHz).
- The differential electric field between the two probes.
- The spacecraft potential over a range of  $\pm 100$  V for sampling frequencies up to 1 kHz.

Coverage will extend over a full  $4\pi$  steradian field. No DC field measurements are possible, as the probes would be too close to the spacecraft body and photo-electrons would interfere. A similar LP concept is described in Wahlund et al. (2005) for the Jupiter Icy Moons Orbiter study.

#### Instrument Description

The notional LP sensors are 5-cm-diameter spheres mounted on 1-m long booms (see Figure B.2.5-10). Since the plasma densities in Europa orbit are assumed to be large ( $>10 \text{ cm}^{-3}$ ), 1-m long low-mass sticks can be used for the booms. The notional LP is similar to the probes flown on Rosetta and as part of the Cassini RPWS instrument. The LP booms will be stowed for launch and deployed once in space. The LP preamps must be located within  $\leq 3$  m of the sensors. This constraint can be met

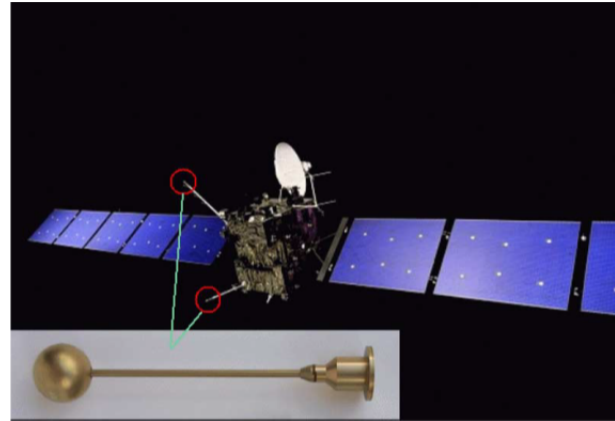


**Figure B.2.5-10.** The dual Langmuir Probe instrument on board Rosetta. A similar setup is considered for the Europa Orbiter.

while housing the preamps with the rest of the LP electronics in the shielded science electronics vault. Dedicated DC/DC conversion is needed, as well as a DPU. In addition, the LP needs bias control and an analyzer board. Two 6U cards will hold the expected electronics. A conceptual physical diagram of the notional LP is shown in Figure B.2.5-11.

#### Radiation Effects and Shielding

A rad-hardened MEMS wafer-level-packaging miniaturized preamplifier (as is currently under development at the Swedish Institute of Space Physics, Uppsala) is envisioned to be housed in the remote shielded vault with the rest of the electronics. All other parts required are rad-hard to  $\geq 100$  krad.

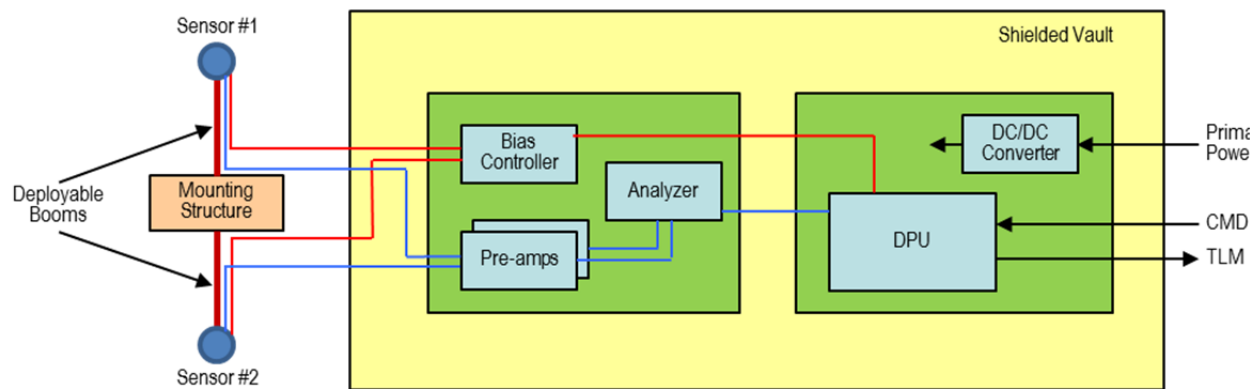


**Figure B.2.5-11.** Block diagram of the notional LP locates remote electronics in a radiation-shielded enclosure.

### Resource Estimates

The estimated LP mass is approximately 2.7 kg. Power consumption is 2.3 W. Telemetry can be varied between 100 bps and several kbps according to availability; 2 kbps is baselined. The preferred mounting would have the first probe located roughly in the ram direction and the second probe at least 90° away from ram. This objective is met by orienting the two booms 180° apart and mounting them on structures that place the deployed sensors far enough out from the spacecraft that a minimum of 15° clearance from the spacecraft structure wake (plasma relative velocity vector) is provided to at least one sensor for all orbital geometries (see Figure B.2.5-1). Spacecraft EMI/EMC cleanliness will be required at levels comparable to those of Rosetta and/or Cassini.

### Planetary Protection

The LP can tolerate the EHM dry-heat microbial reduction plan.

## B.2.6 Mission Design

*A robust mission design is presented, offering healthy margins to accomplish the high-value scientific observations that are best made from orbit around Europa.*

The trajectory design goal for this Europa Orbiter Mission study was to show the feasibility of a Europa Orbiter mission that meets the SDT on-orbit observation and measurement requirements as outlined in the traceability matrix (Foldout B-1). The focus for this study was to deliver sufficient mass into orbit around Europa to accommodate the necessary science instruments while minimizing flight time and total ionizing dose<sup>1</sup> (TID).

The Europa Orbiter Mission flight system assumes a launch on an Atlas V 551 from Cape Canaveral Air Force Station on a Venus-Earth-Earth gravity assist (VEEGA) interplan-

etary trajectory. After a cruise of 6.37 years, the spacecraft would fly by Ganymede just prior to performing Jupiter Orbit Insertion (JOI) via a large main engine maneuver. The spacecraft would then perform additional Ganymede, Callisto and Europa flybys over about 1.5 years to lower its energy with respect to Europa, at which point a relatively low- $\Delta V$  Europa Orbit Insertion (EOI) burn is performed. EOI places the spacecraft into a near-polar, near-circular 100-km altitude orbit, where science operations will be conducted for 30 days. The orbit maintenance  $\Delta V$  of 5 m/s per month is small enough that the spacecraft could remain in orbit for several more months while in good health. Planned end-of-mission is impact on Europa's surface, which occurs due to natural orbit decay over one to two months, or which could be commanded, if impact in a particular region is desired. Foldout B-2 depicts a summary of the mission design.

For discussion of data acquisition scenarios, data return strategies, and communication strategies, see Section B.2.7.7.3.

### B.2.6.1 Mission Overview and Phase Definitions

The general descriptions of each mission phase and the related activities are summarized in Table B.2.6-1.

#### B.2.6.2 Launch Vehicle and Launch Period

In the baseline mission design used for study purposes, Atlas V 551 would launch the spacecraft with a maximum  $C_3$  of 15.0 km<sup>2</sup>/s<sup>2</sup> during a 21-day launch period opening on November 15, 2021. The optimal launch date within the launch period is November 21, 2021 (Figure B.2.6-1). The date of Jupiter arrival is held fixed throughout the launch period, incurring only a negligible penalty while simplifying the design of the tour in the Jovian system. The launch vehicle and launch period parameters are shown on Foldout B-2. The launch vehicle performance is taken as that specified in the NASA Launch Services (NLS)-II Con-

<sup>1</sup> Total ionizing dose Si behind a 100-mil Al, spherical shell.

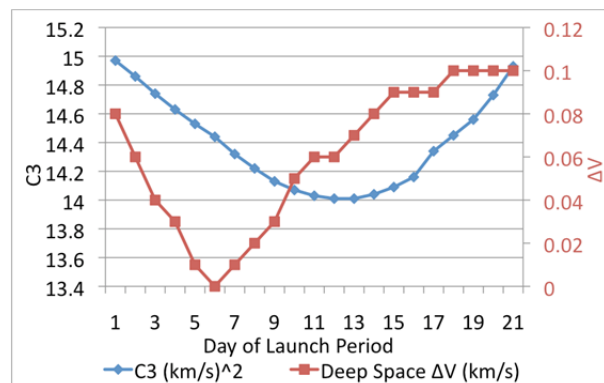
**Table B.2.6-1.** Mission phase definitions and descriptions.

Phase	Subphase	Activity	Start-End
Interplanetary	Launch and Early Operations	Begins with the launch countdown, launch, initial acquisition by the DSN, checkout and deployment of all major flight-system subsystems, and a moderate maneuver to clean up trajectory errors from launch vehicle injection.	Nov./Dec. 2021 + 30 days
	Cruise	Science instrument calibrations, Venus and Earth gravity-assist flyby operations, annual spacecraft health checks, trajectory correction maneuvers, and operations readiness tests (ORTs).	Jan. 2021–Oct. 2027
	Jupiter Approach and JOI	Training, and ORTs for all mission elements in preparation for JOI and Jovian tour. This phase includes the Ganymede (G0) flyby ~12 hours before JOI and ends with completion of JOI which puts the spacecraft into a ~200-day orbit.	Oct. 2027–Apr. 2028
Jovian tour	PJR	Perijove Raise Maneuver near apoapsis of the first Jovian orbit counteracts solar gravitational perturbations and targets Ganymede for the first flyby of the tour.	Apr-2028–Jul. 2029
	Pumpdown	Series of Ganymede, Callisto and Europa flybys to reduce orbital energy around Jupiter, reduce v-infinity at Europa, and obtain the phasing necessary to achieve the desired plane for the orbit around Europa.	
	Endgame and EOI	Two consecutive Europa flybys. The first puts the spacecraft first on a 4:3 resonant return to Europa, and the second in a 6:5 resonant return for EOI. A v-infinity leveraging maneuver is performed on each resonant transfer to reduce v-infinity at Europa for EOI. In the final approach to Europa, multi-body effects are exploited to reduce the EOI maneuver further still.	
Europa Orbit	Science observations and orbital operations. EOI puts the spacecraft in a ~100-km circular, polar orbit with ~2-hr period. The sun-beta angle is 70 deg. Groundtrack has a 3-eurosol repeat. Orbit maintenance maneuvers every 3.5 days or longer.	Jul. 2029 (1 month)	
Spacecraft Disposal	Europa impact due to natural orbital eccentricity growth from Jupiter perturbations: the period remains stable, causing the periapsis to drop.	Aug.-Sep. 2029	

tract, which includes, in particular, a performance degradation of 15.2 kg/yr for launches occurring after 2015. The spacecraft propellant tanks are oversized enough to permit them to be loaded up to the launch vehicle capability. The flight system is designed to launch on any given day in the launch period without reconfiguration or modification.

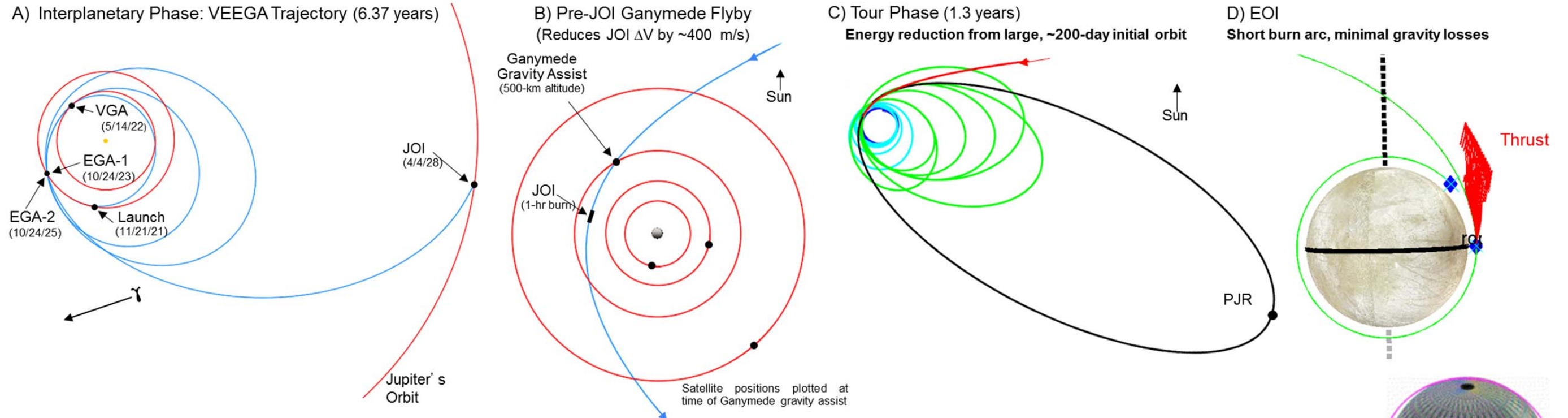
### B.2.6.3 Interplanetary Trajectory

The baseline trajectory used for the Europa Orbiter Mission is a VEEGA (Foldout B-2 and Table B.2.6-2). Cruise navigation would use Doppler and range observations from the Deep Space Network (DSN). The deep-space maneuver (DSM)  $\Delta V$  required on the optimal day of the launch period is zero, but is about 80 m/s at the start of the launch period and

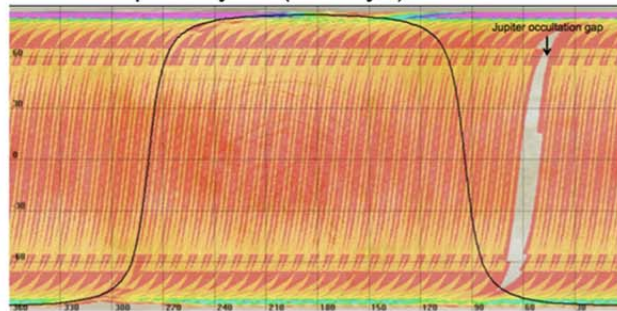
**Figure B.2.6-1.** Baseline interplanetary launch period

reaches its highest level of 100 m/s on the last day. The DSM occurs on the Earth-Venus leg of the trajectory. The interplanetary trajectory design would comply with all required National Environmental Policy Act (NEPA) assess-

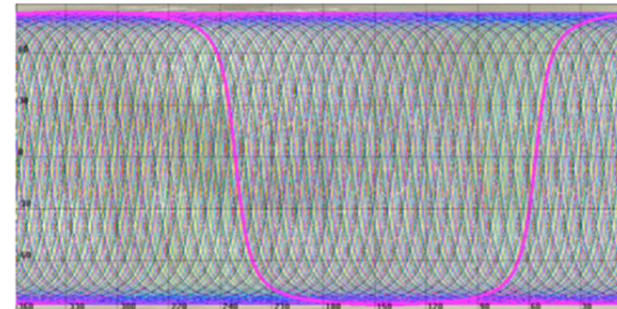
### Europa Orbiter Mission Design: Low-ΔV and Low-Radiation Mission to Explore Europa and Investigate its Habitability from Low-Altitude Orbit



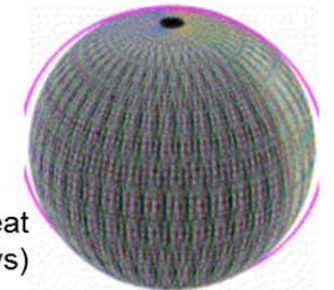
Number of accesses is between 1 and 4 after a repeat cycle (11 days)



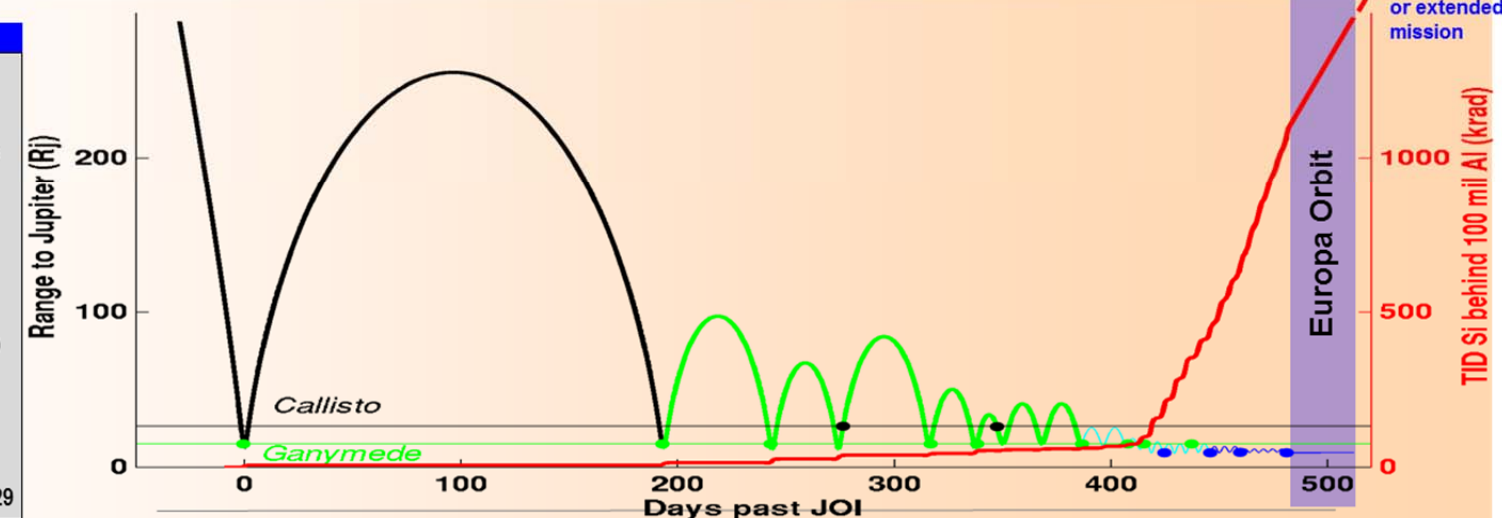
Ground tracks after a repeat cycle (11 days)



Ground tracks after one repeat cycle (11 days)



Key Parameters	Value
Launch Vehicle	Atlas V 551
Earth to Jupiter Trajectory	VEEGA
Earth Launch Period	11/15/21 to 12/05/21
C3 (Max), R.A., Dec.	15 km <sup>2</sup> /s <sup>2</sup> , 334.5°, 11.7°
Jupiter Arrival Date	4/3/2028
Jupiter Arrival V-infinity	5.6 km/s (maximum)
JOI Earth Range	4.52 AU
JOI Periapsis Range	12.8 R <sub>J</sub>
Jupiter Capture Orbit Period	206 days
Tour	4/4/28-8/12/29 (1.3 yrs.)
EOI	8/12/29
Primary Europa Science	8/12/29-9/12/29
Average Orbit Altitude, Inclination, Period	100 km, 95°, 126 min
Initial Orbit Node	4 p.m.
End of Mission	Europa Impact >10/12/29



ment and safety analysis (see Section B.2.9.3). An aim-point-biasing strategy would be used for the Earth flybys. The nominal flyby altitudes of Venus and Earth do not vary significantly over the launch period and are relatively high, as seen in Table B.2.6-2. For comparison, Cassini flew by Earth at an altitude of 1166 km, and Galileo at altitudes of 960 and 304 km.

A 500-km flyby would be performed at Ganymede about 12 hours before JOI, thereby saving about 400 m/s of  $\Delta V$  (compared to the case of no Ganymede flyby). The JOI maneuver lasts about 1 hour and occurs at perijove at a range of 12.8 R<sub>J</sub>, which is in the less intense, outer regions of the radiation belts. Gravity losses are negligible due to the small angle subtended by the burn-arc.

#### B.2.6.4 Backup Interplanetary Trajectories

Besides the baseline trajectory described above, many trajectory options are available, offering at least one launch opportunity every calendar year through 2024. The results of a comprehensive search of all 1-, 2-, 3-, and 4-gravity-assist trajectories are shown in Figure B.2.6-2. The best candidates from the search are shown in Table B.2.6-3, which includes launch period effects. The table shows, for each trajectory, the optimal launch date of the launch period, the flight time to Jupiter, the expected maximum  $C_3$  over the launch period, the launch vehicle capability at maximum  $C_3$  for the indicated launch year

(NLS-II contract), the propellant required for flying the mission (assuming the full launch vehicle capability is used), the maximum dry mass (i.e., the difference between the two preceding numbers), and the propellant required to fly the mission assuming the CBE value for the dry mass. In all cases, the CBE  $\Delta V$  from Table B.2.6-7 is used.

It is worth noting that two types of commonly considered trajectories do not appear in the short list of Europa Orbiter Mission trajectories because of their relatively poor mass performance. The first type is the  $\Delta V$ -Earth gravity assist ( $\Delta V$ -EGA), which is a  $V_\infty$  leveraging type of trajectory involving a large maneuver near aphelion before the first Earth flyby. For the  $\Delta V$ -EGA, the maximum dry mass that can be delivered in the years 2019–2027 is about 1360 kg (about 800 kg less than the “Max Dry Mass” numbers in the short list, Table B.2.6-3). The required  $C_3$  is in the range 25–30 km<sup>2</sup>/s<sup>2</sup>, and the flight time is typically 4–5 years, corresponding to a 2:1  $\Delta V$ -EGA (4.5 years for the maximum-dry-mass case).

**Table B.2.6-2.** Baseline VEEGA interplanetary trajectory (for optimal launch date).

Event	Date	$V_\infty$ or $\Delta V$ (km/s)	Flyby Alt. (km)
<b>Launch</b>	21 Nov 2021	3.77	-
<b>Venus</b>	14 May 2022	6.62	3184
<b>Earth</b>	24 Oct 2023	12.07	11764
<b>Earth</b>	20 Oct 2025	12.05	3336
<b>G0</b>	03 Apr 2028	7.37	500
<b>JOI</b>	04 Apr 2028	0.858	12.8 R <sub>J</sub>

**Table B.2.6-3.** Short list of interplanetary trajectories, including launch period effects. Baseline trajectory is in bold; other listed trajectories represent viable backup opportunities.

Launch Date	Flyby Path	TOF to JOI (yrs.)	$C_3$ (km <sup>2</sup> /s <sup>2</sup> )	Atlas V 551 Capa- bility (kg)	Max MEV Prop Mass (kg)	Max Dry Mass (kg)	Prop for CBE Dry Mass (kg)
25 Mar 2020	VEE	6.03	15.6	4456	2247	2209	1373
27 May 2021	VEE	6.87	14.5	4541	2424	2117	1546
<b>21 Nov 2021</b>	<b>VEE</b>	<b>6.37</b>	<b>15.0</b>	<b>4494</b>	<b>2303</b>	<b>2191</b>	<b>1419</b>
15 May 2022	EVEE	7.22	10.2	4935	2696	2239	1626
23 May 2023	VEE	6.18	16.4	4339	2272	2067	1484
03 Sep 2024	VEE	6.71	13.8	4562	2477	2085	1604
01 Aug 2026	VEE	6.94	10.0	4893	2632	2261	1571
21 Jul 2026	VEE	6.15	15.2	4400	2311	2089	1493

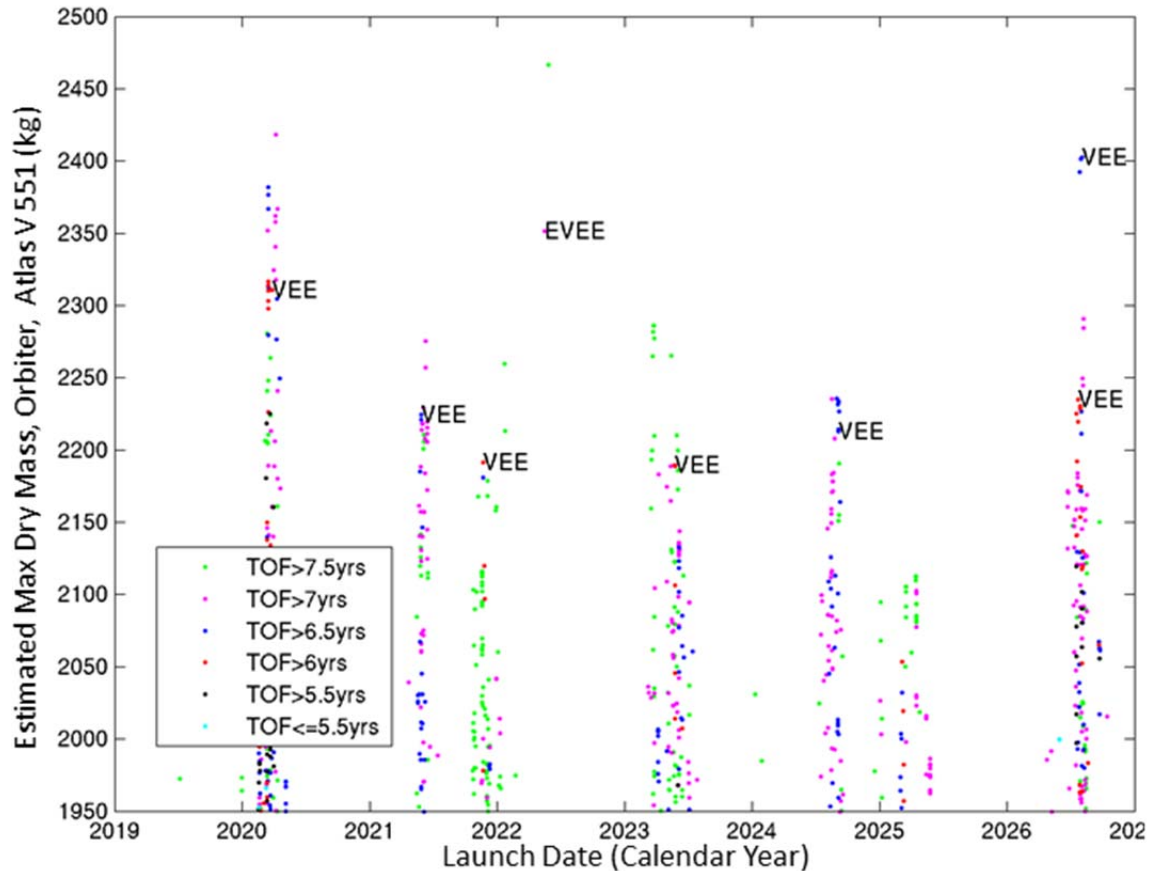


Figure B.2.6-2. Interplanetary trajectory options.

The second type is the Venus-Earth Gravity Assist (VEGA), involving a large maneuver after the Venus flyby. For flight times of around 4.4 yrs, the maximum dry mass for the VEGA is about 1440 kg. For flight times around 5.4 yrs, approaching the VEEGA flight times, the maximum dry mass becomes about 1810 kg. Thus, these two trajectory types significantly underperform in terms of delivered mass compared to the typical VEEGA trajectory. To save some flight time, these trajectory types may be considered in later phases of the mission design, once the vehicle mass is better characterized, assuming it does not grow significantly from current levels.

#### B.2.6.5 Jovian Tour

The three outer Galilean satellites are exploited as gravity-assist bodies to reduce greatly the  $\Delta V$  required for Europa Orbit Insertion. Adding Io gravity assists would reduce the

mission  $\Delta V$  still further, but would involve higher radiation dose and longer flight times. Although the net mass trade between propellant mass and shielding mass would favor using Io gravity assists, the system mass margin was already high enough to make the addition of Io unwarranted. Conversely, shortening the tour will typically add  $\Delta V$  and reduce flight times and radiation dose. The approximate trade-offs are summarized in Table B.2.6-4.

In this design, we assume a tour analogous to the 99-35 tour that has been designed in previous studies [Johannesen & D'Amario 1999]. Tour 99-35 starts with a 200-day orbit post-JOI. On this first Jovian orbit, a perijove raise maneuver (PJR) is performed near apoapsis to counteract perturbations from the Sun's gravity and to target G1, the first flyby of the tour. To keep radiation exposure low, perijove

**Table B.2.6-4.** Trade-offs between Flight-time, deterministic  $\Delta V$ , and TID (Si behind 100 mil Al, spherical shell) for various types of tours as compared to the concept baseline tour

Flight Time (delta yrs)	$\Delta V$ (delta km/s)	TID (delta Mrad)	JOI-to-EOI, inclusive
			Type of Tour
0	> 5.5	~0	No tour, direct insertion to Europa Orbit from interplanetary trajectory
0.25	4	~0	Callisto gravity assists and v-infinity leveraging
0.5	3	~0	Further Callisto gravity assists and v-infinity leveraging
1	2.5	0.1–0.5	Callisto and Ganymede gravity assists (no endgame)
1.5	1.5	0.8–1.2	Callisto, Ganymede, and Europa gravity assists (4:3, 6:5 endgame)
2.5	1.3	1.7	Callisto, Ganymede, Europa and Io gravity assists

ranges are kept high while the orbital period is reduced through Ganymede and Callisto flybys, as shown in the Tisserand Plot in Foldout B-2. By the time of the first Europa flyby, the period has been reduced substantially to about 5.5 days, giving a relatively low v-infinity at Europa. After four phasing orbits and a further Ganymede flyby, a second Europa flyby is performed, which marks the beginning of the tour endgame, whose purpose is to reduce the v-infinity (and hence EOI  $\Delta V$ ) even further. The first part of the endgame is a 4:3 resonance with Europa (approximately 4 Europa revolutions while the spacecraft does 3), followed by a Europa flyby that puts the spacecraft on a 6:5 resonance. On each of the resonances, a small leveraging maneuver is done near an apoapse to reduce the v-infinity at Europa. On the final approach to EOI, multi-body gravitational effects (from Jupiter and Europa) are exploited to give a final, substantial reduction to the EOI  $\Delta V$ . The tour events and EOI are shown in Table B.2.6-5.

The 1.1 Mrad radiation exposure in tour 99-35 is taken as a design point for this study, although it is foreseen that approximately 300 krad can be eliminated without impacting the mission  $\Delta V$  by shifting the phasing orbits to

**Table B.2.6-5.** Flybys of representative tour 99-35, which has a multi-body, v-infinity-leveraging endgame to reduce EOI. Maneuvers are impulsive.

Event		Days to EOI	Altitude (km)	$\Delta V$ or $V_\infty$ (km/s)
Ganymede	1	289.18	100	6.15
Ganymede	2	239.12	2243	6.22
Callisto	3	205.55	1117	6.40
Ganymede	4	165.24	577	5.19
Ganymede	5	143.79	493	5.19
Callisto	6	134.72	607	4.00
Ganymede	7	95.51	127	2.49
Ganymede	8	74.09	1413	2.49
Ganymede	9	66.98	2533	2.48
Europa	10	57.48	4134	2.60
Ganymede	11	44.73	122	1.68
Europa	12	36.34	100	1.57
Leveraging $\Delta V$		29.52		0.118
Europa	13	22.51	6654	0.93
Leveraging $\Delta V$		11.50		0.071
Europa	14	0.06	1765	Elliptical periapsis
EOI		0	100	0.450

the earlier parts of the tour that lie outside of the radiation belts [Grebow et al., 2011; Campagnola et al., 2012]. The correct phasing is needed so that the approach trajectory to EOI is in the plane of the desired science orbit. Also,  $\Delta V$  can be expended to perform EOI earlier if radiation exposure becomes a more pressing concern.

#### B.2.6.6 Europa Orbit, and Orbit Maintenance

After EOI and associated clean-up maneuvers, the spacecraft is in a roughly 100-km circular, near-polar, science orbit with a node of 4pm. The finite burn losses for EOI are minimal as shown in Table B.2.6-6.

**Table B.2.6-6.** Gravity losses for EOI, CBE case and Maximum Dry Mass case (launch vehicle capability fully utilized)

	CBE Dry Mass w/ CBE Prop	Max Dry Mass Case
$\Delta V$ impulsive	450 m/s	450 m/s
$\Delta V$ finite burn	455 m/s	460
Gravity Loss	5 m/s	10 m/s
Gravity Loss, fractional	1 %	2 %
Burn Duration	4 minutes	6 minutes

Weekly orbit maintenance maneuvers are sufficient to control the growth of the eccentricity, which occurs mainly due to Jupiter's gravity, and will fine-tune the orbit period for repeat ground tracks. The total  $\Delta V$  needed for maintenance for a month is only 5 m/s. The maneuver frequency and magnitude can be reduced further still if the orbital eccentricity vector is properly set once the main gravity harmonics of Europa are estimated. The prime science mission ends 30 days after EOI. The TID for a month in the science orbit is about 360 krad, a figure which accounts for the shielding effect of Europa, bringing the total unshielded (i.e. behind 100 mil Al) TID at end of prime mission to about 1.46 Mrad.

#### B.2.6.7 Navigation in the Jovian System

The navigation strategy and statistical  $\Delta V$  are based on experience with Galileo and Cassini. A full-blown navigation study with precise maneuver locations and covariances is beyond the scope of this study. The main uncertainties early in the Jovian cruise are the satellite ephemerides. The maneuver execution errors and perturbing  $\Delta V$ s are much less significant by comparison, except for the large JOI and EOI burns. Thus, up to three statistical maneuvers are envisioned per orbit around Jupiter: About three days after a flyby, near apoapsis, and about three days before a flyby. A cleanup maneuver will be done a few days after JOI to counteract errors both from the 500-km G0 flyby and from JOI itself. Similarly, EOI will have a cleanup maneuver done about 6 to 12 hours after the main burn to give sufficient

time for ground-based orbit determination. Two-way Doppler and range are assumed for orbit determination. Optical navigation is not assumed, but will be studied as a navigation trade option because it has the potential to offer lower statistical  $\Delta V$ s, closer flybys and hence possibly shorter cruise and lower radiation exposure.

#### B.2.6.8 Potential Extended Mission(s)

Given a healthy spacecraft at the end of the Europa Orbiter prime mission (and support from NASA HQ), various options may be considered, depending on the findings of the prime mission and on the propellant reserves available. Extended mission options may include for example:

- Lower orbits for improved mapping and remote sensing
- Long life-time orbits or stable orbits for observing longer temporal variations
  - Higher polar orbits (longer life-time)
  - Low-inclination, stable orbits (assuming significant propellant remains)
- Highly elliptical orbits with very low periapses

#### B.2.6.9 Spacecraft Disposal

Without active maintenance, low, circular orbits above about 40 degrees inclination will naturally impact the surface of Europa due to eccentricity growth (the orbital period does not have any significant secular change). Starting in the science orbit, it would take at least a month for an uncontrolled spacecraft to impact Europa. Thus, if the spacecraft becomes non-functional, it will eventually impact the surface of Europa at a random location. Alternatively, it may be decided after the prime mission to set a still-functioning spacecraft on a deliberate impact course with a specific spot on the surface. There will almost certainly not be sufficient propellant remaining at the end of the prime mission to enable the spacecraft to

**Table B.2.6-7.** Orbiter  $\Delta V$  summary.

Activity	CBE $\Delta V$ (m/s)	MEV $\Delta V$ (m/s)	Comments
Launch Injection Cleanup	20	20	Estimate to correct injection errors from launch vehicle
Earth Bias DV	50	50	Needed for final correction of deliberate aim-point bias away from the earth. ~25m/s/E-flyby. May be performed separately or integrated with other TCMs.
Deep Space Maneuver	100	150	Maneuver on Earth-Earth leg near aphelion. Baseline launch period variation goes from 0m/s up to 100m/s
IP statistical & $\Delta V$ cleanup	50	50	Multiple small maneuvers
JOI at 12.8 R <sub>J</sub> , 500-km G0 flyby	880	900	200-day initial orbit. Includes 3% for cleanup & minimal gravity losses.
Perijove Raise	40	80	Counteracts solar perturbations, targets G1 flyby
Pump-down phase Statistical	120	120	~8 m/s per flyby (conservative) (~15 flybys, incl. endgame). Expected average per-flyby: 3m/s. Deterministic $\Delta V$ can usually be avoided.
Endgame $\Delta V$	188	200	4:3, 6:5 resonance sequence. $\Delta V$ s near an apoapse on each leg.
EOI $\Delta V$ , impulsive	450	600	100 km circular orbit
EOI $\Delta V$ gravity loss	25	30	<~5% for Max mass case and 890N engine
EOI cleanup	10	15	~2% of EOI, probably multiple maneuvers
Orbit Maintenance	5	5	Estimate: ~5 m/s per month, 100km circular orbit
Reserve	0	55	
<b>TOTAL</b>	<b>1940</b>	<b>2275</b>	

escape from Europa. Thus, impact with Europa is the ultimate fate of the spacecraft, which clearly has spacecraft sterilization implications.

#### B.2.6.10 Orbiter Mission $\Delta V$

Table B.2.6-7 summarizes both the current best estimate (CBE) and maximum estimated value (MEV) for the total  $\Delta V$  needed to execute the Europa orbiter mission. The two totals are comprised of both computed values (DSM, JOI, PRM and the tour's deterministic  $\Delta V$ ) and estimated values (launch injection cleanup, Earth bias  $\Delta V$ , interplanetary statistical and cleanup  $\Delta V$ , tour statistical and cleanup  $\Delta V$ , EOI cleanup, orbit maintenance).

See the Master Equipment List (MEL, Sec B.4.3) for calculations of propellant loading based on  $\Delta V$  and thruster usage.

### B.2.7 Flight System Design and Development

*The Orbiter flight system, a capable spacecraft tailored to the Orbiter science objectives, has high heritage and a low-complexity payload.*

The Europa Orbiter Mission Flight System is described first in overview, identifying key components and features, then in detail at the module level. The module description overview discusses cross-cutting subsystem concepts followed by detailed descriptions of the three flight system modules: Avionics, Propulsion and Power Source. Finally, technical resource budgets are described followed by a description of the module and flight system level integration and testing concept.

#### B.2.7.1 Flight System Overview

The conceptual flight system (see Figure B.2.7-1) is comprised of three modules stacked along the Z axis. From top to bottom these are

- Avionics Module—comprising the telecom section (dominated by the 3 m high gain antenna), the upper equipment section containing the payload, and the avionics vault.
- Propulsion Module—containing the tanks, propellant, plumbing, valves and engines

- Power Source Module—Housing the ASRGs, their control electronics and the launch vehicle adapter.

#### *Instruments*

The Orbiter Mission flight system is configured to support the following notional science instruments:

- Mapping Camera (MC).
- Laser Altimeter (LA).
- Magnetometer (MAG).
- Langmuir Probe (LP).

The MC and LA are mounted on a two-axis gimballed platform for nadir pointing during the Europa orbit. The MAG is accommodated on a 10 m boom to provide separation from the spacecraft and to collect magnetic field data in many orientations. The LP is deployed on a 1 m boom to reduce measurement disturbance from spacecraft surface charging. In addition to these four instruments, the flight system X/Ka band telecommunication system supports the Europa gravity science investigation without requiring functionality beyond what is already needed to support nominal communications.

#### *Attitude Control*

The Orbiter flight system is three-axis-stabilized in all phases of flight. Stabilization is achieved through the use of inertial measurement and star measurement for attitude determination and thrusters and reaction wheels for attitude control.

#### *Data Handling*

During an orbit, the volume of science data collected is relative small (~200 MB). This data is stored in the RAD750 radiation-hardened RAM prior to downlinking; the RAD750 is part of the Command and Data Handling Subsystem (C&DH).

#### *Power*

The power source for this spacecraft is four ASRGs. The power system is sized to accommodate the failure of one Stirling engine (each

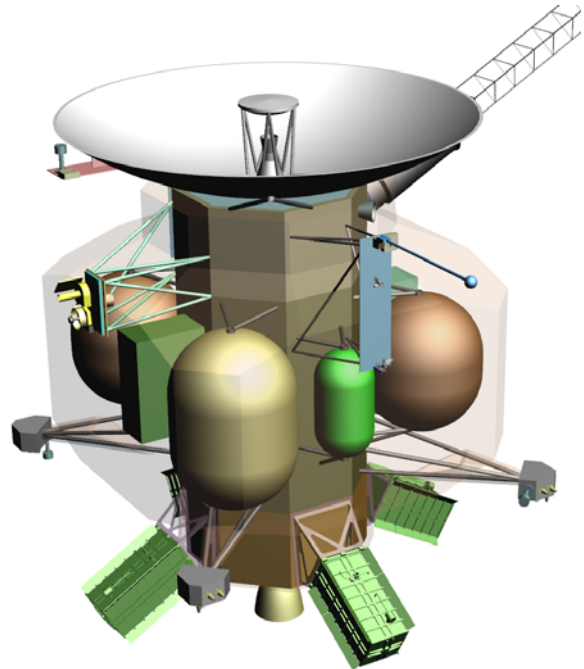


**Figure B.2.7-1.** The flight system (with transparent thermal shroud) provides a robust platform to collect, store, and transmit high volumes of science data.

ASRG uses two Stirling engines). Excess power is stored in an internally redundant 59-Amp-hour lithium-ion battery or dumped as heat through a thermal shunt. For transient mission phases that require more power than produced by the ASRGs in steady state, additional power is temporarily drawn from the battery.

#### *Thermal*

To minimize the power demand of the spacecraft (driven by a desire to minimize the number of ASRGs), the spacecraft was designed to minimize the use of electrical heaters. To achieve this goal, the heat from spacecraft electronics is captured inside a thermal shroud surrounding the Propulsion Subsystem providing enough heat to keep the propellant near room temperature without the need for supplemental electrical heaters. The concept includes 30 radioisotope heater units (RHUs) and/or variable radioisotope heater units (VRHUs) that will be used in extremities and select locations (e.g., thruster cluster assemblies) when heat from the avionics vault is not

available to minimize the need for electrical heaters.

#### *Telecommunications*

The Telecommunications Subsystem is designed to support the gravity science investigation and real-time transmission of science data communicated back to Earth while in Europa orbit. This system consists of X-band uplink for commands, X-band downlink for low-data-rate telemetry, and Ka-band downlink using the fixed 3-meter HGA for high-data-rate telemetry.

#### *Propulsion*

The Propulsion Subsystem provides delta-V and attitude control, momentum management, trajectory correction, Jupiter Orbit Insertion (JOI), and EOI. To support these activities, the Propulsion Subsystem utilizes a dual-mode, bipropellant architecture. The fuel, oxidizer, and pressurant tanks are distributed around the core of the spacecraft to provide radiation shielding to the internal electronics. During Phase A, a risk assessment will be performed on potential micrometeoroid damage to the tanks; if necessary, the thermal shroud can be upgraded with standoff Whipple/bumper shields. The tanks are sized for maximum propellant for spacecraft on the Atlas 551 and can support up to 2.28 km/s of  $\Delta V$ . The engines consist of one 890-N main engine, four 90-N thrust vector control (TVC) thrusters, and sixteen 4.4-N (eight primary, eight redundant) attitude-control thrusters. Each of the four thruster control assemblies (TCA) contains 4 attitude control thrusters and 1 TVC thruster.

#### *Redundancy*

The spacecraft uses a redundancy philosophy similar to that of Cassini: that is, the flight system is redundant with selected cross strapping. The instruments are single string. The structure, main engine, and TVC are also single string; these single-string elements will undergo a risk assessment in Phase A to determine whether the risk is acceptable.

#### *Radiation*

This mission has very demanding total dose radiation requirements (1.56 Mrad (Si) behind 100 mils Al). To support the use of standard aerospace EEE parts, the design uses a multi-layered radiation shield. Most of the spacecraft electronics are housed in a vault (similar to that on the Juno spacecraft). This vault is also buried inside the spacecraft to benefit from shielding provided by spacecraft elements such as the batteries, the structure, tanks, propellant (during Jupiter cruise), and ASRGs. Inside the vault, components will be exposed to less than 150 krads end-of-mission total dose. Parts not capable of meeting even this reduced total dose requirement with proper derating, can be accommodated using additional box level shielding, box and card placement to provide additional self-shielding, and parts-level spot shielding.

##### *B.2.7.1.1 Flight System Configuration*

The engineering configuration of the spacecraft is shown in Figure B.2.7-2. The left side of the figure is the CAD model without the thermal shroud and with the instruments stowed. The right side of the figure is a cross section of the same configuration.

Figure B.2.7-3 shows the spacecraft with the 10-m MAG boom and the LP deployed, and with the thermal shroud. The left side of the figure shows how the HGA and thermal shroud protect the spacecraft from the high solar flux during the Venus flyby portion of the interplanetary cruise. The few elements exposed to the solar flux are the LGA, the thruster clusters, and the LP. These three elements can survive without shading the heating that occurs during the Venus flyby.

##### *B.2.7.1.1.1 Avionics Module*

The topmost portion of the Avionics Module is the telecommunications section. It is composed of a fixed 3-meter HGA, the medium-gain antenna (MGA), one of three low-gain antennas (LGAs) and associated waveguide and amplifiers. Below the HGA is the upper

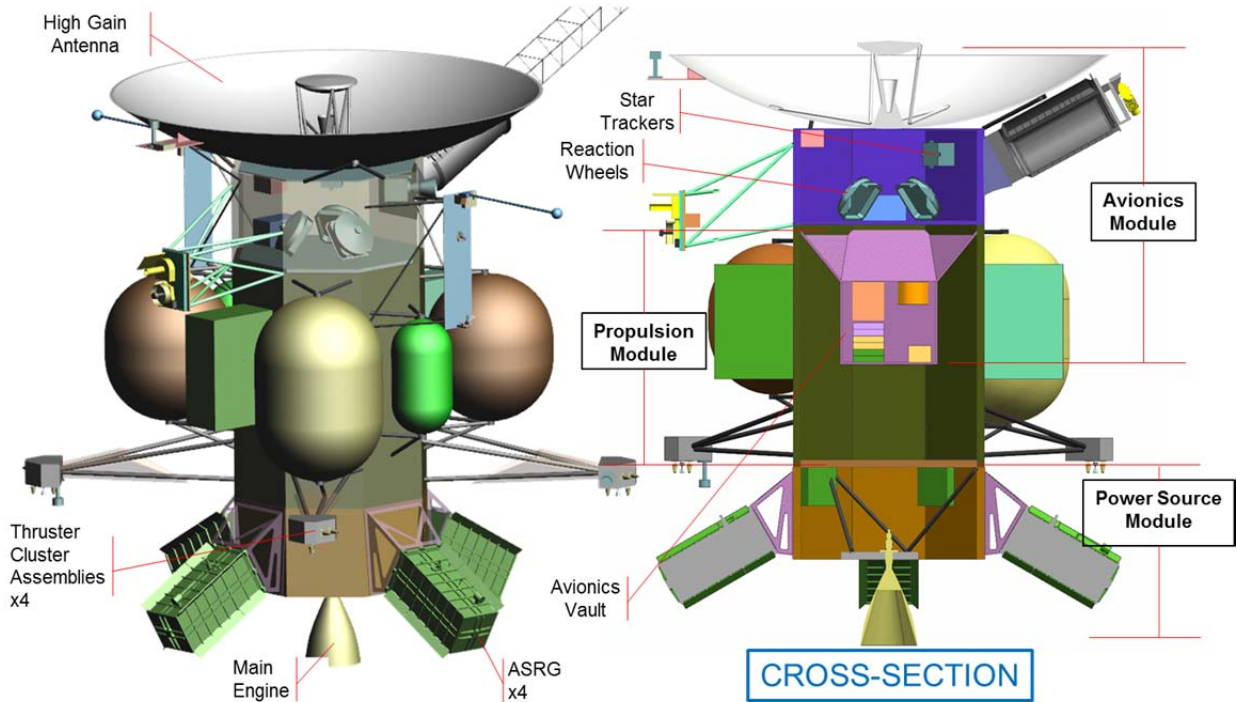


Figure B.2.7-2. The modular configuration shown provides maximum radiation shielding for the electronics (note that the thermal shroud is not shown).

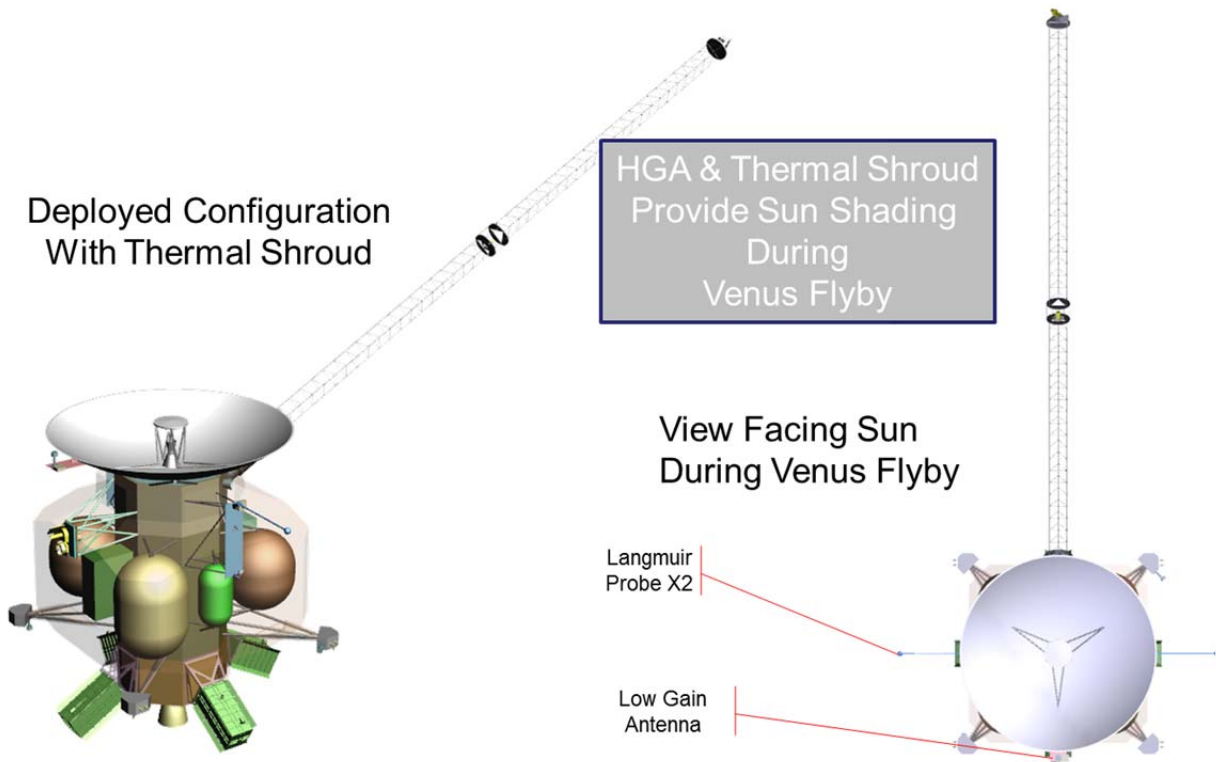


Figure B.2.7-3. The flight system configuration with thermal enclosure and deployed instrumentation.

equipment section. This section holds the instruments, science electronics chassis, reaction wheels, and star-trackers. At the bottom of the Avionics Module is the avionics vault section; inside the vault is a majority of the spacecraft avionics. Note that the vault sits inside the Propulsion Module to maximize the radiation shielding from the tanks, structure, and propellant. The Avionics Module attaches to the Propulsion Module. Until the Avionics Module is mated with the Propulsion Module, all components in the Avionics Module sections are accessible for testing, troubleshooting or rework without significant impact to the System Integration plan. After spacecraft integration, a de-mate operation from the Propulsion Module will enable access to the vault.

#### *B.2.7.1.1.2 Propulsion Module*

The Propulsion Module contains the fuel tanks, oxidizer tanks, and pressurant tanks as shown in Figure B.2.7-2. At the bottom of the Propulsion Module are four thruster clusters holding the attitude-control thrusters; these are supported to maximize the moment arm for attitude control. The main engine is physically attached to the Propulsion Module but protrudes down through the central ring of the Power Source Module after mating. This design allows end-to-end testing of the fully plumbed and sealed Propulsion Module. It also allows system integration of the Propulsion Module to the Avionics and Power Source Modules without breaking the final, tested plumbing configuration.

#### *B.2.7.1.1.3 Power Source Module*

The Power Source Module supports the four ASRGs and their control electronics. The ASRG units would be mounted on the end of a support structure that supports them radially and slightly canted away from the spacecraft. This is to improve the ASRGs thermal view to deep space to improve ASRG efficiency. The support structures also house a passive vibration damping system tuned to the ASRG oscillation frequency of around 100 Hz. This sys-

tem would greatly reduce the vibration transmitted through the spacecraft structure to vibration sensitive components such as the star tracker and optical instruments. The launch vehicle adapter is attached to the underside of the Power Source Module's primary ring.

A main goal of modularizing the ASRG assembly from the rest of the flight system is to decouple the heavily guarded and regulated ASRG fueling and assembly process from the rest of the system. The concept allows for the Power Source Module to be assembled and tested independently from the rest of the spacecraft, only mated to the system at the last possible moment at the launch site before fairing installation. This helps ensure the safest possible handling of the ASRGs.

#### *B.2.7.1.2 System Block Diagram*

Figure B.2.7-4 shows the system block diagram for the Orbiter spacecraft. The top box is the Avionics Module. The middle box is the Propulsion Module. The bottom box is the Power Source Module. Note that items like electrical heaters and temperature sensors are distributed across all of the modules. The legend shows the key interface types between elements.

The Avionics Module holds the majority of the spacecraft avionics. Inside the vault are the C&DH electronics, power electronics, pyro/propulsion drive electronics, inertial measurement units (IMUs), RWA electronics, and SDSTs. Outside the vault are the instruments, science electronics chassis and the following GN&C components: RWA mechanical assemblies, Sun-sensors, and stellar reference units (SRUs). The power subsystem components outside the vault are the shunt radiator and battery. The telecom subsystem components outside the vault are the TWTAs, the coax, the waveguide, switches, and antennas.

The Propulsion Module is an integrated structure comprising all of the tanks (fuel, oxidizer, pressurant), the plumbing, the pressurization control assembly (valves, filters, sensors, etc.),

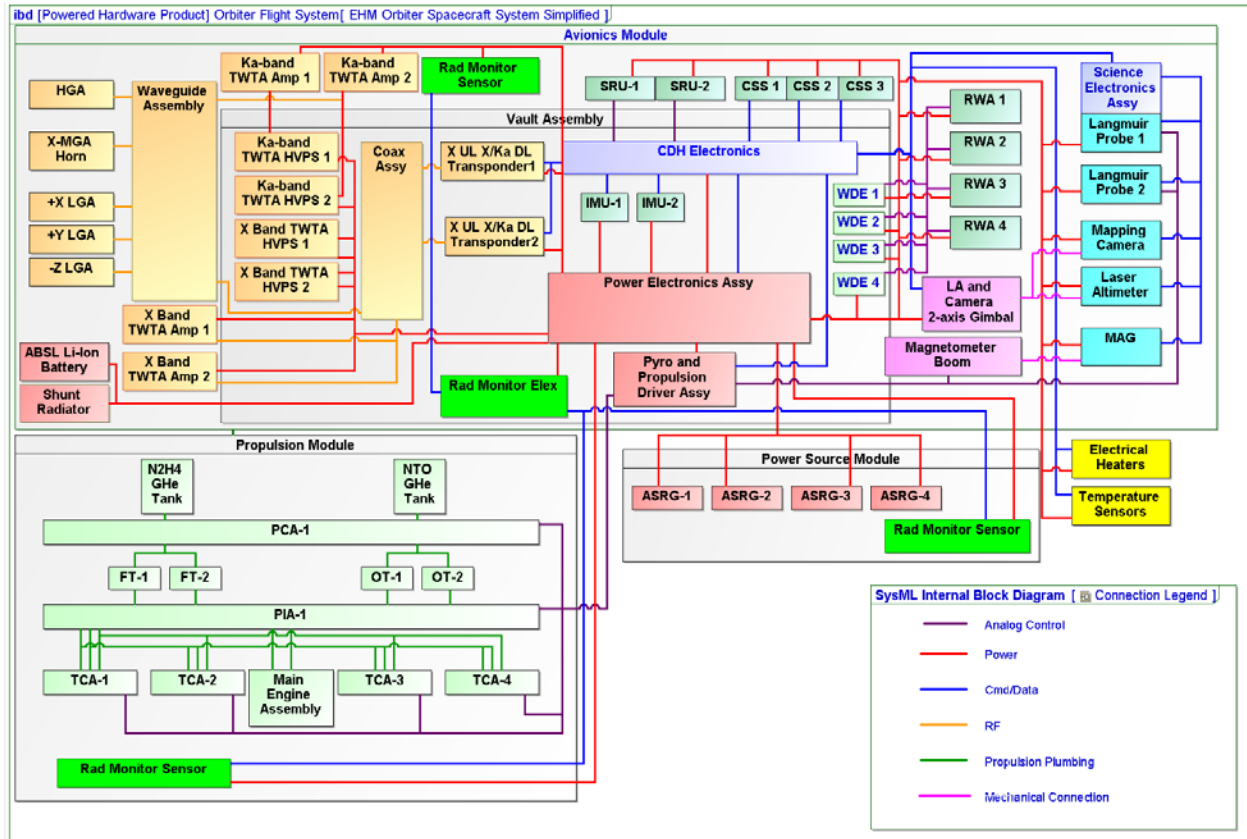


**Figure B.2.7-4.** The system block diagram shows the simple interfaces between the spacecraft modules

the propellant isolation assembly (valves, filters, sensors, etc.), the thrusters, and the main engine.

The Power Source Module is an integrated structure with the launch vehicle adapter and ASRGs. The ASRG consists of the power sources and the control electronics.

Note that some of the boxes (e.g., C&DH) do not show redundancy because they are internally redundant.

**B.2.7.1.3 Flight System Key Drivers**

Table B.2.7-1 shows the key drivers that flow down to the flight system from the science measurements.

Gravity science measurements drive radio Doppler observation of the spacecraft while in orbit around Europa. Long, continuous data sets (i.e. radio Doppler measurements of the spacecraft through several Europa orbits without non-gravitational perturbations from

thruster firings) are highly desired with 24 hour continuous data sets required as a minimum. This requirement drives RWA momentum sizing, telecom performance requirements and power system requirements.

Magnetic field measurements levy two drivers on the flight system design: the system and subsystem design must meet stringent magnetic cleanliness requirements and the magnetometers must be deployed away from the spacecraft. Two magnetometers—one at 5 m along the boom and the other at 10 m—are used to enable post processing removal of any residual spacecraft magnetic field bias.

Charged particle measurement using the Langmuir Probe has two drivers on the flight system design. The system and subsystem design must meet stringent EMI requirements and LP must be deployed away from the spacecraft to provide a clear FOV to the plasma.

**Table B.2.7-1.** The spacecraft driving requirements from the science measurements are mature and have been vetted through numerous Science Definition Team meetings.

Science Measure	Requirement	GN&C	Telecom	Power	CDH	Prop	Thermal	Mech
Gravity Science	Provide continuous “arcs”	RWA Sizing/ Desat Freq	Continuous	# of ASRGs				
	0.1 mm/sec performance		X up, Ka down					
Magnetometry	Provide magnetically clean spacecraft		EMI	EMI	EMI			Deploy two mag
Langmuir Probe	Provide EMI clean spacecraft		EMI	EMI	EMI			Deploy
	“FOV” of Plasma (not in Wake of Spacecraft)							
Mapping Camera	Simultaneous with LA & Gravity Science							Gimbal system
	Stereo Imaging		3-m HGA Ka down		Data Storage			
	Strip overlap & alignment							
Laser Altimetry	Simultaneous with Gravity Science & Mapping Camera							Gimbal system
	10-cm accuracy							

The MC and LA levy several drivers on the flight system. Imaging the surface while simultaneously collecting gravity science with a body-fixed HGA necessitates the use of a two-axis gimbal platform. The surface map creation in stereo is the driver on data storage and downlink; it drives the size of the data storage in the C&DH subsystem and drives the size and power of the telecommunication subsystem. The mapping strip overlap and alignment requires tight pointing knowledge from the GN&C subsystem. The 10-cm accuracy requirement on the LA drives tight pointing knowledge from the GN&C subsystem.

Table B.2.7-2 shows the key drivers that flow down to the flight system from the mission design.

The Venus flyby is a driver for the spacecraft thermal design and results in an approach wherein the spacecraft points the HGA towards the Sun; this enables the HGA and the thermal shroud to shade the vehicle.

During inner-solar-system cruise, there are two key drivers on the flight system design. Commanding and telemetry during this inner-solar-

system cruise require an X-band system for uplink and downlink using near- $4\pi$  steradian coverage from the LGAs. This type of telecom approach is needed since the spacecraft cannot always point the HGA to Earth because of thermal constraints.

During the outer-solar-system cruise, commanding and telemetry require an X-band system for uplink and downlink using the MGA.

During the outer-solar-system cruise and Europa orbital phase, the cold conditions drive the thermal design of the spacecraft. To minimize electrical heater power demand, the internal heating from the electronics is captured within the thermal shroud to keep the spacecraft equipment within flight allowable temperatures. External elements will require electrical heaters or VRHUs.

JOI and EOI are autonomous critical events that drive robust system fault protection. This flows down to the subsystems, resulting in a fault tolerant architecture that allows faults to be detected and isolated so that recovery can

**Table B.2.7-2.** The flight system incorporates design elements that flow down from the mission drivers.

Mission Design	Driver	System	GN&C	Telecom	Power	CDC	Prop	Thermal	Mech
Venus Flyby	Thermal control							Shade with HGA & shroud	
Inner Solar System Cruise	Command & Telemetry								
	Earth Flybys with ASRG	Fault Protection							
Outer Solar System Cruise/Jupiter Cruise/Europa Cruise	Command & Telemetry		Sun sensors						
	Thermal Control							Thermal Shroud/RHU/VRHU	
JOI/EOI	Critical Event	Fault Protection	Dual string/ Hot Sparing	TVC Size Engine Size					
TCM/Europa Orbit Maintenance	Navigation			Doppler					
Jupiter Cruise + Europa Orbit	Radiation	Fault Protection	<300 krad parts	<300 krad parts	<300 krad parts	<300 krad parts			Vault & Config

occur rapidly and without terminating the orbit insertion sequence.

Since the mission has several trajectory correction maneuvers (TCMs), both deterministic and statistical, the onboard communication system must support Doppler tracking to enable navigation on the ground.

The Jupiter cruise and the Europa orbital phase drives one key flight system requirements: a large radiation total dose of approximately 1.56 Mrad (Si) (behind 100 mil Al) is accumulated during these phases with periods of high peak flux; part selection and shielding, sensor noise tolerance and fault-protection requirements.

**B.2.7.2 Structures and Mechanisms**

The overall configuration (Figure B.2.7-5) starts with the Avionics Module at the top, followed by the Propulsion Module and the Power Source Module at the bottom. The primary structure (Figure B.2.7-6) consists of these three octagonal modules. Each module's structure is based on an aluminum forging machined from the outside. Aluminum was chosen because it provides the best balance

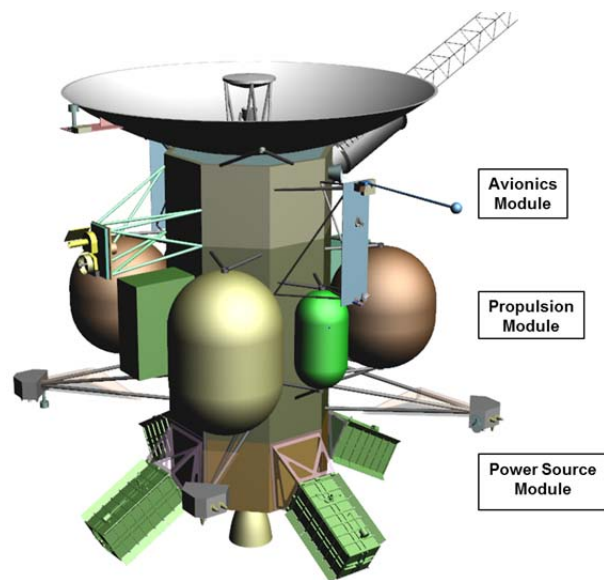


**Figure B.2.7-5.** Structures and mechanisms configuration.

among weight, strength, stiffness, and radiation-shielding and is easily worked into a lightweight, high-strength, and stiff structure. When all three modules are stacked, they form a superstructure that is able to meet the Atlas V launch vehicle's load and frequency requirements.

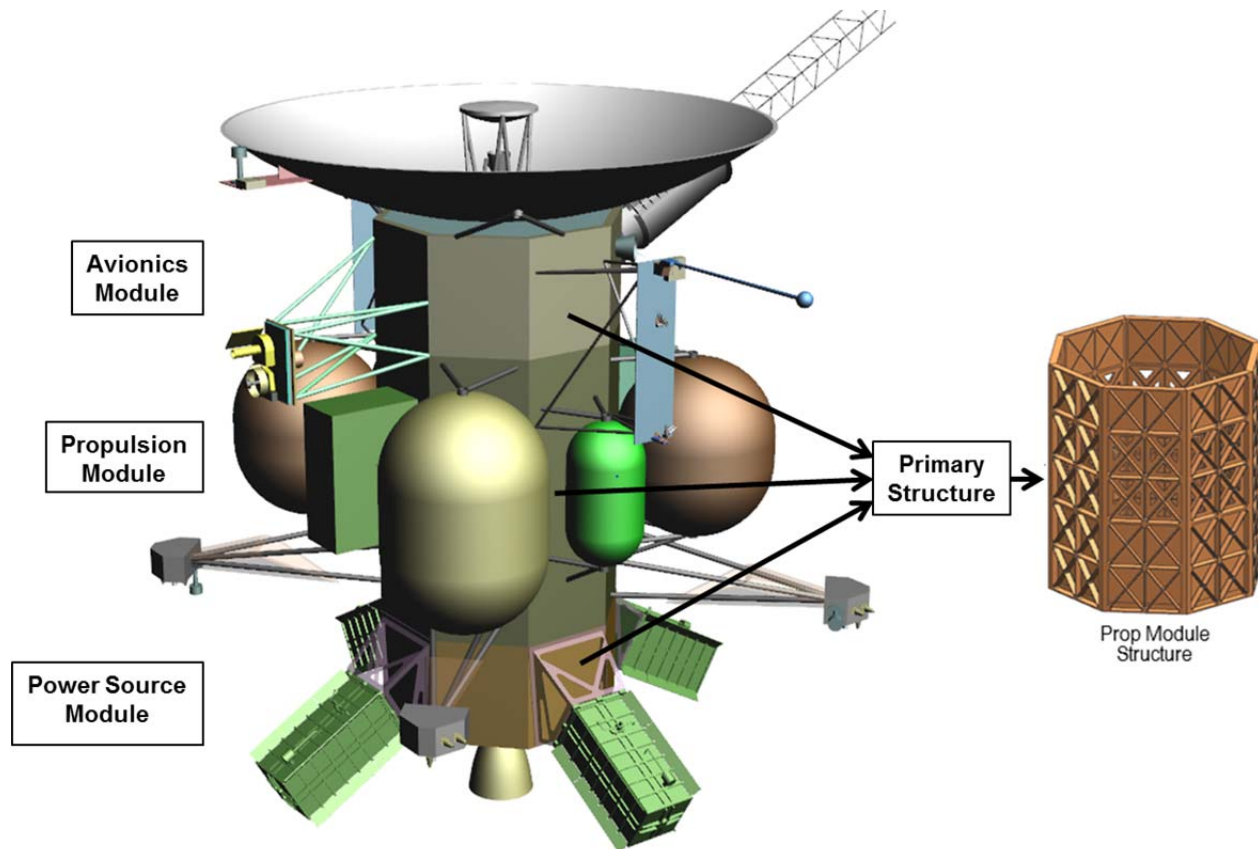


Figure B.2.7-6. Orbiter primary structure.

All brackets, struts, secondary structures, and mechanisms are mechanically grounded to the primary structure. Loads for these appendages are determined using the Atlas V mass acceleration curve.

The orbiter's primary mechanisms are the instrument two-axis gimbal, the LP's deployment system and the MAG boom deployment mechanism (Figure B.2.7-7).

The structures and mechanism do not require any new technology. Designs from past missions can be adapted to meet all of the structural and functional requirements for the Europa Orbiter.

#### B.2.7.2.1 Key Mechanical Drivers

- First mode fundamental frequency: 8 Hz
- Primary structure lateral launch acceleration: 2 G

- Atlas V mass acceleration curve for appendages
- Isolate spacecraft at least 20 Hz from Stirling converter operation frequency (102 Hz)

#### B.2.7.3 Orbiter Thermal Control

The thermal design uses, to the fullest extent practicable, waste heat, insulation, and louvers to control temperatures. This approach consumes little to no operational heater power, is low-mass, and has a flight-proven heritage.

##### B.2.7.3.1 Key Thermal Drivers

- Maintain the propulsion system and battery within allowable flight temperature (AFT) ranges of 15°C to 50°C and 10°C to 25°C, respectively.
- Maintain all instruments within the AFT limits.

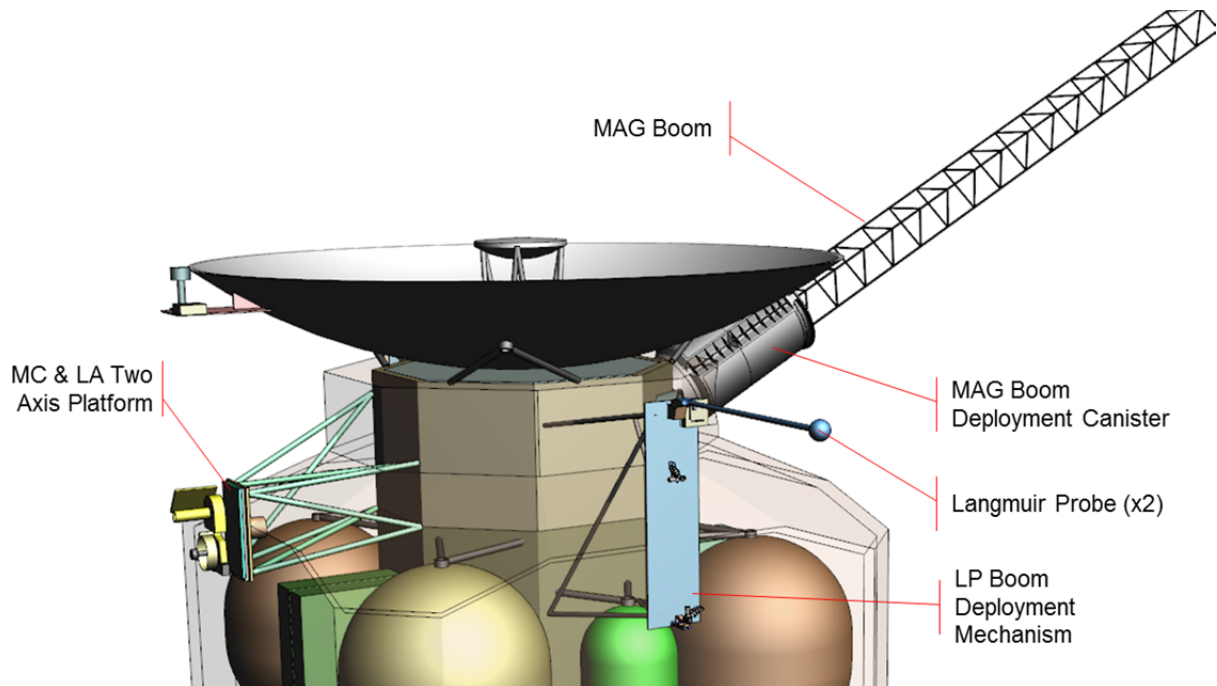


**Figure B.2.7-7.** Laser altimeter and MC and LP.

- Accommodate the variation in environmental heat loads from Venus at 0.7 AU to Jupiter at 5.2 AU (i.e., 2.0 to 0.04 Earth Suns).
- Tolerate limited transient off-Sun exposure at less than 1 AU during fault conditions or trajectory maneuvers.
- Minimize replacement heater power at outer cruise and Jupiter.

#### B.2.7.3.2 Thermal Design

Figures B.2.7-8 and B.2.7-9 show the primary thermal components of the spacecraft. A lightweight thermal shroud surrounds the propulsion tanks and associated plumbing. Consisting of multilayered insulation (MLI) supported by a latticework, this shroud creates a radiative cavity around the tanks. A clearance of 100 mm between the propulsion components and shroud provides adequate view factors for radiation.

Waste heat from the avionics vault and Advanced Stirling Radioisotope Generator (ASRG) electronics radiates into the cavity and warms the propulsion system. Openings in the

primary structure allow heat to radiate from the vault onto the tanks and into the cavity.

A temperature-regulation system is necessary to accommodate the variation in environmental loads and internal dissipations. Accordingly, louvers over external radiators on both ends of the spacecraft regulate the cavity temperature to maintain acceptable vault and propulsion temperatures. Heat from the vault and ASRG electronics, coupled with louvers on the mounting structure, warms the shroud in the cold case and rejects excess heat to space in the hot case, producing acceptable temperatures on the propulsion system and vault.

This system of waste heat and louvers requires no additional electrical heaters for normal operation. With an MLI external area of 26 m<sup>2</sup> and a nominal effective thermal emissivity of 0.01, acceptable tank temperatures occur with a 200-W heat flow. During the mission, 290 W to 418 W is available from the avionics vault and ASRG electronics. Hence, the heat balance is always positive. Fault conditions, where the avionics may be off and waste heat is low, make survival heaters necessary on the

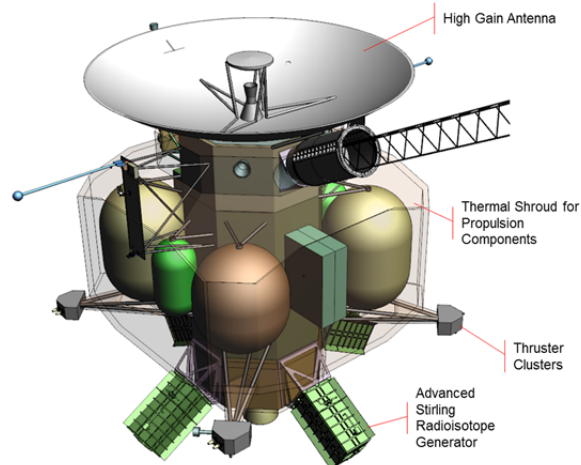


**Figure B.2.7-8.** Orbiter spacecraft with thermal shroud surrounding propulsion tanks.

vault. Survival operation will be studied in Phase A.

The high-gain antenna (HGA) performs an important thermal-control function: It shades the spacecraft from the Sun during the hot conditions near Venus. At Venus, the spacecraft is oriented such that the HGA faces the Sun. This orientation preserves the heat balance on the thermal shroud and louvers. If necessary to tolerate a loss-of-attitude fault at Venus, a hybrid MLI layup with five external layers of embossed Kapton protects against high exterior temperatures. Off-Sun illumination and the impact on temperatures will be studied during Phase A of the project.

A separate thermal-control zone with a dedicated radiator and louver controls the temperature of the battery. This is accomplished by locating the battery in the upper equipment section of the Avionics Module mounted directly to a space exposed bulkhead with a dedicated louver.

Variable radioisotope heating units (VRHUs) control the temperature of the thruster clusters. Local heating from the VRHUs is required due to the remote location of the thrusters. Each VHRU consists of two to three individual RHUs mounted in a rotating cylinder. One half of the cylinder is painted white while the other half is insulated. A bimetallic spring positions

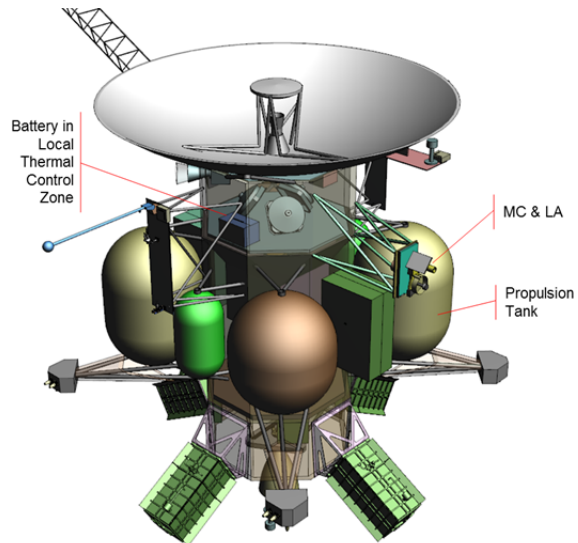


**Figure B.2.7-9.** Orbiter spacecraft with thermal shroud removed.

the cylinder to radiate heat into the thruster cluster when the cluster is cold, or out to space when the cluster is warm. There are four VHRUs per thruster cluster with a total of ten individual RHUs per cluster. Four thruster clusters yield a total of sixteen VHRUs and 40 individual RHUs. This design tolerates a failure mode where one VHRU is stuck fully open or fully closed.

Instrument thermal control is individually customized via local radiators and heaters to maintain acceptable temperatures.

Risk exists, as in any thermal-control system, where thermal performance is affected by workmanship. The effective emissivity of MLI is a notable example. For the Europa Orbiter, this risk is mitigated by design and by test. Margin in the active louver system provides tolerance for hardware variations. Also, thermal development tests of the louvers and critical areas of MLI reduce risk to acceptable levels.

#### B.2.7.3.3 *Heritage*

The thermal design for the Europa Orbiter follows that of Cassini. In the Cassini design, the propulsion system was enclosed in a shroud that formed a radiative cavity. Heat for

the Cassini shroud came from radioisotope thermoelectric generators (RTGs), whereas on the Europa Orbiter spacecraft the heat comes from the avionics vault and the ASRG electronics. VRHUs control the temperature of the thruster clusters for both Cassini and Europa Orbiter. HGA shading protected the Cassini spacecraft from solar loading at Venus and will do the same here. Other thermal hardware, such as louvers, heaters, MLI, and platinum resistance thermometers, also have good heritage based on the flight experience of prior JPL missions.

#### B.2.7.3.4 Heat Balances for Three Governing Conditions

The inner cruise takes the spacecraft near Venus. In this 0.7-AU hot condition, the high-gain antenna points toward the Sun to shade the rest of the spacecraft and prevent overheating. Side-facing louvers automatically control the internal temperatures. All of the heat from the ASRG electronics, 72 W, radiates off the lower louver, and 68 W of the vault power radiates off the upper louver, as shown in Figure B.2.7-10.

The orbiter experiences cold conditions when

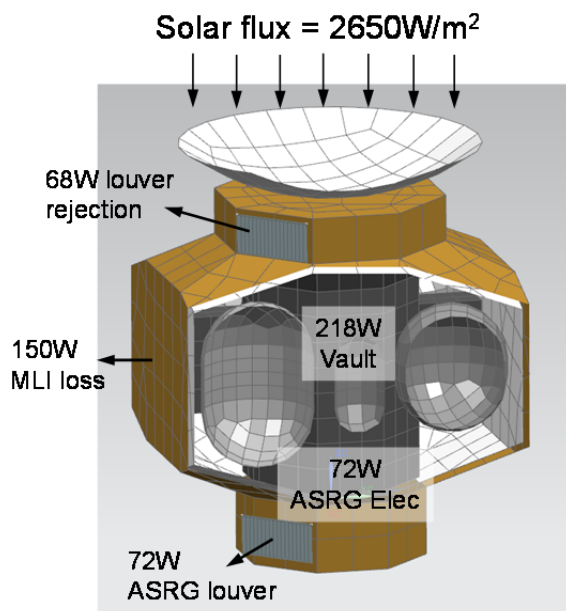


Figure B.2.7-10. Heat balance for inner cruise.

in orbit about Europa without communications. In this cold science mode, the vault power is 169 W. This low level of waste heat is fully used to warm the thermal shroud. Hence, the upper louver is closed. In addition, 31 W of waste heat from the ASRG electronics conducts into the central structure. The remaining 41 W from the ASRG electronics radiates off the lower louver, as shown in Figure B.2.7-11.

Power levels change again for orbit insertion and trajectory correction maneuvers. In this high-power condition, the vault dissipates 346 W. Consequently, the upper louver rejects 146 W while the lower louver rejects 72 W, as shown in Figure B.2.7-12.

Passive thermal control of the propulsion tanks and adjacent lines is by radiation into the thermal shroud. This is the same approach that was used on Cassini. At Jupiter, in the worst-case cold condition, thermal equilibrium occurs with a heat flow of 200 W from the inner structure into the shroud and out through the insulation. An initial thermal analysis shows that the propulsion tanks remain within 25°C to 40°C, in compliance with their AFTs, without direct heating or active control. Fig-

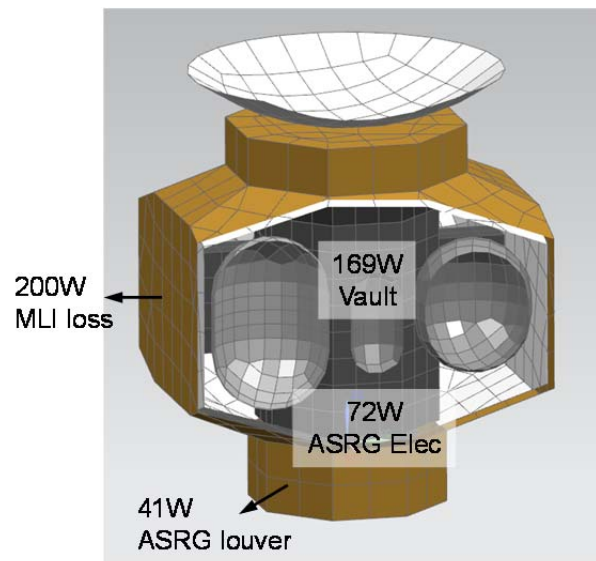
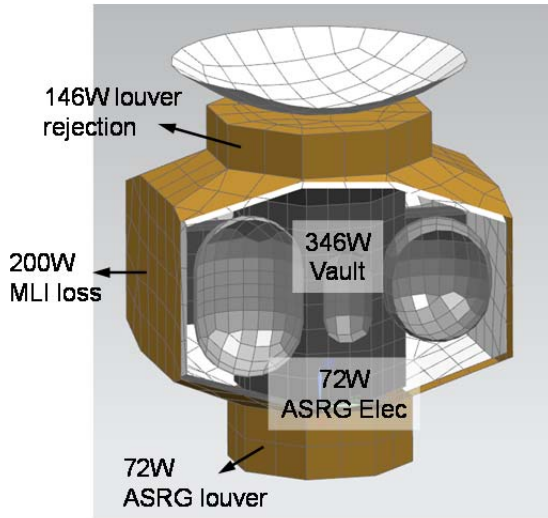


Figure B.2.7-11. Heat balance for Europa orbit with communications off.



**Figure B.2.7-12.** Heat balance for orbit insertion and trajectory correction maneuvers.

ures B.2.7-13 and B.2.7-14 show predictions of the tank temperatures.

#### B.2.7.4 Propulsion Module

##### B.2.7.4.1 Propulsion

*This propulsion subsystem, specifically designed for long-life outer-planet missions, will provide the impulse and reliability necessary to meet the needs of the Europa Orbiter Mission.*

The Europa Orbiter spacecraft propulsion subsystem is a dual-mode bipropellant system. The propellants are hydrazine ( $N_2H_4$ ) and nitrogen tetroxide (NTO). The hydrazine fuel and nitrogen tetroxide oxidizer are used by the bipropellant main engine, and the hydrazine fuel alone is used by the monopropellant reaction-control subsystem (RCS) thrusters and thrust vector control (TVC) thrusters. Figure B.2.7-15 shows a schematic of the propulsion subsystem.

##### B.2.7.4.1.1 Key Performance Drivers

The key drivers of the design of the propulsion subsystem are typical of those for outer-planet missions, with the possible exception of the desire to configure the system to take advantage of the propulsion subsystem mass to provide radiation shielding to sensitive elec-

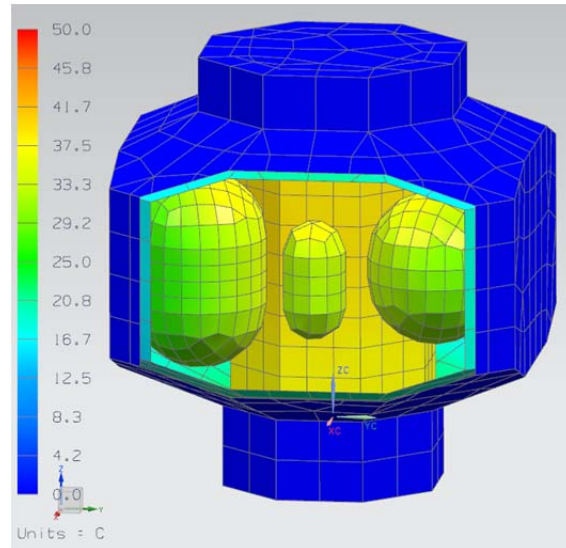


**Figure B.2.7-13.** Tank temperatures.

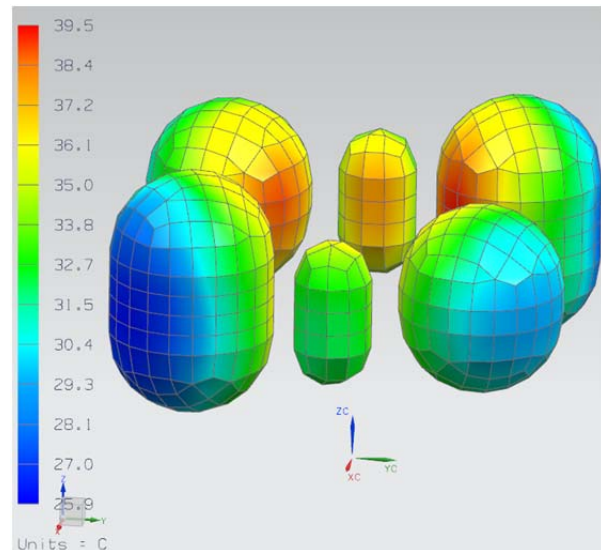


**Figure B.2.7-14.** Predicted tank temperatures, showing only the tanks.

tronics. The key drivers for the propulsion subsystem are to

1. Provide delta-V for maneuvers, including the JOI and EOI maneuvers.
2. Provide thrust vector control during main engine operation.
3. Provide for attitude control when the spacecraft is not using reaction wheels.
4. Provide for reaction wheel unloading.
5. Configure the system to maximize radiation shielding of the spacecraft electronics.

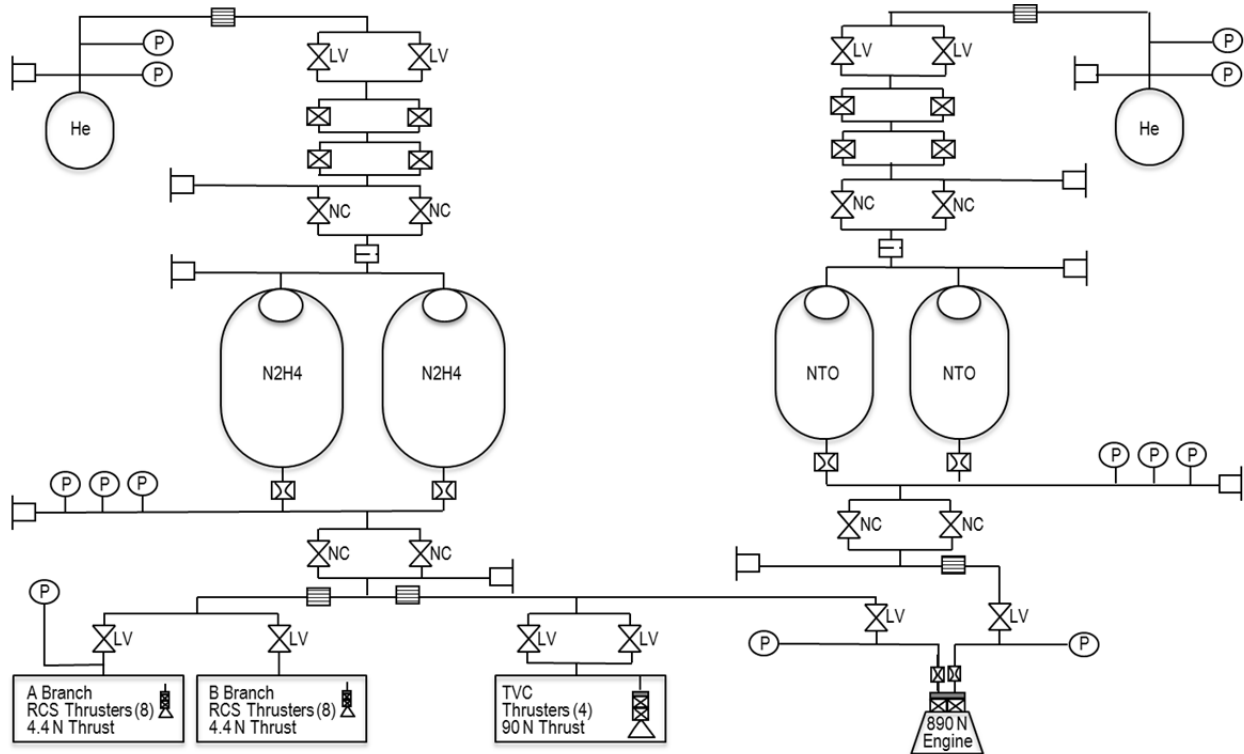


**Figure B.2.7-15.** Dual-mode, bipropellant propulsion subsystem schematic.

#### B.2.7.4.1.2 Propulsion Module Configuration

Figure B.2.7-16 shows that the Propulsion Module configuration is based on a core octagonal structure with the propellant tanks, pressurant tanks, and component plates mounted on the exterior sides of the octagonal structure. This configuration is driven by the desire to maximize the radiation shielding for the spacecraft electronics, mounted on the avionics module and located internal to the Propulsion Module core structure. Note that the propulsion components' plates are mounted perpendicular to the core structure (see Figure B.2.7-16). This is done because there is insufficient real estate to mount the component plates in a more traditional fashion (i.e., parallel) without increasing the length or diameter of the Propulsion Module. It was decided not to mount the component plates to an interior wall of the Propulsion Module because of limited accessibility during ATLO.

A single main engine, mounted using struts at the bottom of the Propulsion Module and pro-

truding through the Power Source Module, provides for primary delta-V. The RCS and TVC thrusters are mounted on four thruster cluster assemblies (TCAs), which in turn are mounted on struts extending away from the spacecraft. This configuration is very similar to that of the Cassini RCS. Each TCA contains four RCS thrusters (two primary and two redundant) and a single TVC thruster. The RCS thrusters are redundant, in that there are two strings of eight thrusters. Each string of eight thrusters is isolated by a single latch valve. The RCS thruster configuration provides for coupled thrust about the Z-axis (roll) and uncoupled thrust in pitch and yaw, identical to the Cassini configuration. Both the main engine and TVC thrusters are single-string in the current concept. A detailed trade of complexity vs. redundancy will be conducted in Phase A to confirm or modify this decision.

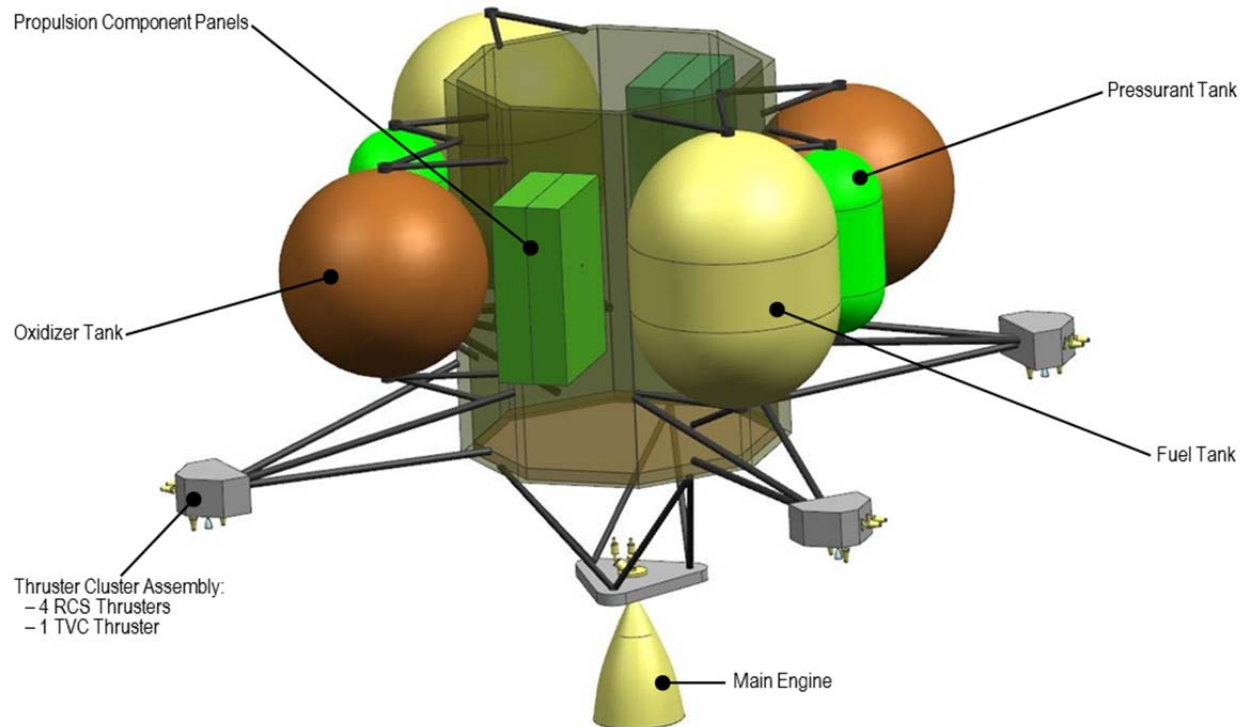


**Figure B.2.7-16.** Propulsion module configuration.

#### B.2.7.4.1.3 Propulsion System Design

##### Engines and Thrusters

An 890-N (200-lbf) main engine operating at a nominal mixture ratio of 1.0 with a minimum specific impulse of 323 seconds has been baselined for the Orbiter Mission concept. As currently planned, the engine is required to support a JOI maneuver on the order of 60 minutes and an EOI maneuver on the order of 25 minutes.

It should be noted that the engine interior wall will most likely have an oxidation-protective coating, which could be subject to micrometeoroid damage. The actual risk of failure and time to failure caused by damage is unknown, and likely indeterminate. The presented concept does not include an engine cover but the design does not preclude its addition either. The decision to include an engine cover will be reevaluated during Phase A.

The TVC thruster currently assumed for the Orbiter spacecraft is the Aerojet MR-107T thruster (or equivalent), providing approxi-

mately 90 N (20 lbf) of thrust. A preliminary analysis has been performed by ACS personnel showing that this thruster provides adequate control authority for the vehicle during main engine operation. The RCS thruster currently assumed is the Aerojet MR-111 thruster (or equivalent), providing approximately 4.4 N (1 lbf) of thrust. Both thrusters are qualified for flight and have high heritage.

##### Pressurization System

The baselined pressurization system allows for independent pressurization and regulation of the oxidizer and fuel tanks. Rather than using a traditional mechanical regulator, this system uses a set of four solenoid valves configured to be parallel and series-redundant (i.e., quad-redundant), allowing for electronic regulation using pressure transducer feedback. Flight software (FSW) would provide closed-loop control using pressure transducers measuring tank pressure. Three pressure transducers would be polled to protect from a transducer failure scenario. There are several advantages of this system over a more traditional pressuri-

zation system using mechanical regulators, especially for long-duration outer-planet missions:

1. Separate pressurization and regulation of the oxidizer and fuel tanks eliminates the risk of propellant vapor mixing in the pressurization system. It also eliminates the need for numerous check valves and pyro-valve isolation, reducing dry mass.
2. Elimination of the mechanical pressure regulator reduces the risk of regulator leakage. The series-redundant solenoid valves are less susceptible to leakage than are mechanical regulators.
3. The design allows for active control of the oxidizer and fuel tank pressures. This is advantageous because the oxidizer-to-fuel mixture ratio can be adjusted during the mission. It allows for more accurate control of mixture ratio, which in turn allows one to reduce residual propellant.

The schematic in Figure B.2.7-15 shows that the quad-redundant solenoid valves are isolated above by parallel redundant, high-pressure latch valves and below by parallel redundant, normally closed pyro valves. The pyro valves would remain closed until first use of the regulators is required.

Systems similar in concept to this have been used in the past on other spacecraft (e.g., MiTE<sub>x</sub> Upper Stage, Clementine, GeoLite, and Orbital Express).

#### *Propellant and Pressurant Tanks*

The propellant tanks are sized for a total propellant load of 2250 kg. This assumes the maximum launch capability of the Atlas V 551 LV on the 20 November 2021 launch window, providing a delta-V of 1.940 km/s. Table B.2.7-3 shows the rack-up of propellant, including residual and ACS propellant. The selected hydrazine tanks are 117 cm (46.0 in.) high by 89 cm (35.1 in.) in diameter (6% ullage), and the oxidizer tanks are a

89-cm (35.1-in.)—diameter sphere. The fuel tanks are based on the ATK P/N 80399-1 tank. The oxidizer tank is based on the ATK P/N 80350-1 tank.

The pressurant tanks are essentially off-the-shelf tanks and significantly oversized for the current propellant load. The pressurant mass load is 5.5 kg. The pressurant tank sizing will be optimized as the design matures.

#### *Propellant Isolation*

The propellant tanks are isolated from the thrusters using parallel redundant, normally closed pyro valves and low-pressure latch valves. The design provides sufficient mechanical inhibits to meet KSC launch safety requirements.

Careful design of the propellant tank surface-tension propellant-management devices (PMDs) and the venturis downstream of the tanks will be necessary in order to prevent propellant transfer between the two tanks, or preferential draw of propellant from one tank. It may be necessary to take more positive measures to prevent propellant transfer, such as the addition of latch valves to isolate the propellant tanks from each other when not in use. Further detailed analyses will be required before this design can be finalized.

#### *B.2.7.4.1.4 Heritage*

The majority of the components used in the Orbiter propulsion system are flight qualified and considered off-the-shelf. This includes the RCS thrusters, TVC thrusters, service valves,

**Table B.2.7-3.** Maximum propellant load case for Orbiter spacecraft propellant tank sizing.

Required Propellant	Mass (kg)
Propellant load for 1.940 km/s delta-V	<b>2054</b>
Hydrazine (MR=1.0)	1027
NTO	1027
Hydrazine for TVC	101
Allocation of ACS propellant (N <sub>2</sub> H <sub>4</sub> )	40
Hydrazine residual/hold up (2.5%)	29
NTO residual/hold up (2.5%)	26
Total hydrazine	1197
Total NTO	1053
<b>Total Propellant Load</b>	<b>2250</b>

pressure transducers, filters, and latch valves. As discussed above, the baselined main engine will require a full qualification program. Regarding the propellant tanks, it is the study team's intent to size them based on a heritage design that makes use of qualified hemisphere forgings. The current design makes use of a 89-cm (35.1-in.) tank, but will likely require a change in length of the cylindrical section. In addition, a new PMD for the oxidizer and fuel tanks will need to be designed and integrated. Hence, the propellant tanks will likely require a new qualification test program. The study team is taking a similar approach with the pressurant tanks, using a qualified design that best meets the requirements for the Europa Orbiter Mission.

The pressurization system, which makes use of electronic regulation, will need to go through a program that develops and qualifies it as an integrated system, including the propulsion hardware, controller, and FSW.

#### B.2.7.4.2 Propulsion Module Structure

The Propulsion Module (Figure B.2.7-17) supports the fuel tanks, attitude-control thrusters, propellant-isolation assembly (PIA), pressurant-control assembly (PCA), and main engine. The propulsion fuel tanks are supported by bipod and tripod combinations and are attached to the primary structure. The main engine is attached at the bottom and extends

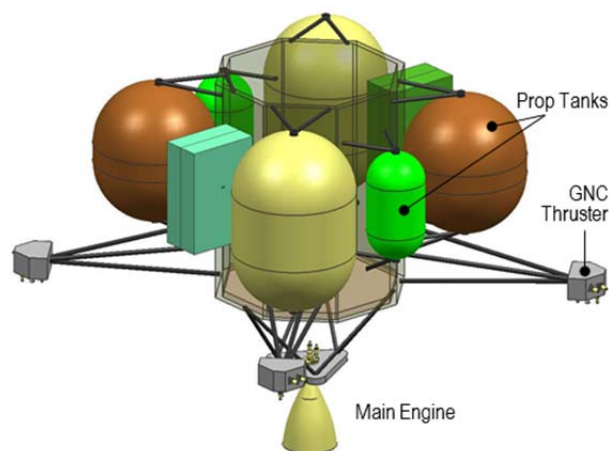


Figure B.2.7-17. Propulsion module.

through and below the Power Source Module. Four thruster clusters are supported at the ends of four tripods and are located as far from the spacecraft's center of mass as the launch vehicle fairing envelop will allow. This configuration maximizes thruster-control authority, and minimizes both plume-impingement forces and fuel required. The PIA and PCA are attached together, back to back and parallel to each other. The PIA/PCA assembly is in turn attached to the Propulsion Module's primary structure.

The Propulsion Module's primary structure has triangular holes in the wall at the location where the warm avionics has a radial view to the propulsion tanks. These holes allow for a direct radiation path to the tanks. In this region, the primary structure's wall thickness is increased to compensate for the holes. The necessary radiation shielding is still maintained due to the position of the tanks and the thickness of the vault.

#### B.2.7.5 Power Source Module

The Power Source Module (Figure B.2.7-18) would contain four ASRGs, the ASRG mounting structure and the launch vehicle adapter. Each ASRG provides a power and command interface to the spacecraft. The Power Source Module would be delivered directly to the launch site for integration. The thermal dissipation of the ASRGs inside the primary structure contributes to the overall thermal input inside the thermal shroud of the spacecraft. The main engine assembly of the Propulsion Module goes through the center of the Power Source Module with a thermal shroud protecting against the heat of the engine.

##### B.2.7.5.1 Power Source

The spacecraft power source interface is to an industry-standard defined power bus with 22 to 36-V range defined at the load interface. The power bus architecture is a direct energy transfer, with the power source interfacing with the power subsystem in the Avionics

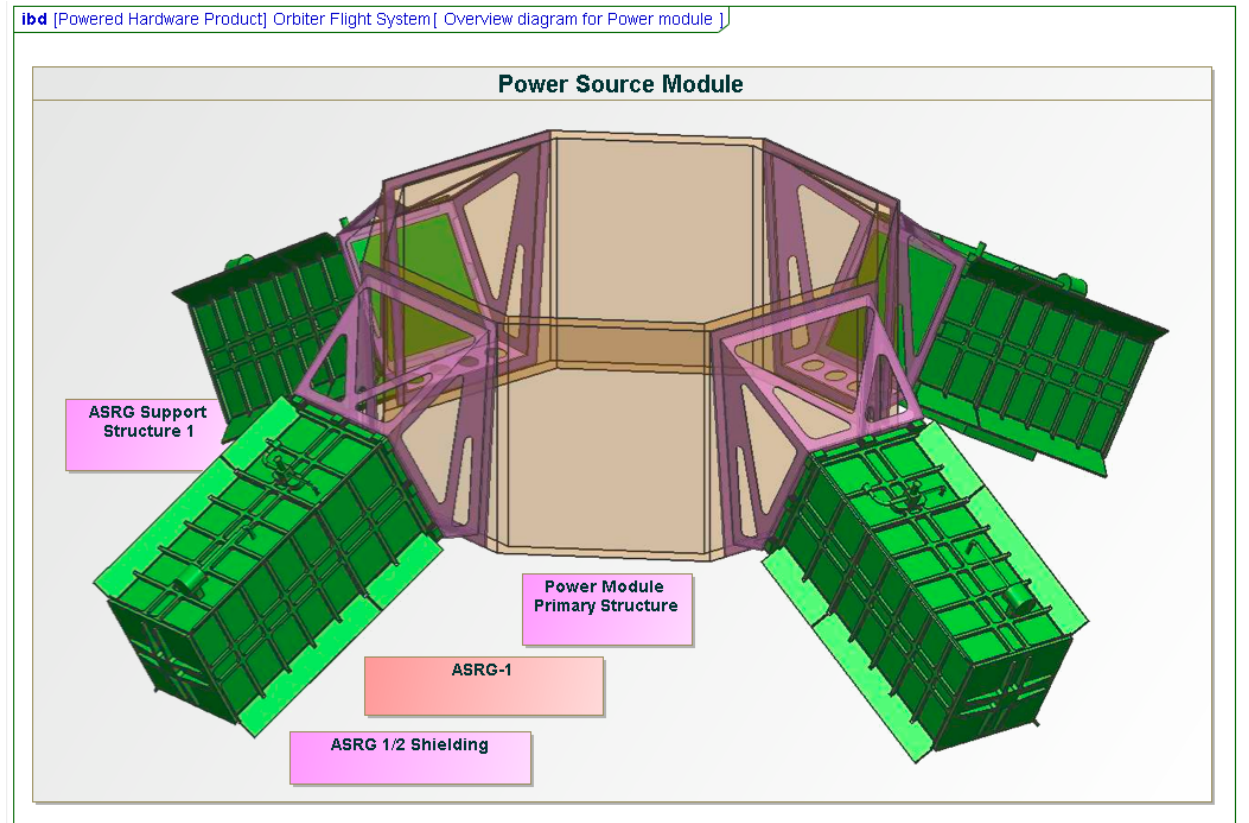
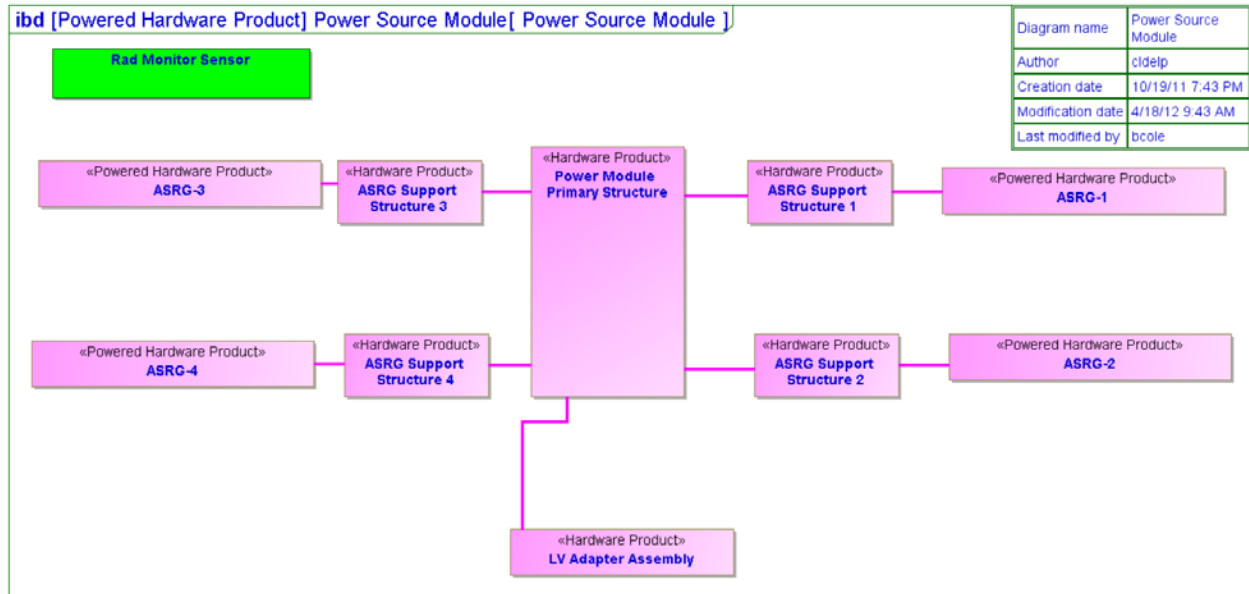


Figure B.2.7-18. Power Source Module block diagram as represented in the system model.

Module. The power subsystem electronics provides the power bus regulation.

*Power Source Drivers*

The key performance drivers for the power source are:

1. Provide 396 W at EOM after a single Stirling engine failure. (Each ASRG has two Stirling engines)
2. Provide a constant power over the nominal power bus voltage operating

range of 22 to 34 V as defined at the power source output.

3. Survive with a power bus voltage over the 34 V and less than 40 V for an indefinite period of time.
4. Provide a diminished power for the power bus voltage less than 22 V to support a bus overload recovery.

The power source is the combined contribution of four ASRGs.

#### B.2.7.5.2 ASRG

##### ASRG Functional Description

Each ASRG (Figure B.2.7-19) consists of two General Purpose Heat Source (GPHS) modules, two ASRG Stirling converters (ASCs), a generator housing assembly (GHA), a shunt dissipater unit (SDU), and an ASC controller unit (ACU).

The GPHS contains plutonium dioxide fuel pellets and is designed to meet all necessary safety and handling requirements. The GPHS produces a range of 244 Watts thermal (Wt) to 258 Wt at encapsulation when the fuel mixture is set in the pellet and placed in the module. From the point of encapsulation, the GPHS thermal output degrades with the radioactive decay rate of plutonium-238, which is approximately 0.8% per year. The study team is assuming that the average GPHS encapsulation will be 3 years before launch.

The ASC converts the thermal energy from the GPHS to AC electrical current using a piston and linear alternator. The ACU rectifies the AC power to DC power and provides it to the power bus with a constant power I-V curve over the power bus voltage range controlled by the spacecraft. The constant power I-V curve

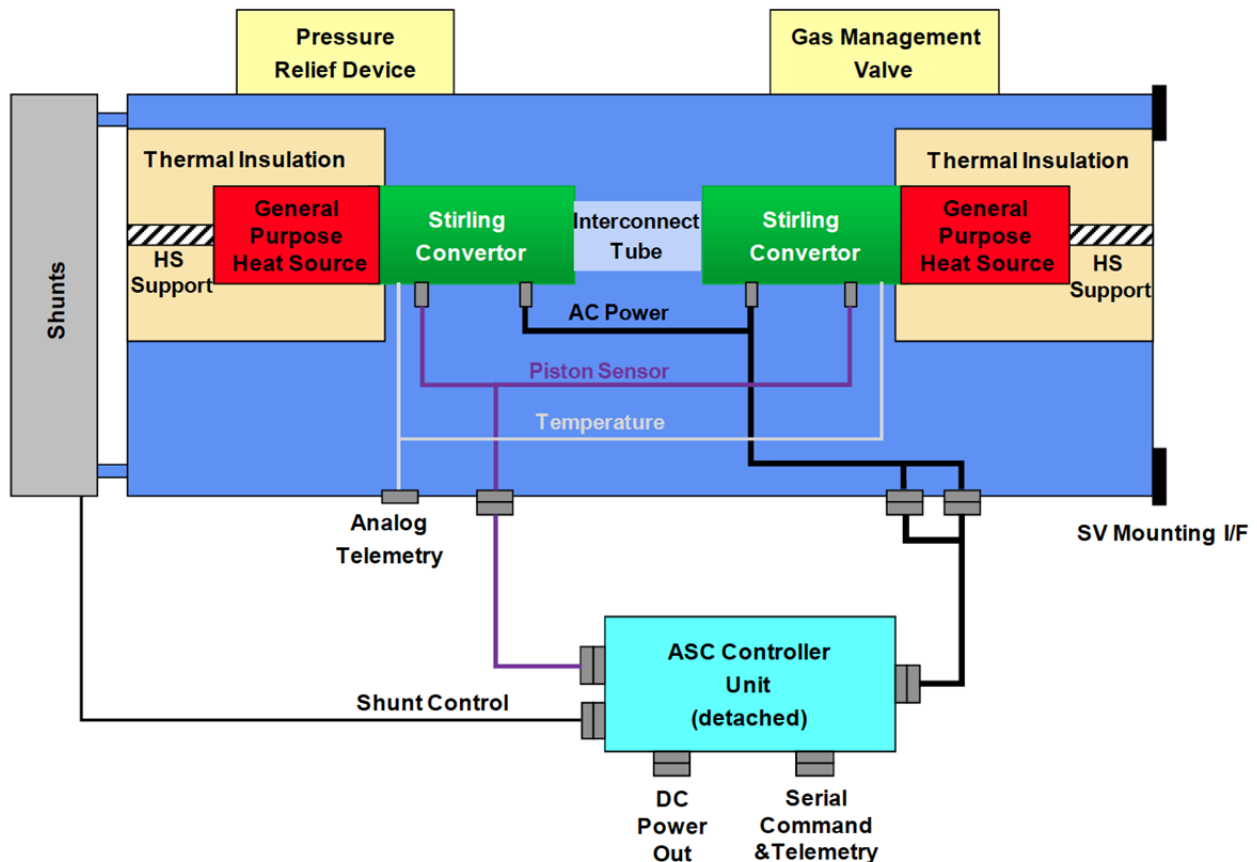


**Figure B.2.7-19.** The ASRG block diagram includes all functional elements that make up the ASRG, with the detached controller that provides the electrical interface with the spacecraft [HS=Heat Source].

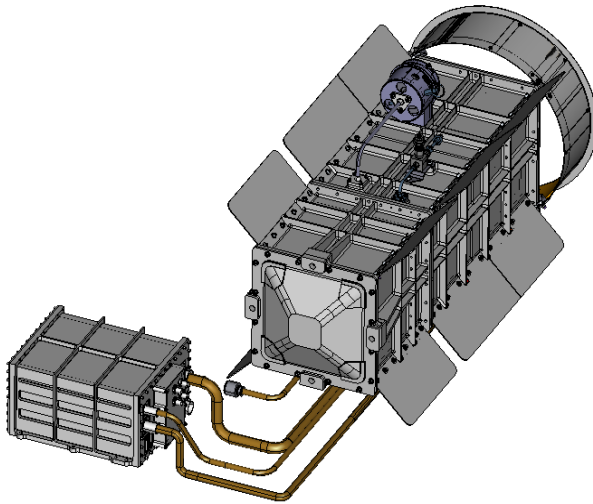


**Figure B.2.7-20.** ASRG CAD model shows the detached controller with cabling and outboard shunt radiator.

allows for more than one ASRG to be connected to the same power bus and share the power.

The ASRG protects itself if the bus voltage goes outside of the specified range of 22–34 V at the ASRG output. The ACU disengages the output from the power bus and shunts the power to the attached radiator if the bus voltage exceeds  $35\text{ V} \pm 1\text{ V}$ . The internal ASRG shunt regulator is independent of the spacecraft shunt regulator used to regulate the power bus. The ASRG shunt radiator is on the outboard end of the GHA and is used only for the off-nominal bus voltage. The power system maintains the bus voltage range at less than 34 V at the ASRG interface to prevent the disengagement. The ASRG reengages once the bus voltage drops back into the range. The ASRG provides a current limited to 3.5 A if the bus voltage drops below 22 V, enabling the system to recover by charging the battery.

The ACU is detached from the GHA (Figure B.2.7-20) and mounted on the inside of the Power Source Module primary structure.

The ACU is single-fault-tolerant with N+1 architecture (Figure B.2.7-21). The ACU needs to be within 3 meters due to impedance constraints from the controller. The ACU also

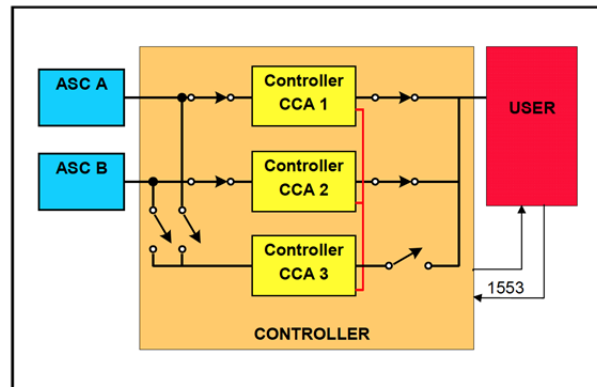


**Figure B.2.7-21.** ASC controller unit block diagram shows the spare controller # 3 that the internal fault protection switches to with the detection of a failure.

needs to be greater than 1 meter away to reduce self-generated radiation levels.

The ACU has internal fault protection to switch automatically to the spare controller board with the detection of a fault. ACU components are currently rated to 50 krad (radiation design factor of 2) total end of mission dose and would need significant additional shielding for use in the Europa Orbiter Mission environment. This additional shielding is included in the system level mass rollout.

#### B.2.7.5.2.1 ASRG Performance

The ASRG output power is a function of time and environment. The power graphs below show power output of the four ASRGs, with degradation due to natural decay of the plutonium dioxide fuel as a function of time from encapsulation, and assuming each GHA has a direct view to space (Figure B.2.7-22). The total power current best estimate (CBE) is with the nominal specified GPHS thermal output of 250 Wt at encapsulation. The total power specification is from the ASRG user guide with a BOM power at 130 W, failure of a single Stirling converter after launch, and 1% degradation per year. The lowest expected value (LEV) is with the minimum specified GPHS thermal output at 244 Wt at encapsulation, 1% degradation per year, and failure of a single Stirling converter after launch. The main difference between the Department of Energy

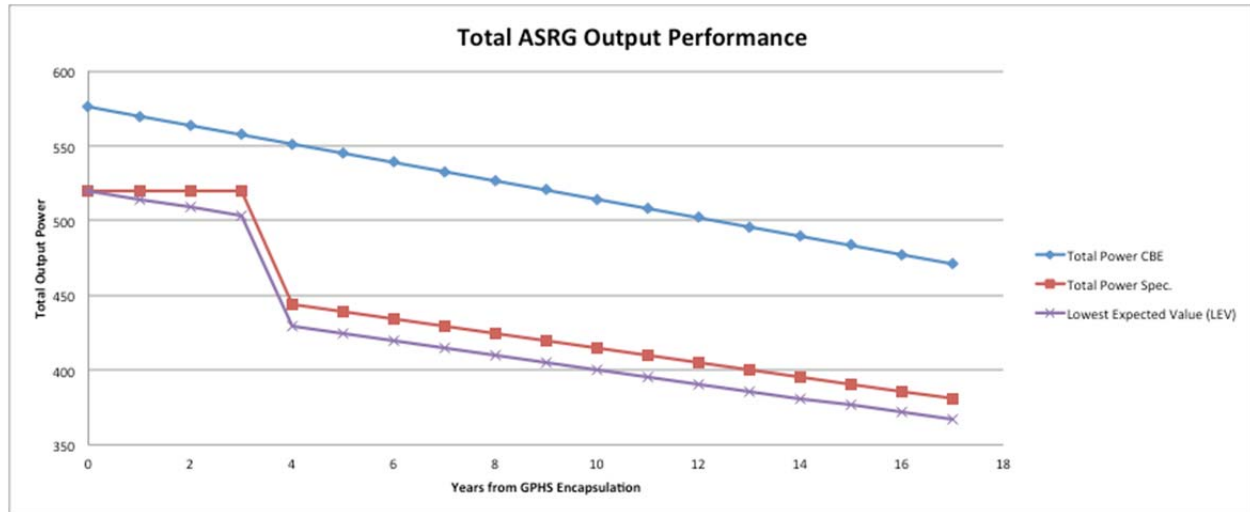


**Figure B.2.7-22.** From the comparison of the ASRG Output CBE to the specification and the LEV with a failure after launch, the LEV degrades performance from GPHS encapsulation; however the specification defines BOM after launch and degrades from that point on.

(DOE) specification and the Europa Study Team's LEV is that the study team chose to start the 1% degradation per year 3 years prior to launch at the average GPHS encapsulation date. With the Europa Orbiter Mission duration at 11 years, the study team expects at least 396 W at EOM.

The curve above assumes a direct view to space with a sink temperature equivalent to 4 K. The power output graph below shows the degradation as the sink temperature increases due to the environment (Figure B.2.7-23).

The spacecraft configuration uses the high-gain antenna and thermal blanket envelope to shade the ASRGs from the Sun within 1 AU. For the changing environment of launch, inner cruise, and Venus gravity assist, a command is sent to the ASRG to adjust the internal operational set point to make sure the ASRG is safe from over temperature which will impact the output power. This operation is independent of the power bus voltage set points controlled by the spacecraft. The spacecraft has adequate power margin for the expected environmentally impacted mission phases. The operation of the ASRG is covered in the ASRG Users Guide.

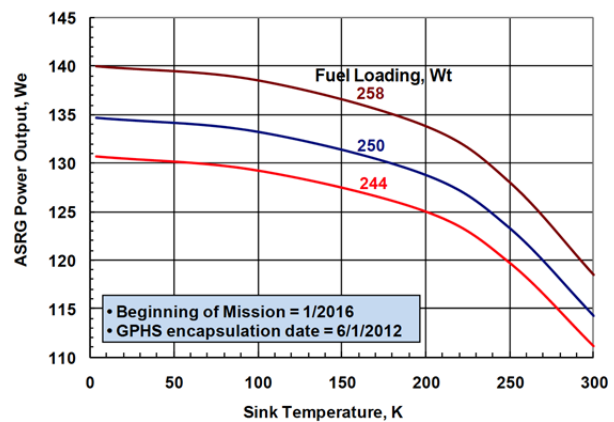


**Figure B.2.7-23.** ASRG output power vs. sink temperature shows that depending on the environment the output power will degrade. The ASRG power output power will depend on the view to space.

#### B.2.7.5.3 Structure/LVA

The four ASRGs and their avionics reside would on the Power Source Module (Figure B.2.7-24). The Propulsion Module's main engine assembly passes through the center but does not directly attach to the Power Source Module's primary structure.

Each ASRG has two opposing and cycling advanced Stirling converter (ASC) pistons. Because they oppose each other, vibration is greatly reduced. If one of these pistons failed to function, the single piston's vibration could

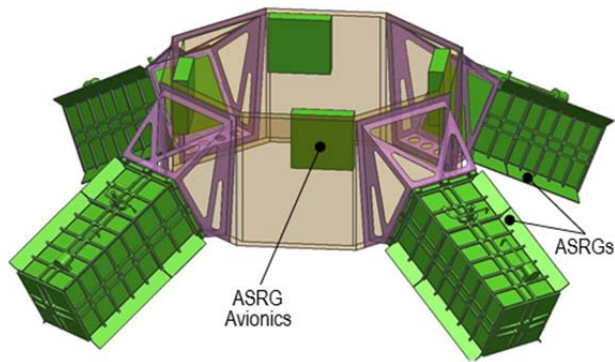


Figure B.2.7-24. Power module.

couple into the structure and imparted large loads on the spacecraft.

In the event of a failed ASC piston, the interface makes use of compression spring assemblies oriented parallel to the long axis of the ASRG. These spring assemblies provide a compliance that yields a 20-Hz axial frequency. At 20 Hz this spring mass system will not couple in with the ASC's frequency of 102 Hz. While the interface is designed to be compliant (20 Hz) axially, the stiffness is still high enough to ensure positive margin for the springs stress when exposed to ASRG launch accelerations.

Because the Power Source Module is the bot-

tommost module, it will experience the largest moment loads during launch. This will require its primary structure to have a slightly greater wall thickness than the propulsion and Avionics Modules.

At the bottom of the Power Source Module is the launch vehicle adapter (LVA, [Figure B.2.7-25](#)). The LVA provides for a transition between the octagonal geometry of the Power Source Module and the circular Marmon clamp separation interface.

#### B.2.7.6 Avionics Module

*The Avionics Module concept results in radiation shielding that enables the use of standard aerospace industry radiation-tolerant parts.*

The Avionics Module will be described in this section of the report. After an overview of the module, the following subsystems included in the Avionics Module will be discussed:

- Telecom
- Power
- Guidance, Navigation, and Control
- Command and Data Handling
- Software
- Structure, along with instrument accommodation

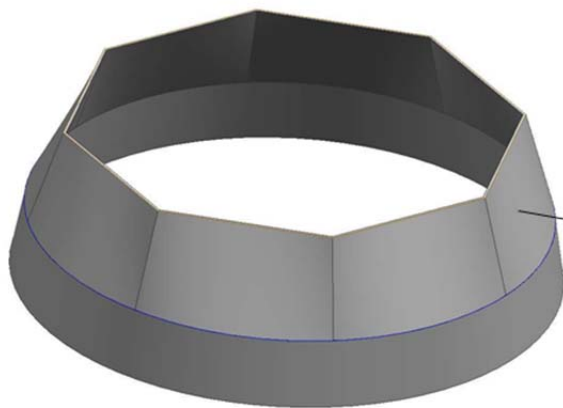
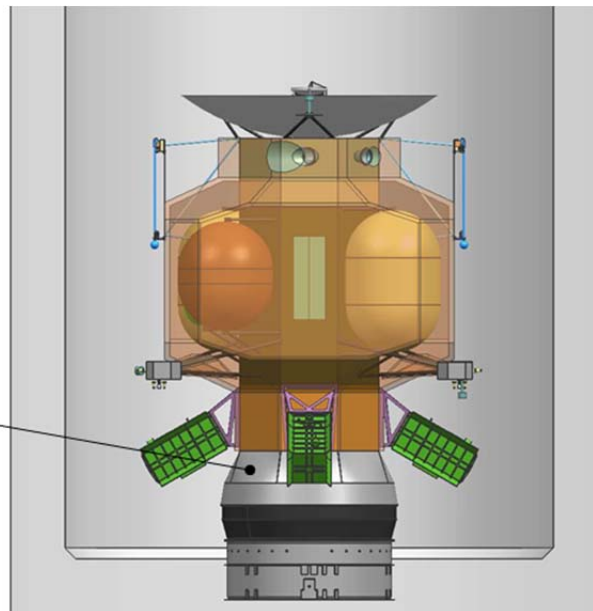


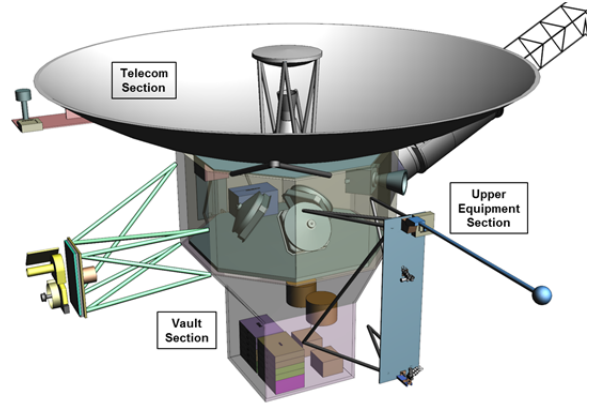
Figure B.2.7-25. Launch vehicle adapter.



Avionics Module Overview

The key design goals for the Avionics Module are:

- A modular design for parallel integration and test with propulsion and Power Source Modules
- A vault to shield a majority of the spacecraft electronics
- Enabling of late integration of instruments
- Simple interfaces with Propulsion and Power Source Modules



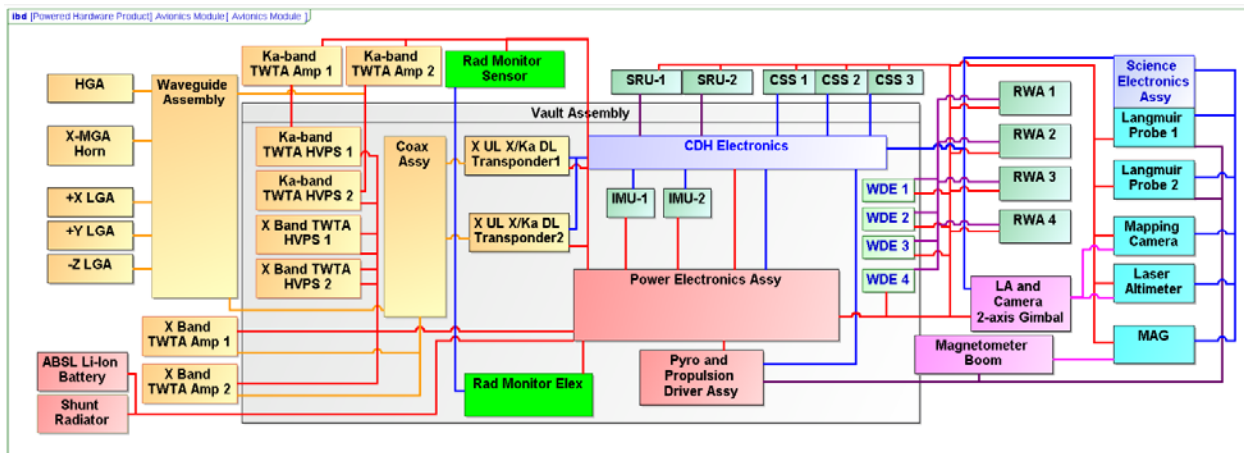
**Figure B.2.7-26.** The three sections of the Avionics Module (telecom, upper equipment, and vault) are configured for simple interfaces to enable parallel integration and test.

Figure B.2.7-26 shows the configuration of the Avionics Module. This module consists of three separate sections: the telecom section, the upper equipment section, and the vault section.

Figure B.2.7-27 shows the system block diagram of the Avionics Module. The red interfaces are 28-V power; the blue interfaces are data; and the gold interfaces are RF.

Inside the vault are the C&DH electronics (this box is internally redundant), the RWA electronics, the power electronics (this box is internally redundant), the pyro/propulsion drive electronics (this box is internally redundant), two block-redundant IMUs, and two block-redundant small deep-space transponders (SDSTs). Outside the vault are the instruments (MAG, LP, MC and LA) and science electron-

ics chassis. Also outside the vault are the following GN&C components: RWA mechanical assemblies, Sun-sensors, and SRUs. All the elements outside the vault are individually shielded for total-dose radiation; in the case of instrument and star-tracker detectors, the shielding also mitigates the effect of the electron flux. The Power Subsystem components outside the vault are the shunt radiator and battery (internally redundant). The Telecom Subsystem components outside the vault are the TWTAs, the coax, the waveguide, switches, and antennas configured in a single-fault-tolerant configuration for Ka-band and X-band communication.



**Figure B.2.7-27.** The system block diagram shows a majority of the spacecraft electronics protected in the vault.

### B.2.7.6.1 *Telecom Subsystem*

The telecom subsystem performs a triple role for the spacecraft: two-way communications with Earth, Earth-to-spacecraft ranging to support navigation as well as precision Doppler velocity measurements for Gravity Science.

#### B.2.7.6.1.1 *Driving Requirements*

There are a number of driving requirements for the subsystem. It must accept uplinked commands through all post launch mission phases as well as send to Earth engineering telemetry and science data. Key data rates required are

- Engineering telemetry: ~2 kbps
- Uplink commanding: ~1 kbps
- Safe mode commanding: ~7.8 bps
- Safe mode telemetry: ~10 bps
- Science data return: ~108 kbps

Implicit in these requirements is communications with the Deep Space Network (DSN) 34-m subnet for routine communications and the 70-m subnet for emergency/safe mode communications.

For Gravity Science, the Telecom System must meet a residual Doppler velocity requirement of 0.1 mm/sec at 60 second integration times. This is met through the subsystem's nominal two-way coherent communications mode through the HGA and the use of the DSN's 34m subnet.

The telecom subsystem is also required to be single-fault-tolerant. This drives the telecom subsystem architecture to include redundant transponders (small deep-space transponders [SDSTs]), redundant X-band and Ka-band travelling-wave tube amplifiers (TWTAs), a complex waveguide transfer switch (WTS) network, as well as a set of low- and medium-gain antennas. One X-band low-gain antenna (LGA) and the medium-gain antenna (MGA) are tolerant of a single WTS failure. Even though there is a single High Gain Antenna (HGA), the HGA features the capability of two

downlink polarizations for fault tolerance to a single failure in the telecom subsystem's transmitter/receiver hardware chain.

#### B.2.7.6.1.2 *Subsystem Features*

The implementation of the telecom subsystem includes X-band uplink and downlink capabilities as well as a Ka-band downlink. The Ka-band downlink enables the mission to meet science data volume requirements concurrently with stringent requirements for DC power. While the downlink data volume requirements could be met with X-band alone (assuming a much more powerful X-band TWTA), a trade study between available DC power and science data volume return informed the selection of a more DC-power-efficient architecture for high-rate science data. For the Europa Orbiter Mission, the use of Ka-band for high-rate science downlink directly reduces the number of ASRGs required to meet mission objectives.

The telecom subsystem features a 3-m-diameter X/Ka-band high-gain antenna (HGA), three LGAs, an MGA with dual polarizations, redundant 25-W (RF power) Ka-band TWTAs, redundant 20-W (RF power) X-band TWTAs, redundant SDSTs, and a complement of microwave waveguide and coax elements. The SDSTs are X-band uplink and downlink capable as well as Ka-band downlink capable. There is no capability or driver for Ka-band uplink.

#### B.2.7.6.1.3 *Block Diagram*

As shown in the telecom subsystem block diagram (Figure B.2.7-28), the equipment configuration is based upon many years of deep-space communications heritage. For example, the -Z LGA is fault-tolerant to a single WTS failure; this provides a robust fault-tolerance posture for communications during the inner-cruise portion of the mission when the spacecraft is required to use its HGA as a sunshield. The LGA configuration enables communications through all cruise periods out to approximately 2 to 3 AU from Earth after which the MGA takes over the safe-mode and

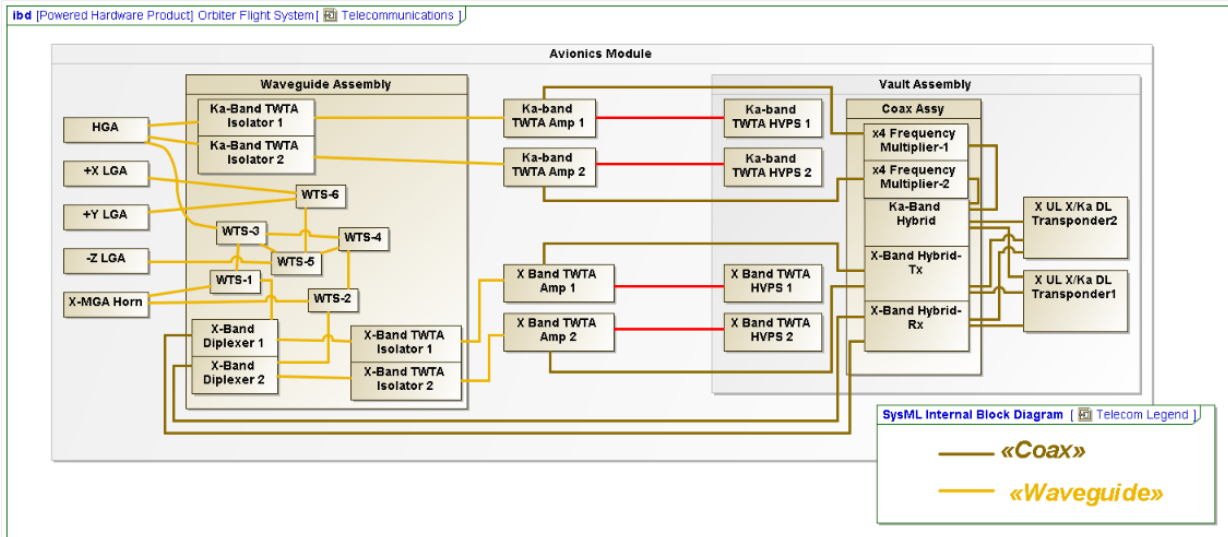
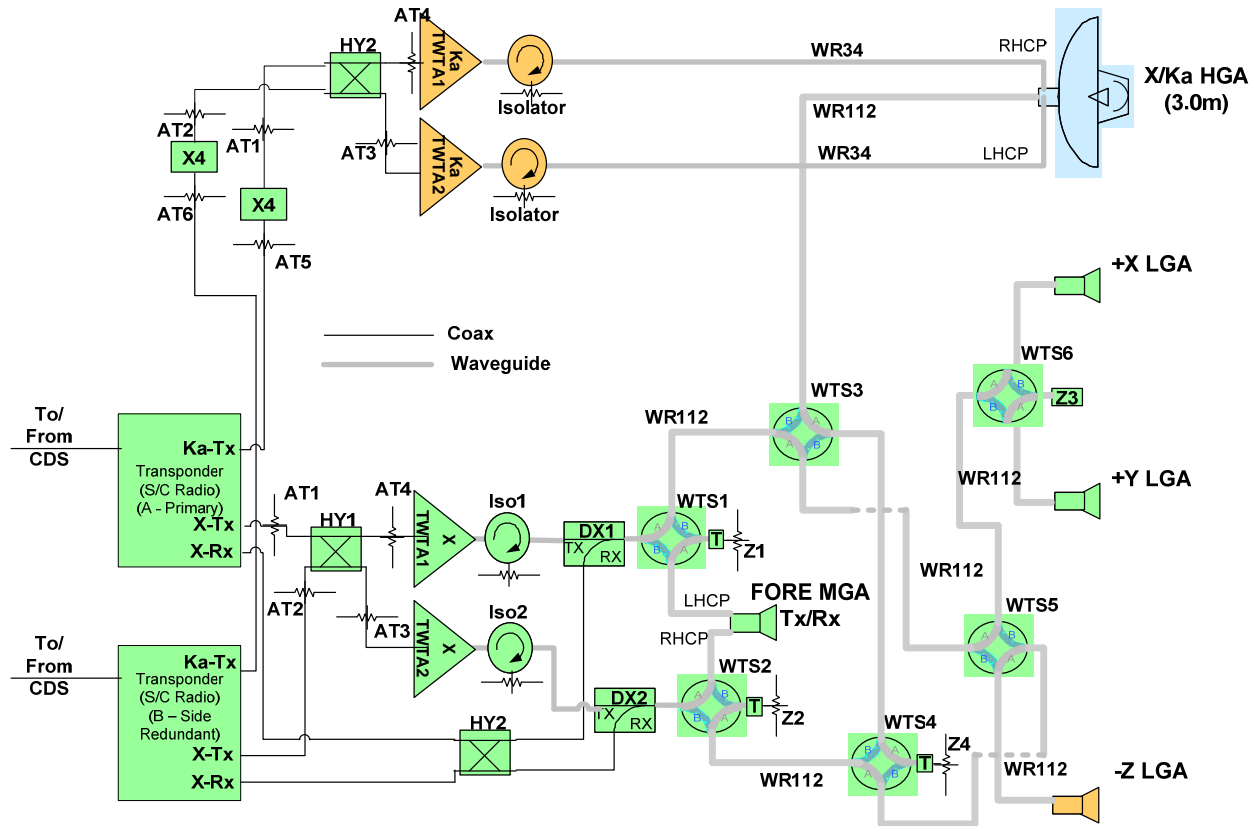


**Figure B.2.7-28.** The telecom subsystem provides robust fault-tolerance through a simplified architecture that minimizes potential for single-point failures.

general cruise communications. Ka-band downlink redundancy is provided through the use of redundant hardware chains and downlink antenna polarizations. This simplified architecture promotes a more robust system

fault-tolerance than could be achieved with the inclusion of an additional WTS to switch between the redundant downlink TWTAs. Similarly, for the X-band uplink an RF hybrid is used (HY2) in place of a WTS. This alone eliminates a potential single-point failure in

the critical X-band uplink path. Similarly the MGA has dual polarizations that enable single fault tolerance safe mode communications at Europa. Overall the Telecom Subsystem presents a robust fault tolerance and presents a low risk posture for the mission.

#### B.2.7.6.1.4 Equipment Heritage

Hardware heritage comes from a number of previous missions. The HGA will be similar to the Juno HGA, but scaled up from Juno's 2.5-m-diameter HGA to 3 m. The Europa Orbiter Mission's HGA will leverage technology developed for the Juno HGA reflector (Figure B.2.7-29) to meet the surface-tolerance requirements for precision Ka-band pointing and efficiency.

The Juno HGA optics will be redesigned to improve Ka-band performance for the Europa Orbiter's high-rate downlink communications requirements.

The TWTAs have heritage from multiple JPL missions: Juno, Dawn, and MRO (X-band) and Kepler (Ka-band). A good example here is the X-band TWTA for the Dawn mission, shown in Figure B.2.7-30. We propose to leverage a long history of downlink TWTAs designed specifically for the requirements of deep-space missions.

The concept proposes to use the SDST, a very mature product, to provide the mission-critical



**Figure B.2.7-29.** Juno's 3-m HGA (X/Ka-band) provides the basis for the Europa HGA.

uplink and downlink function. The SDSTs have heritage from Juno (X/X/Ka-bands), Dawn (X-band), MRO (X/X/Ka-bands), MSL (X-band), Kepler (X/X/Ka-bands), and others. A candidate SDST, flown recently on the Dawn mission, is shown in Figure B.2.7-31. Due to the extensive heritage inherent in the SDST product line, the use of the SDST lowers the overall residual mission risk.

#### B.2.7.6.1.5 Characteristics and Sizing

The telecom subsystem downlink data rate must be at least 108 kbps during Europa science operations. The telecom link budget is designed to meet this requirement with the parameters shown in Table B.2.7-4.

The HGA is body-fixed to the spacecraft and requires a  $\leq 1$ -mrad pointing accuracy to meet

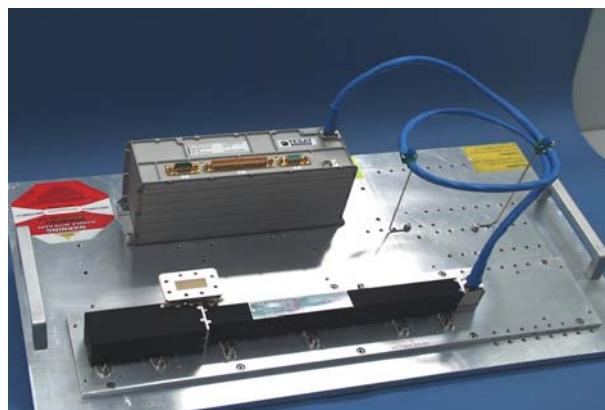


**Figure B.2.7-30.** Candidate X-band TWTA (flown on MRO, MSL, and Dawn).



**Figure B.2.7-31.** The SDST product line provides the mission-critical communications link to Earth.

**Table B.2.7-4.** Telecom link budget.

Parameter	Required Capability	Notes
Throughput Rate (worst case)	108 kbps	Average = 1.2 × worst case
Gravity Science Residual Doppler	≤0.1 mm/sec @ 60 second integration	Met with Two-Way Coherent Mode
TWTA RF Power	25 W (Ka), 20 W (X)	2× for Power Dissipation
HGA Diameter	3.0 m	Body fixed HGA, 60% efficiency
HGA Pointing Error	≤1.0 mrad	Reaction-wheel control
DSN Weather	90% cumulative dist.	
Canberra Elevation	20°	Worst-case, fixed
Earth S/C Range	5.5 AU	Average mission design
Hot Body Noise	16 K	About 0.6 dB loss
Turbo Coding	Rate=1/6, 8920-bit frame	
TWTA to HGA Losses	2 dB	Conservative estimate
Link Margin	3 dB	Per Institutional guidelines
SEP Angle	20°	Worst-case assumption
Operational Configuration	X-band up, Ka-band down	X-band downlink for safe mode & cruise
Hardware Configuration	X-band up, X/Ka-band down 3 LGAs, MGA, HGA, TWTAs	Possible X-band SSPA in lieu of TWTA

communications throughput requirements. A conservative approach was taken with the telecom link by requiring 3 dB margin minimum and by making conservative estimates of individual contributors to the link. Parameters such as RF losses in the downlink path, DSN station performance due to low station elevations, link degradation at low Sun–Earth pointing (SEP) angles and Jupiter’s hot-body noise at Ka-Band are all taken into account. Overall, the X-band and Ka-band communications links are conservative and robust.

The LGA complement provides full  $4\pi$ -steradian coverage; this enables command uplink at any spacecraft attitude. Spacecraft communications during the inner cruise portion of the mission (<1 AU solar distance) use a single-fault-tolerant LGA (-Z LGA). The distances to Jupiter, however, prevent LGA communications at the required safe mode rates. To meet safe mode communications rate requirements, an MGA is needed. All high-rate communications are performed through the HGA. Turbo coding at rate = 1/6 is also part of the baseline communications architecture.

#### B.2.7.6.2 Power

The Orbiter Power subsystem electronics and energy storage provide the power bus regulation and distribute power to the loads.

#### B.2.7.6.2.1 Power Performance Drivers

1. Single-fault-tolerance.
2. Provide energy storage mission load profile.
3. Provide power bus regulation.
4. Provide battery charge control.
5. Distribute power to the loads.
6. Actuate valves.
7. Fire pyro events.

#### B.2.7.6.2.2 Power Subsystem Description

The power subsystem electronics regulates the power bus and distributes power to the loads on the spacecraft. The power subsystem will provide energy storage to cover the transient load profiles of the different Orbiter Mission scenarios. It is single-fault-tolerant, using a combination of block-redundancy with crossstrapping and some majority-voted functions. It provides the valve-drive and pyro-firing functions with range and mission safety inhibits for the hazardous functions.

The power subsystem consists of an ABSL Li-ion battery, a shunt radiator, a shunt driver slice (SDS), two multimission power switch slices (MPSSs), two power bus controllers (PBCs), two power converter units (PCUs), two pyro-firing cards (PFCs), and four propulsion drive electronics slices (PDEs) (Figure B.2.7-32).

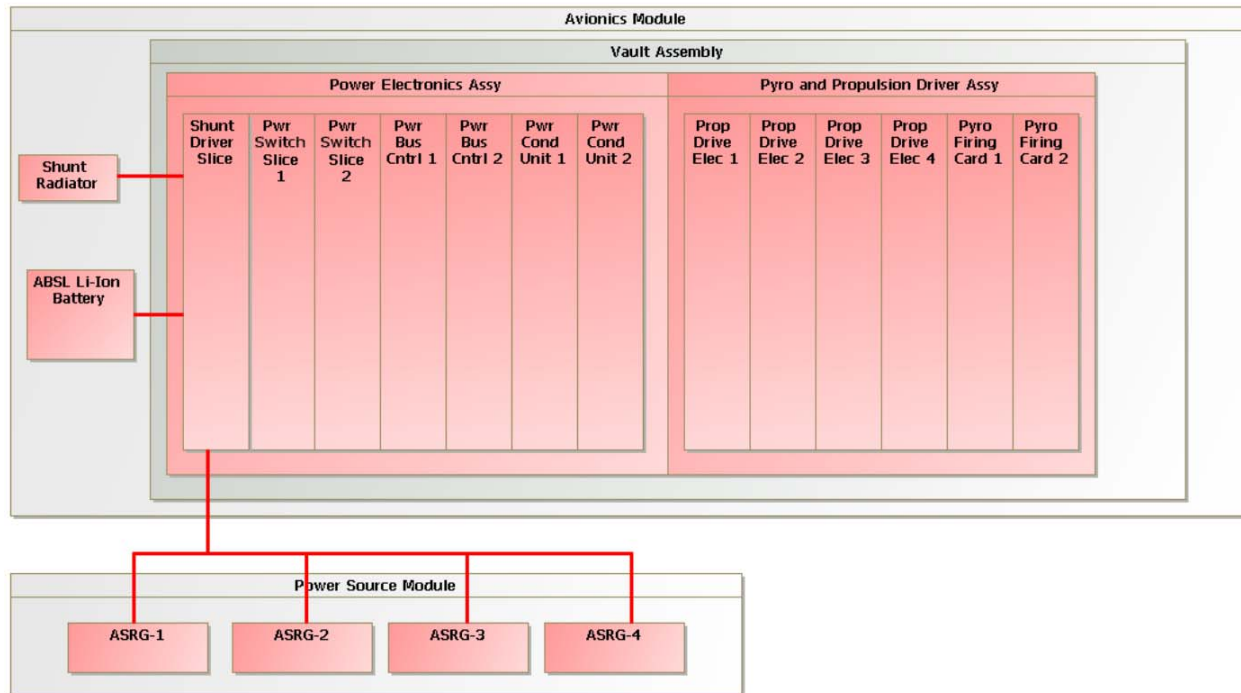


**Figure B.2.7-32.** Power subsystem block diagram is captured in the SysML model. The figure shows that the battery and shunt radiator are outside the vault.

#### B.2.7.6.2.3 Power Control

The PBC slices provide the SpaceWire command interface to C&DH. The PBC provides a low-power serial data bus to all of the other power electronics slices. It converts the commands from C&DH via the SpaceWire interface and distributes them to other slices through the low-power serial data bus. The PBC collects the power subsystem telemetry and makes it available to C&DH via the SpaceWire interface.

The PBC contains the control algorithms for regulating the power bus by commanding the shunt switches in a shunt regulator. The ASRG power source has a constant power I-V curve over a power bus voltage range of 22 to 34 V at the ASRG output. The control function senses the current in the battery and adds or subtracts shunt current to limit the battery charge current to a C/5. The PBC commands discrete shunt driver switches in the SDS that drive power to the shunt radiator to control the power bus. The current regulation will taper to 0 current at the voltage set point correlating to

the desired state of charge. Power analysis uses 32.8 V as the 100% state of charge for the selected Li-Ion battery technology. The PBC has several commanded set points to set the battery at the desired state of charge.

The energy storage technology used for this study is the same small-cell ABSL Li-ion battery used on the Soil Moisture Active Passive (SMAP) mission (Figure B.2.7-33). The battery is configured with eight cells in series to get the desired bus voltage operating range, and 52 cells in parallel to get the desired 59 Ah of energy storage at the beginning of life. It has a capability of 40 Ah at EOM after a single-string failure, including degradation for life, discharge rate, and operating temperature. The reference scenario that defines the energy storage for the Orbiter Mission is the 2-hour JOI, which requires 13 Ah at 10°C with a 6.5-A discharge rate. The JPL Design Principles (DPs) allow for a 70% depth of discharge (DOD), making a 19-Ah battery adequate for the Orbiter Mission (JPL 2010a).

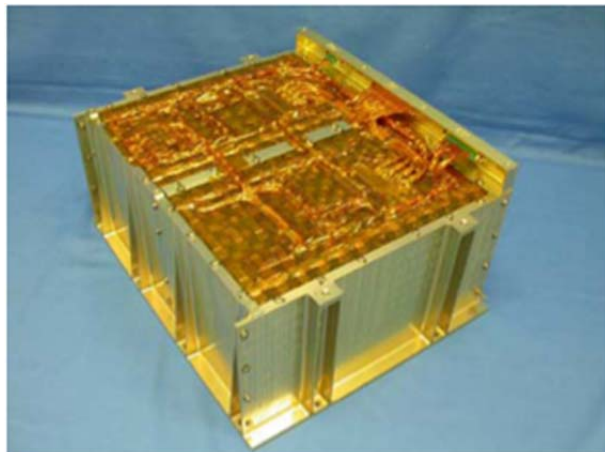


**Figure B.2.7-33.** Small-cell ABSL reference battery is the same size as the SMAP battery configured with 8 cells in series and 52 strings in parallel (Model Number 8S52P).

The small-cell battery approach does not implement individual cell monitoring and balancing due to the matched cell behavior; however, a trade between the large cell with cell balancing and the small cell needs to be studied for this lifetime. This will be considered in Phase A.

#### *B.2.7.6.2.4 Power Distribution*

The power distribution function is a combination of centralized power switches in the MPSS and distributed power switches on the primary side of each PCU. This combination enables the system to optimize the mass of the cabling by using centralized switches for heater buses and other loads that do not require a PCU and distributed switches for each PCU, reducing the point-to-point cabling for the major subsystems. The slice packaging approach enables the addition of centralized power switches while impacting only the mechanical footprint and cabling without modifications to a chassis or backplane. The command and telemetry interface is handled by the addition of addresses on the serial bus implemented in cabling. The thermal interface scales with the mechanical footprint.

Independent high- and low-side switches prevent any single failure from resulting in a stuck-on load. Commanding is cross-strapped

to the power switches through each PBC such that no single failure will prevent the commanding of any power switch. Each set of load switches is part of the load fault-containment region regardless of the location as a centralized or distributed switch.

#### *B.2.7.6.2.5 Power Conversion*

The power conversion function for each subsystem uses a distributed point of load (POL) architecture (Figure B.2.7-34). The approach has a single isolated power converter on the PCU board, providing an intermediate power bus voltage that is distributed to each subassembly in the subsystem. The front end of each subassembly can cross-strap the intermediate power bus and provide on and off capability with fault protection to enable low-power operating modes and improve subsystem fault-containment regions. The primary side power switch is controlled by the power subsystem, and the POL regulators are commanded by the subsystem.

#### *B.2.7.6.2.6 Pyro Firing and Valve Drive*

The pyro-firing and valve-drive functions are provided by a set of centralized power switches in the power subsystem electronics commanded by C&DH via the PBC. The PFCs are fail-safe off, with two cards providing the block-redundancy. Each PFC fires 32 NASA Standard Initiators (NSIs) from a protected load power bus that provides all of the safety inhibits required for launch. The PFC controls the current into each NSI, with an overall capability to fire six simultaneous events.

The PDE actuates the valves for the main engine and the ACS thrusters. The PDE also switches power from the protected load bus with the necessary safety inhibits in place. The PDE is fail-safe off with the single-fault-tolerance provided by a block-redundant set.

#### *B.2.7.6.2.7 Power Subsystem Heritage*

The power subsystem uses the same architecture as SMAP, and many of the slice designs are the same. The power bus control algorithm

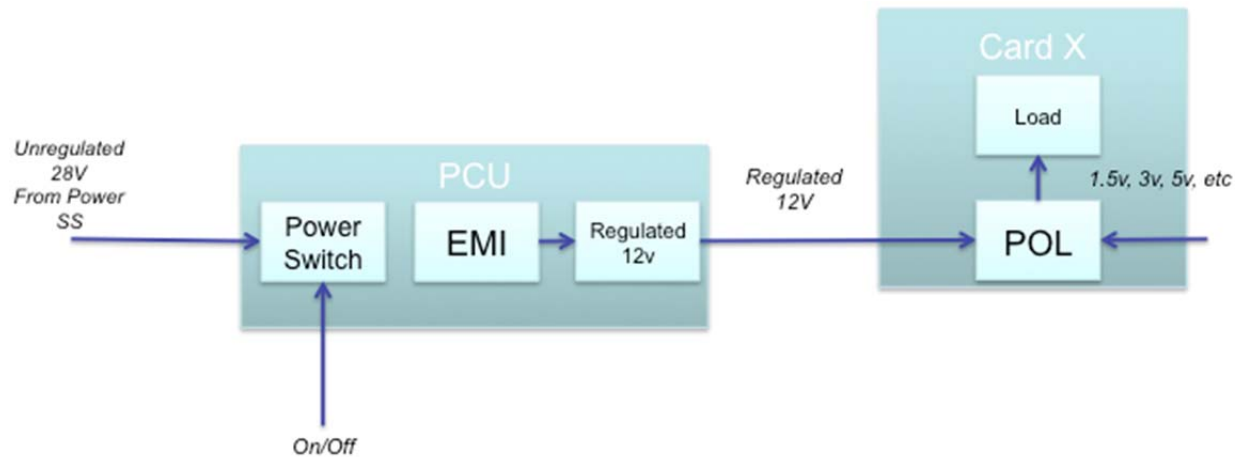


**Figure B.2.7-34.** POL power conversion architecture shows the primary power bus interface with distributed switch controlled by the power subsystem. The distributed POL converters are controlled by the local subsystem.

is the same as used on SMAP, as is the slice packaging design and designs for the PFC and PDE. The MPSS is the high-side and low-side variant of the design used on SMAP. The PBC has a new command interface, but the control of the shunt regulator is the same as for SMAP. The ABSL battery is the same design as used on SMAP, and the cell technology has flight heritage with Kepler.

#### B.2.7.6.3 Orbiter Guidance, Navigation, and Control (GN&C)

*The Orbiter GN&C provides a stable platform for science data collection and telemetry transmission.*

##### Functional Drivers

The GN&C subsystem provides three-axis attitude control through all mission phases to meet the instrument and engineering pointing needs. During TCMs, EOI, or JOI, when the fixed main engine is used, the GN&C provides thrust vector control using dedicated TVC thrusters mounted on the thruster clusters. During Europa orbital science, the spacecraft points the HGA towards Earth to downlink the science data/perform gravity science while using a two-axis gimbal to nadir point the LA/MC.

##### Features

The C&DH subsystem hosts GN&C software, which is developed in a GN&C design and simulation environment. The RWA, IMU, and

SRU are heavily shielded from radiation, allowing the use of standard space products. The SRU head with detector is shielded to reduce the electron/proton flux so that 4<sup>th</sup> magnitude and brighter stars can be tracked. The Europa Study team analyzed attitude determination capabilities in the Europa environment and demonstrated a pointing-knowledge capability exceeding the requirements for HGA pointing. All known targets will be stored onboard, enabling ephemeris-based tracking; Cassini experience indicates that this reduces the operation complexity. Finally, the use of thrusters for TVC reduces the development cost for a gimbaled engine and reduces the number of unique interfaces on the vehicle.

##### Key Characteristics

Table B.2.7-5 shows the key characteristics of the GN&C subsystem. The RWA sizing of 25 Nms is driven by environmental momentum accumulation. This was sized based on vehicle inertias and a desaturation rate of twice per day. Figure B.2.7-35 shows the thruster configuration. The attitude-control thruster sizing of 4.45 N provides a sufficiently small minimum torque impulse for deadband attitude control during interplanetary cruise (or safe mode). The TVC thruster sizing of 40 N provides sufficient control authority for up to a 9-centimeter shift of the vehicle center of mass

**Table B.2.7-5.** The GN&C subsystem design provides an agile platform with precise pointing control.

Item	Value	Sizing
<b>RWA Momentum</b>	25 Nm	Handle gravity gradient momentum accumulation
<b>Attitude-Control Thruster Size</b>	4.45 N	MTIB for deadband control during cruise/safe mode [spell out, as in FB chapter]
<b>TVC Thruster Size</b>	40 N	TVC control for CM offset
<b>Ka Pointing</b>	1 mrad	Support HGA link budget at required data rate with 3 dB of margin
<b>X Pointing</b>	112 mrad	MGA communication while Sun-pointing
<b>LA Pointing Knowledge</b>	1.7 mrad	Pointing knowledge induced altitude error, derived from science traceability requirement
<b>MC Pointing Knowledge</b>	5 mrad	Mapping strip alignment, 1% of FOV

during the mission. Ballast mass is also included in the MEL to provide initial CM/CG alignment. For attitude control and TVC, a thrust-moment arm of approximately 2 meters is used.

The 1-mrad pointing is a radial, three-sigma number derived from the telecom link analysis. Based on error budget analysis of the inertial and stellar reference assemblies in the expected radiation environment, this can be met with a capability of 0.25 mrad (per axis, three-sigma) pointing knowledge. The attitude knowledge is driven by the radiation capability of the SRUs. The X-band pointing for safe mode is 112 mrad based on a beam width that allows Sun-pointing with Sun-sensors while still communicating with Earth from Europa. The pointing knowledge to support laser altimetry is derived as an error budget allocation from the 10-cm accuracy requirement. The pointing knowledge to support surface mapping strip alignment is derived as an error budget allocation from the 1% FOV accuracy requirement.

#### Block Diagram

Figure B.2.7-36 shows the block diagram of the GN&C Subsystem. At the center of the

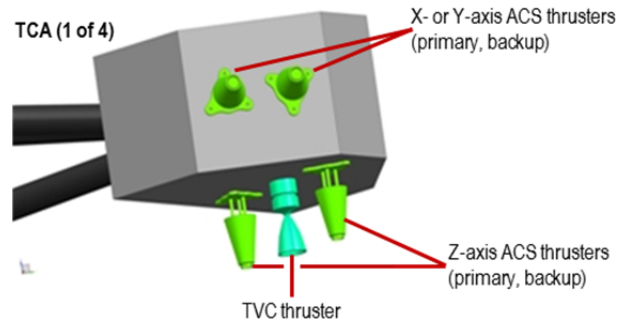


**Figure B.2.7-35.** The Orbiter thruster configuration leverages the proven Cassini approach.

subsystem is the FSW that resides in the RAD750 processor within the C&DH electronics. For Sun-pointing modes of operation, the Sun vector with respect to the vehicle reference frame is provided by the three Sun sensors distributed on the Avionics Module to provide near- $4\pi$  steradian coverage; if there are any gaps in the coverage, a spiral scan attitude maneuver can quickly bring the Sun into a sensor's FOV. For precise attitude determination, a combination of inertial measurements corrected by stellar updates is provided by the IMUs in the radiation vault and shielded SRUs outside the vault.

For precision attitude control, three of four RWAs are used; these are desaturated as needed by the attitude-control thrusters. The RWA wheel-drive electronics are in the vault; mechanical assembly is outside the vault. For less precise attitude control during cruise or during safe mode, the attitude-control thrusters can be used. For attitude control during TCM, EOI, or JOI (when the main engine is fired), the TVC thrusters are used for pitch/yaw control, while the attitude-control thrusters are used for roll control.

The architecture is cross strapped such that any SRU can be used with any IMU to provide the attitude information to any computer. Attitude control can occur with any three of four RWA or with any set of 8 block-redundant thrusters.

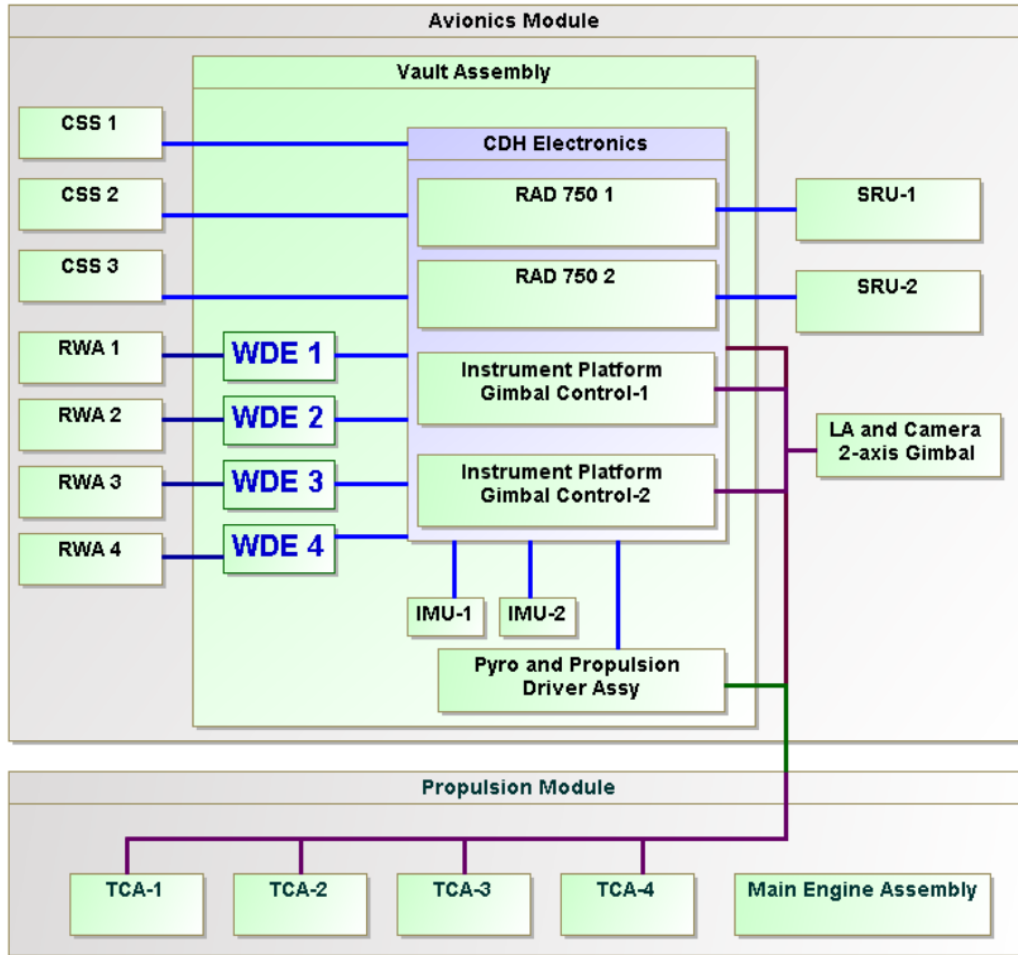


Figure B.2.7-36. The GN&C subsystem is redundant and cross strapped to provide robust fault tolerance to radiation events.

*Heritage*

Given the radiation shielding provided by the spacecraft, the GN&C subsystem can use standard space GN&C products with high TRL. Table B.2.7-6 shows the GN&C hardware items and the approach to deal with radiation.

**B.2.7.6.4 Orbiter Command and Data Handling Subsystem**

*The Orbiter C&DH provides a cross-strapped and redundant radiation-hardened platform to support the data storage and processing needs of orbiter science.*

*Performance Drivers*

The key performance drivers of the C&DH are as follows:

Table B.2.7-6. Standard high-TRL GN&C hardware ensures radiation shielding.

Item	Radiation Approach
RWA	Sensitive wheel-drive electronics in the vault Mechanical assembly radiation-hardened by design
Sun-Sensor	Radiation-hardened by design
Stellar Reference Unit	Shielding for flux and total dose
Inertial Measurement Unit	In vault

- The design should be single-fault-tolerant and cross strapped to enable the C&DH to fail operational.
- The design should allow swapping to enable rapid transition of control during a fault. A RAD750 single-board computer (see Figure B.2.7-37) was se-

lected to leverage the processor flight heritage, radiation hardness, and JPL's extensive experience with this processor.

- The onboard data storage should accommodate buffering science data for 1 missed DSN pass.

#### Features

The C&DH electronics box is a single box that is internally redundant. Given the use of SpaceWire (see Figure B.2.7-38) as the primary interface, there is no need for a backplane or motherboard within the box; this increases the C&DH box reliability. A standard-size chassis of a 6 U×220 mm cards was selected to enable the use of heritage single-board computers and to provide sufficient board area for the I/O and memory cards. Time broadcast and synchronization are part of the SpaceWire standard; therefore, no external timing network is required. The remote I/O handles all the low-level interfaces, such as analogs, discretes, and serial I/O; this I/O also provides the telecom interface, critical relay commanding, and processor swap functions. The I/O is multiplexed through the SpaceWire interface chip; this radiation-hardened chip includes an embedded processor to accommodate programmable I/O functions. The I/O circuits are standard designs from other JPL spacecraft. The RAD750 RAM provides 512 Mbits of storage using radiation hardened RAM; this supports science data storage and program execution. The power-conditioning unit (PCU) takes in unregulated 28 V off the power bus, provides EMI filtering, and converts the power to a regulated 12 V that is distributed to each card in the box. The PCU on/off switch is controlled by the Power Subsystem. The local card on/off is software controlled via the processor and commands issued via the remote I/O.

#### Block Diagram

The system block diagram is shown in Figure B.2.7-39. This diagram shows the cards in the C&DH box. The box is internally redun-



**Figure B.2.7-37.** The RAD750 provides high heritage for both the C&DH electronics and FSW designs.

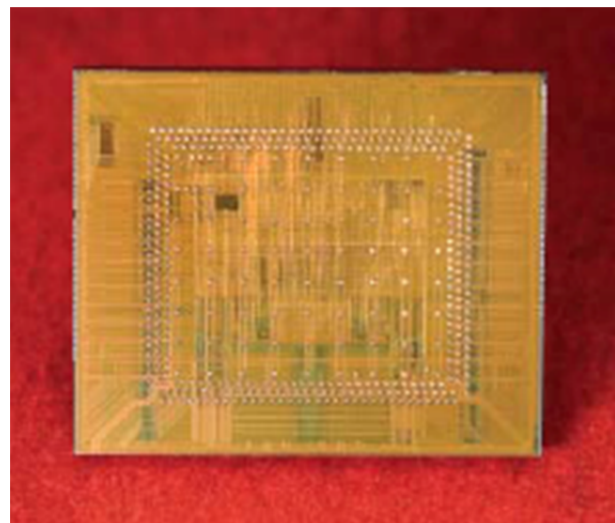


**Figure B.2.7-38.** The SpaceWire interface chip is radiation hardened and provides a high-speed standard interface to the cards in the C&DH.

dant and cross strapped (both data and power). SpaceWire supports multiple topologies (e.g., star or daisy chain). The box consists of two RAD750 single-board computers with a SpaceWire router, two remote I/O cards, and two PCUs. The remote I/O cards interface to the single board computer via SpaceWire. Hosted in the CDH chassis and using the PCU are the remote instrument electronics. This

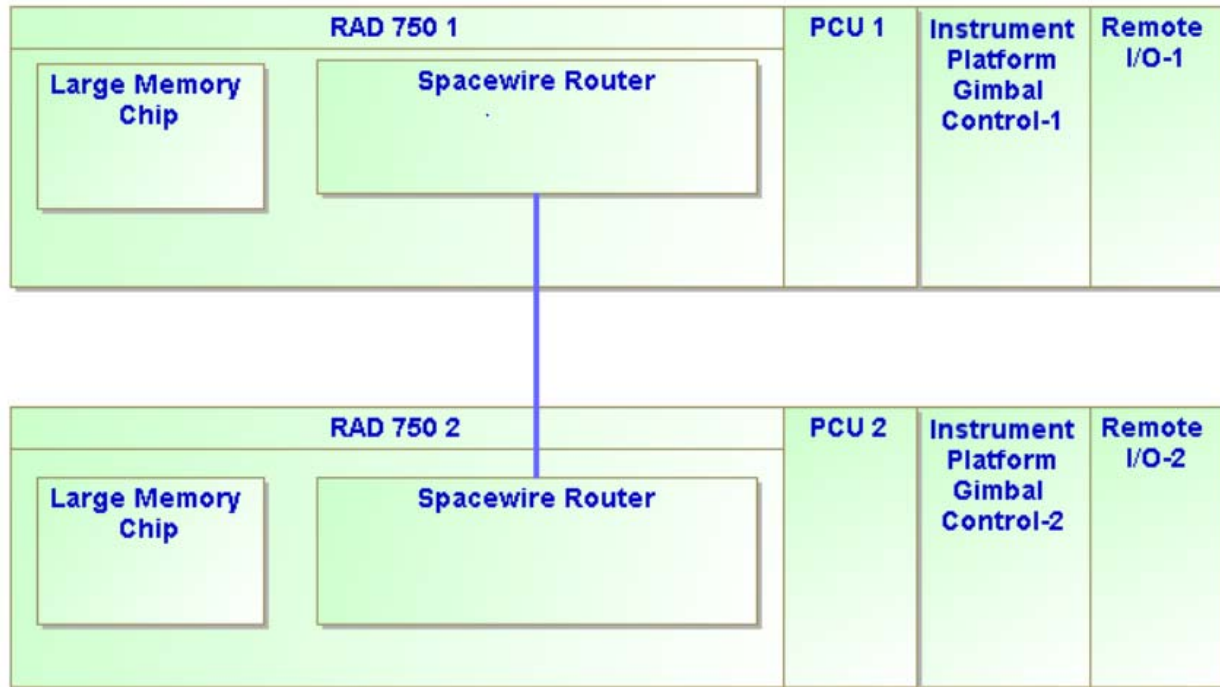


**Figure B.2.7-39.** The C&DH is redundant and cross strapped to provide robust fault tolerance.

integration provides significant savings on mass (including shielding).

#### *Heritage*

The C&DH electronics does not require any new technologies. The RAD750 single-board computer with SpaceWire is an off-the-shelf product. The SpaceWire interface chip is an off-the-shelf product. The I/O circuits and power supply have analogs on previous projects. The 6 U×220 mm packaging standard has been qualified and used on previous projects.

#### *B.2.7.6.5 Software*

Highly reliable software for mission-critical applications is essential for this long-life mission. The FSW baseline extends JPL's long heritage in FSW architecture development, and is implemented in accordance with JPL requirements for NASA Class B (non-human-space-rated) software development. JPL has established a set of institutional software development and acquisition policies and practices as well as Design Principles (DPs) that apply to mission-critical and mission-support

software. These practices conform to NASA Software Engineering Requirements, NPR 7150.2 (NASA 2009b) and are an integral part of the JPL DPs and Flight Project Practices (FPPs) (JPL 2010a, b). All Europa Orbiter Mission FSW would be developed in accordance with JPL institutional policies and practices for deep space missions, including JPL's Software Development Requirements (JPL 2010c), which address all Capability Maturity Model Integration (CMMI) process areas up to maturity level 3. Software identified as safety-critical will comply with safety-critical requirements, regardless of software classification. Software safety-criticality assessment, planning, and management will be performed for all software, including new, acquired, inherited, and legacy software and for supporting software tools. Software is identified and documented as safety-critical or not safety-critical based upon a hazard analysis conducted prior to start of development activities.

Key functions allocated to software include system command and control, health and safety management, attitude control (maintaining concurrent HGA Earth pointing during telecom sessions), science platform articulation, science data collection, onboard data management, reliable delivery using Consultative Committee for Space Data Systems (CCSDS) File Delivery Protocol (CFDP), and thrust vector control during critical propulsion maneuvers. Onboard ephemeris-based pointing and the use of CFDP help to simplify operations and thus reduce long-term operations costs. None of these capabilities are seen as new technology, and significant algorithm and architecture heritage is available from Cassini, MSL, SMAP, MESSENGER, and other missions.

Flight software also has a key role in system fault management. Critical activities are expected to include post launch separation, de-tumble, acquisition, JOI, EOI and Europa orbit science data acquisition. Once in Europa orbit the sequence of behaviors intentionally becomes very repetitive and synchronous with the orbit. During this phase software controls the camera articulation, HGA pointing, and data acquisition and management required for surface mapping, all roughly comparable to MRO except that these behaviors repeat at a more demanding rate than experienced in previous missions, and occur in the hostile radiation environment around Europa. Moreover, coverage objectives require most of the orbital science campaign to complete with minimal disruption. For this reason the FSW coordinates a system fault-management approach, consistent with current best practices, aimed at protecting essential resources, but trying to maintain scheduled operations using automatic fault responses such as resetting devices, switching to redundant devices, or selectively trimming subsets of planned activities.

The FSW is organized in a layered architecture, as shown in Figure B.2.7-40.

The Platform Abstraction layer interfaces directly with the hardware. This layer contains

drivers that provide control, and data abstractions to the device-manager and services layers. The drivers communicate with the hardware using the device-specific syntax and protocol, allowing higher layers of software to interact with these devices using system-standard communication protocols and message formats. Notably, the use of industry-standard SpaceWire as a common hardware communications medium reduces the number of different device types that must be supported, with commensurate reductions in software system complexity. Furthermore, the ability of SpaceWire interface devices to buffer data and perform other control functions in hardware (as demonstrated by MESSENGER) is expected to further reduce the complexity and time-criticality of the FSW implementation.

The Platform Abstraction layer also encapsulates the real-time operating system, device drivers, and all interprocess communications, leveraging flight heritage with the RAD750 platform and all JPL missions since Pathfinder. The commercial operating system provides real-time task scheduling, memory management, and interfaces to I/O devices immediately associated with the processor board.

The Behaviors layer includes software elements that perform closed-loop control around specific system behaviors. These behaviors are typically responsible for the management of one or more hardware devices or subsystems, as well as integrated behaviors associated with them, such as attitude control. Closed-loop behaviors also incorporate fault detection and localized fault management capabilities.

Behavior coordination is provided in a separate Coordination layer that can sequence and coordinate the control of underlying behaviors. This layer is also responsible for coordinating any fault responses at a system level.

The MetaControl layer provides services for initializing and supervising reliable operation of the rest of the software and computing system and for supporting external commanding

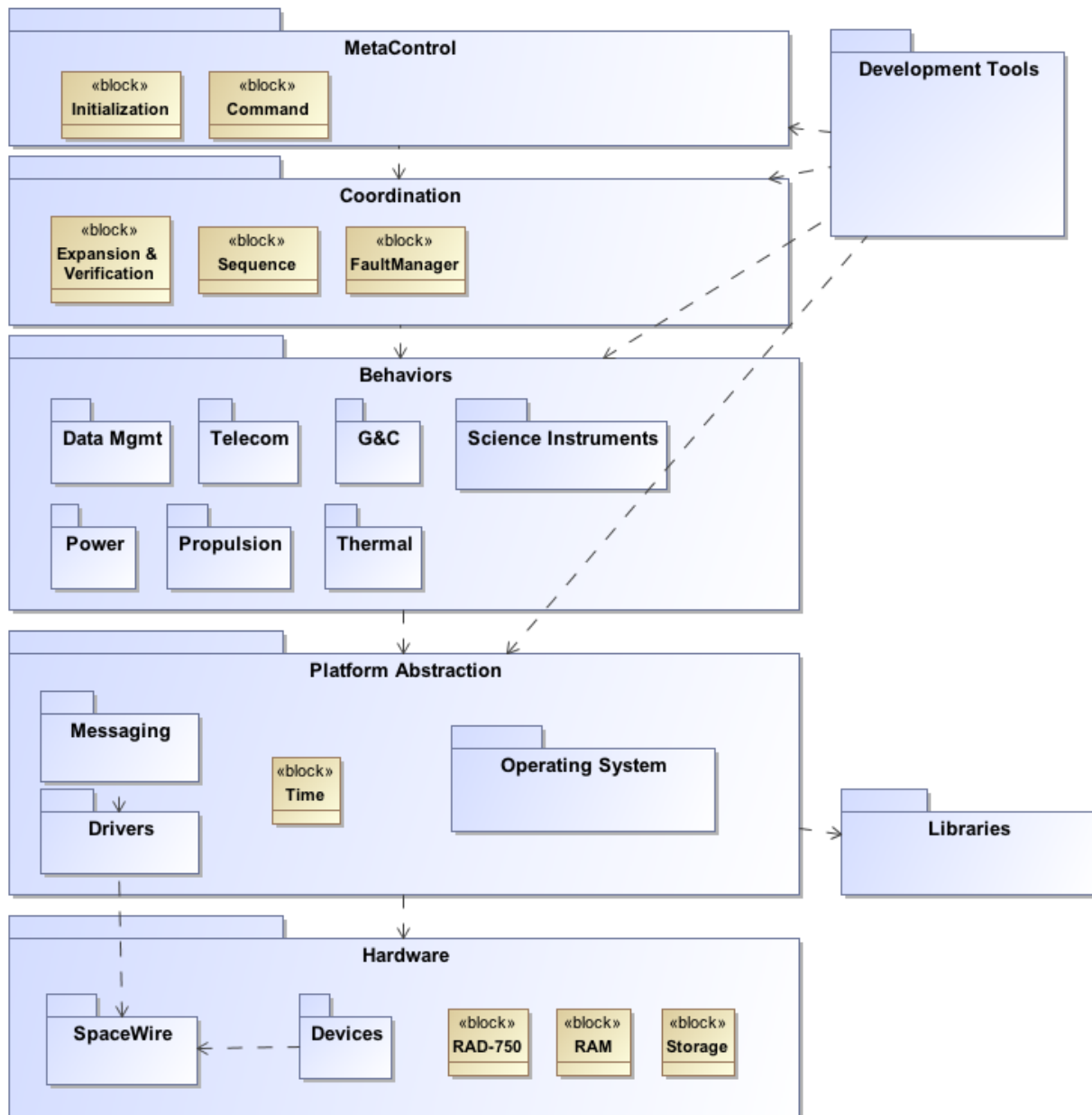


**Figure B.2.7-40.** Flight software benefits from appropriate reuse and evolution within a layered architecture.

and configuration (such as changing system behavior from the ground).

Instrument-embedded software is developed by instrument providers and tested locally using a spacecraft simulator (see Testbed Approach). It is delivered with the instruments. Some engineering devices may also include embedded software. All other software is developed in-house.

#### B.2.7.6.6 Structure

The Avionics Module (Figure B.2.7-41) supports the majority of the avionics, batteries, science instruments, star-trackers, Sun-sensors, and reaction wheels. The vault houses and shields the avionics components that are most sensitive to radiation and extends below the Avionics Module's interface with the Propulsion Module. This configuration optimizes radiation-shielding by making use of the exist-

ing structure in all directions: From the top the octagonal primary structure, reaction wheels, and batteries provide shielding; from the sides the primary structure, tanks, and thermal enclosure provide shielding; and from the bottom the Power Source Module's primary structure and main engine provide shielding, complementing the vault's thick walls. Waste heat from the avionics is allowed to radiate out from the vault to help maintain the propulsion tanks at their required temperatures.

The topmost part of the Avionics Module is also octagonal. The vault is box-shaped. The tapering structure that connects the upper part of the Avionics Module to the vault is composed of machined stringers fastened to sheet-metal panels. An octagonal ring is fastened to the top of the module, and a square interface ring is fastened to the bottom.

The vault consists of six machined panels that are fastened together, with access panels integrated to allow for installation and removal of the avionics. The batteries and reaction wheels reside within the upper section of the Avionics Module.

#### *Instrument Accommodation Structures*

The science instruments on the Orbiter are the LP, LA, MC, and MAG. They are all external-

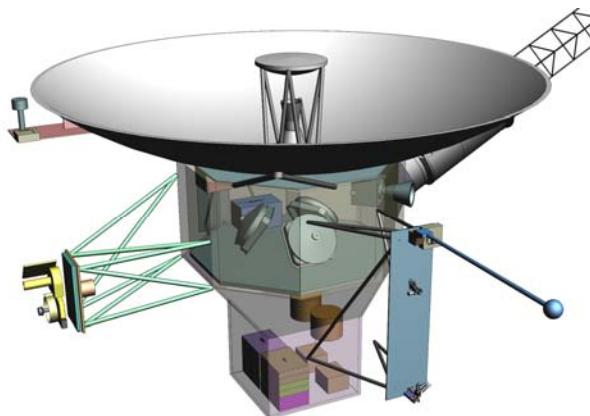


**Figure B.2.7-41.** Avionics module.

ly mounted on the upper section of the Avionics Module.

The LP is passively deployed using a compression spring-based mechanism configured to allow for rotation. This mechanism is based on a device used on MER to retract cables at the cruise stage separation interface. There are launch restraints at the base and end of the probe, held in place by 1/4-inch separation nuts. When the probe reaches end of travel it is latched at full deployment.

The LA and MC are attached to a two-degree-of-freedom gimbal mechanism. On one axis there is a rotating table, driven by a motor and gearbox actuator. The second degree of freedom is driven by a linear actuator.

The MAG boom extends axially. A rate-limiting eddy-current damper at the base of the boom can act as an attenuator. This attenuator is similar to the one currently used on MSL. The attenuator limits the end of travel loads to the required levels.

#### *Thermal Section Structures*

The thermal enclosure (Figure B.2.7-42) consists of blankets made from aluminized Kapton, aluminized Mylar, and Dacron net separa-

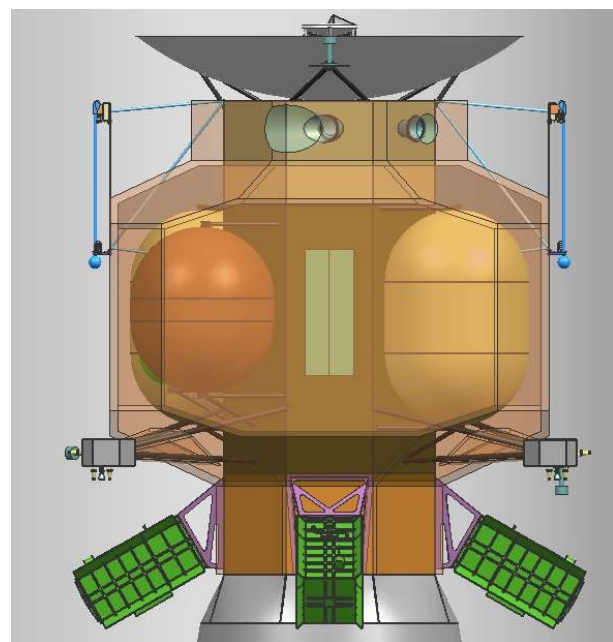


**Figure B.2.7-42.** Thermal enclosure.

tors, supported by a lightweight, carbon-fiber tubular frame.

#### B.2.7.7 Technical Budgets

Three primary technical margins are addressed here: mass, power/energy, and data balance.

Other key technical margins are covered elsewhere in this report: Radiation tolerance margin is treated in Section B.2.6.1.

The approach to technical resources in this study has been to model what is well understood, and then include conservative margin based on past experience to account for items not known well enough to model.

*To minimize cost and schedule risk, the concept strives to achieve high levels of technical margin wherever possible.*

##### B.2.7.7.1 MEL and Mass Margins

The mass margin follows the definitions and conventions specified in the JPL Design Principles, Section 6.3.2 (JPL 2010a). The earliest milestone at which the Design Principles specify a mass margin, however, is the Project Mission System Review (PMSR), when 30% is required. In consideration of the fact that the Europa Orbiter Mission concept is in a much earlier phase, pre-Mission Concept Review (MCR), we have set a more conservative policy of 40% mass margin for this report. This is consistent with the expected evolution of JPL's institutional guidance. The method of calculating the Design Principles margin is shown in Table B.2.7-7.

The dry mass current best estimate (CBE) includes tanks sized to carry the maximum propellant load, radiation shielding, and the launch vehicle adapter (LVA). Each of these is discussed in more detail below.

*Use of "Max Propellant"*

The Design Principles explicitly require that the propellant load assumed for the margin calculation be that amount of propellant needed to provide the required  $\Delta V$  for the maximum possible launch mass on that launch vehicle (LV) (JPL 2010a). In addition, the dry mass of the propellant tanks reflects tanks sized for this maximum propellant load. This approach gives an accurate reading of the overall dry mass margin, *assuming* that the flight system grows to the maximum launchable mass.

Table B.2.7-7. Europa Orbiter Mission mass margin.

Orbiter Mass Margin				
T. Bayer 24 Apr 2012 <a href="#">Orbiter Model - Final Report Update</a>	LAUNCH			
	Flight System Mass, kg			
	CBE	Cont.*	MEV	
Laser Altimeter	10	50%	15	
Langmuir Probe	3	50%	4	
Magnetometer	3	50%	5	
Mapping Camera	4	50%	6	
<b>Payload</b>	<b>20</b>	<b>50%</b>	<b>30</b>	
Power	56	21%	68	
C&DH	19	30%	25	
Telecom	94	30%	122	
Structures	561	27%	715	
Thermal Control	44	30%	57	
Propulsion	193	28%	247	
GN&C	62	29%	80	
Harness	70	50%	105	
Radiation Monitor	8	30%	10	
ASRGs (4)	164	46%	239	
<b>Spacecraft</b>	<b>1271</b>	<b>31%</b>	<b>1668</b>	
<b>Flight System Total Dry</b>	<b>1291</b>	<b>32%</b>	<b>1698</b>	<b>Max Prop</b>
Bipropellant	1129		1837	2054
TVC Monopropellant	101		101	101
ACS Monopropellant	40		40	40
Pressurant	6		6	6
Residual and Holdup	32		49	55
<b>Propellant</b>	<b>1308</b>		<b>2033</b>	<b>2256</b>
<b>Flight System Total Wet</b>	<b>2599</b>		<b>3731</b>	
<b>Capability (21-Nov-21 VEEGA)</b>	<b>Atlas V 551:</b>		<b>4494</b>	
System Margins				
JPL DWVP (Capability - Max Prop - CBE Dry) / (Capability - Max Prop)			42%	

\*Using ANSI/AIAA Guide G-020-1992, "Estimating and Budgeting Weight and Power Contingencies for Spacecraft Systems", applied at the component level.

Specifically, in Table B.2.7-7, propellant mass is computed from the  $\Delta V$  required for the 21 November 2021 Venus-Earth-Earth gravity assist (VEEGA) trajectory. The CBE propellant is computed using the CBE dry mass and CBE  $\Delta V$ . The maximum expected value (MEV) propellant is computed using the MEV dry mass and the MEV  $\Delta V$ . The max propellant is computed using the maximum possible dry mass and the CBE  $\Delta V$ .

#### Radiation Shielding

The model tracks the amount of shielding necessary to protect each piece of sensitive electronics. This mass is accounted for at the appropriate level of assembly (card, box, or module), and shown as a payload and engineering total in Table B.2.7-7.

#### Launch Vehicle Adapter

A standard Atlas LVA is assumed. The mass shown in Table B.2.7-7 includes both the part that remains with the spacecraft and the part that remains with the Centaur upper stage but is considered “payload mass” for the purpose of LV performance.

This margin calculation adds “growth contingency” mass to the CBE masses to arrive at an MEV and the propellant required for that mass, and then compares this value to the LV capability. For determination of contingency factors, the Europa Study Team has used the ANSI/AIAA Guide G-020-1992 (American National Standards Institute 1992), applied at

the component level. This specifies the *minimum* contingency factor based on project phase and component sizing and maturity, and allows a higher factor where the project deems it appropriate. The guideline is generally consistent with traditional JPL practice, but provides a more rigorous grounding through its use of historical data.

As can be seen in Table B.2.7-7, the Europa Orbiter Mission has excellent mass margins. A more detailed mass breakdown can be found in the Master Equipment List (MEL) Section B.4.3.

#### B.2.7.7.2 PEL and Power/Energy Margins

The Power Equipment List (PEL) contains the CBE with a contingency for maturity. The Orbiter Mission power modes are based on the mission scenarios. Europa Orbiter Mission policy is to maintain 40% of the power source capability after a single failure as power margin on the load for all mission power modes. Each mission mode is assessed against the policy. The transient modes are assessed with the power margin on the load and the DPs DOD of actual battery capacity with a single failure (JPL 2010a). Summary results of the mission mode power analysis are shown in Table B.2.7-8.

The PEL provides the current best estimate (CBE) power output and the lowest expected value (LEV) sum output of the ASRG power source for each mission mode. The power

**Table B.2.7-8.** Orbiter power analysis compares the power source capability to the estimated load for all phases of the mission. There are two mission modes that rely on the battery, and the DOD is displayed.

Mission Phase	EHM Orbiter Power Analysis							SS or Transient	Max Bat DoD, %
	ASRG Power, W		Flight System Power, W			Margin, %			
	Spec	LEV	CBE	Cont.	MEV				
Launch	426	334	172	28%	221	48%	SS		
Inner Cruise	535	420	224	19%	266	47%	SS		
Inner Cruise (Safe)	535	420	244	45%	354	42%	SS		
Outer Cruise	514	403	228	46%	334	43%	SS		
<b>Outer Cruise (Safe)</b>	<b>514</b>	<b>403</b>	<b>244</b>	<b>40%</b>	<b>341</b>	<b>39%</b>	<b>SS</b>		
Orbit Insertion/TCM	505	396	356	59%	566	40%	Transient	15%	
Europa—Communications	505	396	241	68%	405	40%	Transient	13%	
Europa—No Communications	505	396	180	98%	358				
Decommissioning	505	396	221	-44%	123	44%	SS		

source estimate takes into account a degraded performance of the ASRG during launch due to the environmental conditions inside the shroud. The LEV of the ASRG assumes a failed Stirling converter after launch, effectively producing the power of 3.45 ASRGs versus a nominal 4.0 ASRGs.

The PEL contains a line item for each load, estimating a CBE load value, an estimated contingency based on maturity, and a maximum expected load value (MEV). Each mode is identified in the PEL, along with a summation of all of the loads that are powered on in that mode. The mission mode total is compared to the power source capability for each mission mode, with the power margin calculated per the DPs approach of  $(\text{Capability} - \text{CBE}) / \text{Capability}$  (JPL 2010a). The transient modes are modeled to estimate the battery DOD with the actual battery capacity.

All mission mode power budgets currently meet the Europa Orbiter Mission 40% margin policy with the exception of outer cruise safe mode, in which the power margin is slightly below policy at 39%. Since safe mode is considered steady state, additional battery capacity does not provide additional margin. Several

options will be examined in Phase A to improve power margin in this mode and it was judged that 39% margin is adequate to assess mission concept feasibility.

The two transient modes are the orbit insertion/TCM and Orbiter science. Orbit insertion is the defining mode for the battery sizing due to the long JOI burn of 1 hour. The battery capacity is estimated to be 40 Ah with a 14-A discharge at 10°C at EOM. The load profile and battery DOD are shown in Figure B.2.7-43.

The JPL DPs allow for a 70% DOD for events such as orbit insertion that are less than 100 cycles (JPL 2010a).

The next transient mode is the science orbit mode, in which the X and Ka band amplifiers are turned on for a continuously for 72 hours to support gravity science. After the continuous track, the X and Ka band amplifiers are 50% duty cycled for the next five orbits until the battery is recharged (see Figure B.2.7-44).

The dominant factor to the Orbiter science mode is the continuous operation of Telecom, driving a 40% DOD for the Orbiter Science with the 72-hour continuous track. The JPL

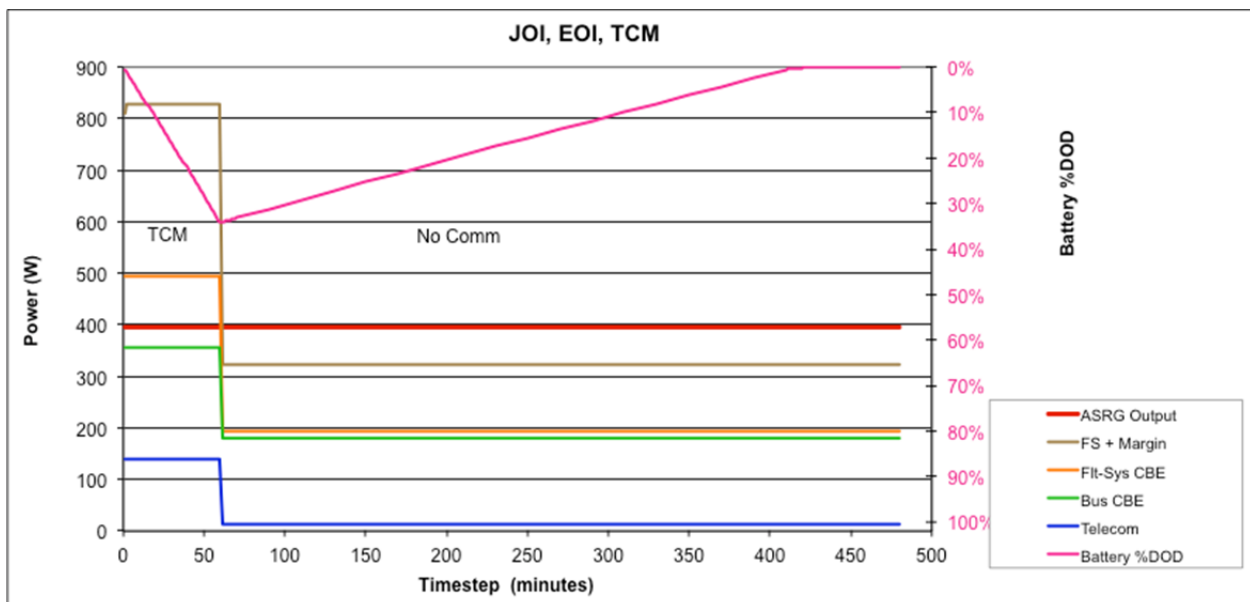


**Figure B.2.7-43.** JOI power analysis shows a 1-hour discharge of the battery using the Europa Study policy of 40% margin on the load profile.



surface map (80% coverage) is needed to meet the science baseline and that the notional orbit would achieve this in 3 Eurosols.

Per orbit downlink margins are shown in Table B.2.7-10 for orbits with continuous telecom. Not shown, but also included in the 549 Mbits of data accumulated, are engineering data collected at 2 kbps. Downlink capacity is computed using the Ka link budget described in Table B.2.7-4, which was computed for a worst-case range of 5.5 AU, and DSN elevation angle of 20 degrees, and then multiplied by a factor of 1.2 to the ability to step downlink bit rates over each pass to maximize the throughput.

The C&DH subsystem provides 256 Mbytes of solid-state storage into which all science data are recorded during observations. When telecom is operating, downlink data is retrieved from storage and queued for transmission by the data manager. Stored data would be managed as products (files) in the onboard store, and the CCSDS File Delivery Protocol (CFDP) would be used to ensure reliable transport of this data to the ground. At the average downlink rate of 129 kbps data would

accumulate on the ground at a rate of about 3.7 Gbit/pass, or 11.1 Gbit/day during the science mission, or about 334 Gbit for the entire science mission.

#### B.2.7.8 Module Development, Integration, and Test

*The modular approach for the spacecraft allows parallel testing before delivery to system integration and test at a higher level of integration than was possible for previous spacecraft.*

The spacecraft is comprised of the Avionics Module, the Propulsion Module, and the Power Source Module.

Development of the spacecraft modules begins with the design and fabrication of a developmental test model (DTM) of the spacecraft structure. The DTM is populated with appropriate mass mockups as required to properly represent the mass properties of the spacecraft. After assembly, a full set of structure qualification tests is to be performed, including static loads, modal survey and pyro-shock testing. The DTM is also be used later as a “trailblazer” to ensure that all facilities (such as the launch site and LV) and mechanical ground support equipment (MGSE) characteristics are compatible. Because the DTM components are built to the same drawings as flight, elements of the DTM could also be used as surrogates for the flight structure, if required.

As the DTM program progresses, the flight model (FM) structural components are fabricated and delivered to the module teams (Avionics Module, Propulsion Module and Power Source Module) for integration with active components and secondary structure, and for

**Table B.2.7-9.** Orbiter Mission Data Balance.

	Gbit
30-day mission data for MAG	10.6
30-day mission data for LA	5
30-day mission data for LP	5.3
30-day mission data for Eng	5.3
Data for one stereo map	38.4
Total mission baseline data (one map)	90
Mission downlink capacity	310
Downlink capacity margin	71%

**Table B.2.7-10.** Data Balance and Margin.

	MC	LA	MAG	LP	Total/Orbit
Raw data rate (Kbps)	375	1.95	4	2	
On-time per orbit (%)	50	100	100	100	
Data reduction factor	3	1	1	1	
Effective output rate (Kbps)	63	1.95	4	2	
Average data per orbit (Mbit)	472.6	14.7	31	15.5	549
Average downlink rate (Kbps)					129
Downlink time required (hour)					47
Downlink time available (hour)					77.5
Downlink margin					39%

module-level testing, including environments, prior to the start of system integration and test. 2 months of schedule margin is allocated for the structure deliveries to the Module Development Teams, and a minimum of 1.5 months schedule margin is allocated for the delivery of the tested flight modules for system integration. Since the Avionics Module is the most complex functionally, 3.5 months of margin are allocated in recognition of its schedule criticality to System Integration and Test.

The module concept adopted for the spacecraft permits testing, both functional and environmental, to be performed with flight cabling and flight structure at a higher level of integration prior to delivery than has been performed on similar previous missions, such as Cassini. Development of more highly integrated modules allows more parallel path testing, reducing the number of interfaces that need to be verified at the system level, compared to a project like Cassini, where individual components and subsystems were delivered and integrated during System Integration and Test.

The major deliveries to system integration are the Avionics Module (consisting of the upper equipment section with science instruments (see below), the avionics vault and its contents, and the telecom assembly), the Propulsion Module (with tanks, other propulsion components, and harnessing), and the Power Source Module. The Power Source Module is populated with advanced Stirling radioisotope generators (ASRG) that are electrically heated to permit realistic testing and evaluation of the end-to-end power delivery system for the spacecraft. Emulations of other modules at electrical interfaces will be used to support module-level integration in each case.

All module deliveries are planned to occur at the start of System Integration and Test to maximize flexibility. The Upper Equipment Section is initially delivered with Engineering-Model (EM) Science Instruments. The Flight Model (FM) science instruments are delivered later as shown in the System Integration and Test flow,

permitting any interface or performance issues to be resolved before the flight deliveries.

#### *B.2.7.8.1 Testbed Approach*

Consistent with longstanding practice, the Europa Orbiter Mission has adopted a system integration approach that is supported by an additional set of software and hardware testbeds, enabling early and thorough integration of key hardware and software interfaces prior to ATLO. This development and validation approach begins with scenario development during formulation and design, and progresses incrementally to system validation using an ever-growing battery of regression tests that verify and validate system architecture as it is designed and developed. Figure B.2.7-45 depicts the proposed testbeds described in the following paragraphs.

Since science instruments are likely to be developed externally, instrument developers must be provided with a testbed environment that includes an emulator for engineering subsystems (hardware and software) that simulates the power, data, and control interfaces with which the instrument must integrate. This ensures that all interface issues have been resolved prior to delivery, thereby helping to keep the ATLO work focused on system integration and on the concerns that can be verified only in an assembled system context. Similar subsystem assembly testbeds are provided for early integration testing of major subsystems (telecom, propulsion, power, etc.).

A high-fidelity model-based simulation capability (known as the workstation test set [WSTS] on MSL and SMAP) is baselined for FSW development test and verification. This includes but is not limited to fault management development and test, attitude control system-level verification and validation (V&V), and mission activity development and test; so several groups will exploit this capability, which can be replicated cheaply as often as necessary. The software simulation of hardware must be of sufficient fidelity to allow seamless

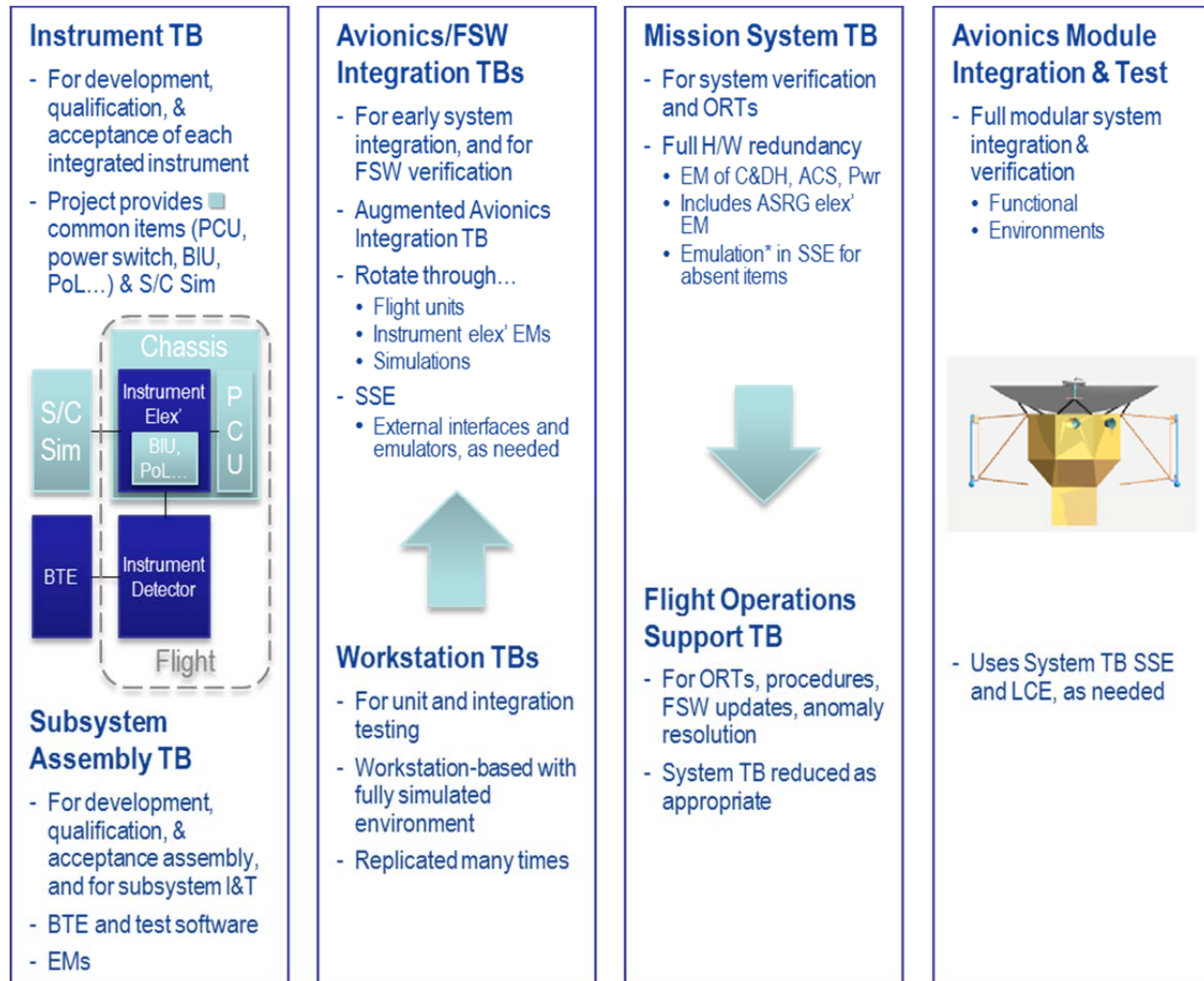


**Figure B.2.7-45.** System integration testbeds. [Define bus interface unit (BIU), launch control equipment (LCE), spacecraft support equipment (SSE). Pester Arden. (will put in acronym list).]

migration of FSW and test cases from simulation to hardware-in-the-loop testbeds. This capability is important and necessary because certain software services are needed to support the instrument testbeds and the testing and integration of devices. Therefore, emphasis will be placed during hardware testing on validating simulation model fidelity.

The first workstation-based spacecraft simulator version will be available in time to support development of the first FSW release, and will progress with expanded capability, as needed to support testing of subsequent FSW builds. It will be available on all software developers', systems engineers', and testers' workstations.

Capabilities will include closed-loop spacecraft behaviors operating in both nominal and off-nominal modes. These simulators are built to allow for interchangeability between software models and hardware engineering models (EMs) later in the "hardware-in-the-loop" testbeds in a manner that is transparent to the FSW and to test scripts, at least at the interface level. This enables use of the same test scripts whenever the testbed models are interchanged with EMs or hardware emulators.

In addition to the simulation capability described above, the Europa Orbiter Mission would have three system testbeds. The first two are the Avionics/FSW integration

testbeds, which are similarly configured with single string avionics. These support the development and test of ground support equipment (GSE) hardware and software, the development and validation of test scripts, and the maturation of databases, such as command and telemetry dictionaries. First on line is the Real-Time Development Environment (RDE), which is dedicated to GSE hardware and software development and test. The next instance of this testbed, the Flight Software Testbeds (FSWTBs), becomes available later in the development process to allow V&V to proceed in parallel with FSW development. The third system testbed is the Mission System Testbed (MSTB), a full redundant, high-fidelity testbed dedicated to system V&V, FSW fault management tests, mission system tests, and AT-LO support.

These system testbeds include the C&DH, GN&C, power, telecom, and harness subsystems, as well as Ground Data System (GDS) hardware and software. The EM versions of all flight system engineering subsystems and instruments will pass through these testbeds for integration and interface verification and the testbeds can support flight hardware testing, if needed. The V&V simulation environment can offload the hardware-in-the-loop testbeds and use the EM integration effort to help evaluate model fidelity. The simulation environment interfaces and procedures are compatible with those of the hardware testbeds. These testbeds are also used to train test analysts to support system testing, as well as to support ATLO procedure development and anomaly investigation. All FSW versions are verified on the system testbeds prior to being loaded onto the flight system during ATLO or flight operations. The flight system testbed transitions to operational use for this purpose after launch.

#### **B.2.7.8.2 System Integration and Test**

***The conservatively derived system integration and test program is based on actual durations from the Cassini project. Launch operations***

***durations are based on actuals from the MSL project along with operations unique to the Europa Orbiter Mission.***

The System Integration and Test (SI&T) Phase, described graphically in Figure B.2.7-46, would begin with the delivery of the flight Avionics Module components, Propulsion Module, and Power Source Module for system integration. The Avionics Module components, consisting of the telecom assembly, Upper Equipment Section (with EM science instruments) and the Avionics Vault, is integrated initially using extender cables. These permit access to circuits for integration and troubleshooting, as well as for connection of direct access equipment needed for closed-loop operation of the Attitude Control Subsystem during mission scenario and comprehensive performance testing. During integration, interface signal characteristics are measured and recorded for comparison with requirements.

Even though traditional EMC/EMI system engineering methods would be employed during development, the early integration of the telecom subsystem permits monitoring of spectral characteristics as other hardware is added to the system for detection and identification of any interfering spurious signals. A thorough telecom functional test is included in the flow to establish baseline performance while operating with the rest of the Avionics Module.



The Propulsion Module is electrically integrated through extended cables next in the flow to demonstrate signal characteristics to propulsion valves and thrusters, and to perform an initial verification of proper phasing. The design of the extender cables and the layout of the modules in the test facility address cable length issues, as appropriate. Phasing of propulsion components (as well as G&C components) is repeated after spacecraft stacking to remove any influence of the extender cables.

Finally, the Power Source Module is electrically integrated through extended cables. Plans call for fully functional ASRGs that are electrically heated and can be used to verify end-to-end performance, as well as to verify integration procedures that will be used for the flight ASRG integration at KSC.

A Deep Space Network (DSN) compatibility test is performed at this point (with the DSN compatibility test trailer) followed by an Engineering Baseline Comprehensive Performance Test (CPT). This and other configuration-dependent baseline tests are performed throughout the ATLO program in order to detect performance changes resulting from either trending or environments.

A series of fault management tests is performed to establish correct operation of the fault management system software in conjunction with associated hardware detections and responses.

The first mission scenario test is the launch sequence test, executed both nominally and with selected fault and off-nominal conditions. Subsequently, a trajectory correction maneuver test (including orbit insertion) is performed in both nominal and off nominal conditions. Other capabilities of the spacecraft to support required operational modes, science observations, and other noncritical mission scenarios will be incorporated in CPT(s) rather than in specific scenario tests so that spacecraft capabilities are fully established, rather than merely performing point-design mission scenario

verifications. Since all operations described above are first-time events, one-month schedule margin is included at this point to prevent any delay to the science instrument integration.

At this point, any remaining science instruments are delivered and integrated into the Avionics Module, replacing their EMs that have been serving as surrogates throughout system testing. An Engineering and Science CPT follows integration, with all spacecraft components present to establish the performance of the spacecraft before reconfiguration for environmental test.

The environmental test program starts with the mechanical and electrical integration of the upper equipment section, avionics vault and the telecommunications assembly to complete the Avionics Module. Stacking of the Propulsion Module, Power Source Module, and Avionics Module to each other, stacking the spacecraft on the Launch Vehicle Adapter (provided by the Launch Service) and the installation of pyro devices needed for pyro-shock testing. An Abbreviated Baseline CPT is performed, as well as an RF radiation test using the flight antennas, and a phasing test to demonstrate proper phasing without extender cables. This is the first time the spacecraft is in a flight-like electrical and mechanical configuration.

Radiated emissions and radiated susceptibility tests are then performed, as well as a self-compatibility test. This is followed by an alignment verification to establish pre-environmental alignment data. Thermal blankets (including the thermal shroud) and environmental test instrumentation are installed after the spacecraft is stacked.

The spacecraft is then transported to the Environmental Test Lab (ETL), where acoustics tests and pyro-shock tests are performed. The pyro-shock test also verifies the LV separation mechanical interfaces.

The spacecraft is then moved to the 25-foot Space Simulator, where a baseline test is performed to verify configuration and performance prior to starting solar thermal-vacuum (STV) tests. The STV test is primarily a verification of worst-case hot and cold performance, as well as selected thermal balance conditions. Additional tests (such as science instrument modes that require vacuum conditions) are performed during thermal transitions, if they are not otherwise required for the worst-case thermal tests that verify margins required by JPL Design Principles and Flight Project Practices (JPL 2010a, b).

After STV test, the spacecraft is transported back to the Spacecraft Assembly Facility (SAF), where post-environmental alignment verifications are performed. The Engineering and Science CPT is repeated for post-environmental performance verification. Launch sequence tests, trajectory correction maneuver tests, countdown and scrub/recycle tests, and engineering and science performance tests are performed prior to shipment to KSC. Two months of schedule margin are included at this point to protect the ship date and KSC operations. Shipment to KSC is performed at the module level because of the large size of the stacked spacecraft and to permit access to direct access signals for the final comprehensive performance testing at KSC.

After arrival at the KSC Payload Hazardous Servicing Facility (PHSF), the spacecraft modules, interconnected with extender cables, are put through a System Test Configuration Baseline CPT to reestablish the health of all spacecraft systems. Spacecraft stacking is then performed, followed by a DSN Compatibility Test with MIL-71, alignment re-verification, and a final Phasing Test using the launch version of flight software. A Launch Configuration Baseline Test is performed, followed by a Launch Sequence Test from prelaunch through early cruise. Flight pyrotechnic devices (excluding those for spacecraft separation) are installed. A dry-run installation of the flight

ASRGs is performed as well. After the flight ASRGs are removed and secured, the spacecraft is transported to the KSC Operations and Checkout (O&C) facility for dry heat microbial reduction (DHMR). The descriptions of operations with the ASRG assume that they can be handled in similar fashion to the MMRTG used on Mars Science Laboratory (MSL). These operations will be refined as the ASRG requirements and development proceed.

At the O&C the spacecraft is installed in an existing thermal chamber in the O&C high bay. Vacuum bakeout of the spacecraft is performed, followed by backfill to an appropriate convective atmospheric environment for heating (either nitrogen or filtered air at the preference of the Planetary Protection Engineer). Spacecraft temperatures are elevated and verified, at which point the DHMR operation is conducted. Because of uncertainty in the durations of each of these operations, five days of schedule margin are allocated at this point. Over one month of schedule is allocated to the end-to-end DHMR operation. The spacecraft is then transported back to the PHSF. Conservative planetary protection handling is planned beyond this point, consistent with a spacecraft that could impact Europa.

At the PHSF, a baseline test is performed to confirm the status of all spacecraft systems after DHMR. Since the ASRGs would not be present, the spacecraft will be powered by ground support equipment power supplies. Final spacecraft closeouts and walk-down inspections are performed, followed by propellant and pressurant loading of the Propulsion Module. Three weeks of schedule margin are included at this point to protect the date of delivery to the LV for integrated operations.

At this point, the spacecraft is ready for integrated operations with the LV, including mating to the flight LVA, encapsulation with the fairing, transport to the launch pad, and fueled ASRG installation for flight, countdown, and launch.

Durations for most of the spacecraft test operations (including setup, reconfiguration, preps, and transportation) are based on actual “as-executed” durations from Cassini. Cassini was used as a reference because its ATLO plan was executed without any holiday work, or any work on a holiday weekend, minimal Saturday work, and a nominal five-day-per-week, single-shift operation. Integrated operations with the LV are based on actuals from MSL, which had similar operations with the same/similar LV and integration of an MMRTG. These estimates have been informed by MSL complications of MMRTG installation inside the MSL aeroshell and implementation of required cooling systems. Cooling may not be required for the Europa Orbiter Mission, given the characteristics of ASRGs.

The ATLO flow described above has not been optimized to incorporate opportunities for parallel operations, except in the case of preparations for environmental testing, where such operations are customary. The flow described also includes the 20% schedule margin at JPL, and one day per week schedule margin at KSC, as required by the JPL Design Principles (JPL 2010a).

### **B.2.8 Mission Operations Concept**

Europa and its vicinity is a challenging and hazardous environment for operating any science mission. The central guiding theme of mission operations is to deliver the spacecraft to Europa safely, and fully capable of conducting science observations. No other activities are allowed to drive the design of the operations systems and concepts. For the Orbiter Mission, operations consist of repeated measurements made via one orbital template that is replicated over multiple orbits.

Operations development has drawn much wisdom from the many NASA-wide studies of Europa exploration from as early as 1997. In addition, two key studies in 2008 were conducted to capture relevant lessons learned from past and present operations missions, incorpo-

rating members from JPL, APL, and NASA Ames (Clark, 2008). These studies focused in particular on flight and ground system capabilities needed to simplify science operations; early development of flight and ground concepts to ensure appropriate implementation; and postlaunch activities and development to ensure functional capabilities and simplified operations. All of the operations assessments, from the many studies and scenario work of highly experienced engineers, emphasize early consideration of operability issues in the system architecture and design. All system trades (spacecraft, operations, science, etc.) are treated as mission trades to work toward the best cost/risk for the overall mission, rather than optimizing a single element and unknowingly adding significant cost/risk to another.

#### **B.2.8.1 Operations Concept— Interplanetary and Jupiter Cruise**

After launch, mission focus is on the checkout, characterization, and deployment of all flight systems. In the first few weeks of cruise, coverage is continuous, driven by real-time commanding for schedule flexibility based on the high variability associated with early checkout activities. Once postlaunch checkouts are complete, the mission transitions to interplanetary cruise.

Interplanetary cruise is quiescent, save for elevated activity required for gravity assists and maneuvers. The spacecraft is minimally operated, with basic telemetry expected only once per week; however, 24-hour coverage is expected around maneuvers, and daily to continuous tracking is expected prior to gravity assists, particularly for nuclear safety maneuvers prior to gravity assists involving Earth. After JOI, instrument characterization and checkout resume, and operations readiness tests (ORTs) and instrument calibrations could be conducted during Jupiter system flybys prior to Europa orbit.

**B.2.8.2 Operations Concept—Science Phase**

The Orbiter Mission science phase, described in Section B.3.1, begins after Europa Orbit Insertion and circularization and is achieved via 30 days of operations at Europa. Each orbit has a very similar geometry; simple, repeated observations flowing from one conceptual design are capable of delivering all of the science goals. The Europa orbit geometry that will be used is shown in Figure B.2.8-1.

The science phase concept is a 30-day mission at an altitude of 100 km. The inclination is 95°, and at a 4:30 pm local solar time as shown in Figure B.2.8-1, near-constant communications with Earth are possible, for the spacecraft never enters occultation by Europa (though it does by Jupiter). The Laser Altimeter, LP, MAG, and Radio Science experiments can be on nearly all the time, except for maneuvers and Jupiter occultation (because both the spacecraft and Europa are occulted). Imaging is conducted on the day-side (shown by the

yellow swath in Figure B.2.8-1).

There are many candidate repeat orbits available for use in accomplishing global mapping. The best repeat orbits have a comfortable swath-to-swath overlap, complete the repeat quickly, and are close enough to Europa to satisfy resolution requirements. Figure B.2.8-2 shows the candidate repeat cycles for the Europa Orbit Mission. The best option, marked in



Figure B.2.8-1. Europa orbit geometry as seen from Earth.

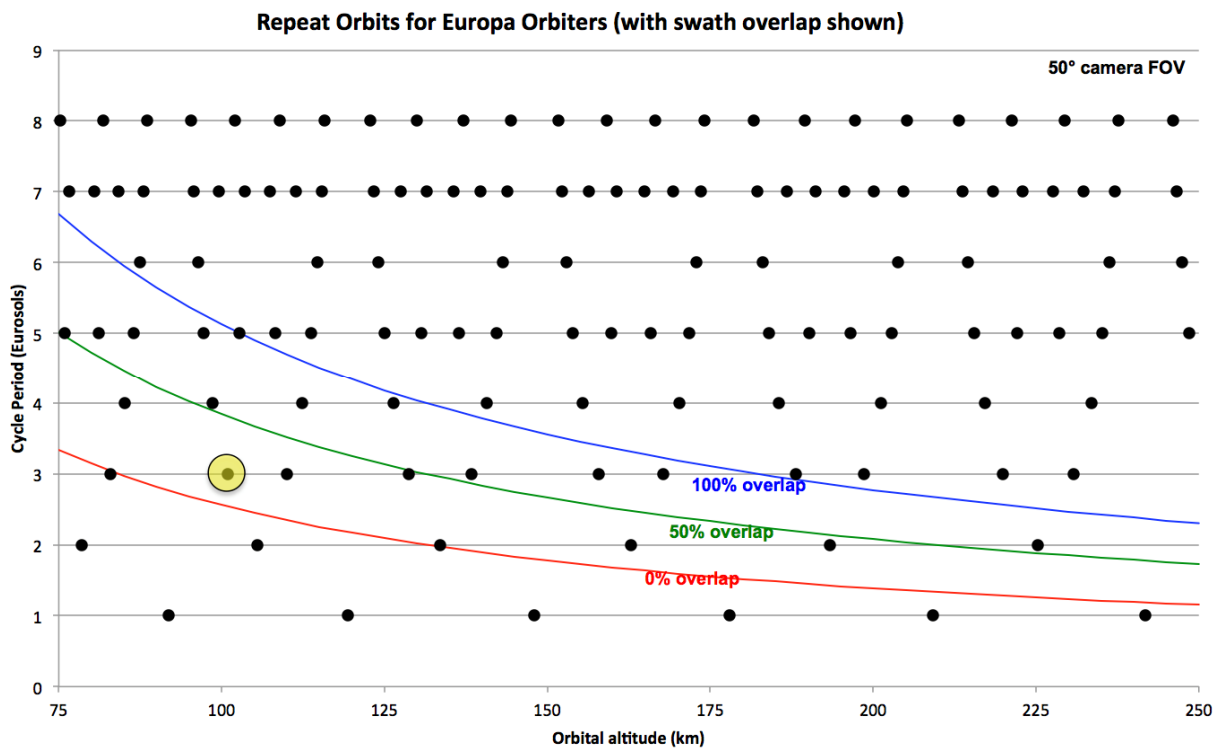


Figure B.2.8-2. Candidate repeat orbits.

the figure with a yellow circle, is a 122:3 repeat orbit; that is, 122 orbits of Europa are executed over 3 eurosols (about 11 days). This repeat cycle gives a swath-to-swath overlap of 18% at the equator at the end of the cycle. Since this repeat cycle only takes 11 days, continuing the cycle would provide up to three opportunities to map each point on the surface over the 30-day mission.

Imaging might be curtailed at the poles after the first Eurosol, as the groundtracks converge and higher overlap is achieved. At the equator, the overlap is 18% from one Eurosol to the next; however, above about 50 degrees latitude, only every other swath need be imaged for full coverage; and above about 65 degrees latitude, only every fourth swath is needed for full coverage. This strategy might be utilized to conserve resources (power, data) if needed, or to enable other operations, such as maneuvers.

Figure B.2.8-3 illustrates the imaging coverage achievable after one repeat cycle of 11 days. The only gap shown is that due to occultation by Jupiter, as the satellite (and spacecraft)

passes into shadow.

Figure B.2.8-4 shows the Laser Altimeter spacing and coverage after the full 30-day science phase. Equatorial spacing of 25 km is achieved by allowing the groundtracks to drift after the first imaging repeat cycle.

The data collection and pointing profile is identical in nature for each orbit, save for curtailing of imaging coverage over time. No negotiation for resources or case-by-case optimization is necessary.

The orbiter concept employs frequent to continuous coverage for data downlink. The spacecraft is Earth-pointed except for trajectory correction maneuvers (TCMs), with science playback, engineering telemetry, and two-way navigation during DSN passes. Instruments that require pointing to the surface are on a two-gimbal science platform. The data balance described in Section B.2.4 allows for reasonable DSN tracking and healthy data volume margin in returning each orbit's science observations.

Simple, repeated operations are sufficient to

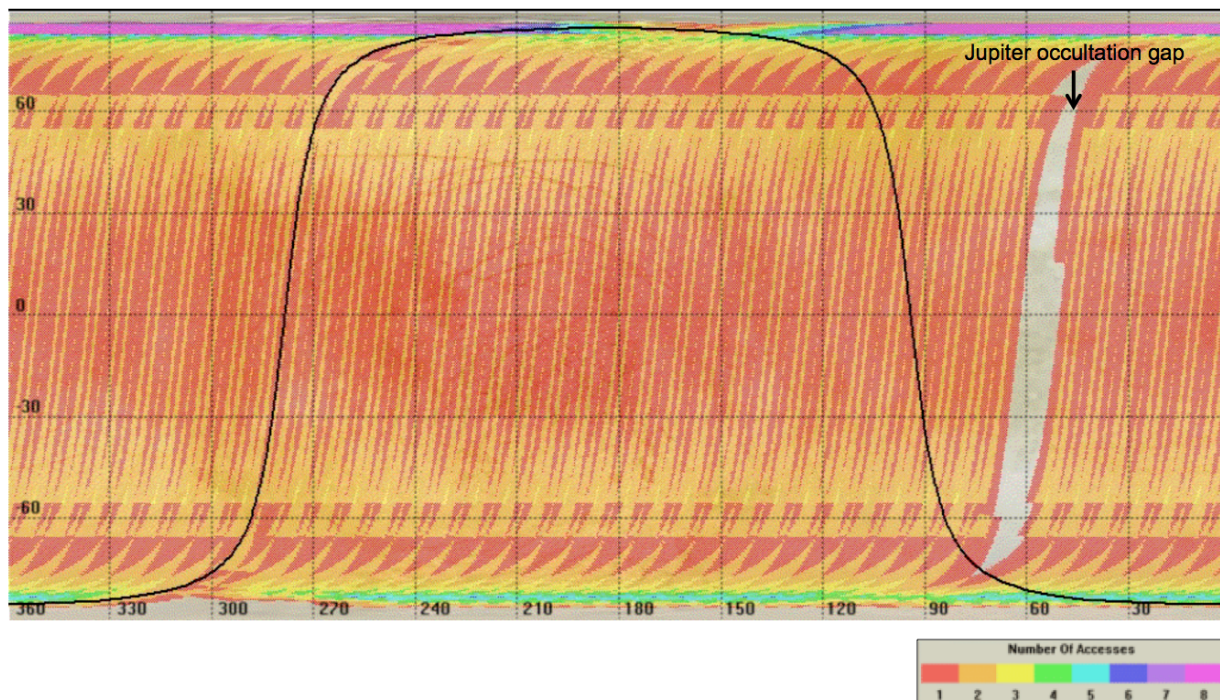
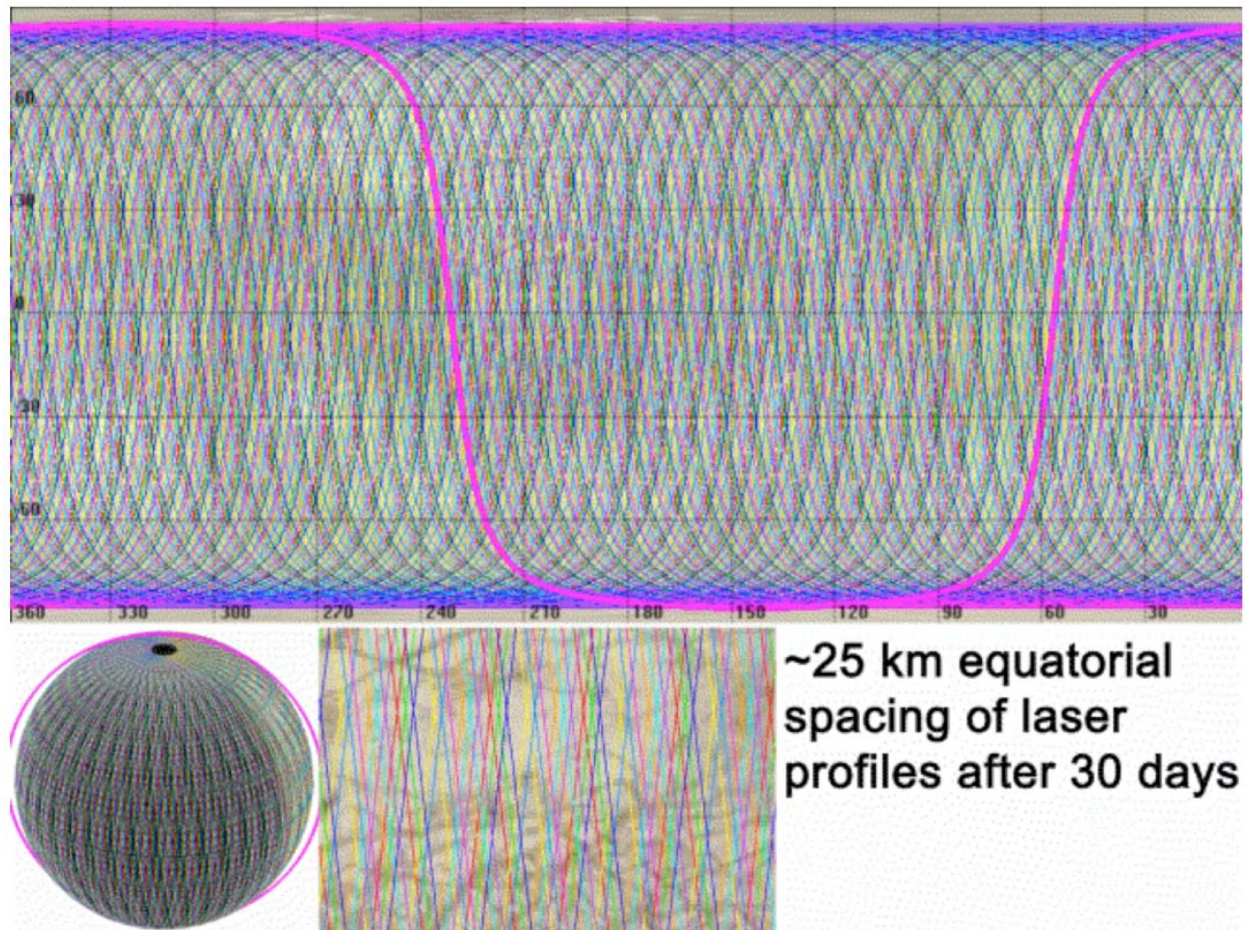


Figure B.2.8-3. Imaging coverage after one repeat cycle.



**Figure B.2.8-4.** Laser Altimeter coverage after one repeat cycle.

accomplish the above operations concepts. All orbits follow a single science profile of activities. There is no optimization per orbit or sharing of pointing or data volume, so negotiation is negligible. Maneuvers occur every few days; overall, activity intensity is low, with mostly continuous, simply sequenced background activities.

### B.2.8.3 Development Supporting Europa Operations

Early consideration of operability issues in the system architecture and design is of great importance. The Europa Flyby Mission plans significant operations scenario development during Phases A-D. Science operations will be a strong element of the prelaunch flight systems engineering. Science operations scenarios will be developed early and at a level of detail that permits flight system design choices to be

assessed thoroughly. Operations and ground system architecture, requirements, models, and software will be developed to a level sufficient to support prelaunch development and flight system trade studies. Science planning tools will be developed such that they can be used to evaluate the ground and flight system requirements and capabilities. Based on these preparations, refinements can then be made much more confidently in cruise and throughout the mission to this unified ground and flight system architecture and its software requirements.

Modeling will be conducted to simulate representative operations in deep space, including Europa flyby operations. The ATLO phase includes testing of at least one representative operational sequence to be used during Europa encounters. These efforts, though they add early cost, should bring net savings to the

project over all life cycle phases because they make possible more efficient operations, and uncover problems at a time when something can be done to mitigate them.

Opportunities for process improvement are built into the schedule after launch. A long cruise period presents some challenges, among them the risks of personnel attrition and ground system obsolescence. However, the varying level of intensity—lower between gravity assists, for example—also offers opportunities to improve processes, software, IT infrastructure, and operations concepts and the science template for Europa observations. A Europa Orbiter Mission project would aim to fill the “bathtubs” between major events in cruise with periods of further development and training. The Europa Orbiter Mission would strategically defer some operations development until after launch. Doing so has several advantages. First, it obviates the need to staff the project up for major cruise events and down afterwards. Second, it allows the project to take advantage of improvements in technology as they become available and to work with a flight team more likely to be present during later operations than is the flight team in place at launch. Third, it affords the flight team enticing opportunities to contribute to the design of the operations system, improving staff skill and possibly retention as team members choose to remain with the project in part to see their efforts bear fruit in Europa orbit. Finally, it ensures that the operations team on the line during science operations is deeply familiar with the system, such that disruptions from faults or radiation issues can be handled in an expeditious, reliable, and expert manner. Staffing levels should remain at approximately the late Phase D workforce level through launch and initial checkouts, after which it can drop to a more sustainable cruise staffing level. Cruise staffing should be relatively flat thereafter, with a moderate increase in development staff in the later portion of interplanetary cruise. Because the navigation team must

be fully capable for JOI, they would staff up to Jupiter cruise levels no later than six months before JOI. Spacecraft system and subsystem support needed to support navigation and maneuvering would also be added at this time. Other operations teams would staff up at around JOI to prepare for EOI, finalize the orbital science operations plan and supporting software, with the first ORTs for Europa science operations beginning 4 to 6 months after JOI.

### **B.2.9 Systems Engineering**

*Through key investments in infrastructure, engineering products, and team-building, the Europa Study Team is well positioned to move into pre-project formulation.*

This section outlines the overall systems engineering approach and plan. The subsections that follow address three specific systems engineering challenges: radiation, planetary protection, and nuclear safety.

In general the Europa Orbiter Mission can be said to have the following technical and programmatic characteristics:

- Technical
  - Functioning in the presence of radiation flux, SEEs, radiation damage to parts and materials
  - Satisfying planetary protection of the European ocean, as well as of Ganymede and Callisto, from delivered bioburden
  - Lifetime and reliability over a long mission
  - Maintaining conservative resource margins
  - Integrating a suite of competitively selected science instruments from a diverse field of providers
  - Integrating radioisotope power sources
  - Contrasting thermal environments at Venus flyby and Jupiter
  - Critical orbit insertion at Jupiter and Europa

- Intense science operations schedule at Europa after years of unhurried cruise
- Keeping a 10-year-plus “corporate memory” of the requirements, detailed design, and the rationales for design choices
- Programmatic
  - Succeeding in a cost- and cost-profile-constrained environment
  - Coordinating the efforts of a large, diverse engineering team
  - Integrated the project and design with competitively selected instruments
  - Accommodating development and maturation issues of the radioisotope power sources
  - Multi-institution and potential multinational partnerships (JPL, APL, PIs)

To help address these concerns, the following overarching systems engineering objectives have been set for formulation:

- By System Requirements Review (SRR), produce a Baseline System Specification (L1-L3 Baseline; L4 Preliminary; L5 Key and Driving), a committed systems engineering schedule and cost profile, and a committed mission architecture.
- By Preliminary Design Review (PDR), produce a released set of procurement specifications, a fully developed preliminary design, and a committed project schedule and cost.

Institutional project and line management is uniformly committed to making major strides in systems engineering, supporting and enforcing the following approach:

- Exercise rigorous engineering discipline. Expect engineering rationale to be documented as complete and logical chains of thought, and in appropriate

tools (Mathematica/Maple not PowerPoint; IOMs not emails)

- Make use of emerging new systems engineering capabilities as appropriate, including system modeling language standards and tooling, model integration and exchange standards and tooling, and Web-based report generation.
- Starting from the beginning, build persistent and evolvable artifacts.
- Starting from the beginning, build a core team of systems engineers who can faithfully promulgate the architecture later as the project grows.
- Proactively align with forthcoming NPR 7120.5E (NASA 2012).
- Emphasize architecture and design space exploration through MCR. An architectural approach keeps the team properly focused on the “why,” and design space keeps us properly focused on the concept rather than a point design. In this endeavor, trusted models and analytical tools are essential investments.
- Make decisions by a process that is explicitly guided by Architecture, is timely and responsive, is transparent to all stakeholders, and includes balanced consideration of multiple experienced viewpoints.

The Europa OrbiterOrbiter Mission is well positioned to move into pre-project formulation. The Europa Study Team has made key investments in infrastructure, engineering artifacts, and team-building, as described below:

- Infrastructure has been under development for the long term. Already set up and in initial use are a collaborative Systems Modeling Language (SysML) environment (MagicDraw/Teamwork Server), a collaborative architecture development environment (Architecture Framework Tool), the project doc-

ument repository (DocuShare), and the project workflow management system (JIRA).

- Key plans and processes are in place. Key parts of the architecture description are in preliminary form, as outlined in this report. The core of a system model is established.
- Our team processes and practices are maturing. Cost estimates, some technical margin estimates, and mechanical configuration changes have been improved over past practice.

From this strong starting point, a plan that achieves robust maturity at SRR and PDR has been constructed. The sketch of this plan, expressed as key artifacts per life-cycle phase through PDR, is shown in Tables B.2.9-1 through B.2.9-4. In these tables the changes from one table to the next are shown in **bold**

**blue font**, and the parentheticals following the artifact names denote required maturity levels:

- (A): Approach is defined, and possibly a sketch of the artifact.
- (K&D): Key and Driving cases are identified and covered.
- (P): Preliminary. A full version for review and discussion leading to a baseline version.
- (B): Baseline. The artifact is under configuration control.
- (U): Update.

After PDR, systems engineering focus changes from development to implementation: managing change control process, while maintaining architectural integrity; implementing I&T and V&V programs; and preparing for flight operations.

**Table B.2.9-1.** Present maturity of systems engineering artifacts.

Systems Engineering Plan: Key Artifacts per Life-Cycle Phase							
At Tech Review	Artifact Type						
	Plan	Scenario	Model	Analysis & Sim	Report	Spec	
<b>SCOPE</b>	Program (L1)						L1 Rqmts (K&D)
	Project (L2)	Arch Dev Plan (P) SEMP (A) Model Mgt Plan (A)	Driving Mission (K&D)	Trajectory (P) Science Margin (A) Data Margin (P) FS Radiation (P)	Delta-V/Prop (P) Science Margin (A) Data Margin (P) FS Radiation Life (P)	Concept Report (P) Msn Arch Descr (P) Ops Concept (A) Tech Assessment (A) Eng Dev Assess (A) Top Risks (A)	L2 Rqmts (A) Env Definition (A)
	System (L3)		Flight Sys Ops (K&D)	FS Functional (P) FS Physical (P) FS Shielding (P) FS Power (P) FS Static Mech (P) FS Thermal (P) FS Telecom Link (P) FS Attitude Ctrl (P)	FS Mass Margin (P) FS Shield Mass (P) FS Pwr Margin (P) FS Mass Props (P) FS Therm Balance (P) FS Link Margin (P) FS Pntg Margin (P)		L3 Rqmts (A)
	Subsystem (L4)			Power (K&D) Thermal (K&D) Propulsion (K&D) Telecom (K&D) Avionics (K&D) Structure (K&D)	Power Bus Sim (P) Therm Balance (P) JOI Perf (A) EIRP, G/T (P) C&DH Throughput (A) LV Static Envel (P)		
	Component (L5)			Radiation Effects (P) DHMR Effects (P)	Component Life (P) Parts/Matl Issues (P)	Approved Parts (A) Approved Matls (A)	

(A) Approach (K&D) Key & Driving (P) Preliminary (B) Baseline (U) Update **Blue = Change**

**Table B.2.9-2.** Maturity of systems engineering artifacts at MCR.

Systems Engineering Plan: Key Artifacts per Life-Cycle Phase							
At MCR	Artifact Type						
	Plan	Scenario	Model	Analysis & Sim	Report	Spec	
<b>SCOPE</b>	Program (L1)					L1 Rqmts (P)	
	Project (L2)	Arch Dev Plan (B) SEMP (P) Model Mgt Plan (P) Integr Plan (A) V&V Plan (A)	Driving Mission (P)	Trajectory (B) Science Margin (B) Data Margin (B) FS Radiation (B)	Delta-V/Prop (P) Science Margin (P) Data Margin (P) FS Radiation Life (P) Rqmt Traceability (P)	Concept Report (B) Msn Arch Descr (P) Ops Concept (P) Tech Assessment (P) Eng Dev Assess (P) Top Risks (P)	L2 Rqmts (P) Env Definition (P) External ICDs (K&D) Intersystem ICDs (K&D) S/C-P/L ICD (K&D)
	System (L3)		Flight Sys Ops (P)	FS Functional (P) FS Physical (P) FS Shielding (P) FS Power (P) FS Static Mech (P) FS Thermal (P) FS Telecom Link (P) FS Attitude Ctrl (P) FS Behavior (P) FS Fault Contnmt (P)	FS Mass Margin (P) FS Shield Mass (P) FS Pwr Margin (P) FS Mass Props (P) FS Therm Balance (P) FS Link Margin (P) FS Pntg Margin (P)	L3 Rqmts (K&D) Intra-FS ICDs (K&D)	
	Subsystem (L4)			Power (P) Thermal (P) Propulsion (P) Telecom (P) Avionics (P) Structure (P)	Power Bus Sim (P) Therm Balance (P) JOI Perf (P) EIRP, G/T (P) C&DH Throughput (P) LV Static Envel (P)		
	Component (L5)			Radiation Effects (P) DHMR Effects (P)	Component Life (P) Parts/Matl Issues (P)	Approved Parts (P) Approved Matls (P)	

(A) Approach (K&D) Key & Driving (P) Preliminary (B) Baseline (U) Update Blue = Change

**Table B.2.9-3.** Maturity of systems engineering artifacts at SRR.

Systems Engineering Plan: Key Artifacts per Life-Cycle Phase								
At SRR	Artifact Type							
	Plan	Scenario	Model	Analysis & Sim	Report	Spec		
<b>SCOPE</b>	Program (L1)						L1 Rqmts (B)	(A) Approach (K&D) Key & Driving (P) Preliminary (B) Baseline (U) Update <b>Blue = Change</b>
	Project (L2)	Arch Dev Plan (U) SEMP (B) Model Mgt Plan (B) Integr Plan (P) V&V Plan (P) S/W Mgt Plan (P)	Mission Plan (K&D)	Trajectory (U) Science Margin (U) Data Margin (U) FS Radiation (U)	Delta-V/Prop (B) Science Margin (B) Data Margin (B) FS Radiation Life (B) Rqmt Traceability (B)	Concept Report (U) Msn Arch Descr (B) Ops Concept (B) Tech Assessment (B) Eng Dev Assess (B) Top Risks (B) Instrument AO PIP (B)	L2 Rqmts (B) Env Definition (B) External ICDs (B) Intersystem ICDs (P) S/C-P/L ICD (P)	
	System (L3)		Flight Sys Ops (B)	FS Functional (B) FS Physical (B) FS Shielding (B) FS Power (B) FS Static Mech (B) FS Thermal (B) FS Telecom Link (B) FS Attitude Ctrl (B) FS Behavior (B) FS Fault Contnmt (B)	FS Mass Margin (P) FS Shield Mass (P) FS Pwr Margin (P) FS Mass Props (P) FS Therm Balance (P) FS Link Margin (P) FS Pntg Margin (P) FS PRA (A) FS Func FMECA (A) FS TAYF Exceptions (A)	Ground Sys Arch (P) Payload Arch (P)	L3 Rqmts (B) Intra-FS ICDs (P) Procurement Specs (P)	
	Subsystem (L4)			Power (B) Thermal (B) Propulsion (B) Telecom (B) Avionics (B) Structures (B)	Power Bus Sim (P) Therm Balance (P) JOI Perf (P) EIRP, G/T (P) C&DH Throughput (P) LV Static Envel (P)		L4 Rqmts (P) Intrasubsystem ICDs (P)	
	Component (L5)			Radiation Effects (B) DHMR Effects (B)	Component Life (P) Parts/Matl Issues (P)	Approved Parts (P) Approved Matls (P)		

**Table B.2.9-4.** Maturity of systems engineering artifacts at PDR.

		Systems Engineering Plan: Key Artifacts per Life-Cycle Phase						
At PDR	Artifact Type							
	Plan	Scenario	Model	Analysis & Sim	Report	Spec		
<b>SCOPE</b>	Program (L1)					L1 Rqmts (B)	(A) Approach (K&D) Key & Driving (P) Preliminary (B) Baseline (U) Update <b>Blue = Change</b>	
	Project (L2)	Arch Dev Plan (B) SEMP (U) Model Mgt Plan (U) Integr Plan (B) V&V Plan (B) S/W Mgt Plan (B)	Mission Plan (P)	Trajectory (U) Science Margin (U) Data Margin (U) FS Radiation (U)	Delta-V/Prop (U) Science Margin (U) Data Margin (U) FS Radiation Life (U) Rqmt Traceability (U) <b>Mission Fault Tree (P)</b>	Concept Report (U) Msn Arch Descr (U) Ops Concept (U) Tech Assessment (U) Eng Dev Assess (U) Top Risks (U) Instrument AO PIP (B)		L2 Rqmts (B) Env Definition (B) External ICDs (B) Intersystem ICDs (B) S/C-P/L ICD (B)
	System (L3)		Flight Sys Ops (U)	FS Functional (B) FS Physical (B) FS Shielding (B) FS Power (B) FS Static Mech (B) FS Thermal (B) FS Telecom Link (B) FS Attitude Ctrl (B) FS Behavior (B) FS Fault Contnmt (B)	FS Mass Margin (B) FS Shield Mass (B) FS Pwr Margin (B) FS Mass Props (B) FS Therm Balance (B) FS Link Margin (B) FS Pntg Margin (B) FS PRA (P) FS Func FMECA (P) FS TAYF Exceptions (P)	Ground Sys Arch (B) Payload Arch (B)		L3 Rqmts (B) Intra-FS ICDs (B) Procurement Specs (B)
	Subsystem (L4)			Power (B) Thermal (B) Propulsion (B) Telecom (B) Avionics (B) Structures (B)	Power Bus Sim (B) Therm Balance (B) JOI Perf (B) EIRP, G/T (B) C&DH Throughput (B) LV Static Envel (B)	<b>Subsys Des Desc (P)</b> <b>P/L Design Desc (P)</b>		L4 Rqmts (B) Intrasubsystem ICDs (B)
	Component (L5)			Radiation Effects (B) DHMR Effects (B)	Component Life (B) Parts/Mat Issues (B)	Approved Parts (B) Approved Matls (B)		L5 Rqmts (P)

### B.2.9.1 Radiation

*The effects of radiation on the spacecraft are mitigated by the efficient use of inherent shielding provided by the spacecraft itself and additional dedicated shield mass, combined with radiation-tolerant materials and electronics.*

The Europa Orbiter spacecraft would be exposed to naturally occurring and self-generated radiation from launch to the end of mission. The self-generated radiation, composed of neutrons and gamma rays, is evolved from the natural decay of nuclear fuel used in the Advanced Stirling Radioisotope Generators (ASRGs). The naturally occurring radiation encountered during the cruise phase between launch and Jupiter Orbit Insertion (JOI) consists of solar flare protons and background galactic cosmic ray heavy ions. Between JOI and the end of the mission, the spacecraft is exposed to protons, electrons, and heavy ions trapped in the Jovian magnetosphere.

The radiation encountered during the mission can affect onboard electronics, nonmetallic materials, thermal control materials, and surface coatings by depositing energy through ionization, henceforth called total ionizing dose (TID), and can cause noise in science instrument and star-tracker detectors due to the intense proton and electron flux encountered in the Jovian system. The expected accumulated TID from launch to end of mission as a function of effective aluminum shielding thickness is shown in Table B.2.9-5. Peak electron and

**Table B.2.9-5.** Expected Orbiter Mission accumulated total ionizing dose as a function of shield thickness.

Aluminum Thickness (mil)	Total Ionizing Dose (krad Si)				
	Electron	Photon	Proton	ASRG	Total
100	1500	5.3	51.7	1.3	1560
200	685	6.0	12.1	1.3	704
400	258	7.0	2.1	1.3	268
600	134	7.6	1.0	1.3	140
800	80.5	8.1	0.6	1.3	90.5
1000	53.4	8.4	0.4	1.3	63.5
1200	37.9	8.7	0.3	1.3	48.2
1400	28.1	8.8	0.2	1.3	38.4
1600	21.6	8.9	0.2	1.3	32.0

proton fluxes for the mission are shown in Table B.2.9-6.

The selection of electronic parts with respect to their radiation tolerance and reliability in the Europa radiation environment will be achieved through a combination testing and analysis. The minimum acceptable total ionizing dose hardness of electronic devices will be 100 kilorad. The minimum single event effects (SEE) hardness will be documented in a Parts Program Requirements (PPR) document. A combination of radiation testing (TID, DDD, and SEE) of electronic devices and buying vendor guaranteed radiation hardened parts that meet the minimum TID and SEE requirements will ensure that robust electronics will be used in spacecraft and instrument electronics. Radiation testing will be done at industry standard high dose rates and at low dose rate for electronic devices types that are susceptible to Enhanced Low Dose Rate Sensitivity (ELDRS) effects (primarily bi-polar devices). Electronic part parameter degradation observed during radiation testing will be documented and used as input into the spacecraft and instrument electronics end of mission Worst Case Analysis (WCA). Electronic devices that do not meet the minimum TID and SEU hardness requirements will not be used within the spacecraft electronics or instruments unless approved by a requirements waiver.

The selection guidelines of non-metallic materials for radiation susceptibility and reliability has been documented in a report entitled, "Materials Survivability and Selection for Nuclear Powered Missions" by Willis [JPL D-34098].

**Table B.2.9-6.** Expected Orbiter Mission peak electron and proton flux.

Particle Energy (MeV)	Flux (#>Energy cm <sup>-2</sup> sec <sup>-1</sup> )	
	Electron	Proton
10	1.6E6	1.5E5
20	4.6E5	2.8E4
30	2.1E5	7.3E3
50	7.0E4	6.9E2
100	1.5E4	1.5E1

Detailed evaluations will be performed for these materials after exposure to end of mission radiation environment to ensure end of life performance requirements are met. Radiation testing will be performed for materials which do not have available radiation data.

The Europa Orbiter mission will develop an Approved Parts and Materials List (APML) for the purpose of identifying standard parts approved for flight equipment developed under the project's cognizance. The APML will be populated with EEE parts and materials, as well as many critical parts such as sensors, detectors, power converters, FPGAs, and non-volatile memories. Each entry will be accompanied with a Worst Case Datasheet (WCD) and application notes describing proper use of the part at selected radiation levels. Dissemination of this information early in the design process is critical to enable the spacecraft electronics and instrument providers to adequately design for the radiation environment.

Every approved part listed on the APML will meet the reliability, quality, and radiation requirements specified in the PPR. The APML will be updated as new radiation data become available. Parts not listed as approved on the APML are defined as non-standard parts and will require a Non-standard Part Approval Request (NSPAR) for use in the Europa Orbiter mission. All non-standard parts will be reviewed, screened, and qualified to the requirements of PPR.

Every part on the APML will be approved by the Parts Control Board (PCB). The PCB recommends and approves parts for inclusion in the APML. Criteria will be based on absolute need, the number of subsystems requiring the part, qualification status, TID, Single Event Effects (SEE), and procurement specification review. Mission designers should use standard parts to the maximum extent possible so that they can reduce the radiation testing and qualification expenditure to the minimum.

Radiation-induced effects on instrument detectors and other key instrument components can ultimately impact the quality and quantity of the mission science return and the reliability of engineering sensor data critical to flight operations. High-energy particles found within the Europa environment will produce increased transient detector noise as well as long-term degradation of detector performance and even potential failure of the device. Transient radiation effects are produced when an ionizing particle traverses the active detector volume and creates charges that are clocked out during readout. Radiation-induced noise can potentially swamp the science signal, especially in the infrared wavebands where low solar flux and low surface reflectivity result in a relative low signal. Both TID and DDD effects produce long-term permanent degradation in detector performance characteristics. This includes a decrease in the ability of the detector to generate signal charge or to transfer that charge from the photo active region to the readout circuitry; shifts in gate threshold voltages; increases in dark current and dark current non-uniformities, and the production of high-dark-current pixels (hot pixels or spikes). It is important to identify and understand both the transient and permanent performance degradation effects in order to plan early for appropriate hardware and operations risk mitigation to insure mission success and high-quality science returns.

A JEO Detector Working Group (DWG) was formed in FY08 to evaluate the detector and laser components required by the planning payload and stellar reference unit. The DWG participants included experienced instrument, detector, and radiation environment experts from APL and JPL. For each technology required for the payload, the DWG (i) reviewed the available radiation literature and test results, (ii) estimated the radiation environment incident on the component behind its shield, and (iii) assessed the total dose survivability (both TID and DDD) and radiation-induced

transient noise effects during peak flux periods. The assessment included the following technologies: visible detectors, mid-infrared and thermal detectors, micro-channel plates and photomultipliers, avalanche photodiodes, and laser-related components (pump diode laser, solid-state laser, fiber optics).

The DWG assessment, reported in “Assessment of Radiation Effects on Science and Engineering Detectors for the JEO Mission Study” [JPL D-48256], concluded that the radiation challenges facing the JEO notional payload and SRU detectors and laser components are well understood. With the recommended shielding allocations, the total dose survivability of these components is not considered to be a significant risk. In many cases, the shielding allocation was driven by the need to reduce radiation-induced transient noise effects in order to meet science and engineering performance requirements. For these technologies—notably mid-infrared detectors, avalanche photodiode detectors, and visible detectors for star tracking—the extensive shielding (up to 3-cm-thick Ta) for transient noise reduction effectively mitigates all concern over total dose degradation. For the remaining technologies, more modest shielding thicknesses (0.3–1.0 cm Ta, depending upon the specific technology) were judged to be sufficient to reduce the total dose exposure and transient noise impact to levels that could be further reduced with known mitigation techniques (detector design, detector operational parameters, algorithmic approaches and system-level mitigations). The DWG conclusions reached for the JEO are applicable for the science detectors and the SRU onboard the Europa Orbiter mission.

A rigorous “test-as-you-fly” policy with respect to detector radiation testing, including irradiation with flight-representative species and energies for TID, DDD, and transient testing, will be adopted for the Europa Orbiter mission.

The Jovian electron environment also causes dielectric materials and ungrounded metals to collect charge on spacecraft external surfaces and within the spacecraft. This causes transient voltage and currents in the spacecraft when an electrostatic discharge (ESD) event occurs. Surface charging effects are mitigated by limiting the differential charging of external materials. This is accomplished by using materials that have surface coatings and treatments that allow the accumulated charges to bleed to spacecraft ground. A significant number of such surface materials have been used extensively in severe charging environments for spacecraft with long lifetimes (typically geosynchronous communications spacecraft, but also Juno) and are usable for the Europa Orbiter Mission. These materials include

- Carbon-loaded Kapton thermal blankets
- Indium-tin-oxide-coated gold Kapton thermal blankets
- Germanium-coated, carbon-loaded Kapton thermal blankets
- Electrostatic-conductive white paint
- Electrostatic-conductive black paint
- Composite materials
- Metallic materials

When surface discharge does occur, the voltage and current transients are mitigated by shielding around harness lines and using interface electronic devices that can tolerate the energy from ESD-induced transients that couple into the harness center conductors.

Internal ESD is controlled by shielding to reduce the electron flux present at dielectric materials within the spacecraft (typically circuit boards) and by limiting the amount of ungrounded metal (ungrounded harness conductors, connector pins, device radiation shields, part packages). The shielding required to reduce the TID to acceptable levels for the Europa Orbiter Mission is more than sufficient to reduce the electron flux enough to preclude discharge events to circuit boards. Grounding

of radiation shields, part packages, harness conductors, and connector pins through ESD bleed wires or conductive coatings limits the ungrounded metals to small areas that cannot store enough energy to cause discharges that can damage electronic devices.

The surface and internal charging methodology has been used extensively in a severe charging environment for spacecraft with long lifetimes and was used specifically on the Juno project.

The spacecraft's exposure to radiation is attenuated to acceptable levels by providing shielding between the external environment and the sensitive materials and electronic parts in the spacecraft. Most of the spacecraft electronics are placed in a shielded vault. Payload electronics and sensor heads external to the vault have shielding tailored for their design and location on the spacecraft. Science instrument detector shielding to suppress radiation-induced background noise and permanent damage effects is achieved through a combination of instrument-level shielding for detector support electronics and internal high-Z material shielding for the detector devices.

Efficient use of dedicated shield mass is achieved through a nested shield design, shown in Figure B.2.9-1. Spacecraft structure and placement of the propulsion subsystem hardware (fuel tanks, oxidizer tanks, helium pressurant tanks, and propellant that remains in the tanks after JOI) provide significant collateral shielding to the electronics packaged within the vault. The vault's wall thickness and material composition, 5.3-mm-thick aluminum, limit the Orbiter Mission TID to 150 krad for the enclosed electronics. Localized shielding at the assembly level reduces the Orbiter Mission TID from 150 krad to 50 krad at the device level for all electronics.

The dedicated shield mass for the Orbiter Mission is a total of 167 kg, as shown in Table B.2.9-7. The shield mass was calculated based on a detailed radiation transport analysis

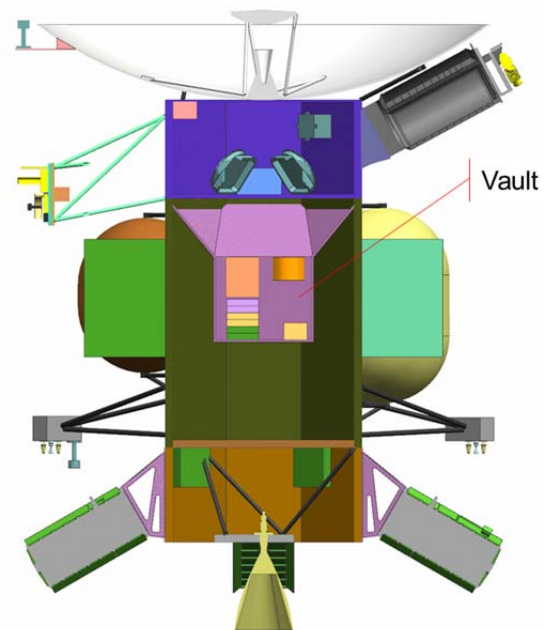


**Figure B.2.9-1.** Orbiter Mission electronics are shielded by the spacecraft structure, propulsion tanks, and a dedicated electronics vault.

that takes into account the spacecraft configuration shown in Figure B.2.9-1; material composition and thickness of the spacecraft structural elements and propulsion tanks; and the locations of electronic units and science instruments. Analysts used the following process:

1. Generate spacecraft element configuration and locations from a CAD model.
2. Explicitly calculate the shielding effectiveness of materials used in spacecraft structure, propulsion tanks, electronics unit chassis, dedicated vault, and added electronics assembly shielding based on material composition, density, and location using the NOVICE radiation transport code. For this analysis, the propulsion tanks are modeled with 436 kg of fuel and oxidizer in the tanks for the portion of the mission between Jupiter Orbit Insertion (JOI) and Europa Orbit Insertion (EOI). After EOI, the propellant tanks are modeled as empty tanks.

3. To minimize the cost and risk of assuming electronic parts with higher radiation tolerance, assume all spacecraft electronics to use 300-krad-tolerant electronic parts.
4. Understand science instrument electronics co-located with detectors to have radiation tolerances that are instrument-specific (see Section B.2.2).
5. Through adjustments to assembly-level shielding mass, shield all spacecraft electronics assemblies to a TID of 150 krad or less at end of mission (i.e., to account for environmental uncertainty, they are given a radiation design factor [RDF] greater than or equal to 2 at the end of the mission).
6. Shield science instrument electronics to have a minimum RDF of 2 for TID at the end of the mission.
7. To minimize cost, use aluminum shielding for all spacecraft electronics except science instrument and star-tracker detectors.
8. To minimize the radiation-induced noise at the detector location, shield science instrument and star-tracker detectors using high-atomic-number materials (such as tantalum) (see Section B.2.2).
9. At the individual assembly level, to allow the use of off-the-shelf electronics without modification, wrap shielding around each assembly rather than integrating it into the assembly chassis.
10. Model circuit boards within the electronic assemblies as unpopulated boards. (Modeling component layouts on boards will be performed as the project progresses into Phase B. Including component layout in the radiation transport model will further reduce TID at the device level.)

Significant opportunities to reduce the dedicated shield mass have been identified alt-

**Table B.2.9-7.** Calculated shield masses to reduce the mission TID below 150 krad within each assembly.

Item	Shield Mass (kg)
Vault Structure	40.6
C&DH Subsystem	4.3
Power Subsystem	9.8
MIMU (2)	7.8
SDST (2)	4.7
WDE (4 slices)	3.5
Ka HVPS (2)	5.4
X HVPS (2)	4.8
ASRG (5)	48.2
Star-Tracker (2)	13.7
Pressure Transducer (10)	3.9
Science Electronics	13.7
Topographic Imager	1.5
Laser Altimeter	4.7
Orbiter Mission Total	167

though they have been unexercised at this time. These opportunities include the following:

1. Change electronics unit placement within the vault to protect units with lower-TID-capable electronic parts.
2. Place electronics cards within units to provide the lowest local TID at the part level.
3. Use a more efficient shield material than aluminum.
4. Add rigor to the radiation transport model by including populated boards and individual device shielding.
5. Integrate the shielding into the electronics chassis.
6. Use multiple-material layered shielding.

The shield masses in Table B.2.9-7 have been incorporated into the spacecraft MEL.

### B.2.9.2 Planetary Protection

NASA Planetary Protection policy (NPR 8020.12C [NASA 2005]) specifies requirements for limiting forward contamination in accordance with Article IX of the 1967 Outer Space Treaty.

As Europa is a body of extreme interest to the astrobiological community as a possible loca-

tion for the emergence of extra-terrestrial life, contamination of Europa with Earth-derived biology must be carefully avoided.

The mission's plan for responding to planetary protection requirements is to perform Dry Heat Microbial Reduction (DHMR) on as much of the spacecraft as possible, as late in the integration flow as possible. DHMR involves raising the bulk temperature of the spacecraft above the survival threshold for microbes and their spores. For materials contamination reasons, this bake out is typically done in vacuum or inert gas (nitrogen). To the extent possible, all spacecraft components will be designed to accommodate late integration DHMR without disassembly or recalibration. However, components or instrumentation unable to comply with DHMR requirements may be removed and sterilized through other means.

The extent to which DHMR sterilization and subsequent recontamination must reduce the spacecraft bioburden before liftoff is greatly influenced by the expected impact of post-launch sterilization processes and contamination probabilities. These include:

- a) Probability of organism survival during interplanetary cruise
- b) Probability of organism survival in the Jovian radiation environment
- c) Probability of impacting Europa
- d) Probability of organism survival on the surface of Europa before subsurface transfer
- e) The duration required for transport to the European subsurface
- f) Organism survival and proliferation after subsurface transfer

Each of these factors will be carefully examined to determine the ultimate allowable bioburden at launch and the required effectiveness of DHMR to maintain compliance with NASA regulation and international treaty.

### B.2.9.3 Nuclear Safety

The Europa Orbiter Mission concept requires the use of nuclear energy sources for electrical power and heating. The radioactive material used for this purpose is potentially hazardous to humans and the environment unless precautions are taken for its safe deployment. The following circumstances are of concern:

- Handling: People would be in the vicinity while nuclear sources (ASRGs or RHUs) are being constructed, transported, and installed on the spacecraft.
- Launch: In the event of a catastrophic LV failure, the spacecraft with its nuclear components would be potentially subject to explosion, fire, impact, or the heat and forces of immediate reentry.
- Injection: If injection into interplanetary flight is not achieved, the spacecraft may be left in an Earth orbit that could decay to reentry after some time, thus exposing nuclear components to reentry conditions.
- Earth Flyby: If unplanned trajectory errors cause the spacecraft to reenter Earth's atmosphere, nuclear components would be exposed to reentry conditions.

Safety from nuclear hazards in each of these circumstances is essential.

The National Environmental Policy Act of 1969 (NEPA) specifies measures intended to mitigate these concerns. [This is enough ID for a public law—no need to put it in the References.] Project compliance with NEPA is mandatory and is described in more detail below.

#### B.2.9.3.1 NEPA Compliance

Environmental review requirements would be satisfied by the completion of a mission-specific Environmental Impact Statement (EIS) for the Europa Orbiter Mission. In accordance with the requirements of NPR 7120.5D, NPR 7120.5E (pending) and NPR 8580.1 (NASA 2007, 2012), the Record

of Decision (ROD) for this EIS would be finalized prior to or concurrent with project PDR.

The Europa Orbiter Mission Launch Approval Engineering Plan (LAEP) is completed no later than the Mission Definition Review (MDR). This plan describes the approach for satisfying NASA's NEPA requirements for the mission, and the approach for complying with the nuclear safety launch approval process described in Presidential Directive/National Security Council Memorandum #25 (PD/NSC-25) (1977) and satisfying the nuclear safety requirements of NPR 8715.3 (NASA 2010b). The LAEP provides a description of responsibilities, data sources, schedule, and an overall summary plan for preparing the following:

- A mission-specific environmental review document and supporting nuclear safety risk-assessment efforts
- LV and flight system/mission design data requirements to support nuclear risk assessment and safety analyses in compliance with the requirements of NPR 8715.3 (NASA 2010b) and the PD/NSC-25 nuclear safety launch approval process
- Support of launch site radiological contingency planning efforts
- Earth swing-by analysis
- Risk communication activities and products pertaining to the NEPA process, nuclear safety, and planetary protection aspects of the project.

It is anticipated that NASA HQ would initiate the Europa Orbiter Mission NEPA compliance document development as soon as a clear definition of the baseline plan and option space has been formulated. The Department of Energy (DOE) provides a nuclear risk assessment to support the environmental review document, based upon a representative set of environments and accident scenarios compiled by the KSC Launch Services Program working

with JPL. This deliverable might be modeled after the approach used for the MSL EIS.

DOE provides a Nuclear Safety Analysis Report (SAR) based upon NASA-provided mission-specific launch system and flight system data to support the PD/NSC-25 compliance effort. The SAR is delivered to an ad hoc Interagency Nuclear Safety Review Panel (INSRP) organized for the Europa Orbiter Mission. This INSRP reviews the SAR's methodology and conclusions and prepares a Safety Evaluation Report (SER). Both the SER and the SAR are then provided by NASA to the Environmental Protection Agency, Department of Defense, and DOE for agency review. Following agency review of the documents and resolution of any outstanding issues, NASA, as the sponsoring agency, would submit a request for launch approval to the Director of the Office of Science and Technology Policy (OSTP). The OSTP Director reviews the request for nuclear safety launch approval and can either approve the launch or defer the decision to the President.

As part of broader nuclear safety considerations, the Europa Orbiter Mission would adopt ATLO, spacecraft, trajectory (e.g., for sufficiently high orbit at launch, and for Earth flybys), and operations requirements that satisfy the nuclear safety requirements of NPR 8715.3 (NASA 2010b).

Development of coordinated launch site radiological contingency response plans for NASA launches is the responsibility of the launch site Radiation Protection Officer. Comprehensive radiological contingency response plans, compliant with the National Response Framework and appropriate annexes, would be developed and put in place prior to launch as required by NPR 8715.2 and NPR 8715.3 (NASA 2009a, 2010b). The Europa Orbiter Mission would support the development of plans for on-orbit contingency actions to complement these ground-based response plans.

A project-specific Risk Communication Plan would be completed no later than the MDR. The Risk Communication Plan details the rationale, proactive strategy, process, and products of communicating risk-related aspects of the project, including nuclear safety and planetary protection. The communication strategy and process would comply with the approach and requirements outlined in the Office of Space Science Risk Communication Plan for Deep Space Missions (JPL D-16993, 1999).

### B.3 Programmatic

#### B.3.1 Management Approach

The management approach draws upon extensive experience from Galileo and Cassini. It follows NPR 7120.5E and incorporates NASA lessons learned.

The project approach includes a work breakdown structure (WBS), technical management processes conducted by veteran systems engineers, and integrated schedule/cost/risk planning and management. The project will take advantage of existing infrastructure for planning, acquisition, compliance with the National Environmental Policy Act (NEPA), compliance with export control regulations (including International Traffic in Arms Regulations), independent technical authority (as called for in NPR 7120.5E), mission assurance, ISO 9001 compliance, and earned value management (EVM).

The Europa Orbiter Mission employs JPL's integrated project controls solutions to manage and control costs. Skilled business and project control professionals are deployed to projects, utilizing state of the art tools and executing processes that support the project cost, schedule, and risk management requirements. Key attributes of the project controls solution are as follows:

- The Business Manager, project focal point on all business management issues, and the project control staff lead

project planners and managers in application of the most effective and efficient implementation of project control processes.

- Mature and successfully demonstrated cost and schedule tools are employed.
- Cost and schedule data are tied directly to work scope.
- “Early warning” metrics are provided monthly to key decision makers. Metrics include 1) cost and schedule variances based on the cost value of work performed and 2) critical-path and slack analysis derived from fully integrated end-to-end network schedules. Each end-item deliverable is scheduled with slack to a fixed receivable. Erosion of this slack value is tracked weekly and reported monthly.
- An integrated business management approach is applied to all system and instrument providers. This approach includes relative performance measurement data integrated into the total project database for a comprehensive understanding of project cost and schedule dynamics.
- Risk management processes are integrated with the liens management process for full knowledge of project reserve status. Early risk identification is maintained as a potential threat to project reserves. Reserve utilization decisions are made with the knowledge of risks and risk mitigation, project performance issues, and increases in scope.

JPL flight projects that have used this integrated project controls approach include Juno, Grail, MSL, and Phoenix.

Requirements for project controls evolve throughout the project life cycle. Pre-Phase A and Phase A will require less support than phases B, C, and D. During Phase B, the project controls capability is established at full strength to establish all the appropriate data-

bases and gate products required for a successful Confirmation Review. During phases C and D, the project controls will be fully functioning with recurring performance measurement analysis and cost and schedule tracking reports. During phases E and F, the project controls function reduces to minimal levels.

### **B.3.2 WBS**

The Europa Orbiter Mission Work Breakdown Structure (WBS) is structured to enable effective cost, schedule and management integration. The WBS is derived from JPL's Standard Flight Project WBS Version 5 and is fully compliant with NPR 7120.5E. This WBS is a product-oriented hierarchical division of the hardware, software, services, and data required to produce end products. It is structured according to modular design of the spacecraft, and reflects the way the work would be implemented, and the way in which project costs, schedule, technical and risk data are to be accumulated, summarized, and reported.

The top-level WBS is shown Figures B.3.2-1 and B.3.2-2.

### **B.3.3 Schedule**

A top-level schedule and implementation flow is shown in Figure B.3.3-1. The phase durations draw on experience from previous outer planet missions and are conservative. A bottom-up, WBS-based integrated schedule would be generated during Pre-Phase A.

#### **B.3.3.1 Pre-Phase A**

Up to and including this report, many alternative concept studies have been conducted. Those studies form the basis of an assessment of alternatives that have resulted in the current mission concept and its readiness to complete Pre-Phase A. To complete Pre-Phase A, a pre-project team would be formed to refine the baseline mission concept and implementation plan to align with programmatic goals and objectives. This refinement, along with interactions with NASA and other potential stakeholders, will result in further definition of the

mission concept and draft project-level requirements.

The Pre-Phase A activities include completion of Pre-Phase A Gate Products specified in NPR 7120.5D and the forthcoming revision NPR 7120.5E (NASA 2007, NASA 2012 (pending)), preparation of a Project Information Package (PIP) in support of NASA's development of an AO for instrument acquisition, and a Mission Concept Review leading to Key Decision Point (KDP) A. In addition to those activities required for transition to Phase A, the team will identify additional planning, advanced development, and risk-reduction tasks that could provide a prudent and cost-effective approach to early reduction of cost and schedule risk and have the potential to reduce the estimated cost of the mission. Primary activities include reducing the radiation and planetary protection risks associated with instrument and spacecraft development.

#### **B.3.3.2 Phases A-F**

The Phase A-F schedule reflects the total project scope of work as discrete and measurable tasks and milestones that are time-phased through the use of task durations, interdependencies, and date constraints. To ensure low risk, the schedule includes slack for all tasks.

The Project Manager controls the project schedule, with support from a Project Schedule Analyst. An Integrated Master Schedule identifies key milestones, major reviews, and receivables/deliverables (Rec/Dels). Schedule reserves included in the schedule for the November 2021 launch opportunity meet or exceed JPL DP requirements (schedule reserves of 1 month per year for Phases A through D, with schedule reserves of 1 week per month for activities at the launch site [JPL 2010a]). The project uses an integrated cost/schedule system in Phase B to fully implement an EVM baseline in Phases C, D, and E. Inputs are supplied to NASA's Cost Analysis Data Requirement (CADRe) support contractor for reporting at major reviews. Schedule and cost





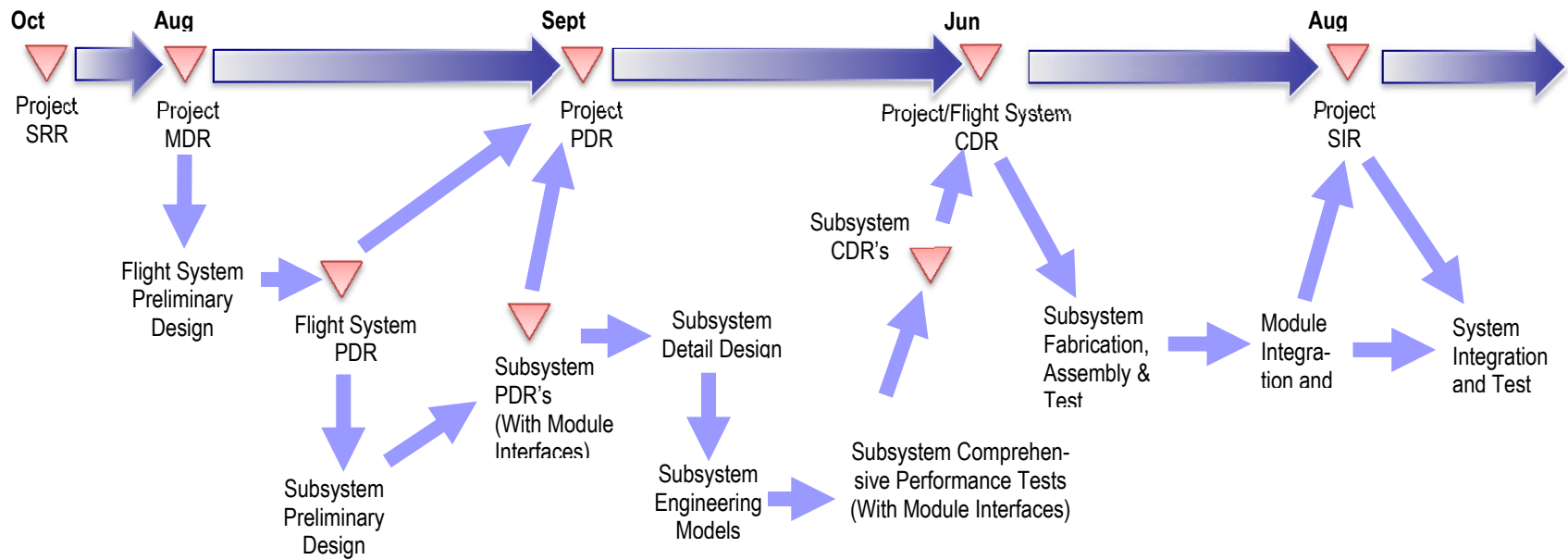
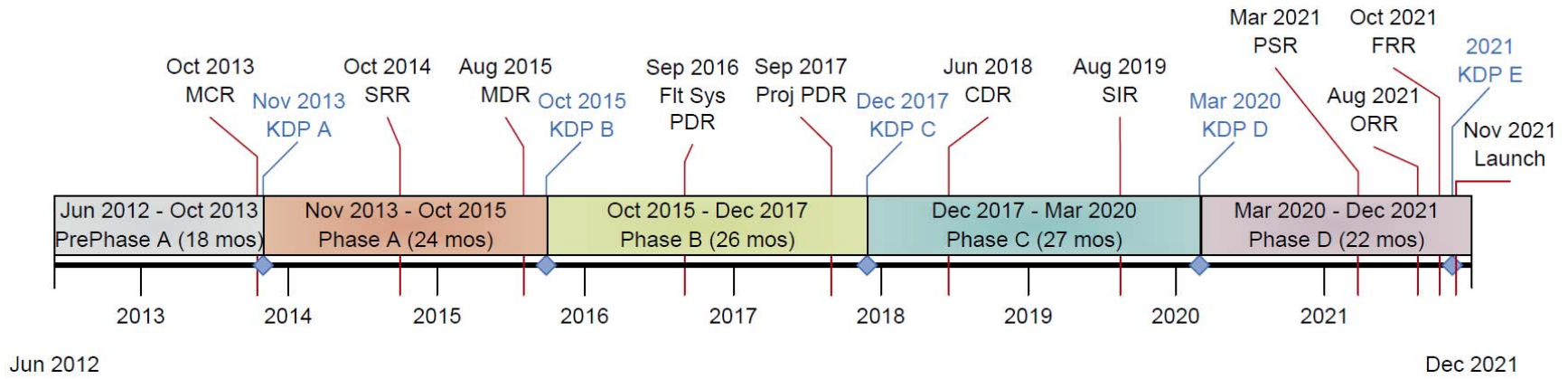


Figure B.3.3-1. Top-level schedule and Implementation Flow for the Europa Orbiter Mission.

estimates at completion (EACs) are prepared at regular intervals as part of the EVM process. Major project review milestones (not all shown) are consistent with NPR 7120.5D (NASA 2007) and will be reviewed for compliance with NPR 7120.5E (NASA 2012 [pending]).

#### B.3.3.3 Phases A–B

The length of phases A and B (24 months for A, 26 months for B) is driven by the need to mature the mission architecture in advance of selecting instruments in response to an AO and need to develop the selected instruments to adequate maturity before PDR. In Phase A, the primary tasks are completing the Gate Products required and facilitating the selection of the science instruments. The 8-month period between instrument selection and the system Mission Definition Review (MDR) allows instrument designers to work directly with the project personnel on issues related to accommodation, requirements, radiation, and planetary protection. The schedule is front-loaded with a long Phase A to give adequate time to define requirements early in the mission development life cycle.

#### B.3.3.4 Phases C–D

The length of phases C and D (27 months for C, 22 months D) is primarily driven by the schedule to bring the flight system to launch readiness. Phase C is longer than typical due to the added time required to implement the radiation and planetary-protection requirement-mitigation aspects of the design. The long Phase C also allows for a lower staff-level profile, which keeps the mission cost profile flat. Phase D was developed using the Cassini model of ATLO and includes 1.5 months to perform the system-level dry-heat sterilization.

A trailblazer activity is scheduled to occur at the launch facility in Phase D to ensure that the spacecraft design is compatible with the launch vehicle and facility limitations at the launch site for transporting and loading of the ASRGs. This activity starts at a very low level

in Phase B and continues with increasing activity until the approach to ASRG installation is validated in Phase D. The trailblazer activity is also used to dry-run the system-level dry-heat sterilization activities that will take place in a thermal vacuum chamber at KSC.

#### B.3.3.5 Phases E–F

Phase E (9.5 years) is driven by the interplanetary trajectory and science requirements at Europa. Phase F (6 months) is structured to carry out the end-of-mission scenario and to complete data analysis and archiving.

### B.3.4 Risk and Mitigation Plan

*The main risks and their mitigation approaches are understood.*

The primary challenges of a mission to Europa are Jupiter's radiation environment, planetary protection, trajectory management for numerous consecutive Jovian tour flybys, and the large distance from the Sun and Earth. Driving technical risks are

1. Advanced Stirling radioisotope generator (ASRG) development
2. Performance in a radiation environment
3. Instrument development
4. Planetary protection

#### B.3.4.1 ASRG

NASA is developing the ASRG as the long-term solution for reducing the plutonium requirements for future planetary missions. Any problems with the development and validation of the ASRG could have a serious impact on the Europa Orbiter Mission, since it is baselining a radioisotope power system. ASRG development and qualification risks could have high consequences and are outside the control of the Europa Orbiter Mission project. The ASRGs are a new development, and the likelihood of problems is not known; however, successful development of new radioisotope thermoelectric generators can be difficult. Risks to the mission associated with this development can be mitigated if well-defined

and stable ASRG characteristics are known early in Phase A to allow the system designers to adequately incorporate them into the spacecraft system. However, if these characteristics are not known and stable early in Phase A, late design changes and impacts on mass, power, cost, and schedule are likely. The Europa Power Source Module concept allows for later ASRG delivery, thereby diminishing some of the development risk, as does the Europa Study Team's close work with NASA to clearly delineate the mission requirements on the ASRGs. Mitigation of these risks also requires that the project work closely with the Program Executive at NASA Headquarters for the ASRG Development Program to ensure that the technology is flight-qualified with completed life tests, no later than Phase B. A robust ground-test program is essential to migrating the ASRG risks. The NASA ASRG development efforts are currently underway (see Section B.2.7.5.2).

#### B.3.4.2 Performance in a radiation environment

The radiation environment to which the Europa Orbiter Mission hardware would be exposed, and its accumulated effects by end of mission, are significant. Radiation effects expected in the mission are TID effects and SEE in electronic components, displacement damage (DD) effects in components and materials, noise effects in detectors, and surface and internal charging (IC). The primary risk considered here is the likelihood that premature component failure or compromised performance could have a serious impact on spacecraft functionality if the radiation problem is not addressed appropriately. Sensors for instruments used for pointing and navigation and in science instruments are particularly sensitive to radiation effects, primarily due to noise and displacement effects. Test techniques used to verify component suitability might over-predict component hardness due to inadequate accounting for radiation rate or source type effects that are negligible at lower

doses. Also, unanticipated failure mechanisms might be present or might become important at high doses or at high DD levels that are not of concern for missions conducted at nominal total-dose exposures. The measures described here reduce both the likelihood and the consequences of such impacts, with designs for this radiation environment robust beyond the level normally accomplished for spaceflight design. The Europa Orbiter Mission design concept uses an approach similar to that taken by Juno, using an electronics vault to shield the electronic components to a mission dose of 150 krad, thereby reducing the likelihood of radiation-related problems while increasing the likelihood of parts availability. There has been significant effort exerted by experts to mitigate this risk over the past decade. In 2007, the Europa Study Team convened several review teams to assess the particular risks in each area. The results of the reviews were presented in Appendix C of the 2007 Europa Explorer Mission Study report (Clark et al. 2007). As a result of those reviews, a Risk Mitigation Plan: Radiation and Planetary Protection (Yan 2007, outlined in Clark et al. 2007) was further developed and executed to make strategic investments related to reducing even further the likelihood of component failure and degradation, and the related radiation risk. Results of this work were reported in the 2008 JEO final report (Clark et al. 2008). An expanded systems engineering approach focuses on graceful degradation and reduces the consequences of any component failures in electronic parts.

#### B.3.4.3 Instrument Development

Instrument development and delivery will undoubtedly be on the critical path, as has historically been the case. Only four instruments are needed to fulfill the Europa Orbiter Mission science requirements. An Approved Parts and Materials List (APML), addressing planetary protection and radiation constraints, will be available in time for the instrument AO. In addition, design guidelines will be incorporated into the AO. This facilitates mat-

uration of instrument concepts prior to selection. The instruments in the model payload are all based on mature technologies, and if deployed on a mission in the inner solar system, would represent low risk. For a Europa mission though, radiation can be expected to have a detrimental impact on instrument performance. If such problems cannot be resolved satisfactorily, the science objectives of the mission would not be met. Therefore, instruments will be selected as early as possible in Phase A, and early funding will be made available in order to alleviate development risks. In addition, the project will assign instrument interface engineers to work with each instrument provider to ensure that the instrument meets interface requirements and the spacecraft accommodates specific instrument needs.

To reduce the likelihood that the instruments fall short of their desired specifications or run into resource and schedule problems due to radiation issues, typical interface engineering support will be augmented for each instrument with personnel experienced in the area of radiation design. Design guidelines will be generated for the instrument teams to describe radiation constraints and to provide recommendations for design issues, and for parts and material selection. Development of a knowledge base for potential instrument providers has already begun. Four instrument workshops were held to engage the instrument provider community in a dialogue on needs and potential driving requirements for a mission to Europa. Information regarding radiation and planetary protection requirements was disseminated. The Europa Orbiter Mission development schedule provides abundant time plus reserves after selection for instrument developers and the project to work through and understand the particular design implications for each instrument of radiation and planetary protection. The project schedule also allows ample time for the instruments to be developed and delivered to system test. In

addition, the modular spacecraft approach, early local testing with spacecraft emulators, and a straightforward instrument interface allow instruments to be integrated last in the system integration process, if necessary.

#### B.3.4.4 Planetary Protection

The planetary protection requirements for a mission to Europa are significant and can drive mission design, schedule, and cost. The final fate of the Europa Orbiter Mission, impacting on the European surface, means that the mission will be classified as at least Category III under current Committee on Space Research (COSPAR) and NASA policy (COSPAR 2002). If prelaunch cleanliness levels are not met, expenditure of cost and schedule reserves might be required to address contamination problems late in the process to prevent contamination of Europa. This risk is cross-cutting and is mitigated in part by a review added in Phase B to confirm the approach and assess implementation. This risk is also mitigated by the previous Europa Study activities. The approach to planetary protection compliance for the Europa Orbiter Mission concept, at this time is 1) prelaunch DHMR to control bioburden for those areas not irradiated in-flight and 2) in-flight microbial reduction via radiation prior to Europa orbit insertion. The prelaunch method is to perform a full system DHMR as one of the last steps in the ATLO process at KSC. A chamber has been identified at KSC that is capable of performing DHMR, though specific details will need to be worked during Phase A. A pathfinder activity is planned as a dress rehearsal to resolve any procedural challenges. Compilation of the Europa Orbiter Mission APML will address compliance of materials with the DHMR process.

#### B.3.5 Cost

##### B.3.5.1 Cost Summary

The Total Mission Cost for the Europa Orbiter Mission concept is estimated at \$1.6B to \$1.7B FY15, *excluding the launch vehicle, which is costed separately*. The mission base-

line comprises an Orbiter spacecraft carrying four instruments—Laser Altimeter (LA), Mapping Camera (MC), Magnetometer (MAG), and Langmuir Probe (LP)—that will spend one month taking geophysical measurements of Europa from orbit. The Europa Orbiter Mission enables investigators to characterize the extent of the European ocean and investigate Europa’s habitability for life.

Table B.3.5-1 summarizes the Europa Orbiter Mission cost estimate at WBS level 2.

The Total Mission Cost is broken down into \$1.4B for the Phase-A through -D development period and \$0.25B for operations during Phases E and F. The Europa Orbiter Mission holds 37% in cost reserves that is broken down into 40% for Phases A, B, C, and D, and 20% for Phases E and F.

The estimated cost is based on the implementation approach described in Section B.2, which includes the following key features in the baseline plan:

- Redundant flight system with selected cross-strapping
- No new technologies requiring extraordinary development
- Simple, repeated, algorithm-driven observations capable of achieving all of the science goals
- Experienced providers of key systems and subsystems

#### B.3.5.2 Cost Estimating Methodology

To estimate the cost for the Europa Orbiter Mission concept, JPL used their institutional cost estimation process applicable for the design maturity of a concept study in early formulation. This process focuses on using parametric cost models, analogies, and other non-grassroots estimating techniques, which provide the following advantages:

- Provide rapid turnaround of extensive trade studies

**Table B.3.5-1.** Europa Orbiter cost summary by WBS (FY15 \$M).

WBS Element	PRICE-H	SEER
01 Proj Mgmt	55	54
02 Project System Engineering	45	43
03 Safety & Mission Assurance	49	47
04 Science	64	64
05 Payload System	75	75
06 Spacecraft System	507	482
ASRG	200	200
07 Mission Operations System	161	161
08 Launch System	-	-
09 Ground Data System	39	39
10 Proj Sys I&T	51	43
11 Education and Public Outreach	10	10
12 Mission Design	21	20
<b>Subtotal (FY15\$M)</b>	<b>1,276</b>	<b>1,238</b>
Reserves	386	371
<b>Total (FY15\$M)</b>	<b>1,661</b>	<b>1,609</b>

- Enable design-to-cost to narrow the trade space and define a baseline concept
- Establish reasonable upper and lower bounds around a point estimate

A cost estimation process begins with the Europa Study Team developing a Technical Data Package (TDP) that describes the science requirements, technical design, mission architecture, and project schedule. Next, all work is organized, defined, and estimated according to the NASA standard WBS. The Europa Study Team then tailors the WBS as needed for cost estimation and planning.

The institutional business organization uses the TDP and WBS to develop the cost estimate by applying estimating methods and techniques appropriate for each WBS element, based on the maturity of design and manufacturing requirements, availability of relevant historical information, and degree of similarity to prior missions. For the Europa Orbiter Mission, the tools and methods used include the following:

- Calibration of commercial, off-the-shelf (COTS) tools PRICE-H and

SEER to Juno, the most relevant JPL planetary mission

- Use of the NASA Instrument Cost Model (NICM) for the notional payload, tailored for the Europa environment
- Use of the NASA Space Operations & Cost Model (SOCM) for Phases E and F
- Wrap factors based on analogous historical planetary missions for Project Management, Project Systems Engineering, Safety and Mission Assurance, and Mission Design

The Europa Study Team's estimate is a compilation of these multiple techniques. The Europa Study team then vets the integrated cost rollup and detailed basis of estimate (BOE), and reviews the results for consistency and reasonableness with the mission design, WBS, and NASA requirements to ensure that technical and schedule characteristics are accurately captured and a consistent cost-risk posture is assumed.

To validate the resulting proposed cost, the Europa Study Team used Team X to independently cost the baseline concept with the JPL Institutional Cost Models (ICMs): 33 integrated, WBS-Level-2 through -4 models built by JPL line organizations to emulate their grassroots approach. The Europa Study Team also contracted with the Aerospace Corporation to perform an Independent Cost Estimate (ICE) and Cost and Technical Evaluation (CATE.) The Aerospace results are discussed in Section B.4.5.

The Europa Study Team then used an S-curve cost risk analysis to validate and bound the cost reserves. The reserves substantiation is discussed in Section B.3.5.7.

#### B.3.5.3 Basis of Estimate

The integrated Europa Orbiter Mission cost estimate is based on the science and mission implementation approach described in Section B.2. In addition, the Master Equipment

List (MEL) provided the key inputs for mass, quantities, and the quantification of electronics versus structures that are needed to run the parametric tools. The cost estimating methodologies and assumptions used to develop the Europa Orbiter Mission cost estimate are summarized in Table B.3.5-2.

#### B.3.5.4 Instrument Cost Estimates

The NASA Instrument Cost Model (NICM) system model with an augmentation to account for radiation and planetary protection was used to estimate instrument costs. Each notional instrument was characterized for performance establishing instrument type, aggregate power estimates, and subsystem level mass. Table B.3.5-3 shows the input parameters used for each instrument for the NICM system model.

##### B.3.5.4.1 NICM Adjustments

NICM outputs at the 70 percentile were reported in FY15\$. This reference cost estimate was then augmented for radiation and planetary protection. The NICM model does not

Table B.3.5-2. Cost estimation methodology.

WBS Element	Methodology
<b>01 Project Management</b>	Historical wrap factor based on analogous historical planetary missions. Estimate was augmented by \$15M to account for Nuclear Launch Safety Approval (NLSA) and National Environmental Policy Act (NEPA) costs associated with usage of the advanced Stirling radioisotope generators (ASRGs).
<b>02 Project Systems Engineering</b>	Historical wrap factor based on analogous historical planetary missions.
<b>03 Safety &amp; Mission Assurance</b>	Historical wrap factor based on analogous historical planetary missions.
<b>04 Science</b>	Expert-based estimate from the science team based on mission class, schedule, and the number and complexity of instruments. Cost estimate captures the level of effort for a Project Scientist, two Deputy Project Scientists, the Science Team, and participating scientists, with additional workforce requirements for Phases C and D, based on the size of the team, the number of meetings with the team, and the products required from this group. For Phases E and F, the cost estimate also assumes a science team for each instrument, with the estimated level of effort based on existing instrument teams supporting current mission, and on the number of months in hibernation, cruise, and science operations.
<b>05 Payload System</b>	Historical wrap factor for Payload Management, Systems Engineering, and Product Assurance based on analogous historical planetary missions. Instrument costs developed using the NASA Instrument Cost Model (NICM), Version 5.0. The 70% confidence-level estimate was selected as a conservative point estimate for each notional instrument. Instrument costs are then augmented for radiation shielding, detector radiation redesign, and planetary protection for any DHMR material properties issues. For payload radiation shielding, the cost was estimated separately using PRICE-H and SEER, and the cost is included under WBS 06 Spacecraft System. For planetary protection a flat fee was then added to each instrument, based on instrument complexity. For radiation redesign, an additional fee of \$2M was assessed per detector.
<b>06 Spacecraft System</b>	Historical wrap factor for Flight System Management, Systems Engineering, and Product Assurance based on analogous historical planetary missions. Spacecraft hardware costs estimated using PRICE-H and SEER calibrated to Juno at the subsystem level. Juno selected as an analogous mission for the calibration due to the operation of the flight system in a comparable radiation environment. Software costs estimated using a wrap factor of 10% on the hardware cost. ASRG cost provided by NASA Headquarters in the Europa Study Statement of Work, dated October 4, 2011 (NASA 2011). Estimate includes four ASRGs at \$50M each (FY15\$).
<b>07 Mission Operations System</b>	Team X estimate based on historical data for a Class A mission for Phases A-D; SOCM estimate for Phases E-F
<b>08 Launch System</b>	Launch Vehicle costs, including nuclear processing costs, are not included and will be provided by NASA Headquarters as directed in the Europa Study Statement of Work.
<b>09 Ground Data System</b>	Team X estimate based on historical data for a Class A mission for Phases A-D; SOCM estimate for Phases E-F
<b>10 Project Systems I&amp;T</b>	PRICE-H and SEER estimate calibrated to Juno.
<b>11 Education &amp; Public Outreach</b>	1.0% wrap factor on the total mission cost excluding the launch system (WBS 08), ASRG, and DSN tracking costs. Based on the percentage prescribed in the recent AOs for Discovery 2010 and New Frontiers 2009 (NASA 2010a, 2009c).
<b>12 Mission Design</b>	Historical wrap factor based on analogous historical planetary missions.
<b>Reserves</b>	40% for Phases A–D and 20% for Phases E–F on the total mission cost excluding the launch system (WBS 08), ASRG, and DSN tracking costs. These percentages were based on historical experience with recent planetary missions.

**Table B.3.5-3.** NICM System Model Inputs for Baseline.

Instrument Name	Langmuir Probe (LP)	Laser Altimeter (LA)	Magnetometer (MAG)	Mapping Camera (MC)
<b>Remote Sensing or In-Situ?</b>	Remote Sensing	Remote Sensing	Remote Sensing	Remote Sensing
<b>Environment</b>	Planetary	Planetary	Planetary	Planetary
<b>Remote Sensing Instrument Type</b>	Particles	Optical	Fields	Optical
<b>Total Mass (kg)</b>	2.7	5.5	3.3	2.5
<b>Max Power (W)</b>	2.3	15	4	6
<b>Design Life (months)</b>	108	108	108	108
<b>Number of Detectors</b>	0	0	0	1

**Table B.3.5-4.** Instrument Cost Estimation Process.

Master Instrument Costing Matrix	Instrument Cost (excluding radiation shielding) (A)	Detector Radiation Design Costs (B)	Planetary Protection Fee (C)	Total Instrument Cost	Radiation Shielding Cost – Included in WBS 06
Instrument X	NICM 70th percentile estimate	\$2M per detector	Based on complexity	A+B+C	Estimated in PRICE-H/SEER

**Table B.3.5-5.** Instrument Cost Estimation Details (FY15\$M).

Instrument	Acronym	NICM 70% Cost	Detector Radiation Design Costs	Planetary Protection Fee	TOTAL INSTRUMENT COST
Laser Altimeter	LA	28.8	0.0	1.4	30.2
Langmuir Probe	LP	7.1	0.0	0.1	7.1
Mapping Camera	MC	14.3	2.0	0.7	17.1
Magnetometer	MAG	10.9	0.0	0.3	11.2
<b>TOTAL</b>		<b>61.1</b>	<b>2.0</b>	<b>2.6</b>	<b>65.6</b>

have parameters or characteristics sufficient to model planetary protection requirements or radiation environments. A flat fee for Planetary Protection was added to each instrument, based on instrument complexity. An estimate for the number of electronic boards and detectors was made for each instrument, and an additional fee of \$2M was assessed per detector for radiation redesign costs. The instrument radiation shielding masses were estimated separately in PRICE-H and SEER, and are included in WBS 06 spacecraft costs under Payload Radiation Shielding. Table B.3.5-4 summarizes the instrument cost estimation process.

#### B.3.5.4.2 NICM Estimate

Table B.3.5-5 provides the final NICM system cost estimate including all adjustments for radiation and planetary protection.

#### B.3.5.5 Spacecraft Hardware Costs

The Europa Orbiter Mission spacecraft hardware costs were estimated using PRICE-H and SEER, calibrated to Juno. The Orbiter spacecraft is most closely analogous to the Juno spacecraft. Configuration, avionics subsystems, radiation environment, mission complexity and design lifetime match closely to the corresponding aspects of the Juno mission.

##### B.3.5.5.1.1 PRICE-H and SEER Cost Estimates

The Spacecraft System costs generated for PRICE-H and SEER are shown in Table B.3.5-6. The Spacecraft System is bookkept in in WBS 06. The Payload Radiation Shielding is captured as part of the Mechanical Subsystem and the costs are bookkept under WBS 06.07b. The RPS System was estimated at a cost of \$50M per ASRG unit as directed by NASA HQ, and included in WBS 06, separate from the Spacecraft System costs. The I&T

**Table B.3.5-6.** PRICE-H and SEER Cost Estimates for the Europa Orbiter Mission. (FY15\$M).

Spacecraft System	PRICE-H	SEER
<b>06 Spacecraft System</b>		
06.04 Spacecraft Power SS	50	68
06.05 Spacecraft C&DH SS	37	27
06.06 Spacecraft Telecom SS	93	54
06.07 Spacecraft Mechanical SS	54	46
06.07a Radiation Shielding	9	9
06.07b Payload Radiation Shielding	2	1
06.08 Spacecraft Thermal SS	10	10
06.09 Spacecraft Propulsion SS	41	60
06.10 Spacecraft GN&C SS	51	56
06.11 Spacecraft Harness SS	6	6
06.12 Spacecraft Flight SW	35	34
<b>06C RPS System</b>	<b>200</b>	<b>200</b>
<b>10 I&amp;T</b>	<b>51</b>	<b>43</b>

costs are kept in WBS 10. Spacecraft flight software was estimated as a 10% wrap factor based on hardware cost, which is a high-level rule of thumb derived from JPL's historical software cost data.

### B.3.5.6 Phase E and F Cost Estimates

The NASA Space Operations Cost Model (SOCM) was used to estimate operations costs in Phases E and F. The Europa Study science team provided an expert-based estimate for WBS 04 Science based on schedule and the number and complexity of instruments. The Europa Orbiter Mission Phase E and F Cost Estimate are shown in Table B.3.5-7.

### B.3.5.7 Estimate Reasonableness (Validation)

A JPL Team X cost session was used to assess the reasonableness of the parametrically derived PRICE-H and SEER-based Flight System (WBS 06) and Project Systems I&T (WBS 10) estimates and associated wraps. In addition, Aerospace Corporation independently ran an Independent Cost Estimate (ICE) and Cost and Technical Evaluation (CATE). Aerospace Corporation found the project cost estimate to be reasonable and found no cost or schedule threats. The results of the Team X cost session and Aerospace Corporation analysis are presented in Table B.3.5-8 along with

**Table B.3.5-7.** Phase E and F Cost Estimate for the Europa Orbiter Mission. (FY15\$M).

WBS Element	Phase E & F Cost
01 Project Management	7
02 Project Systems Engineering	7
03 Safety & Mission Assurance	7
04 Science	38
05 Payload	0
06 Spacecraft	0
07 Mission Operations	119
08 Launch System	0
09 Ground Data Systems	12
10 Project System Integration & Test	0
11 Education & Public Outreach	2
<b>SUBTOTAL</b>	<b>193</b>
DSN Tracking	15
20% Reserves (excluding DSN)	39
<b>TOTAL</b>	<b>246</b>

**Table B.3.5-8.** Comparison of Team X, and Aerospace Corporation cost estimates. (FY15\$B).

	Team X	Aerospace ICE	Aerospace CATE
<b>Total FY15\$B)</b>	<b>1.5</b>	<b>1.7</b>	<b>1.8</b>

the PRICE- and SEER-based project estimates for comparison. The Aerospace CATE report is located in Appendix B.4.5.

### B.3.5.8 Cost-Risk Assessment and Reserve Strategy

The Europa Study Team conservatively applied project-level reserves of 40% for Phases A–D and 20% for Phases E and F on all elements except for Launch Services, ASRGs, and DSN tracking. These reserve levels are more conservative than the reserve guidelines set forward in JPL Flight Project Practices, Rev. 8 (JPL 2010b).

The Europa Orbiter Mission cost risk and uncertainty assessment is a natural extension of the cost modeling discussed in Sections B.3.5.1-7, and is consistent with standard practice at NASA and JPL. This assessment considers the wide band of uncertainty that typically accompanies missions at early phases of development, as well as the technical risk and uncertainties of the Europa Orbiter Mission as

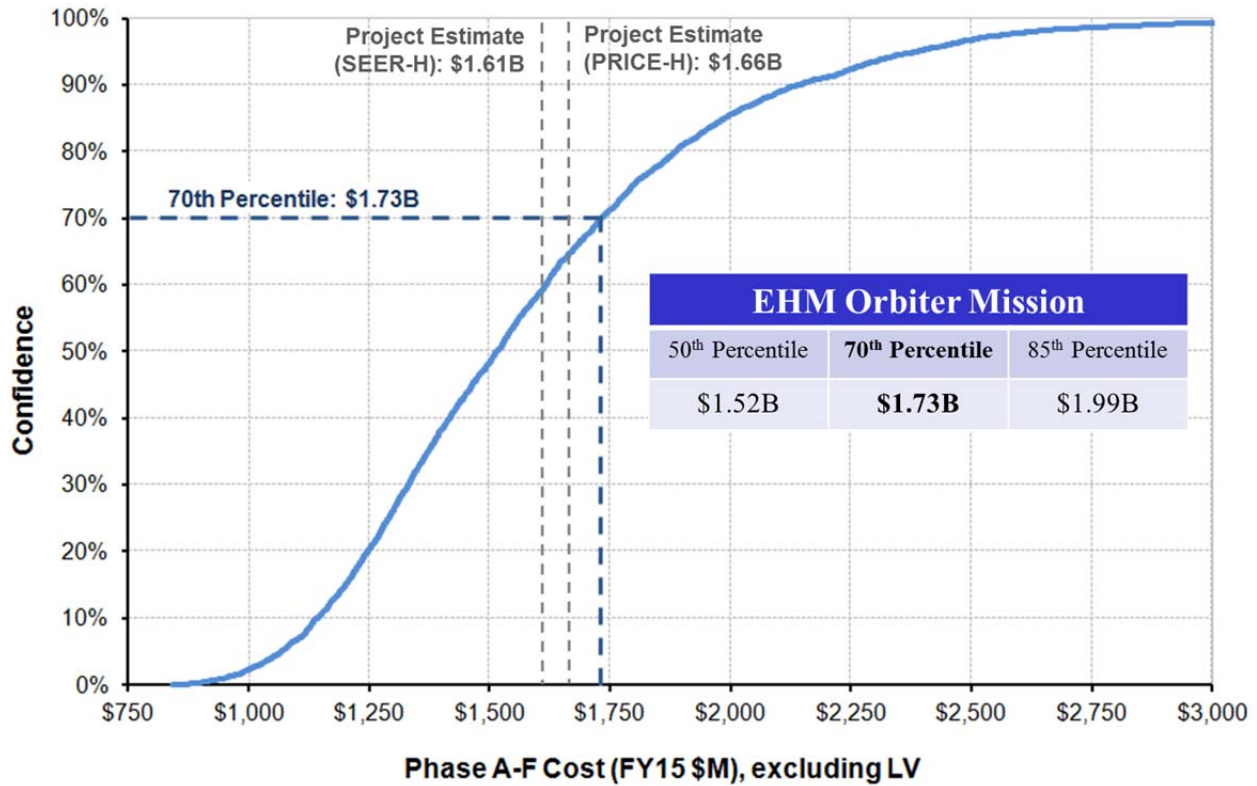


Figure B.3.5-1. Europa Orbiter Mission cost estimate S-curve analysis.

understood at this time and as experienced on prior competed and directed missions (e.g. Juno, MRO, MSL).

The primary technique utilized for this assessment is an S-Curve. This provides a statistically-based distribution of total project cost around the project’s point estimate based on the cost models used in this analysis and the historical JPL data to which they are calibrated. Equivalently, this technique provides a probabilistic estimate of total project cost based on variability and uncertainties in the model-based estimates.

An S-curve analysis was performed on the study cost estimate, and demonstrated a 70<sup>th</sup>-percentile cost estimate of \$1.73B (FY15\$) (Figure B.3.5-1). Comparing the Europa Study Team estimate (including cost reserves) to the S-Curve indicates that the Europa Study Team estimate of \$1.6B to \$1.7B is at approximately 65<sup>th</sup>-percentile. To be at 70<sup>th</sup>-percentile, the Europa Study Team would need to increase reserves by ~\$70M to ~\$120M, resulting in a reserve position of 45% overall (Phase A-F).

## B.4 Appendices

### B.4.1 References

- Anderson, J.D., Schubert, G., Jacobson, R.A., Lau, E.L., Moore, W.B., et al., 1998. Europa's differentiated internal structure: Inferences from four Galileo encounters. *Science* 281, 2019–2022.
- Becker, H., Miyahira, T., Johnston, A., 2003. The influence of structural characteristics on the response of silicon avalanche photodiodes to proton irradiation, *IEEE Trans. Nucl. Sci.* 50(6), 1974–1981.
- Bierhaus, E.B., Zahnle, K., Chapman, C.R., 2009. Europa's crater distributions and surface ages. In: Pappalardo, R.T., McKinnon, W.B., Khurana, K.K. (Eds.), *Europa*, U. Arizona Press, Tucson, 161–180.
- Billings, S.E., Kattenhorn, S.A., 2005. The great thickness debate: Ice shell thickness models for Europa and comparisons with estimates based on flexure at ridges. *Icarus* 177, 397–412.
- Bills, B.G., 2005. Free and forced obliquities of the Galilean satellites of Jupiter. *Icarus* 175, 233–247.
- Bills, B.G., Nimmo, F., 2008. Forced obliquity and moment of inertia of Titan. *Icarus* 196, 293–297.
- Bills, B.G., Lemoine, F.G., 1995. Gravitational and topography isotropy of the Earth, Moon, Mars, and Venus. *J. Geophys. Res.* 100, 26,275–26,295.
- Bills, B.G., Nimmo, F., Karatekin, Ö., Van Hoolst, T., Rambaux, N., et al., 2009. Rotational dynamics of Europa. In: Pappalardo, R.T., McKinnon, W.B., Khurana, K.K. (Eds.), *Europa*, U. Arizona Press, Tucson, 119–136.
- Boldt, J., et al., 2008. Assessment of radiation effects on detectors and key optical components. JPL D-48256.
- Carr, M.H., Belton, M.J.S., Chapman, C.R., Davies, M.E., Geissler, R., Greenberg, R., McEwen, A.S., Tufts, B.R., Greeley, R., Sullivan, R., Head, J.W., Pappalardo, R.T., Klaasen, K.P., Johnson, T.V., Kaufman, J., Senske, D., Moore, J., Neukum, G., Schubert, G., Burns, J.A., Thomas, P., Veverka, J., 1998. Evidence for a subsurface ocean on Europa. *Nature* 391, 363–365.
- Cavanaugh, J., Smith, J., Sun, X., Bartels, S., Bartels, A., Ramos-Izquierdo, L., Krebs, D., McGarry, J., Trunzo, R., Novo-Gradac, A., Britt, J., Karsh, J., Katz, R., Lukemire, A., Szymkiewicz, R., Berry, D., Swinski, J., Neumann, G., Zuber, M., Smith, D., 2007. The Mercury Laser Altimeter instrument for the MESSENGER mission. *Space Sci. Rev.* 131, 451–479.
- Clark, K., 2008. EJSM Europa Orbiter Mission Design and Architecture (presentation slides). Outer Planets Flagship Mission Instrument Workshop, June 3, 2008.
- Clark, K., et al., 2007. Europa Explorer Mission Study: Final Report, JPL D-41283.
- Clark, K., et al., 2008. Jupiter Europa Orbiter Mission Study 2008 Final Report, JPL D-48279.
- Clark, K., et al., 2009. Europa Jupiter System Mission Joint Summary Report, January 16, 2009.
- Cole, T., Boies, M., El-Dinary, A., Cheng, A., 1997. The Near-Earth Asteroid Rendezvous Laser Altimeter. *Space Sci. Rev.* 82, 217–253.
- Collins, G., Nimmo, F., 2009. Chaotic terrain on Europa. In: Pappalardo, R.T., McKinnon, W.B., Khurana, K.K. (Eds.), *Europa*, U. Arizona Press, Tucson, 259–282.
- Committee on Space Research, 2002. COSPAR Planetary Protection Policy, as amended March 2005). <<http://www.cosparhq.org/scistr/PPPPolicy.htm>>.

- Comstock, R.L., Bills, B.G., 2003. A solar system survey of forced librations in longitude. *J. Geophys. Res.* 108, doi: 10.1029/2003JE002100.
- Constable, S., Constable, C., 2004. Observing geomagnetic induction in magnetic satellite measurements and associated implications for mantle conductivity. *Geochemistry, Geophysics, Geosystems* 5, doi: 10.1029/2003GC000634.
- Doggett, T., Greeley, R., Figueredo, P., Tanaka, K., Weiser, S., 2009. Geologic stratigraphy and evolution of Europa's surface. In: Pappalardo, R.T., McKinnon, W.B., Khurana, K.K. (Eds.), *Europa*, U. Arizona Press, Tucson, 137–160.
- Dyal P. and Parkin C. W. (1973) Global electromagnetic induction in the moon and planets. *Phys. Earth Planet. Inter.*, 7, 251–265.
- Figueredo, P.H., Greely, R., 2004. Resurfacing history of Europa from pole-to-pole geological mapping. *Icarus* 167, 287–312.
- Geissler, P.E., Greenberg, R., Hoppa, G., McEwen, A., Tufts, R., Phillips, C., Clark, B., Ockert-Bell, M., Helfenstein, P., Burns, J., Veverka, J., Sullivan, R., Greeley, R., Pappalardo, R. T., Head, J. W., Belton, M. J. S., Denk, T., 1998. Evolution of lineaments on Europa: Clues from Galileo multispectral imaging observations. *Icarus* 135, 107–126, doi: 10.1006/icar.1998.5980.
- Greeley, R., Chyba, C.F., Head, J.W. III, McCord, T.B., McKinnon, W.B., Pappalardo, R.T., Figueredo, P., 2004. Geology of Europa. In: Bagenal, F., Dowling, T.E., McKinnon, W.B. (Eds.), *Jupiter: The Planet, Satellites, and Magnetosphere*, Cambridge U. Press, Cambridge, U.K., 329–362.
- Greenberg, R., G.V. Hoppa, B.R. Tufts, P. Geissler, J. Riley, and S. Kadel, 1999. Chaos on Europa. *Icarus* 141, 263–286.
- Hand, K.P. and C.F. Chyba 2007. Empirical constraints on the salinity of the european ocean and implications for a thin ice shell. *Icarus* 189, 424–438.
- Hand, K.P., C.F. Chyba, J.C. Priscu, R.W. Carlson, and K.H. Nealson 2009. Astrobiology and the potential for life on Europa. *Europa* (R.T. Pappalardo, W.B. McKinnon, and K.K. Khurana, Eds.), Univ. of Arizona Press, Tucson, 589–630.
- Head, J.W., Pappalardo, R.T., 1999. Brine mobilization during lithospheric heating on Europa: Implications for formation of chaos terrain, lenticula texture, and color variations. *J. Geophys. Res.*, Planets 104, 27143–27155.
- Henschel, H., Köhn, O., Schmidt, H., Bawirzanski, E., Landers, A., 1994. Optical fibres for high radiation dose environments. *IEEE Trans. Nucl. Sci.* 41(3), 510–516.
- Hoppa, G.V., et al. 1999. Formation of cycloidal features on Europa. *Science* 285, 1899–1902.
- Hussman, H., Spohn, T., 2004. Thermal-orbital evolution of Io and Europa. *Icarus* 171, 391–410.
- Jet Propulsion Laboratory, 2009. JPL Standard Flight Project Work Breakdown Structure Template, Rev. 5, JPL Rules! DocID 59533, March 18, 2009.
- Jet Propulsion Laboratory, 2010a. Design, Verification/Validation and Ops Principles for Flight Systems (Design Principles), Rev. 4, JPL Rules! DocID 43913, September 20, 2010.
- Jet Propulsion Laboratory, 2010b. Flight Project Practices, Rev. 8, JPL Rules! DocID 58032, October 6, 2010.
- Johnston, A., 2001. Proton displacement damage in light-emitting and laser diodes. *IEEE Trans. Nucl. Sci.* 48(5), 1713–1720.
- Kattenhorn, S.A., Hurford, T., 2009. Tectonics of Europa. In: Pappalardo, R.T., McKinnon, W.B., Khurana, K.K. (Eds.), *Europa*, U. Arizona Press, Tucson, 199–236.

- Khurana, K.K., M. Kivelson, D. Stevenson, G. Schubert, C. Russell et al. 1998. Induced magnetic fields as evidence for subsurface oceans in Europa and Callisto. *Nature* 395, 777–780.
- Khurana, K.K., M.G. Kivelson, and C. T. Russell, 2002. Searching for Liquid Water in Europa by Using Surface Observatories. *Astrobiology* 2, 93-103.
- Khurana, K.K., M.G. Kivelson, K.P. Hand, and C.T. Russell 2009. Electromagnetic induction from Europa's ocean and the deep interior, Europa (R.T. Pappalardo, W.B. McKinnon, and K.K. Khurana, Eds.), Univ. of Arizona Press, Tucson, 571–588.
- Kivelson, M.G., K.K. Khurana, C.T. Russell, M. Volwerk, R.J. Walker et al. 2000. Galileo magnetometer measurements: A stronger case for a subsurface ocean at Europa. *Science* 289, 1340–1343.
- Klaasen, K., Clary, M., Janesick, J., 1984. Charge-coupled device television camera for NASA's Galileo mission to Jupiter. *Optical Engineering* 23, 334–342.
- Konopliv, A.S., C.F. Yoder, E.M. Standish, D-N. Yuan, and W.L. Sjogren 2006. A global solution for the Mars static and seasonal gravity, Mars orientation, Phobos and Deimos masses, and Mars ephemeris. *Icarus* 182, 23–50.
- Kwok, J., Prockter, L., Senske, D., Jones, C., 2007. Jupiter System Observer Mission Study: Final Report, JPL D-41284.
- Lock, R., 2008. EISM Europa Orbiter Science Scenarios (presentation slides). Outer Planets Flagship Mission Instrument Workshop, June 3, 2008.
- Lock, R., 2010. Concept of Operations (presentation slides), Jupiter Europa Orbiter Internal Mission Concept Review, June 7–9, 2010.
- Ludwinski, J., 1997. Galileo Mission Planning Office Closeout (Lessons Learned), JPL IOM 311.1/98/01, January 19, 1997.
- Luthcke, S.B., C. Carabajal, and D. Rowlands 2002. Enhanced geolocation of spaceborne laser altimeter surface returns: Parameter calibration from the simultaneous reduction of altimeter range and navigation tracking data. *J. Geodynamics* 34, 447–475.
- Luthcke, S.B., D. Rowlands, T. Williams, and M. Sirota 2005. Reduction of ICES at systematic geolocation errors and the impact on ice sheet elevation change detection. *Geophys. Res. Lett.* 32, L21S05.
- Luttrell, K. and D. Sandwell 2006. Strength of the lithosphere of the Galilean satellites. *Icarus* 183, 159–167.
- Moore, J.M., Asphaug, E., Belton, M., Bierhaus, B., Breneman, H., et al. 2001. Impact features on Europa: Results of the Galileo Europa Mission (GEM). *Icarus* 151, 93–111.
- Moore, J.M., Black, G., Buratti, B., Phillips, C.B., Spencer, J., Sullivan, R., 2009. Surface properties, regolith, and landscape degradation. In: Pappalardo, R.T., McKinnon, W.B., Khurana, K.K. (Eds.), Europa, U. Arizona Press, Tucson, 369–380.
- Moore, W.B. and G. Schubert 2000. The tidal response of Europa. *Icarus* 147, 317–319.
- NASA, 2005. NASA Procedural Requirements (NPR) 8020.12B. Planetary Protection Provisions for Robotic Extraterrestrial Missions. NASA, Washington, DB.
- NASA, 2007. NASA Program and Project Management Processes and Requirements, NASA Procedural Requirements (NPR) 7120.5D, March 6, 2007. NASA, Washington, DC.
- NASA, 2010a. Discovery 2010 Announcement of Opportunity, NNH10ZDA007O, June 7, 2010.
- NASA, 2010b. NASA Emergency Preparedness Plan Procedural Requirement, NPR 8715.3, December 16, 2010. NASA, Washington, DC.
- NASA, 2011. Europa Study Statement of Work, October 4, 2011. NASA, Washington, DC.

- Neumann, G.A. D. Rowlands, F. Lemoine, D. Smith, and M. Zuber 2001. Crossover analysis of Mars Orbiter Laser altimeter data. *J. Geophys. Res.* 106, 23,753–23,768.
- Newhall, X. X. and J. C. Williams 1997. Dynamics and astrometry of natural and artificial celestial bodies: proceedings of IAU Colloquium 165, Poznan, Poland, July 1-5, 1996 / edited by I.M. Wytrzyszczak, J.H. Lieske, R.A. Feldman. Dordrecht; Boston : Kluwer Academic Publishers, QB1 I56 no.165, p. 21.
- Nimmo, F. and M. Manga 2009. Geodynamics of Europa's icy shell. *Europa* (R.T. Pappalardo, W.B. McKinnon, and K.K. Khurana, Eds.), Univ. of Arizona Press, Tucson, 381–404.
- Nimmo, F., Giese, B., Pappalardo, R.T., 2003. Estimates of Europa's ice shell thickness from elastically supported topography. *Geophys. Res. Lett.* 30, 1233.
- O'Brien, H., Brown, P., Beek, T., Carr, C., Cupido, E., Oddy, T., 2007. A radiation tolerant digital fluxgate magnetometer. *Meas. Sci. Technol.* 18, 3645–3650.
- Ojakangas, G.W., D.J. Stevenson 1989. Thermal state of an ice shell on Europa. *Icarus* 81, 220–241.
- Paczkowski, B., et al., 2008. Outer Planets Flagship Mission Science Operations Concept Study Report, JPL D–46870. June 2008.
- Pappalardo, R.T., et al., 1998. Geological evidence for solid-state convection in Europa's ice shell. *Nature* 391, 365.
- Pappalardo, R.T., Head, J.W., Greeley, R., Sullivan, R.J., Pilcher, C., et al., 1999. Does Europa have a subsurface ocean? Evaluation of the geological evidence. *J. Geophys. Res.* 104, 24,015–24,056. [[Move other authors over to Lander chapter.](#)]
- Parkinson, W. D., 1983. *Introduction to Geomagnetism*. Scottish Academic Press, Edinburgh, 433 pp.
- Peale, S.J., 1976. Orbital resonances in the solar system. *Ann. Rev. Astron. Astrophys.* 14, 215–246.
- Prockter, L.M., Head, J.W., Pappalardo, R.T., Sullivan, R.J., Clifton, A.E., Giese, B., Wagner, R., Neukum, G., 2002. Morphology of European bands at high resolution: A mid-ocean ridge-type rift mechanism, *J. Geophys. Res.* 107, 4-1–4-28. doi:10.1029/2000JE001458.
- Prockter, L.M., Pappalardo, R.J., 2000. Folds on Europa: Implications for crustal cycling and accommodation of extension. *Science* 289, 941–943.
- Prockter, L.M., Patterson, G.W., 2009. Morphology and evolution of Europa's ridges and bands. In: Pappalardo, R.T., McKinnon, W.B., Khurana, K.K. (Eds.), *Europa*, U. Arizona Press, Tucson, 237–258.
- Rasmussen, R., 2009. System architecture for JEO (presentation slides), EJSM Instrument Workshop, July 15–17, 2009.
- Riley, J., Hoppa, G.V., Greenberg, R. Tufts, B.R., Geissler, P., 2000. Distribution of chaotic terrain on Europa. *J. Geophys. Res.* 105, 22,599–22,616.
- Rose, T., Hopkins, M., Fields, R., 1995. Characterization and control of gamma and proton radiation effects on the performance of Nd:YAG and ND:YLF Lasers. *IEEE J. Quantum Electron.* 31(9), 1593–1602. doi: 10.1109/3.406369.
- Rowlands, D.D., D. Pavlis, F. Lemoine, G. Neumann, and S. Luthcke 1999. The use of laser altimetry in the orbit and attitude determination of Mars Global Surveyor. *Geophys. Res. Lett.* 26, 1191–1194.
- Sarid, A.R., R. Greenberg, G.V. Hoppa, T.A. Hurford, B.R. Tufts et al. 2002. Polar wander and surface convergence of Europa's ice shell: Evidence from a survey of strike-slip displacement. *Icarus* 158, 24–41.

- Schenk, P. 2009. Slope characteristics of Europa: Constraints for landers and radar sounding. *Geophys. Res. Lett.* 36, L15204.
- Schenk, P., Pappalardo, R., 2004. Topographic variations in chaos on Europa: Implications for diapiric formation. *Geophys. Res. Lett.* 31, L16703 1–5.
- Schenk, P.M., Chapman, C.R., Zahnle, K., Moore, J.M., 2004. Ages and interiors: The cratering record of the Galilean satellites. In: Bagenal, F., Dowling, T.E., McKinnon, W.B. (Eds.), *Jupiter: The Planet, Satellites, and Magnetosphere*, Cambridge U. Press, Cambridge, U.K., 427–457.
- Schenk, P.M., Turtle, E.P., 2009. Europa's impact craters: Probes of the icy shell. In: Pappalardo, R.T., McKinnon, W.B., Khurana, K.K. (Eds.), *Europa*, U. Arizona Press, Tucson, 181–198.
- Schilling, N., F.M. Neubauer, and J. Saur, J. 2007. Time-varying interaction of Europa with the Jovian magnetosphere: Constraints on the Conductivity of Europa's subsurface ocean. *Icarus* 192, 41–55.
- Schmidt, B.E., Blankenship, D.D., Patterson, G.W., Schenk, P.M., 2011. Active formation of “chaos terrain” over shallow subsurface water on Europa. *Nature* 479, 502–505. doi: 10.1038/nature10608.
- Schubert, G., F. Sohl, and H. Hussmann 2009. Interior of Europa. *Europa* (R.T. Pappalardo, W.B. McKinnon, and K.K. Khurana, Eds.), Univ. of Arizona Press, Tucson, 353–368.
- Seas, A., Li, S., Stephen, M., Novo-Gradac, A-M., Kashem, N., Vasilyev, A., Troupaki, E., Chen, S., Rosanova, A., 2007. Development and vacuum life test of a diode-pumped Cr:Nd:YAG laser (heritage laser) for space applications, Conference on Lasers and Electro-Optics. doi: 10.1109/CLEO.2007.4452342.
- Sotin, C., G. Tobie, J. Wahr, and W.B. McKinnon 2009. Tides and tidal heating on Europa. *Europa* (R.T. Pappalardo, W.B. McKinnon, and K.K. Khurana, Eds.), Univ. of Arizona Press, Tucson, 85–118.
- Space Studies Board, 2000. Preventing the Forward-Contamination of Europa. National Academy Press, Washington, DB.
- Space Studies Board, 2003. New Frontiers in the Solar System: An Integrated Exploration Strategy 2003–2013. The National Academies Press, Washington, DC.
- Space Studies Board, 2011. Visions and Voyages for Planetary Science in the Decade 2013–2022. The National Academies Press, Washington, DC.
- Sullivan, R., Greeley, R., Homan, K., Klemaszewski, J., Belton, M.J.S, Carr, M.H., Chapman, C.R., Tufts, R., Head, J.W. III, Pappalardo, R., Moore, J., Thomas, P., and the Galileo Imaging Team, 1998. Episodic plate separation and fracture infill on the surface of Europa. *Nature* 391, 371–373.
- Tsang, T., Radeka, V., 1995. Electro-optical modulators in particle detectors. *Rev. Sci. Instrum.* 66(7), 3844–3854.
- Tufts, B.R., Greenberg, R., Hoppa, G., Geissler, P., 2000. Lithospheric dilation on Europa. *Icarus* 146, 75–97.
- Tyler, R.H., S. Maus, and H. Luhr 2003. Satellite observations of magnetic fields due to ocean tidal flow. *Science* 299, 239–241.
- Valavanoglou, A., Oberst, M., Magnes, W., Hauer, H., Neubauer, H., Baumjohann, W., Falkner, P., 2007. Magnetometer front-end ASIC (MFA). *Geophys. Res. Abstr.* 9, 3645–3650.

- Wahlund, J.-E., Blomberg, L.G., Morooka, M., Cumnock, J.A., Andre', M., Eriksson, A.I., Kurth, W.S., Gurnett, D.A., Bale, S.D., 2005. Science opportunities with a double Langmuir probe and electric field experiment for JIMO. *Adv. Space Res.* 36, 2110–2119.
- Wahr, J.M., M. Zuber, D. Smith, and J. Lunine 2006. Tides on Europa, and the thickness of Europa's icy shell. *J. Geophys. Res.* 111, doi: 10.1029/2006JE002729.
- Ward, W.R. 1975. Past orientation of the lunar spin axis. *Science* 189, 377–379.
- Wu, X.P., Bar-Sever, Y.E., Folkner, W.M., Williams, J.G., Zumberge, J.F., 2001. Probing Europa's hidden ocean from tidal effects on orbital dynamics. *Geophys. Res. Lett.* 28, 2245–2248.
- Wu, X.P., Y. Bar-Sever, W. Folkner, J. Williams, and J. Zumberge 2001. Probing Europa's hidden ocean from tidal effects on orbital dynamics. *Geophys. Res. Lett.* 28, 2245–2248.
- Yoder, C.F. and S. Peale 1981. Tidal variations of Earth rotation. *J. Geophys. Res.* 86, 881–891.
- Zahnle, K., Dones, L., Levison, H.F., 1998. Cratering rates in the Galilean satellites. *Icarus* 136, 202–222.
- Zahnle, K., Schenk, P., Levison, H., Dones, L., 2003. Cratering rates in the outer solar system. *Icarus* 163, 263–289.
- Zimmer, C., K.K. Khurana, and M. Kivelson 2000. Subsurface oceans on Europa and Callisto: Constraints from Galileo magnetometer observations. *Icarus* 147, 329–347.
- Zombeck, M.V, 1982. *Handbook of Space Astronomy and Astrophysics*. Cambridge U. Press, Cambridge, U.K.
- Zuber, M.T., D. Smith, S. Solomon, D. Muhleman, J. Head 1992. The Mars Observer Laser Altimeter investigation. *J. Geophys. Res.* 97, 7781–7797.

**B.4.2 Acronyms and Abbreviations**

$\Delta V$	delta velocity, delta-V	$C_3$	injection energy per unit mass ( $V_{\infty}^2$ ), km <sup>2</sup> /s <sup>2</sup> (also C3)
3D	three-dimensional	CAD	computer-aided design
A	ampere	CADRe	Cost Analysis Data Requirement
A	approach	CATE	Cost and Technical Evaluation
A/D	analog to digital	CBE	current best estimate
ABSL		CCD	charge-coupled device
AC	alternating current	CCSDS	Consultative Committee for Space Data Systems
ACS	attitude control subsystem	CDR	Critical Design Review
ACU	ASRG controller unit	CEM	channel electron multiplier
ADC	analog-to-digital converter	CFDP	CCSDS File Delivery Protocol
AFT	allowable flight temperature	CG	center of gravity
Ah	ampere-hour	CM	center of mass
anti-jovian		CMMI	Capability Maturity Model Integration
AO	Announcement of Opportunity	CMOS	complementary metal-oxide semiconductor
APL	Applied Physics Laboratory	COSPAR	Committee on Space Research
APML	Approved Parts and Materials List	COT	crank over the top
APS	active pixel sensor	CPT	comprehensive performance test
ASC	Advanced Stirling converter	CRAM	chalcogenide random-access memory
ASIC	application-specific integrated circuit	CRISM	Compact Reconnaissance Imaging Spectrometer for Mars
ASRG	Advanced Stirling Radioisotope Generator	CU	cleanup
ATK/PSI		DC	direct current
ATLO	assembly, test, and launch operations	DC/DC	direct current to direct current
B	baseline	DD	displacement damage
BIU	Bus Interface Unit	DDD	displacement damage dose
BOM	beginning of mission		
BTE	bench-test equipment		
C&DH	command and data handling/ command and data handling subsystem		

DHMR	dry-heat microbial reduction	FPPs	Flight Project Practices
DOD	depth of discharge	FS	flight system
DOE	Department of Energy	FSW	flight software
DPs	Design Principles	FSWTB	flight software testbed
DSM	deep-space maneuver	FWHM	full width at half maximum
DSN	Deep Space Network	G/T	gain to equivalent noise temperature
DTM	developmental test model	GDS	Ground Data System
DWG	Detector Working Group	GHA	generator housing assembly
EEE	electrical, electronic, and electromechanical	GM	product of gravitational constant and mass
EFM	Europa Flyby Mission	GN&C	guidance, navigation, and control
EGA	Earth gravity assist	GN&C	guidance, navigation, and control
EHM	Europa Habitability Mission	GPHS	General Purpose Heat Source
EHS	electrical heater source	GRAIL	Gravity Recovery and Interior Laboratory
EIRP	effective isolated radiated power	GSE	ground-support equipment
EIRP	Environmental Incident Response Plan?	H/W	hardware
EIS	Environmental Impact Statement	HCIPE	High-Capability Instrument for Planetary Exploration
EJSM	Europa Jupiter System Mission	HEPA	high-efficiency particulate air
EM	engineering model	HGA	high-gain antenna
EMI	electromagnetic interference	HQ	NASA Headquarters
EOI	Europa Orbit Insertion	HS	heat source
EOM	end of mission	HY	RF hybrid
ES	Europa Study	I&T	integration and test
ESA	European Space Agency	I/O	input/output
ESD	electrostatic discharge	IC	internal charging
ETL	Export Technical Liaison	ICD	Interface Control Document
EVEE	Earth-Venus-Earth-Earth	ICE	Independent Cost Estimate
FMECA	failure modes, effects, and criticality analysis	ICM	Institutional Cost Model
FOV	field of view	ID	identification/identifier

ID	inner diameter	M3	Moon Mineralogy Mapper
IFOV	3.2.2, p 2	MAG	Magnetometer
IFOV	instantaneous field of view	MARCI	Mars Color Imager
IMU	inertial measurement unit	MARSIS	Mars Advanced Radar for Subsurface and Ionosphere Sounding
INMS	Ion and Neutral Mass Spectrometer		
INSRP	Interagency Nuclear Safety Review Panel	MC	Mapping Camera
		MCP	microchannel plate
IOM	interoffice memorandum	MCR	Mission Concept Review
IP	interplanetary		
IPR	Ice-Penetrating Radar	MDIS	Mercury Dual Imaging System
IR	infrared	MDR	Mission Definition Review
ITAR	International Traffic in Arms Regulations	MEL	Master Equipment List
		MER	Mars Exploration Rover
I-V	current-voltage	MESSENGER	Mercury Surface, Space Environment, Geochemistry, and Ranging
JEO	Jupiter Europa Orbiter		
JOI	Jupiter Orbit Insertion		
JPL	Jet Propulsion Laboratory	MEV	maximum expected value
K&D	key and driving	MGA	medium-gain antenna
KSC	Kennedy Space Center	MIC	Mars Imaging Camera
L1, L2	Level-1, Level-2, etc.	MLI	multilayer insulation
LAEP	Launch Approval Engineering Plan	MMM	Moon Mineralogy Mapper
		MMRTG	multimission radioisotope thermoelectric generator
LAT	limited angle torque		
LCE	Launch Control Equipment	MOLA	Mars Orbiter Laser Altimeter
LEV	lowest expected value	MPSS	multimission power switch slice
LGA	low-gain antenna		
LORRI	Long-Range Reconnaissance Imager	MRO	Mars Reconnaissance Orbiter
		MSL	Mars Science Laboratory
LP	Langmuir Probe	MSTB	Mission System Testbed
LST	local solar time	MTIB	minimum torque impulse bit
LVA	launch vehicle adapter	MVIC	Multispectral Visible Imaging Camera
LVDS	Low-voltage differential signaling	NASA	National Aeronautics and Space Administration

NEPA	National Environmental Policy Act	PJR	perijove raise
NICM	NASA Instrument Cost Model	PMD	propellant-management device
NIMS	Near-Infrared Mapping Spectrometer	PMSR	Project Mission System Review
NLS	NASA Launch Services	PoL	point of load
NLSA	Nuclear Launch Safety Approval	PRA	probabilistic risk assessment
NR	nonresonant, nonres	PRA	Project Resource Analyst
NSI	NASA Standard Initiator	PRICE-H	Parametric Review of Information for Costing and Evaluation—Hardware
NTO	nitrogen tetroxide	PSA	Project Schedule Analyst
O&C	Operations & Checkout	RAD750	radiation-hardened microprocessor
OD	orbit determination	ram	direction of forward velocity vector
OPAG	Outer Planets Assessment Group	RAM	random-access memory
ORT	operations readiness test	RCS	reaction-control subsystem
OSTP	Office of Science and Technology Policy	RDE	Real-Time Development Environment
OTS	off the shelf	RDF	radiation design factor
P	preliminary	RDM	radiation design margin
P/L	payload	RF	radio frequency
P/N	part number	RHU	radioisotope heater unit
PBC	power bus controller	Rj	jovian radii
PCA	pressurant-control assembly	ROD	Record of Decision
PCU	power converter unit	ROIC	readout integrated circuit
PDE	propulsion drive electronics	ROSINA	Rosetta Orbiter Spectrometer for Ion and Neutral Analysis
PDR	Preliminary Design Review	RTG	radioisotope thermoelectric generator
PEL	Power Equipment List	RTOF	reflectron time-of-flight
PFC	pyro-firing card	RWA	reaction wheel assembly
PHSF	Payload Hazardous Service Facility	S/N	signal-to-noise ratio
PI	Principal Investigator	S/S	subsystem
PIA	propellant-isolation assembly	SAF	Spacecraft Assembly Facility
PIP	Project Information Package		

SAR	Safety Analysis Report	TCM	trajectory correction maneuver
SDS	shunt driver slice	TDP	Technical Data Package
SDST	small deep-space transponder	TI	Topographical Imager
SDT	Science Definition Team	TID	total ionizing dose
SDU	shunt dissipater unit	TOF	time of flight
SEE	single-event effect	TRL	technology readiness level
SEER	System Evaluation and Estimation of Resources	TVC	thrust vector control
SEL	single-event latchup	TWTA	traveling-wave tube amplifier
SEMP	Systems Engineering Management Plan	U	update
SER	Safety Evaluation Report	UES	Upper Equipment Section
set point		V	volt, velocity, vector
SEU	single-event upset	V&V	verification and validation
SHARAD	Shallow Radar	VEE	Venus-Earth-Earth
SMAP	Soil Moisture Active Passive	VEEGA	Venus-Earth-Earth gravity assist
SNR	signal-to-noise ratio	VIMS	Visual and Infrared Mapping Spectrometer
SQRT	mean radiation signal per pixel	VRHU	variable radioisotope heating unit
SRAM	static random-access memory	W	watts
SRR	System Requirements Review	We	watts electrical
SRU	stellar reference unit	Wt	watts thermal
SS	subsystem	WBS	work breakdown structure
SSE	Spacecraft Support Equipment	WSTS	workstation testset
SSI	solid-state imager	WTS	waveguide transfer switch
SSPA	solid-state power amplifier		
SSR	solid-state recorder		
STV	Solar Thermal Vacuum		
SWIRS	Shortwave Infrared Spectrometer		
SysML	Systems Modeling Language		
TAYF	test as you fly		
TB	testbed		
TCA	thruster cluster assembly		

**B.4.3 Master Equipment List**

Master Equipment List (MEL) removed for compliance with export-control (ITAR) regulations. Available upon request.”

**B.4.4 Europa Orbiter Mission Senior Review Board Report**

DURAND BUILDING, 496 LOMITA MALL  
 STANFORD, CA 94305-4035  
<http://aa.stanford.edu>  
 (650) 723-3317, fax: (650) 723-0279

Dr. Firouz Naderi  
 Solar System Exploration Directorate  
 JPL  
 Pasadena, CA

December 1, 2011

Dear Dr. Naderi

The recent Planetary Decadal Survey determined that the Europa Jupiter Science Mission (EJSM) had compelling science but was not affordable based on an independent cost estimate of \$4.8B provided to the National Research Council by The Aerospace Corporation. The Decadal Survey recommended that the mission be descoped to significantly reduce cost. In response, the Europa Jupiter System Mission (EJSM) was separated into two elements (i.e., Orbiter and Flyby) and focused solely on Europa science. Subsequently, NASA directed that a soft lander be added to the options under consideration.

As requested by JPL and consistent with the direction from NASA HQs, a Review Board was created to assess the viability of the three mission options to be provided to NASA HQ. These options were to focus on Europa only and develop Orbiter, Flyby (multiple) and Lander concepts, identifying the lowest achievable cost with a target value of  $\approx$ \$1.5B for each concept, not including launch vehicle. It was recognized by the Board that at a  $\approx$  70% reduction in cost from the original EJSM concept any new mission design and corresponding science content would be dramatically different and go far beyond the usual meaning of a simple “descope”.

In the charge to the Board, it was emphasized that the Board’s responsibility was to conduct an “existence proof” evaluation of a pre-pre Phase A concept. In addition, each project was to be evaluated independently, not as one element of a program series.

The Board listed below was assembled and on November 15, convened at JPL to review the Orbiter and Flyby mission designs.

Scott Hubbard	Chair – NASA Ret.
Orlando Figeroa	NASA Ret. (via telephone)
Mark Saunders	NASA Ret.
Dave Nichols	JPL Div. 31
Jeff Srinivasan	JPL Div. 33
Barry Goldstein	JPL Div. 34
Cindy Kahn	JPL Div. 35
Rosalyn Lopes	JPL Div. 32

Gentry Lee	JPL 4X Chief Engineer
Will Devereux	APL
Douglas Eng	APL

To assist the Board in assessing the concepts, members of the JPL staff provided presentations and responded to many questions. This entire effort was applauded by all of the members of the Board and contributed to a most successful meeting.

The high level Europa Review Board conclusions can be summarized in a few statements:

- The overall approach to spacecraft modularity and radiation shielding was unanimously lauded as a creative approach to reducing technical risk and cost. No engineering “showstoppers” were identified.
- Both the Orbiter and Flyby mission concepts satisfied the “existence proof” test as missions that met Europa science requirements, could be conducted within the cost constraints provided and have substantial margins.
  - o However, several Board members expressed a strong opinion that a “science per dollar” criterion such as applied by the Decadal Survey would find the Flyby mission to yield much greater benefits than the Orbiter Project.
- The Board was unanimous in identifying two technical risks that impact both mission concepts:
  - o The Advanced Stirling Radioisotope Generator (ASRG) has been selected as a critical enabling technology. The Board recommends that the study teams thoroughly familiarize themselves with the development status, schedule and performance of the current version of the ASRG and identify any potential modifications from the Discovery version for Europa. In addition, availability of  $^{238}\text{Pu}$  stock and ASRG performance elicited concerns from the Board. In particular, there was a recommendation that much more data be collected on ASRG response to the space mission environment, *e.g.*, microphonics and performance under loads.
  - o While the “nested” approach to radiation shielding clearly mitigated the risk to the spacecraft and instrument electronics, the detectors will be exposed to the space environment. The Board found that early assessment and investment must be provided to ensure proper sensor performance.
- Consistent with the above statement, a Board consensus emerged that if either of these mission concepts moves ahead, particular attention must be paid to the Announcement of Opportunity (AO) for the science investigations so that the AO enables a simple approach and clearly specifies the PI-mission interface in critical areas such as total detector dose.

#### Detailed Considerations:

In the charter distributed to the Board prior to the review, we were asked to consider the following criteria:

- Ability of the mission to satisfy the Science Objectives
- Mission design approach
- Robustness of the mission and system architectures

- Robustness of mission and system margins; compliance with JPL design principles.
- Proposed scope, including available options, is consistent with funding target value to complete the mission
- Cost risk Project planning risks, including design, environment mitigation plans, integration and test plans, schedule and margins.

Within this overall review framework the following more specific comments were noted where at least two or more Board members addressed similar issues:

#### Science and Mission Design:

- During the science presentations, there were numerous questions about the changes from the original EJSM instrument suite and experiment goals. Following a request from the Board, Dr. Pappalardo gave a summary of science traceability. A number of the Board members suggested that more work be done by the SDT to clearly define the relationship of a given mission concept to the Decadal Survey.
- The Orbiter mission is challenging in that the science campaign occurs in the last 30 days of the mission and after significant radiation exposure. The Flyby mission has a much slower accumulation of total dose. This distinction needs to be sharpened.

#### Robustness and Margins:

- Systems margins presented for power, mass, and data were substantial, and of course have implications for launch vehicle requirements and cost. There was considerable discussion and some disagreement about whether maintaining such large technical margins may inappropriately drive the costs at this stage of maturity. A majority of the Board concluded that a conservative approach was appropriate at this point in the life cycle, particularly with the uncertainty in the launch vehicle capabilities a decade or more away from now.

#### Cost and Cost Risk:

- A majority of the Board appeared satisfied that the two study teams had produced credible cost estimates using a variety of tools and approaches. While the Flyby mission was slightly higher than the \$1.5B FY15 target, both projects were deemed to be “in the ballpark”. There was a minority opinion that expressed concern over an inconsistency in trends between two parametric tools. Clearly, ongoing cost evaluation and the Aerospace CATE are needed to track these concepts.

#### Schedule:

- The Study leader (Gavin) noted at the beginning of the review that detailed schedules would not be available. While the Board accepted this limitation as a necessary element of an “existence proof” review, there was clear concern about whether the schedule supported the hardware development as proposed. At subsequent reviews more explicit schedule data is required in order to understand the risks involved.

On behalf of the entire Board, I wish to express again our congratulations to the JPL team in the high quality of the studies. We look forward to the Lander review early in 2012.

Sincerely,

A handwritten signature in blue ink, appearing to read "G. Scott Hubbard".

Prof. G. Scott Hubbard  
Chair, Europa Mission Review Board  
Cc: Board members, Tom Gavin

**B.4.5 *Aerospace Independent Orbiter Concept CATE: Cost and Technical Evaluation***

(see next page)



# Europa Habitability Mission: Orbiter Concept CATE: Cost and Technical Evaluation

April 24, 2012

Randy Persinger<sup>1</sup>, Robert Kellogg<sup>2</sup>, Mark Barrera<sup>3</sup>

<sup>1</sup>Advanced Studies and Analysis Directorate, NASA Programs Division

<sup>2</sup>Space Architecture Department, Systems Engineering Division

<sup>3</sup>Vehicle Concepts Department, Systems Engineering Division

Prepared for:

Jet Propulsion Laboratory  
4800 Oak Grove Drive  
Pasadena, CA 91109

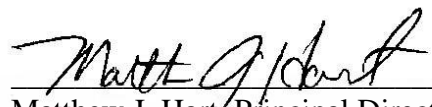
Contract No. 1393581

Authorized by: Civil and Commercial Operations

**PUBLIC RELEASE IS AUTHORIZED.**

# Europa Habitability Mission: Orbiter Concept CATE: Cost and Technical Evaluation

Approved by:



---

Matthew J. Hart, Principal Director  
Advanced Studies and Analysis Directorate  
Ground Enterprise  
NASA Programs Division  
Civil and Commercial Operations

## **Acknowledgments**

The following individuals are recognized for their contributions as authors, reviewers, and editors of the Cost and Technical Evaluation (CATE) for the Europa Habitability Mission: Orbiter concept.

David Bearden  
Ray Nakagawa  
Anh Tu  
Mark Cowdin  
Gary North

## Contents

1. Purpose .....	1
2. Executive Summary.....	3
3. CATE Background .....	5
4. Technical Evaluation .....	7
5. Cost and Schedule Evaluation .....	11

## Figures

Figure 1.	EHM Orbiter Mission Concept Overview .....	1
Figure 2.	Europa Orbiter Cost Estimates.....	3
Figure 3.	EHM Orbiter Mission Concept Features .....	7
Figure 4.	EHM Orbiter Launch Mass Margin.....	8
Figure 6.	CATE Cost Estimating Process .....	11
Figure 7.	Analogy-Based Estimating Process .....	12
Figure 8.	Orbiter Bus Cost Estimates.....	12
Figure 9.	Orbiter Laser Altimeter Cost Estimates.....	13
Figure 10.	Orbiter Langmuir Probe Cost Estimates .....	13
Figure 11.	Orbiter Magnetometer Cost Estimates.....	14
Figure 12.	Orbiter Mapping Camera Cost Estimates .....	14
Figure 13.	Total Payload Cost Comparison .....	15
Figure 14.	Europa Orbiter Planned Development Schedule .....	16
Figure 15.	Cost Reserve Estimate Process Overview .....	17
Figure 16.	Contingency Values Used For Threat Estimates .....	18
Figure 17.	Independent Schedule Estimate Process Overview .....	19
Figure 18.	Analogous Mission Development Time Comparison.....	20
Figure 19.	Europa Orbiter ISE S-Curve .....	20
Figure 20.	Europa Orbiter Analogous Mission Phase Comparison .....	21
Figure 21.	Europa Orbiter Key Cost Element Comparison.....	22
Figure 22.	Europa Orbiter Cost Estimates.....	22
Figure 23.	Complexity-Based Risk Assessment Cost Analysis .....	23
Figure 24.	Complexity-Based Risk Assessment Schedule Analysis.....	24

## Tables

Table 1.	Europa Orbiter Mass Properties.....	18
Table 2.	Europa Orbiter Cost Estimate Comparison (FY15\$M) .....	21

# 1. Purpose

The Aerospace Corporation was tasked in November 2011 to participate as an independent party to review three separate, but related, Europa Habitability Mission (EHM) concepts under study by the Jet Propulsion Laboratory (JPL) to visit Europa in the continuing search for life in our solar system. The three concepts were being studied by JPL in the context of guidance provided by the National Research Council (NRC) Planetary Decadal Survey report released to the public in March 2011. In this report, a mission to the Jupiter/Europa system was rated very high with regard to science importance to the United States in the next decade. However, based on the expected high cost of the baseline reference mission evaluated by the NRC Planetary Decadal Steering Committee, the guidance was to descope the reference mission and significantly reduce mission cost while providing sufficient scientific investigation capability considered to be of paramount importance over the next decade. Aerospace, having participated as the NRC Cost and Technical Evaluation (CATE) contractor in the cost, technical, and schedule risk assessment of the planetary concepts evaluated by the Planetary Steering Committee, was a logical choice to independently evaluate the three updated EHM concepts with the same CATE techniques and processes. The three separate EHM mission concepts evaluated were: Orbiter, Flyby and Lander. This report presents the cost, technical, and schedule risk assessment for the **EHM Orbiter Mission** using the CATE process originally established by the NRC.

The key parameters of the EHM Orbiter Mission can be found in Figure 1.

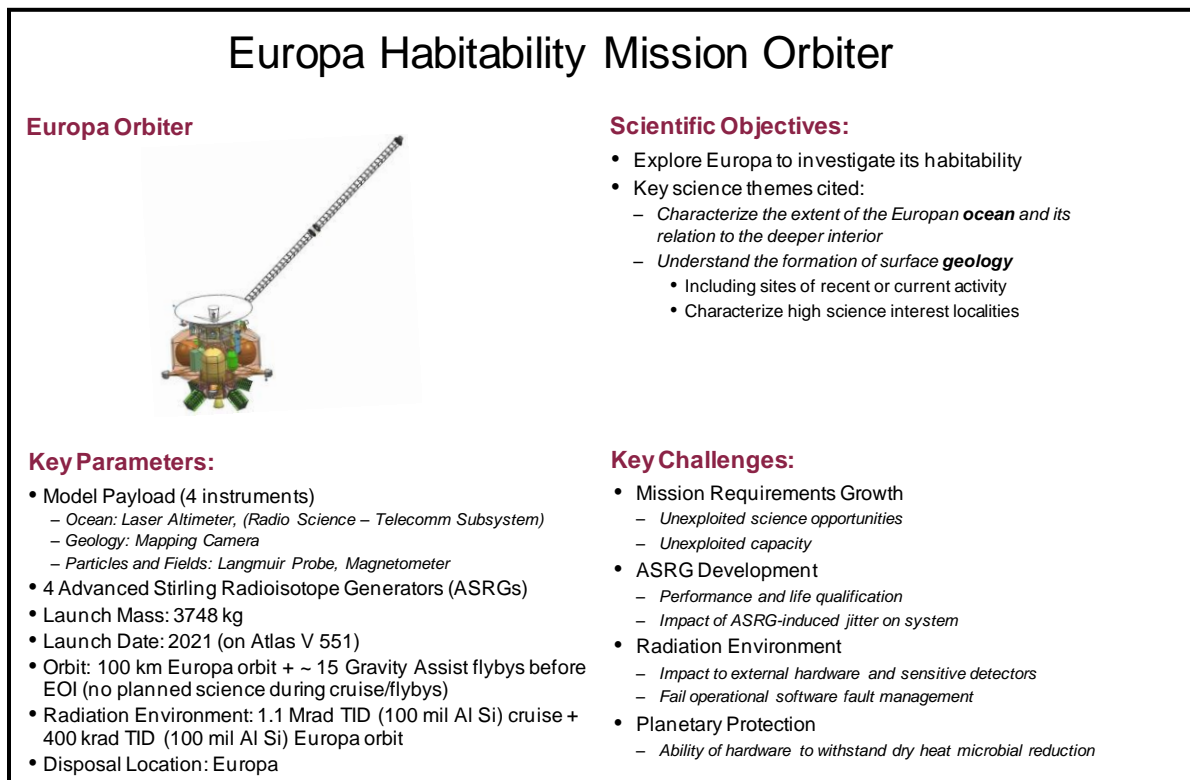


Figure 1. EHM Orbiter Mission Concept Overview

## 2. Executive Summary

The EHM Orbiter concept was found to have a Medium technical risk and is well designed for an orbiter mission to Europa. Mass and power margins are robust, and the design incorporates modularity with well-defined interfaces. Technology development is mainly related to engineering implementation; however, concern does exist with the technology development of the radioisotope power source (ASRGs) currently under development by NASA. An additional concern is the selection of hardware that is tolerant to the dry heat microbial reduction process planned to ensure satisfaction of Planetary Protection requirements. The impact of radiation for this mission is also a concern but has been mitigated by compartmentalization and the modular design, as well as the mission design.

The CATE cost estimate for the EHM Orbiter concept is \$1.8B in FY15 dollars excluding launch services. The EHM Orbiter CATE, estimate excluding launch services, is compared to the Project's cost estimate in Figure 2. Including a launch service cost of \$272M, consistent with CATE estimates for the Planetary Decadal Survey Steering Committee, the CATE estimate including launch services is \$2.0B. The cost estimate for four ASRGs is assumed to be \$200M based on guidance provided by NASA. The cost risk associated with the ASRG technology development required for the EHM mission concepts has not been included in the CATE cost estimate, nor have the associated schedule risk to the project and technical risk to the flight system.

The project schedule of 73 months is considered to be realistic with the independent estimate being 75 months. The concept's use of modularity provides the opportunity to focus and minimize risk through parallel development paths.

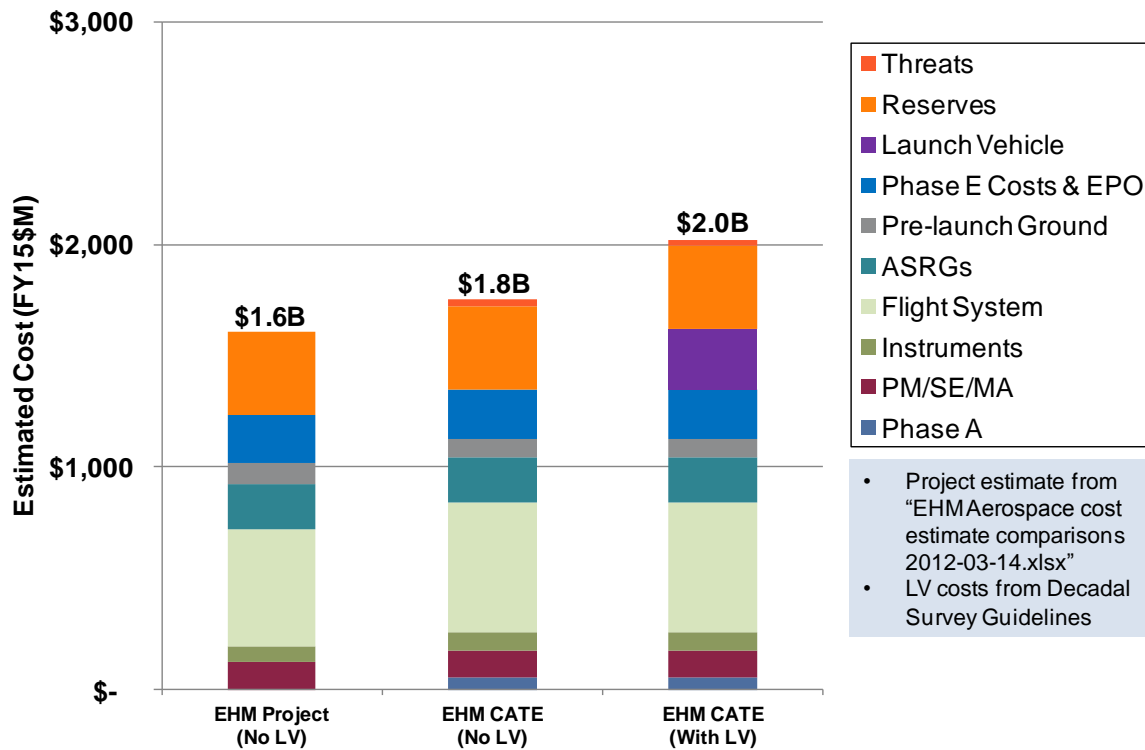


Figure 2. Europa Orbiter Cost Estimates

### 3. CATE Background

The NRC Astro2010 Decadal Survey Steering Committee established the CATE process in June 2009. The CATE process was then used for three NRC Decadal Surveys: Astro2010, Planetary, and Heliophysics. Previous NRC Decadal Surveys had underestimated the costs associated with the recommended science priorities. The NRC and others recognized that mission costs were being underestimated, so the US Congress mandated that an independent contractor be utilized to provide more realistic cost, technical and schedule risk assessment directly to the decadal steering committees for consideration and evaluation in executing their charter. Select portions of the Planetary Decadal report, *Vision and Voyages*, from Appendix C are provided below to summarize the CATE process. It is important to note that the CATE process is intended to inform future NASA Science Mission Directorate (SMD) budget decisions, not to decide if a specific concept meets a cost target or to decide if a specific mission concept should be selected for flight versus another mission. Because the CATE process is used for future budgetary decisions, it incorporates potential cost threats that may occur in the future based on concept maturity at the time of evaluation.

The CATE process focuses on cost and schedule risk assessment, but limited technical evaluation is also required to categorize concept maturity, technology development, and the potential impact that insufficient margins and contingency (mass and power) may have on schedule or cost.

***Vision and Voyages, Planetary Decadal Report, Appendix C:** The objective of the CATE process is to perform a cost and technical risk analysis for a set of concepts that may have a broad range of maturity, and to ensure that the analysis is consistent, fair, and informed by historical data. Typically, a concept evaluated using the CATE process is early in its life cycle and therefore likely to undergo significant subsequent design changes. Historically, such changes have resulted in cost growth. Therefore, a robust process is required that fairly treats a concept of low maturity relative to one that has undergone several iterations and review. CATEs take into account several components of risk assessment.*

*The primary goal of the CATE cost appraisal is to provide independent estimates (in fiscal year [FY] 2015 dollars) that can be used to prioritize various concepts within the context of the expected NASA budgetary constraints for the coming decade. ... To be consistent for all concepts, the CATE cost process allows an increase in cost resulting from increased contingency mass and power, increased schedule, increased required launch vehicle capability, and other cost threats depending on the concept maturity and specific risk assessment of a particular concept. ... All cost appraisals for the CATE process are probabilistic in nature and are based on the NASA historical record and documented project life-cycle growth studies.*

*The evaluation of technical risk and maturity in the CATE process focuses on the identification of the technical risks most important to achieving the required mission performance and stated science objectives. The assessment is limited to top-level technical maturity and risk discussions. Deviations from the current state of the art as well as system complexity, operational complexity, and integration concerns associated with the use of heritage components are identified. Technical maturity and the need for specific technology development, including readiness levels of key technologies and hardware, are evaluated. ... The CATE technical evaluation is limited to high-level technical risks that potentially impact schedule and cost. The CATE process places no cost cap on mission concepts, and hence risk as a function of cost is not considered. Concept maturity and technical risk are evaluated in terms of the ability of a concept to meet performance goals within proposed launch dates with adequate mass, power, and performance margins.*

*To aid in the assessment of concept risk, independent schedule estimates are incorporated as part of the CATE cost estimate.*

## 4. Technical Evaluation

The EHM Orbiter technical risk rating is Medium. The mission will require medium new development, mostly in the engineering implementation. Radioisotope, or ASRG, power source qualification, radiation mitigation for external hardware, software fault management, bake stable treatment of detectors for planetary protection, and qualification of the AMBR 890 N (HiPAT) engine will be some of the key challenges associated with this mission. Mass margins are high, with an average mass contingency of 64% for the bus and 88% for the instruments. Power margins and battery depth of discharge are adequate assuming four ASRGs. The concept design is within the capability of the Atlas V 551 and 541 launch vehicles, with greater than 10% launch mass margin. The radiation environment contributes to Medium operational risk. The proposed “fail operational” approach to fault management of radiation upsets also contributes to this risk. An additional concern is the development of hardware to withstand Planetary Protection measures, given the vehicle will be disposed of on the surface of Europa.

The top technical risks associated with the EHM Orbiter Mission are:

1. **Mission Requirements Growth** to utilize additional capacity
2. **Advanced Stirling Radioisotope Generator (ASRGs)** development impact
3. Survival of flight system in **Radiation Environment**
4. Development of hardware to withstand **Planetary Protection** methods

These top risks are discussed below. Figure 3 illustrates some key aspects of the EHM Orbiter concept.

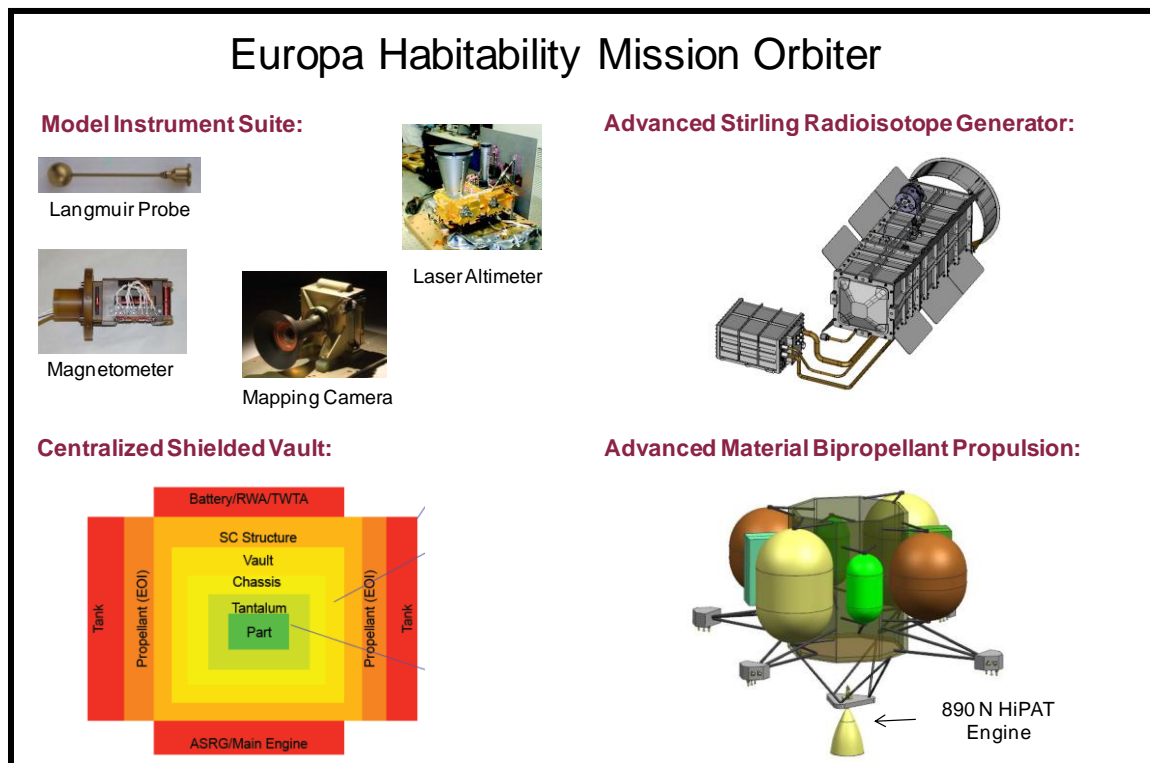


Figure 3. EHM Orbiter Mission Concept Features

## Mission Requirements Growth

The anticipated high mass margins for the EHM Orbiter mission have the benefit of mitigating the risk of unplanned mass growth; however, they also offer a temptation to increase the science payload from the current focused concept, which may impact the overall complexity and cost of the mission. As illustrated in Figure 4, the proposed concept has a launch mass margin of greater than 10% on Atlas V 541 and 551. This margin already considers the best-estimate mass as well as an average 64% mass growth contingency for the bus and 88% mass growth contingency for the instruments. Since the mass margins are high, there is a concern that instrument providers may wish to utilize excess capacity. Competitively chosen instruments may have higher mass or complexity than the model instruments for the EHM concept. Also, there is a concern that instrument types from the EHM Flyby concept may be added to the Orbiter mission. Neither of these potential scenarios was included in the CATE cost estimate.

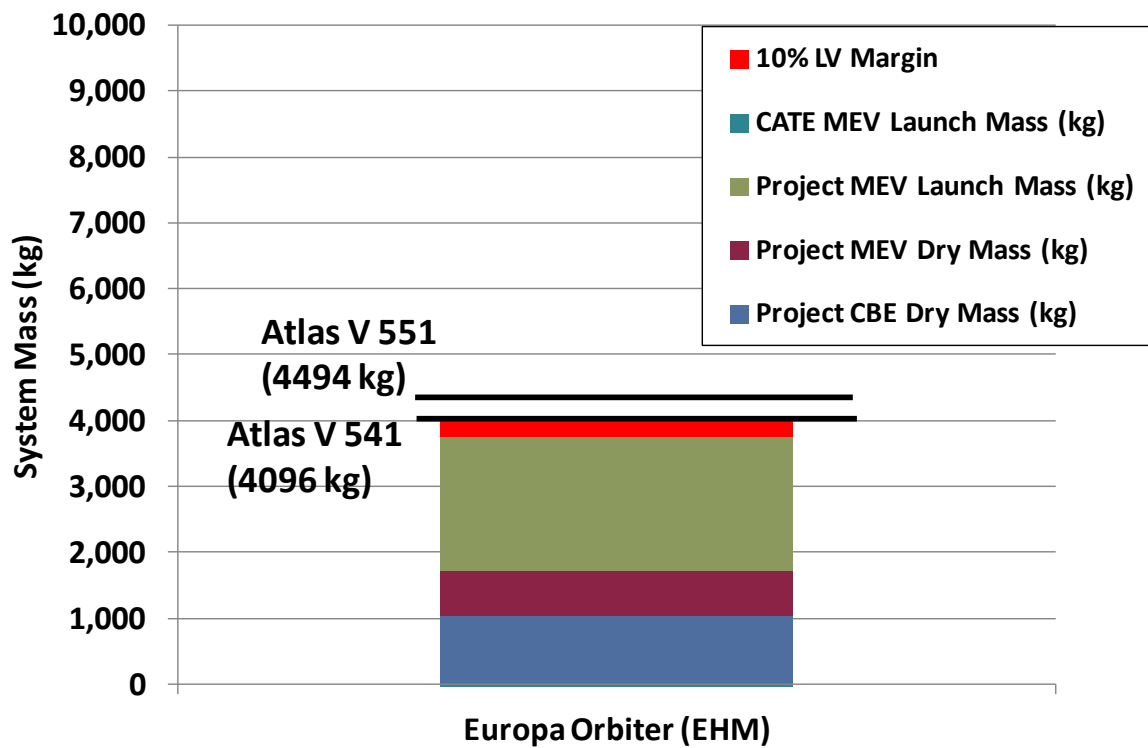


Figure 4. EHM Orbiter Launch Mass Margin

Power margins during normal operations are acceptable assuming 4 ASRG power, as shown in Figure 5. There are small differences in the expected maximum battery depth of discharge due to differences in power growth allowances in CATE estimates versus project estimates; however, all estimated power margins are within acceptable limits. Battery depth-of-discharge is held to 28% or lower in the worst case (at either telecom or Jupiter orbit insertion).

## Advanced Stirling Radioisotope Generator (ASRGs)

Uncertainty associated with technology development for the ASRGs contributes to risk of design changes and schedule delays for the project. The ASRG is currently estimated at TRL 5 and is part of an ongoing development effort. Results from the ground based testing program may possibly lead to changes in the ASRG interface to the spacecraft. Items that are of particular concern include the contribution of jitter from the ASRGs to the Mapping Camera and Laser Altimeter as well as the

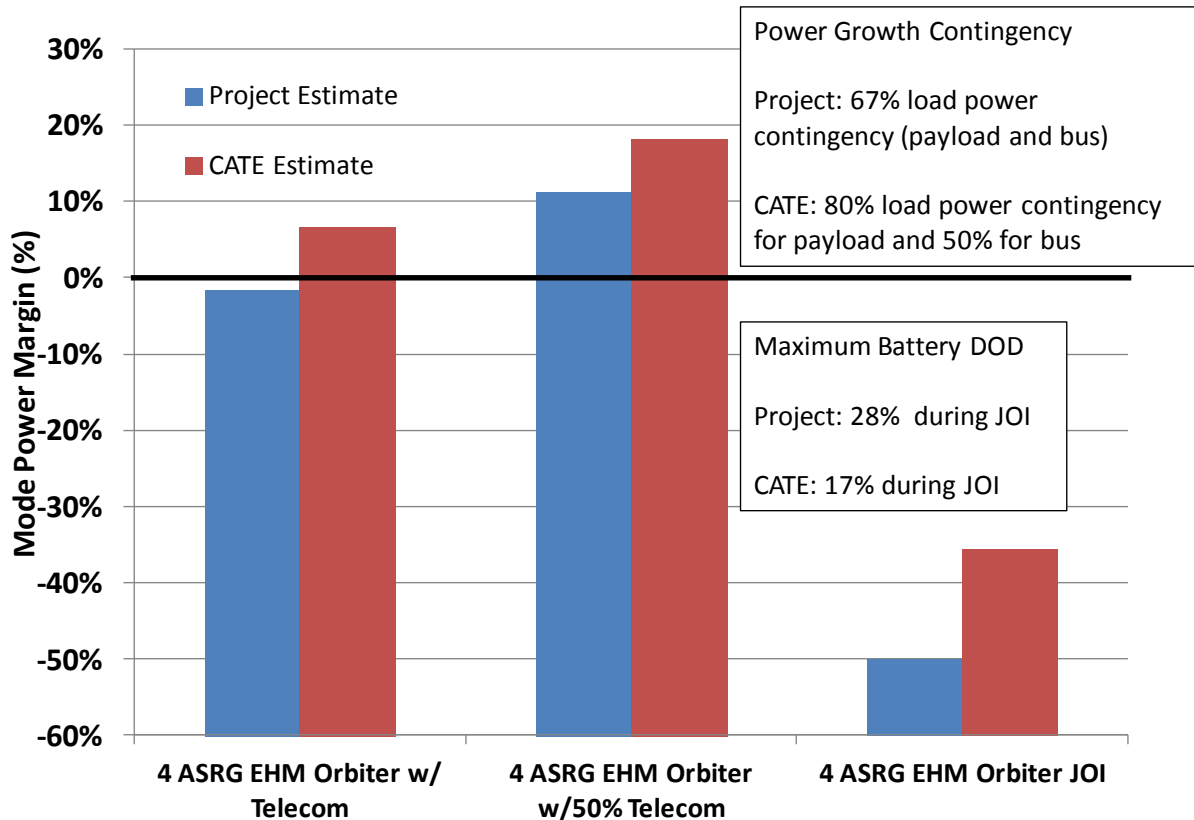


Figure 5. EHM Orbiter Power Margin

impact of electromagnetic interference (EMI). Also, there is concern that the ASRG may not provide the expected power for the mission environment. If the ASRGs provide less power than expected, then either a fifth ASRG may need to be considered or a modification to mission operations may be necessary. No additions to the CATE cost or schedule estimates were made based on possible delays in ASRG development.

### Radiation Environment

The radiation environment for the EHM Orbiter mission contributes to uncertainty in mass, cost, and schedule. Hardware that is external to the radiation vault, particularly exposed sensor heads, will require qualification for the mission radiation environment. Delays in radiation qualification of sensor detectors or optics may adversely impact project cost and schedule. Hardware that is internal to the radiation vault may need to be assessed for compatibility (EMI and thermal) within the common enclosure. Additional systems engineering effort is anticipated for successful integration of electronics within the common radiation vault. In order to maintain operations through radiation upsets, the EHM Orbiter mission proposes a “fail operational” software fault management approach. While this approach may help to maintain operations pacing, it will require a more complete understanding of hardware failure modes than a “fail safe” approach. Some delays in fault management software are anticipated as the hardware implementation matures. The impact to the CATE cost estimate was considered by using the Juno mission as a cost analogy and adding a 5% multiplier to the bus and camera estimates for radiation issues.

## **Planetary Protection**

The EHM Orbiter is intended for disposal on the surface of Europa and as a result is subject to Planetary Protection requirements. These requirements will place a stringent limit on spores on surfaces, in joints, and in the bulk of nonmetallic materials. Currently, the project plans to use dry heat microbial reduction to meet these requirements and possibly other means if necessary. Hardware used on the EHM Orbiter must be tolerant to the high heat (~110°C-125°C) microbial reduction process or other processes as needed. These requirements will constrain hardware selection and may result in adverse impacts to cost and schedule. In order to ensure satisfaction of Planetary Protection requirements, the project will need to implement a compliance effort throughout the system development. In order to account for instrument and bus planetary protection, a 5% multiplying factor was used in the cost estimate.

## **Technology Development**

Technology development items for the EHM Orbiter mission include development of the ASRG, radiation-hardened detectors for the Europa mission environment, and qualification of the AMBR 890 N (HiPAT) engine. The ASRG is currently estimated at TRL 5 based on DoE engineering unit testing with further testing by NASA Glenn Research Center. Further life testing is anticipated as well as a modified housing design. Additional development of radiation hardened detectors is anticipated to advance beyond TRL 5-6. The current level of maturity depends on the selected manufacturers and their proposed manufacturing techniques for hardening of CCD and CMOS type detectors. The AMBR engine is currently estimated at TRL 6, based on unit level environmental and performance testing, although additional performance and life testing is ongoing.

## 5. Cost and Schedule Evaluation

Figure 6 illustrates the CATE cost estimating approach in the form of a flow diagram. The initial focus is to estimate, with multiple analogies and cost models, the concept hardware such as instruments and spacecraft bus. Following the estimation of other cost elements based on historical data, a probabilistic cost-risk analysis is employed to estimate appropriate cost reserves. To ensure consistency for all concepts, the cost estimates are updated with information from the technical team with regard to mass and power contingencies and potentially required additional launch vehicle capacity. Using independent schedule estimates, costs are adjusted using appropriate burn rates to properly reflect the impact of schedule delays or multiple work shifts to ensure meeting a launch date. Finally, the results are integrated, cross-checked with other independent cost and schedule estimating capabilities, and verified for consistency.

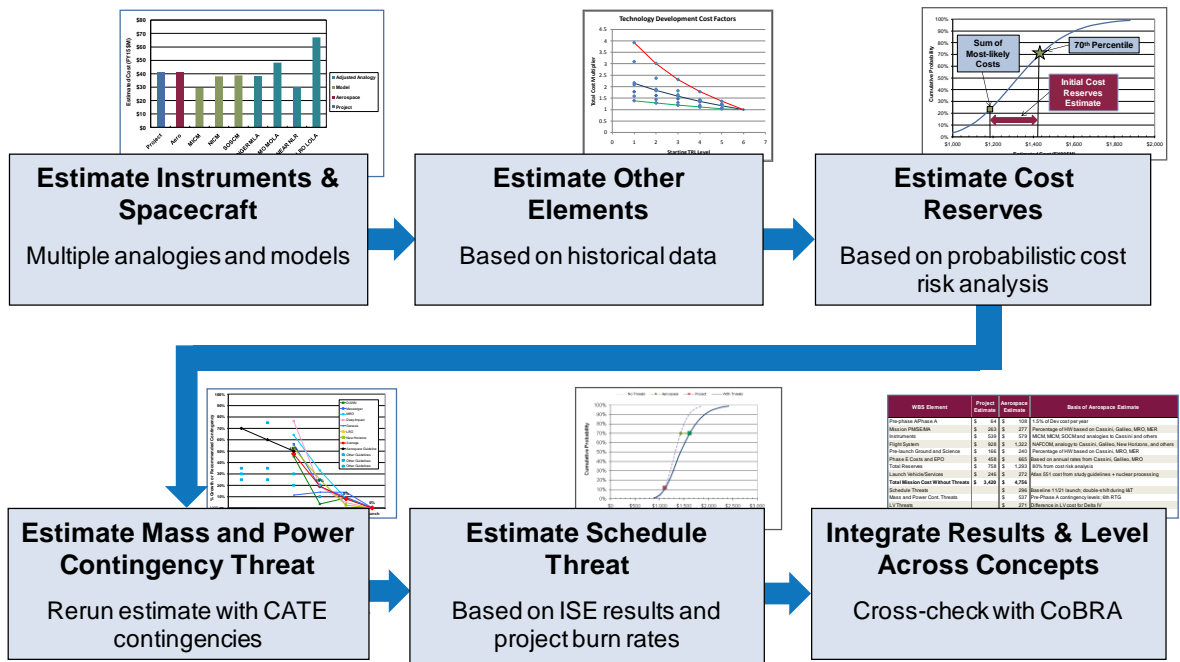


Figure 6. CATE Cost Estimating Process

### Hardware Cost Estimates

The hardware cost elements estimated for the Europa Orbiter concept are the spacecraft bus and the four instruments. Multiple estimates are developed for each of these elements. Both parametric cost models and analogy-based estimates are used. Figure 7 illustrates the analogy-based estimating process, which uses a cost estimating relationship (CER) to adjust the actual costs of past missions. By using the actual costs of past missions, unique attributes of those missions or performing organizations, which are similar to the mission being estimated, can be captured. This can provide insight that is different from most parametric cost models, which are based more on an “industry average” approach.

For the spacecraft bus, a total of five estimates were developed using the NASA and Air Force Cost Model (NAFCOM), the PRICE-H cost model and analogy-based estimates using Juno, Cassini, and Mars Reconnaissance Orbiter (MRO). The final CATE estimate is an average of these five estimates. The results of these estimates are depicted in Figure 8. The cost estimates shown include the spacecraft hardware, Project Management and Systems Engineering at the bus level, as well as bus

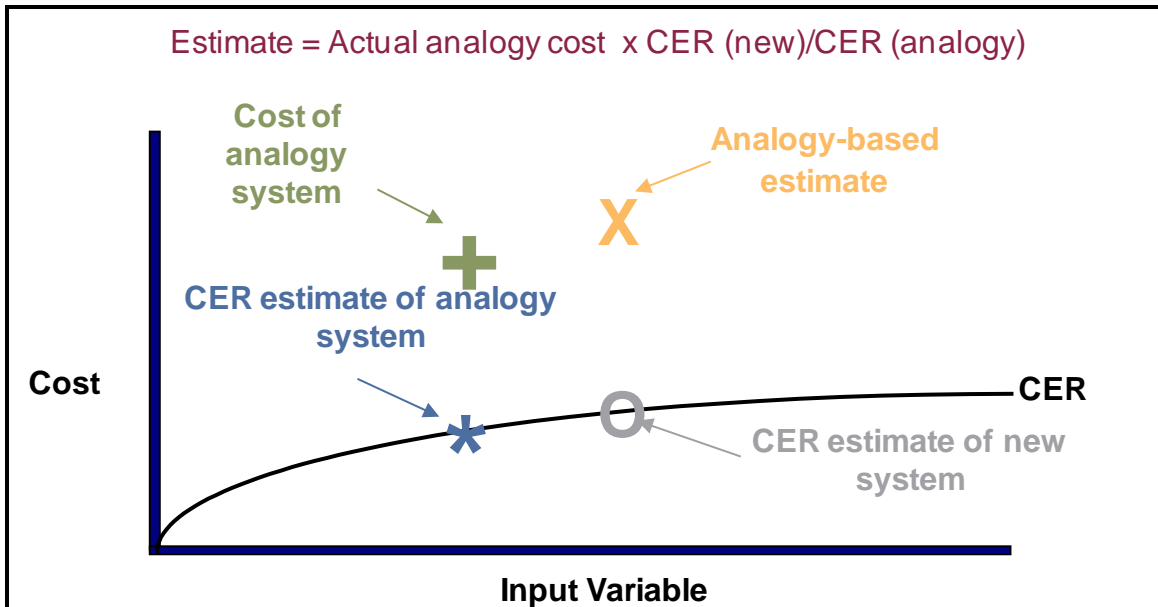


Figure 7. Analogy-Based Estimating Process

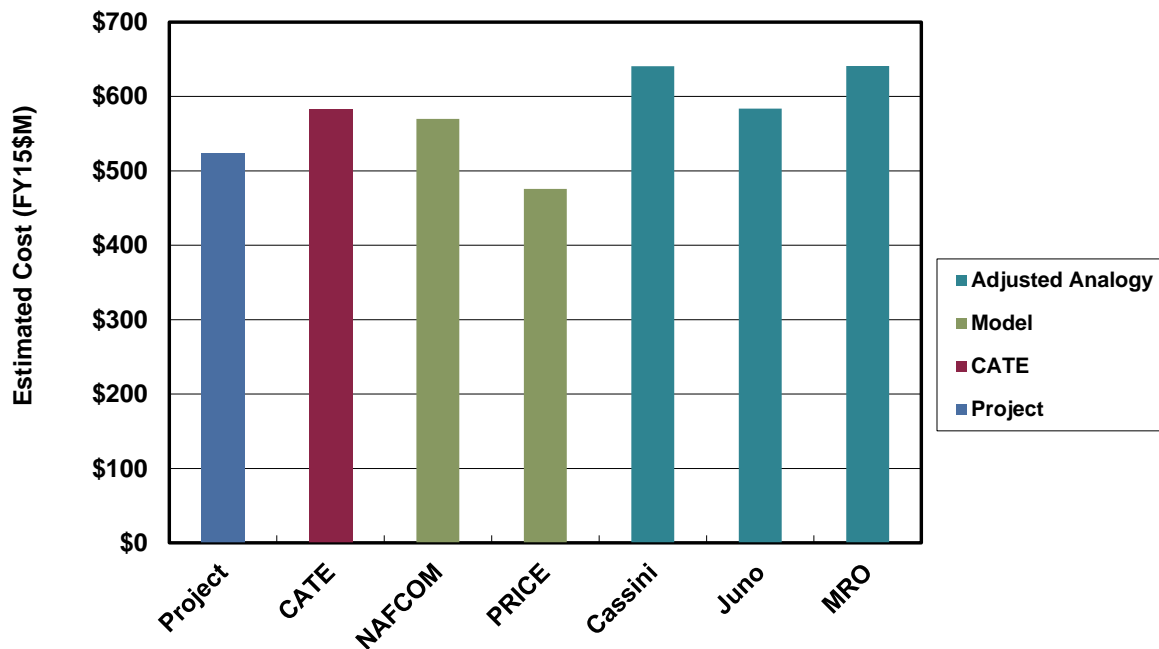


Figure 8. Orbiter Bus Cost Estimates

and system-level integration and test. ASRG costs are not included in these estimates. As can be seen, there is reasonable agreement between the CATE (\$582M) and Project (\$523M) cost estimate for the spacecraft bus or flight system.

For the Orbiter instruments, the cost estimates are based on either two or three parametric cost models and three to five analogy-based estimates. The parametric models used for the Orbiter instruments include the NASA Instrument Cost Model (NICM), The Multivariate Instrument Cost Model (MICM), and the Space-based Optical System Cost Model (SOSCM). The results for the instruments are depicted in Figures 9 to 12. In addition to the individual instrument estimates, the total payload

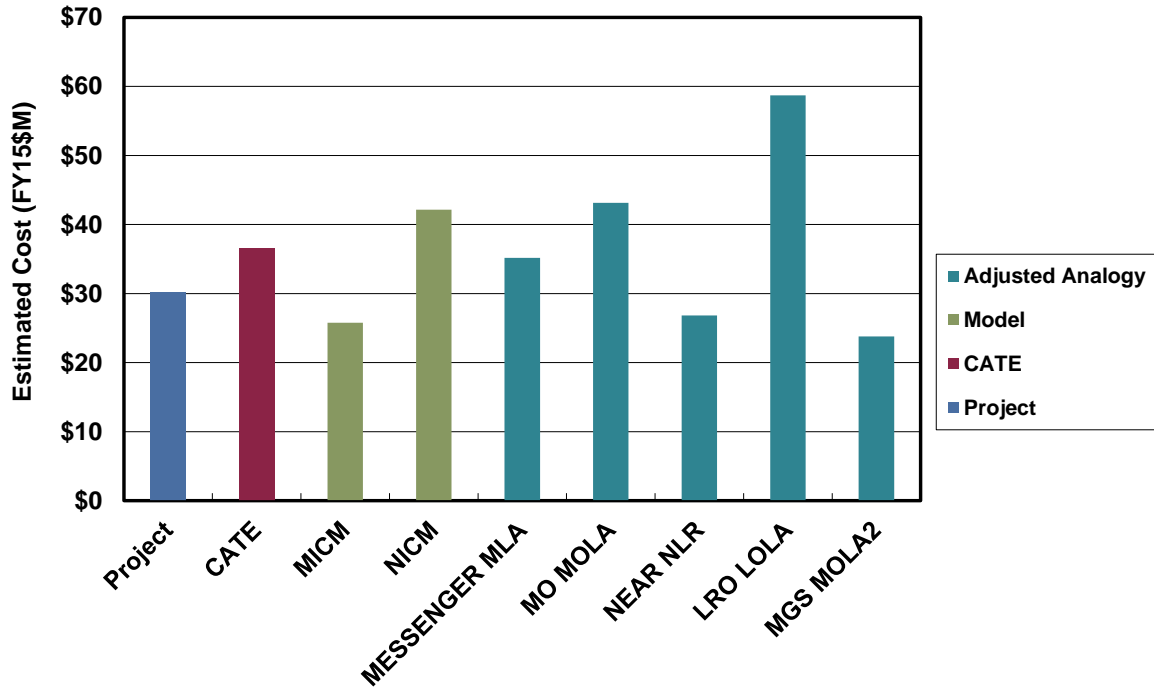


Figure 9. Orbiter Laser Altimeter Cost Estimates

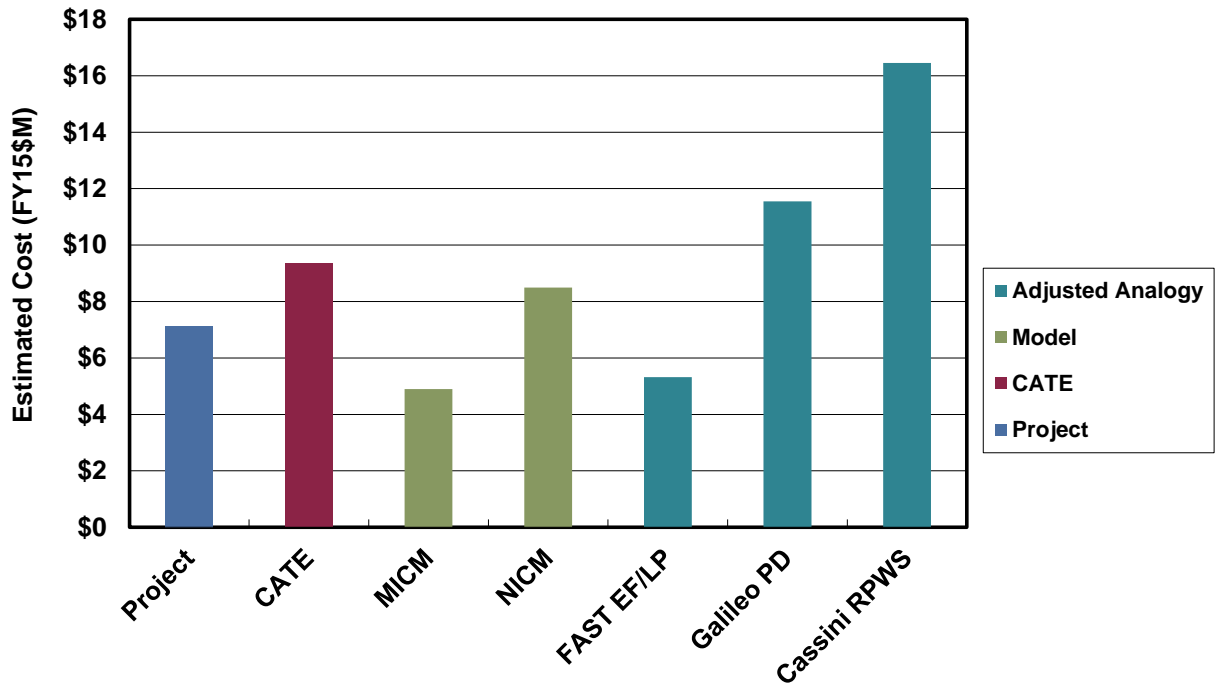


Figure 10. Orbiter Langmuir Probe Cost Estimates

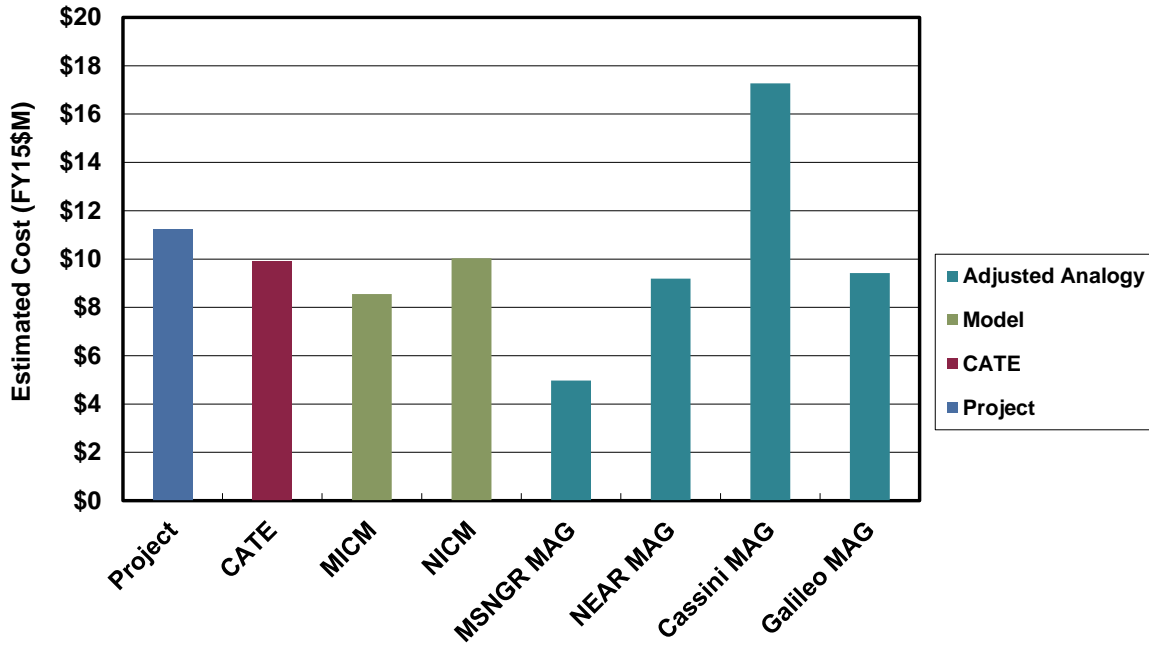


Figure 11. Orbiter Magnetometer Cost Estimates

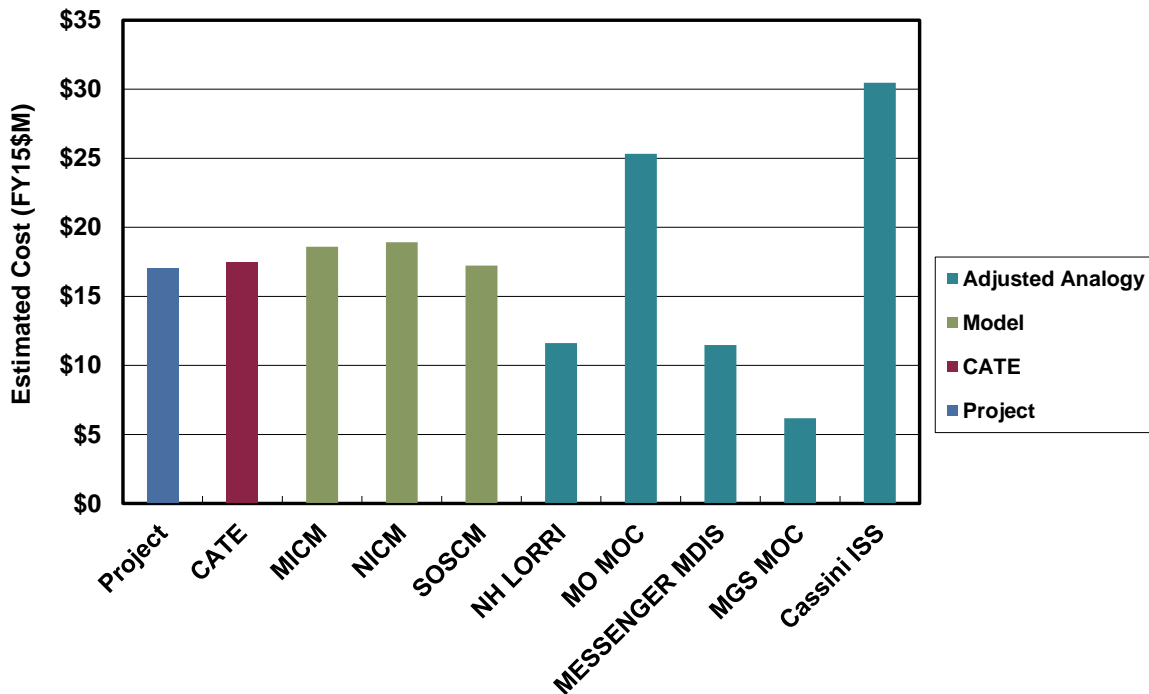


Figure 12. Orbiter Mapping Camera Cost Estimates

estimates include an estimate of the payload-level Project Management and Systems Engineering. For the total payload, there is good agreement between the CATE (\$81M) and Project (\$75M) cost estimates, as shown in Figure 13.

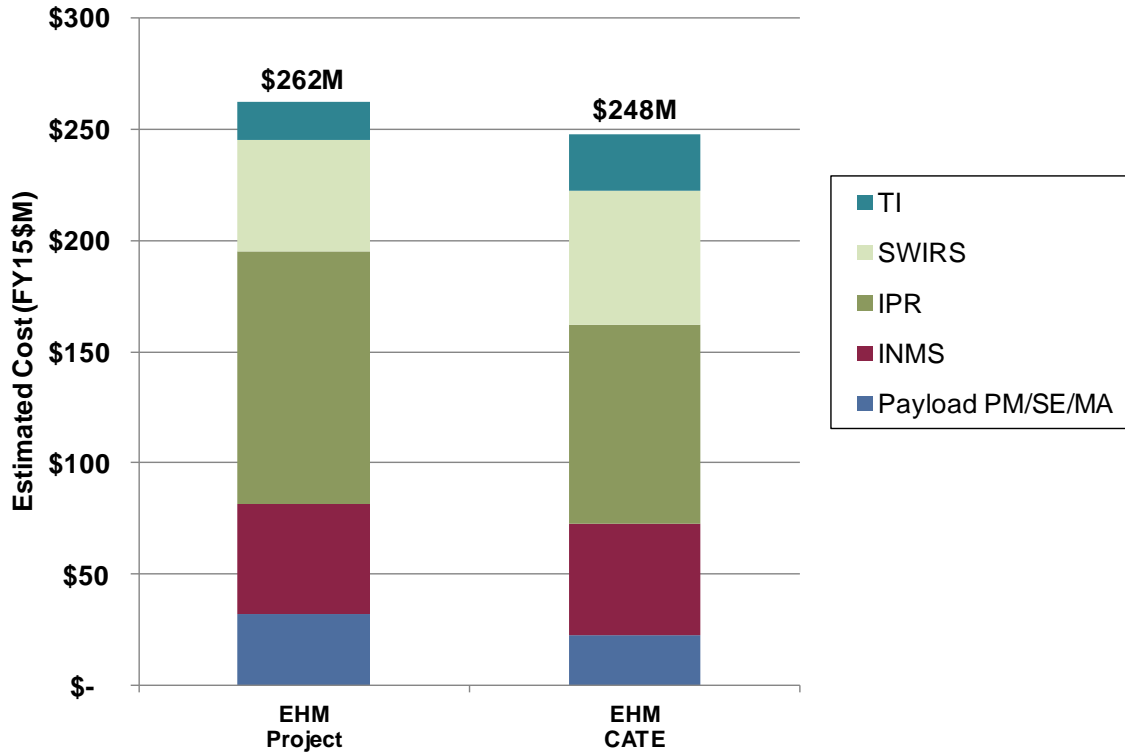


Figure 13. Total Payload Cost Comparison

### Other Cost Elements

Other cost elements estimated for the EHM Orbiter concept include project-level Project Management, Systems Engineering, and Mission Assurance, pre-launch Science and Ground System Development, Pre-Phase A/Phase A, Phase E, and Education and Public Outreach (EPO). Other cost elements included in the total cost estimated, but not independently estimated, are the ASRGs and launch vehicle.

Project Management, Systems Engineering, and Mission Assurance were estimated as a single total (PM/SE/MA) using “wrap factors” based on similar historical projects. The historical missions used for the Orbiter PM/SE/MA estimate are Cassini, Juno, MER, and Mars Exploration Rover (MRO). The “wrap factors” are calculated as a percentage of hardware costs for the historical missions. These percentages are then applied to the estimated hardware cost of the Orbiter concept. Specifically, the average percentage wrap factor is applied to the total of the average estimate for each hardware element.

Pre-launch Science and Ground System Development estimate is similarly developed using wrap factors based on historical missions. The historical missions used are Cassini, Juno, MER, and MRO.

Pre-Phase A/Phase A costs are estimated using a rule of thumb of 1.5% of the Phase B-D development costs per year of Pre-Phase A/Phase A. For the EHM Orbiter concept, the total duration used was 40 months starting in June 2012 and ending in October 2015. This is actually earlier than the Phase A end date shown on the project schedule (Figure 14). However, significant activities are planned to start in October 2015. These activities have historically been a part of Phase B, so an adjusted Phase B start date is used for all schedule-related analyses.

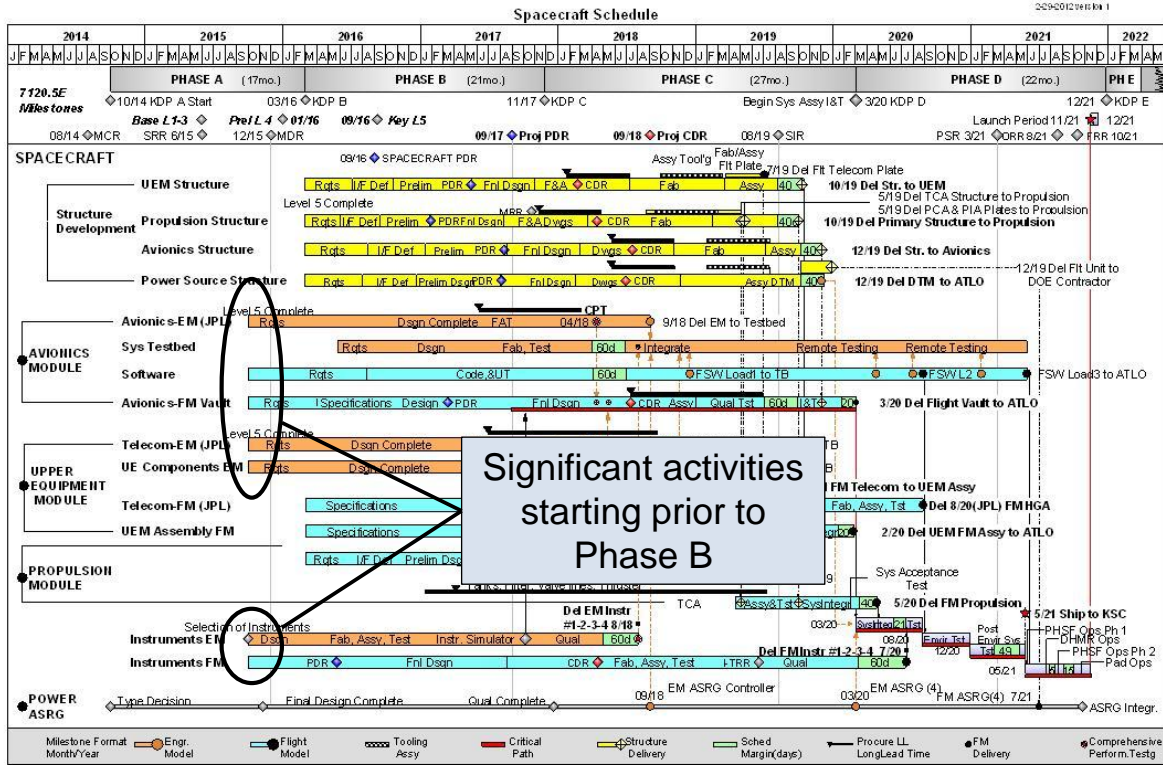


Figure 14. Europa Orbiter Planned Development Schedule

Phase E costs were estimated using annual spend rates from similar historical projects. Because of the potentially different staffing required during cruise and encounter, these phases were estimated separately using historical rates appropriate for the respective phase. For the cruise phase, annual rates from MESSENGER, Juno, and New Horizons cruise phases were used. For the encounter phase, annual rates from MRO and the predicted annual rate from Juno encounter phases were used.

EPO costs are estimated as 1% of total project costs excluding launch vehicle.

For the ASRGs, the project estimate of \$50M each, supplied by NASA HQ, was used in the CATE estimate. For the Atlas V 551 launch vehicle, a \$272M estimate from the Planetary Decadal Survey was assumed for consistency.

### Cost Reserves

Cost reserves are estimated using a process illustrated in Figure 15. For each Work Breakdown Structure (WBS) element, a triangular distribution of possible costs is developed. The cost values for the triangle are derived from the range of cost estimates as illustrated in the bus and instrument figures above. The lowest of the multiple estimates is used as the low value of the triangular distribution. The average of the multiple estimates is used as the mode or most-likely value of the triangular distribution. The high value of the triangular distribution starts with the highest of the multiple estimates but then adds an additional Design Maturity Factor. The DMF is a multiplier based on the maturity of the proposed design and the experience of the team. This factor helps ensure that the high value of the distribution truly represents a worst case.

Once the triangular distributions are developed for each WBS element, they are statistically combined to produce a total cost probability distribution. This distribution is typically plotted as a cumulative

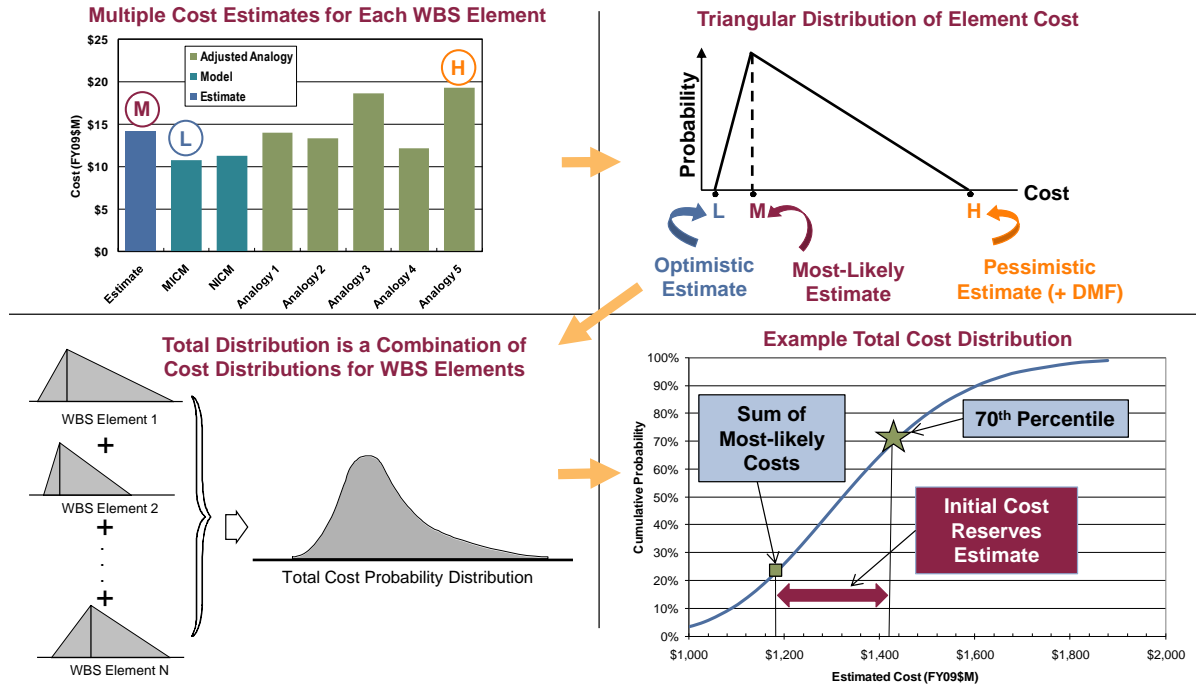


Figure 15. Cost Reserve Estimate Process Overview

distribution, which takes the familiar “S-curve” shape. The difference between the 70th percentile value from this curve and the sum of the most-likely estimates is the cost reserves estimate.

### Mass and Power Contingency Threat

The mass and power contingency threat is a concept that was developed to support the CATE estimates, initially for the Astro2010 Decadal Survey, then later applied to the Planetary Science and Heliophysics Decadal Surveys. The motivation was to provide a methodology to account for the design evolution that has historically occurred from early conceptual design through development and launch. In order to assign a cost to these design changes, historical mass and power growth data was examined. This data showed values that were well above the typical guidelines of roughly 30% at Phase B start. Because data prior to Phase B start was sparse, the available data was extrapolated back to early conceptual phases.

Figure 16 shows an example of the data used for the mass and power contingency threats. This plot shows payload mass growth data for seven historical planetary missions. The red line is the average of this historical mission data. The black line is the CATE contingency that is used for the threat calculation.

To estimate the threat cost, the project-proposed mass and power contingencies (used in the hardware estimates described above) are replaced with the CATE contingencies. The estimates, including reserves, are then recalculated and the difference between this result and the result using project contingencies is recorded as the mass and power contingency threat.

For most projects, the CATE contingencies are well above the contingency values assumed in the proposed concept. However, the Europa Orbiter concept already carried significant contingencies, so the estimated contingency threat was insignificant (\$15M). Table 1 is a summary of the mass properties provided for the CATE assessment.

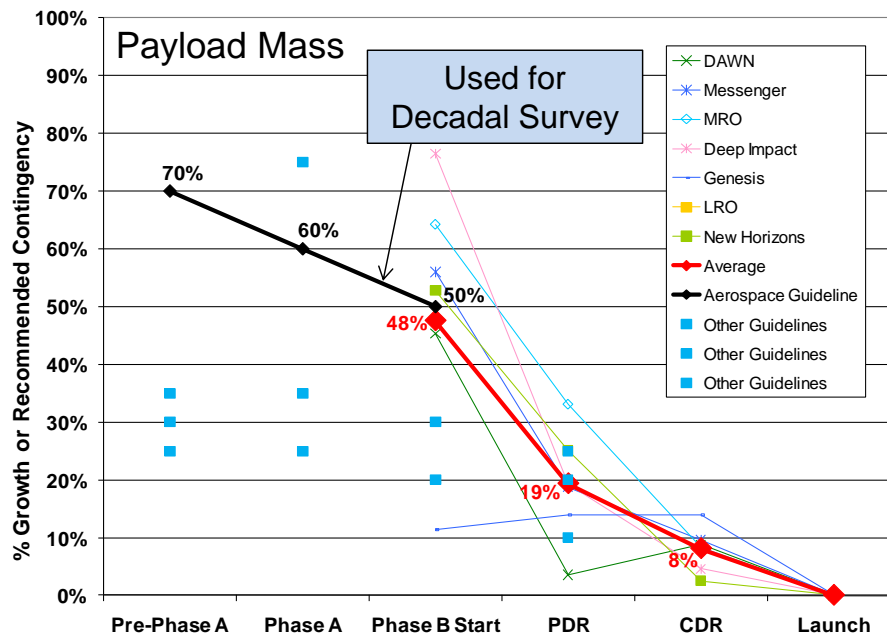


Figure 16. Contingency Values Used For Threat Estimates

Table 1. Europa Orbiter Mass Properties

	Project CBE (kg)	Project Cont. (%)	Project MEV (kg)	CATE Cont. (%)	CATE MEV (kg)
<b>Orbiter Flight System Total</b>	<b>1033.4</b>	<b>63%</b>	<b>1685.7</b>	<b>51%</b>	<b>1555.9</b>
<b>Orbiter Payload Total</b>	<b>29.1</b>	<b>76%</b>	<b>51.4</b>	<b>70%</b>	<b>49.5</b>
Instrument Chassis	2.0	63%	3.3	70%	3.4
Laser Altimeter	4.4	88%	8.2	70%	7.4
Langmuir Probe	2.2	88%	4.1	70%	3.7
Magnetometer	2.7	88%	5.0	70%	4.5
Mapping Camera	2.0	88%	3.8	70%	3.4
Payload Shielding	15.9	70%	27.1	70%	27.1
<b>Orbiter Bus Total</b>	<b>1004.2</b>	<b>63%</b>	<b>1634.3</b>	<b>50%</b>	<b>1506.4</b>
C&DH	12.0	63%	19.5	50%	18.0
GN&C	31.5	44%	45.2	50%	47.2
Harness	56.0	88%	105.0	50%	84.0
Mechanical	436.2	59%	694.3	50%	654.2
Power (w/o ASRGs)	41.5	34%	55.4	50%	62.2
ASRGs (4)	102.4	88%	192.0	50%	153.6
Propulsion	153.7	57%	241.6	50%	230.6
Telecom	60.9	71%	103.8	50%	91.3
Thermal	35.0	63%	56.9	50%	52.5
Bus Shielding	75.2	60%	120.6	50%	112.8

### Schedule Threat

The base cost estimate described above uses the project-proposed development schedule. Historically, project schedule estimates have proven to be optimistic. As part of the CATE process, a probabilistic

Independent Schedule Estimate (ISE) is developed. If the 70th percentile duration from the ISE is longer than project schedule, then a schedule threat is added.

Figure 17 illustrates the ISE process. The ISE is based on actual schedule durations from similar, historical missions. The duration of each schedule phase is treated as a triangular distribution, which can be statistically combined to yield a probability distribution of total project development time. The triangular distribution of durations for each phase is derived from the actual phase durations from the historical missions. The lowest duration is used as the low end of the triangular distribution, the average duration is used as the mode or most-likely value, and the highest historical value is used as the high value of the triangular distribution.

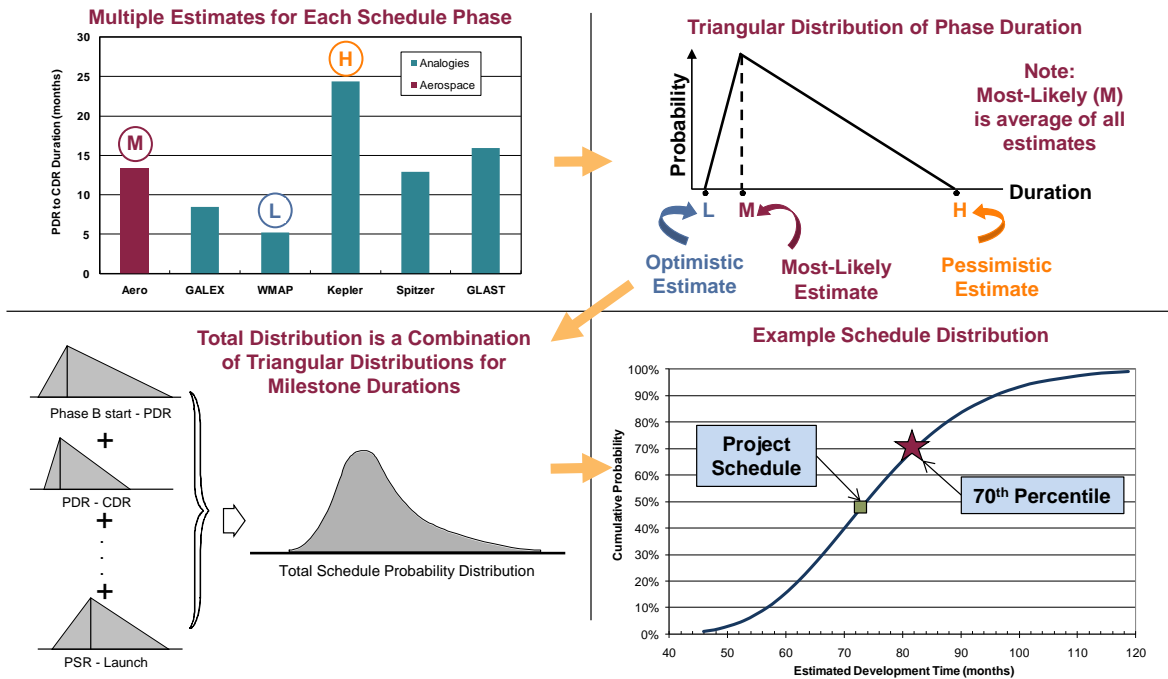


Figure 17. Independent Schedule Estimate Process Overview

Figure 18 compares the actual Phase B-D duration of the four analogous missions used in the ISE with the proposed Europa Orbiter Phase B-D duration. Figure 19 shows the results of the ISE as a cumulative probability distribution or S-curve. The 70th percentile ISE value is 75 months while the Europa Orbiter proposed value is 73 months (after adjusting the effective Phase B start date as described above). Figure 20 is a breakdown of the results by project phase. While the overall durations agree quite well, the 70th percentile historical duration for the CDR to start of spacecraft I&T phase is significantly longer than the project value. Although this difference does not contribute to the CATE cost estimate, the plan for this phase should be examined to ensure its adequacy.

The difference between the 70th percentile value and the proposed project duration is then converted to a cost threat using a burn rate based on the project budget without reserves or launch vehicle. For Europa Orbiter, the roughly two months' difference is multiplied by a burn rate of roughly \$7M per month to yield a schedule threat of \$17M.

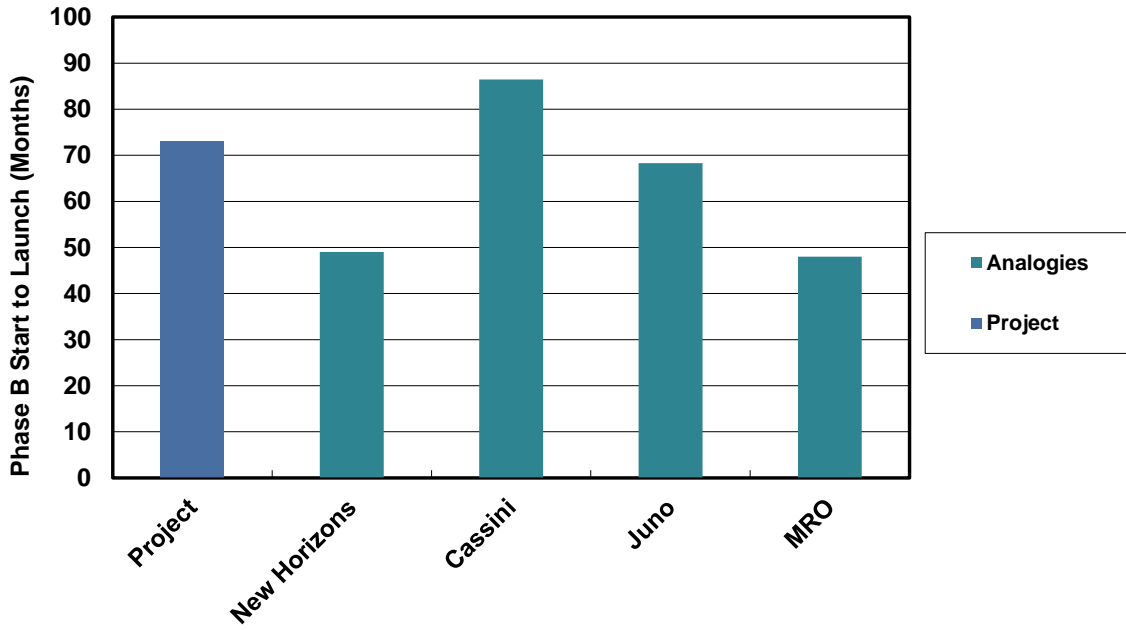


Figure 18. Analogous Mission Development Time Comparison

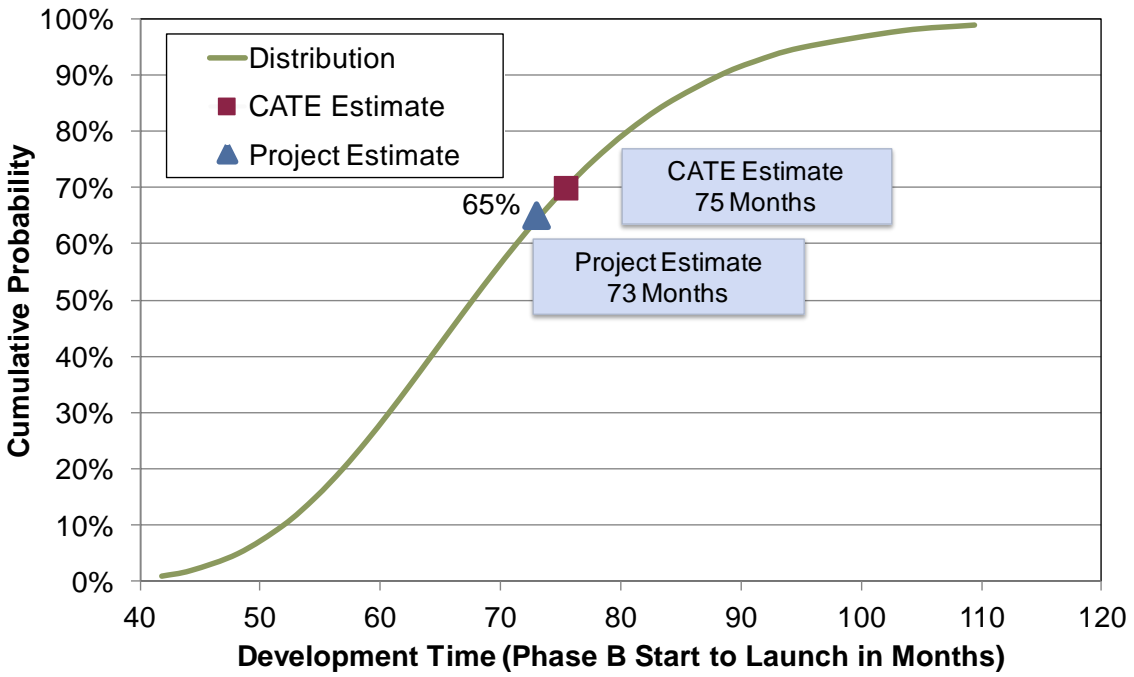


Figure 19. Europa Orbiter ISE S-Curve

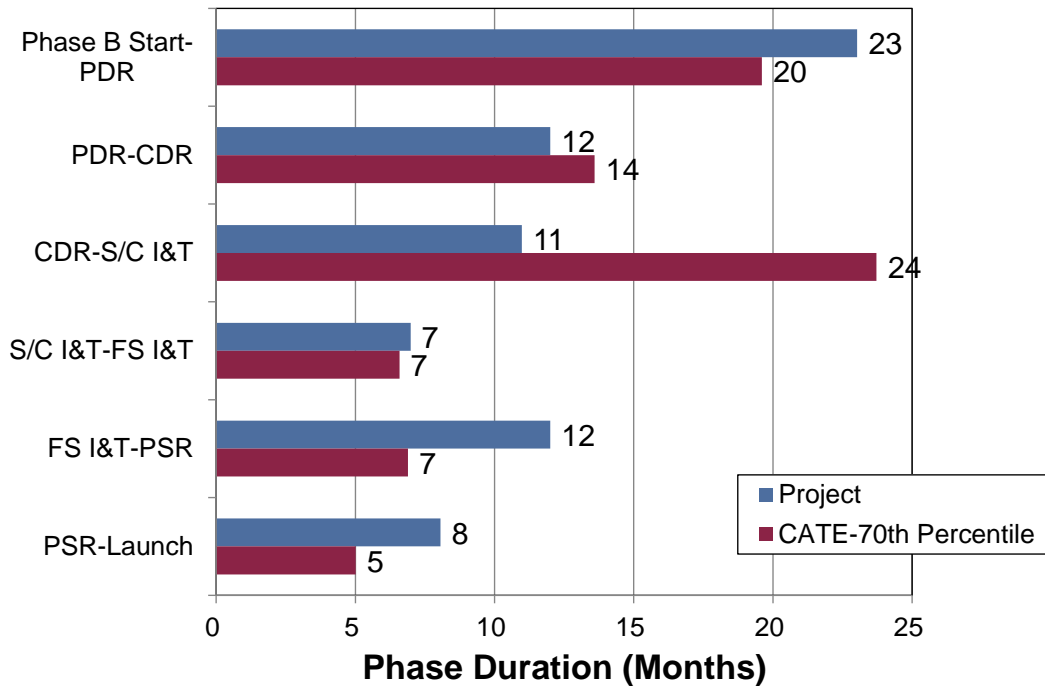


Figure 20. Europa Orbiter Analogous Mission Phase Comparison

## Results

Table 2 presents the final CATE cost results compared to the current Europa team cost estimate. The agreement between the two estimates is quite close in all WBS elements. Figures 21 and 22 present the same data in graphical form.

Table 2. Europa Orbiter Cost Estimate Comparison (FY15\$M)

WBS Element	Project Estimate	CATE Estimate	Basis of CATE Estimate
Pre-Phase A, Phase A	incl. below	\$ 54	1.5% of Dev cost per year for 40 months
Mission PM/SE/MA	\$ 123	\$ 125	Percentage of HW based on Cassini, Juno, MRO, MER + NEPA
Instruments	\$ 75	\$ 81	MICM, NICM, SOCM and analogies to planetary instruments
Flight System	\$ 523	\$ 582	NAFCOM11, PRICE, Juno, MRO, Cassini
ASRGs	\$ 200	\$ 200	Project Value for 4 ASRGs
Pre-launch Ground and Science	\$ 99	\$ 85	Percentage of HW based on Cassini, Juno, MRO, MER
Phase E and EPO	\$ 216	\$ 225	Based on annual rates from MESSENGER, NH, Juno, MRO
Total Reserves	\$ 370	\$ 369	70% from cost risk analysis
<b>Mission Cost Before Threats</b>	<b>\$ 1,606</b>	<b>\$ 1,719</b>	
Schedule Threats		\$ 17	2 months at Phase D burn rate (\$7M/month scaled from JEO)
Mass and Power Contingency Threats		\$ 15	Based on 2/14 MEL
LV Threats		\$ -	Adequate margins on Atlas V 551
<b>Mission Cost With Threats</b>	<b>\$ 1,606</b>	<b>\$ 1,751</b>	
Launch Vehicle/Services	\$ 272	\$ 272	Atlas V551 cost from DS guidelines + nuclear processing
<b>Total Mission Cost With Threats</b>	<b>\$ 1,878</b>	<b>\$ 2,023</b>	

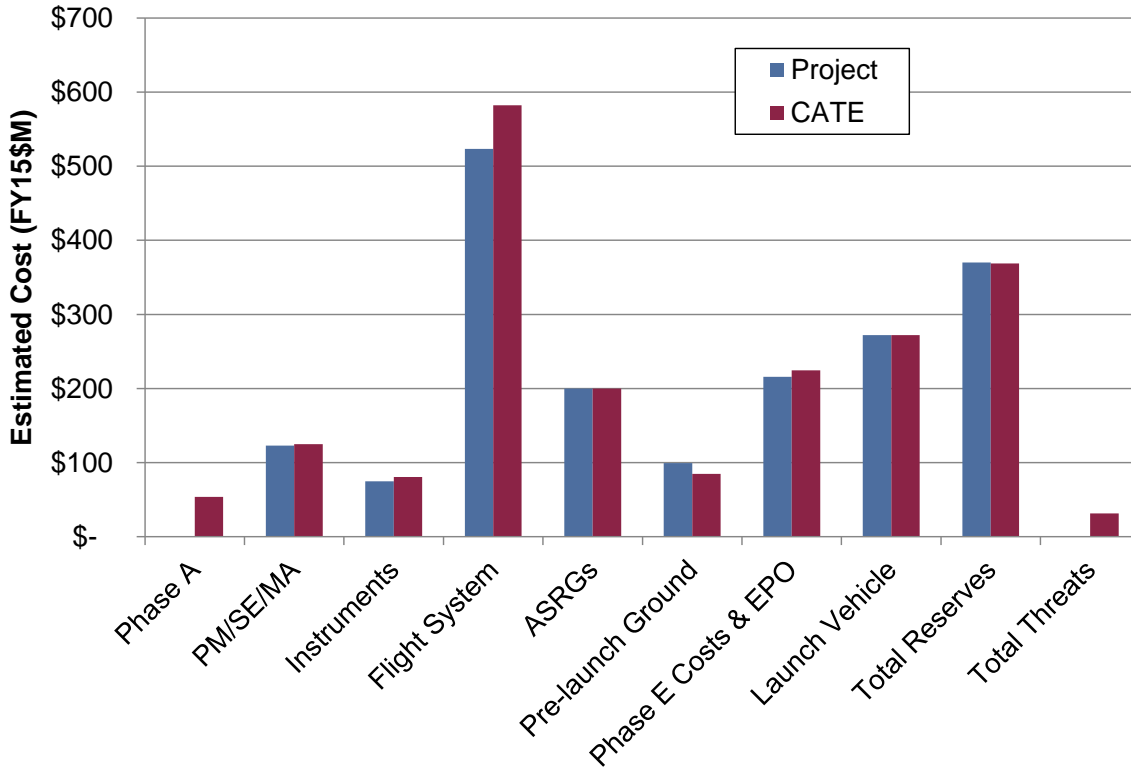


Figure 21. Europa Orbiter Key Cost Element Comparison

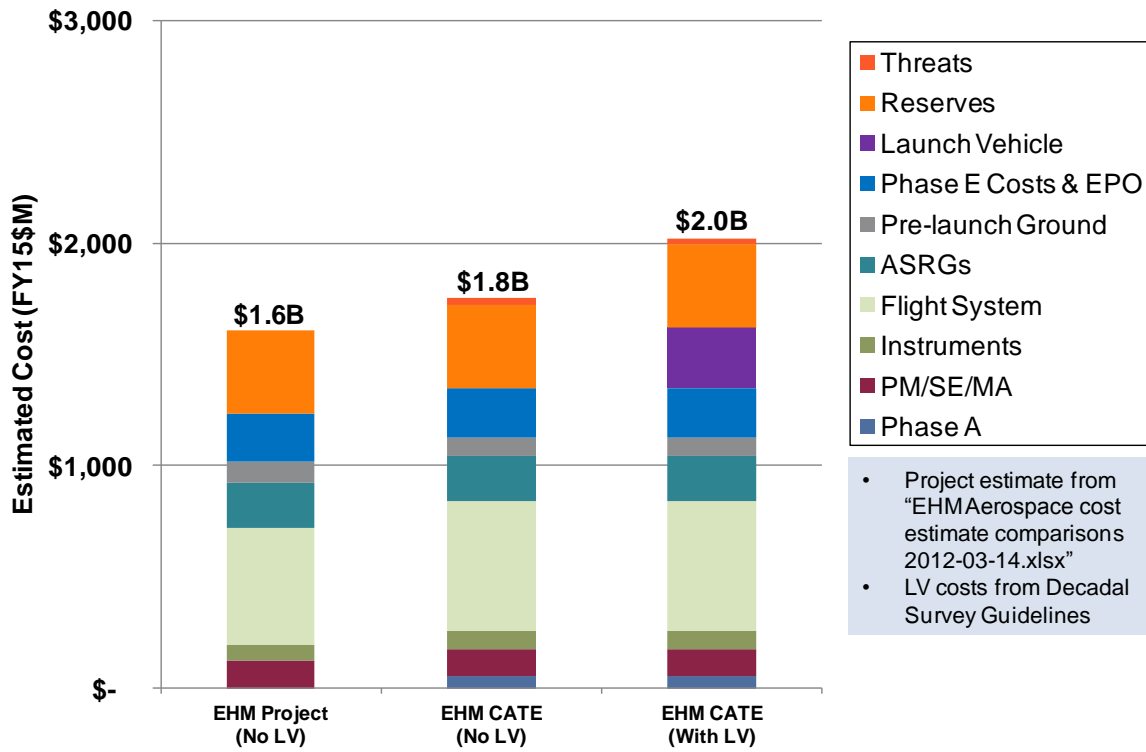


Figure 22. Europa Orbiter Cost Estimates

## Complexity-Based Risk Assessment (CoBRA)

As a cross-check of the CATE results, the Complexity-Based Risk Assessment (CoBRA) process was also applied to the Europa Orbiter concept. The CoBRA process uses technical and programmatic parameters from the conceptual design to calculate a complexity value for the design. This is done by ranking each of the individual parameters against a database of historical space missions. The calculated complexity values for the historical missions are plotted against development cost and schedule. The missions are classified as successful, partially successful, failed, or yet to be determined. A best-fit line is drawn through the successful missions, and the estimated cost and schedule of the Europa Orbiter concept can be compared to missions of similar complexity. Figures 23 and 24 show the CoBRA cost and schedule analysis results. Both the project and CATE cost estimates are slightly above the green trend line, which is in family with successful past missions of this complexity. Both the project and CATE schedule estimates are below the green trend line but above the blue trend line, which is drawn through successful missions that had a planetary launch window constraint. Again, this result adds confidence that the Europa Orbiter schedule estimates are in family with comparable successful missions.

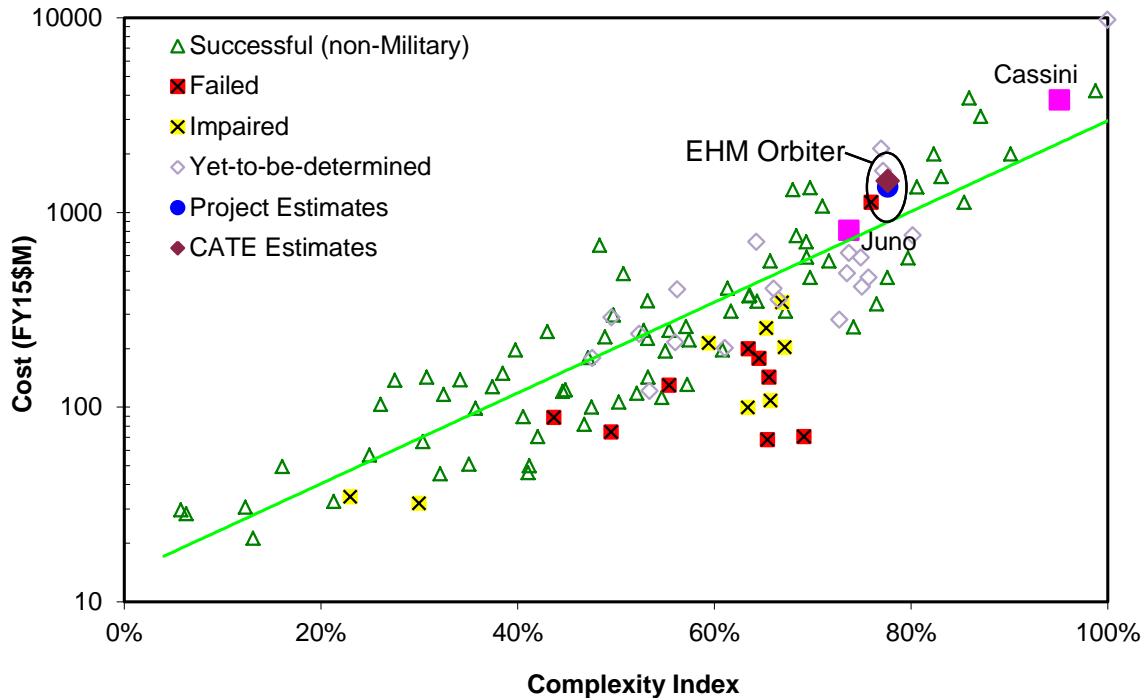


Figure 23. Complexity-Based Risk Assessment Cost Analysis

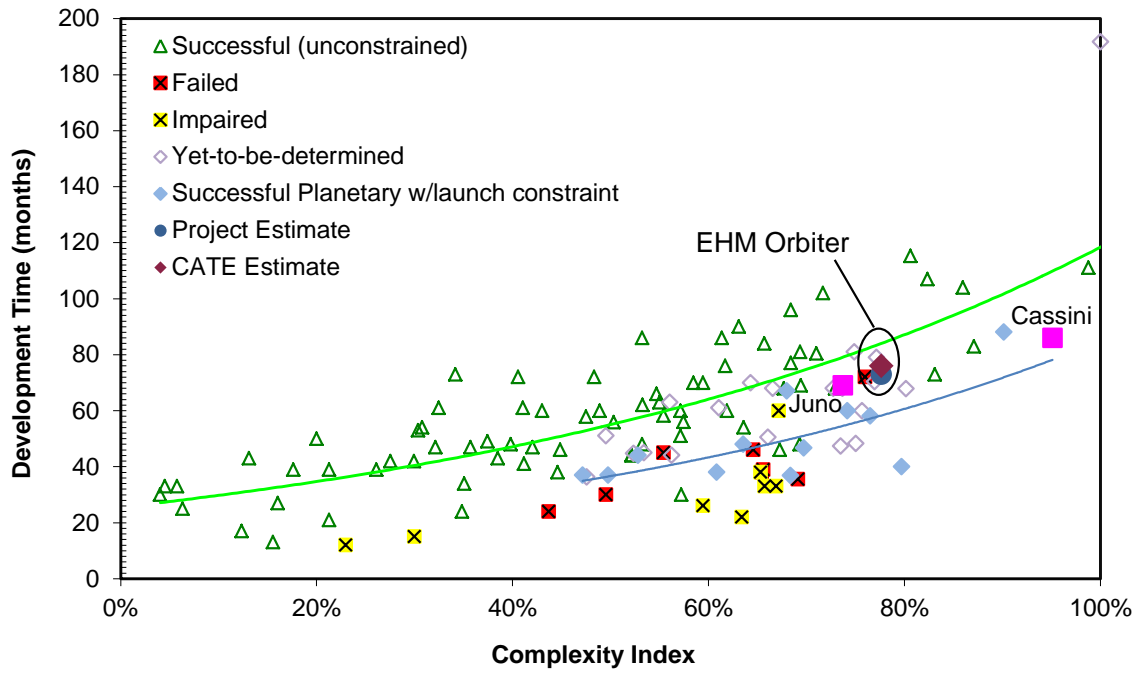


Figure 24. Complexity-Based Risk Assessment Schedule Analysis